



HAL
open science

Designing biomaterials for controlled cardiac stem cell differentiation and enhanced cell therapy in the treatment of congestive heart failure

Yohan Farouz

► **To cite this version:**

Yohan Farouz. Designing biomaterials for controlled cardiac stem cell differentiation and enhanced cell therapy in the treatment of congestive heart failure. Biomechanics [physics.med-ph]. Université Sorbonne Paris Cité, 2015. English. NNT : 2015USPCB114 . tel-01541523

HAL Id: tel-01541523

<https://theses.hal.science/tel-01541523>

Submitted on 19 Jun 2017

HAL is a multi-disciplinary open access archive for the deposit and dissemination of scientific research documents, whether they are published or not. The documents may come from teaching and research institutions in France or abroad, or from public or private research centers.

L'archive ouverte pluridisciplinaire **HAL**, est destinée au dépôt et à la diffusion de documents scientifiques de niveau recherche, publiés ou non, émanant des établissements d'enseignement et de recherche français ou étrangers, des laboratoires publics ou privés.



Sorbonne Paris Cité – Université Paris Descartes
Ecole Doctorale ED474 : Frontières du Vivant

Sorbonne Paris Cité – Université Paris Descartes – PARCC – HEGP – Fondation Carpentier
INSERM U970 : Regenerative therapies for cardiac and vascular diseases

Paris Sciences et Lettres – Ecole Normale Supérieure de Paris – Institut Pierre-Gilles de Gennes
CNRS UMR8640 : Microfluidics, chemical organization and nanotechnologies

Designing biomaterials for controlled cardiac stem cell differentiation and enhanced cell therapy in the treatment of congestive heart failure

[Conception de biomatériaux pour le contrôle de la différenciation cardiaque à partir de cellules souches et pour l'amélioration de la thérapie cellulaire dans le traitement de l'insuffisance cardiaque sévère]

Par Yohan Farouz

Thèse de doctorat,

Spécialité : Biophysics, Biomaterials and Regenerative Medicine (Biophysique, Biomatériaux et Médecine régénératrice)

Dirigée par :
Philippe Menasché
Yong Chen

En vue d'une soutenance publique le 30 septembre 2015 devant un jury composé de :

Cesare Terracciano, MD, PhD	rapporteur
Abdul Barakat, PhD	rapporteur
Matthieu Piel, PhD	examinateur
Onnik Agbulut, PhD	examinateur
Yong Chen, PhD	co-directeur de thèse
Philippe Menasché, MD, PhD, PU-PH	co-directeur de thèse

© 2015 Yohan Farouz
All rights reserved

Abstract

Cell therapy is a promising strategy to help regenerate the damaged heart. Recent studies have placed a lot of hopes in embryonic stem cells and our lab had previously found a way to differentiate them into cardiac progenitors, cells that can only differentiate into cardiomyocyte, endothelial cells or smooth muscle cells. This early commitment decreases their proliferative capabilities, yet maintains their plasticity for better integration inside the host tissue. However, clinical and pre-clinical injection studies did not really meet the expectations. Even though slight improvements in cardiac function were demonstrated, very low cell viability has been observed, as well as a very low retention of the cells inside the myocardium. To address this problem, my PhD projects not only focus on the design of new biomaterials to act as a vehicle for cell delivery and retention in the infarcted area, but also on the design of biomaterials that control the cellular environment during the differentiation of pluripotent stem cells into cardiomyocytes. Going back and forth between the labs and the clinics, we first developed new techniques for the fabrication and the characterization of a cell-laden fibrin patch that is now undergoing phase I clinical trial. From the approved clinical formulation, we then propose new blends of clinical materials that will eventually improve the maturation of the cardiac progenitors once grafted onto the failing heart. In this perspective, we developed an *in vitro* model to investigate the combined influence of matrix elasticity and topographical confinement on stem cell differentiation into cardiomyocytes. By using microfabrication techniques to pattern pluripotent stem cells on substrates of controlled stiffness, we demonstrate that even using a widely recognized chemical-based protocol to modulate signaling cascades during differentiation, much heterogeneity emerges depending on the cellular physical environment. We thus extracted the main features that led to controlled and reproducible cardiac differentiation and applied it to the fabrication of next generation of multi-layered anisotropic cardiac patches in compliances with clinical requirements. This work opens new routes to high-scale production of cardiomyocytes and the fabrication of cell-laden or cell-free clinical patches.

Keywords: Cell therapy, regenerative medicine, biomaterials and tissue engineering, cardiac development, mechanotransduction, microfabrication, human pluripotent stem cells.

Résumé

La thérapie cellulaire se positionne comme une stratégie prometteuse pour inciter le cœur infarcté à se régénérer. A cet effet, des études récentes placent des espoirs considérables dans l'utilisation des cellules souches embryonnaires et notre laboratoire a déjà démontré comment les différencier en progéniteurs cardiovasculaires, un type de précurseurs cellulaires qui ne peut aboutir qu'à la formation de cardiomyocytes, de cellules endothéliales ou de cellules de muscles lisses. Cet engagement précoce réduit leur capacité de prolifération anarchique et en même temps leur permet de rester suffisamment plastiques pour éventuellement s'intégrer plus facilement avec le tissu hôte. Cependant, les études précliniques et cliniques d'injection de ces cellules s'avèrent décevantes. Malgré de légères améliorations de la fonction cardiaque, on observa une trop faible survie cellulaire ainsi qu'un taux de rétention des cellules dans le myocarde remarquablement bas. Afin d'étudier ce problème, mes travaux de thèse ont porté non seulement sur la conception de nouveaux biomatériaux pouvant servir de moyen de transport et d'intégration des cellules dans la zone infarctée, mais aussi sur la conception de biomatériaux permettant de contrôler précisément l'environnement cellulaire au cours du processus de différenciation de cellules souches pluripotentes humaines en cardiomyocytes. Grâce aux importantes interactions entre nos laboratoires de recherche fondamentale et de recherche clinique, nous avons tout d'abord développé de nouvelles techniques de fabrication et de caractérisation de patches de fibrine cellularisés qui sont récemment entrés dans un essai clinique de phase I. A partir de cette formulation clinique approuvée par les autorités de régulation, nous avons élaboré toute une gamme de matériaux composites uniquement à base de matières premières pertinentes dans ce cadre clinique, dans le but d'améliorer la maturation des progéniteurs cardiovasculaires une fois greffés sur le cœur défaillant. Dans cette optique, nous avons également développé un modèle *in vitro* permettant d'étudier précisément l'influence combinée de la rigidité du substrat et du confinement spatial sur la différenciation des cellules souches en cardiomyocytes. Grâce à des techniques de microfabrication sur substrat mou, il a été possible de positionner précisément les cellules souches pluripotentes dans des espaces restreints d'élasticité variable. Ainsi, nous avons pu observer que même en utilisant des protocoles chimiques éprouvés basés sur la modulation de cascades de signalisation impliquées dans le développement cardiaque, une très forte hétérogénéité pouvait apparaître en fonction de l'environnement physique des cellules. Nous avons ainsi pu extraire les caractéristiques principales permettant une différenciation cardiaque efficace, reproductible et standardisée et les avons appliquées à la fabrication d'une nouvelle génération de patches composés de matériaux cliniques et de couches multiples de bandes synchrones de cardiomyocytes. De fait, ces travaux ouvrent de nouvelles voies dans l'utilisation de biomatériaux pour la production industrielle de cardiomyocytes et pour la fabrication de patches cliniques, cellularisés ou non, dans le traitement de l'insuffisance cardiaque.

Mots clés : Thérapie cellulaire, médecine régénératrice, biomatériaux et ingénierie tissulaire, développement cardiaque, mécanotransduction, microfabrication, cellules souches pluripotentes humaines.

Acknowledgements - Remerciements

The work presented in this dissertation is not the fruit of a single man, but rather the fortunate consequence of many interactions with people who raised me, guided me, assisted me and encouraged me relentlessly to make this journey instructive and worthwhile. I apologize in advance for any involuntary omission I am about to make.

Before anything, lets acknowledge our many sponsors for their generous funding and support: Ecole Polytechnique Paris Saclay for the 3-year PhD scholarship, Université Paris Descartes – Sorbonne Paris Cité for the 3-year teaching assistantship, Fondation pour la Recherche Médicale for funding the 4th and final year, Fondation Bettencourt-Schueller for travelling stipends, and all the other institutions that help the various laboratories I have spent time in: Labex Revive, ShapeHeart Leducq Transatlantic Network, ANR, AFM, Fondation de France, the PARCC/HEGP, INSERM, CNRS, the FdV Doctoral School and the Ecole Normale Supérieure de Paris.

Then, I would like to thank my two supervisors, Philippe Menasché and Yong Chen, who could not have been more complementary in their mentoring advice and my training. Philippe Menasché, for his open-mindedness, his trust and positivity, for involving me in the pre-clinical experience and for introducing the clinical world to me. Yong Chen, also for his open-mindedness, trust and positivity, and for brainstorming the most challenging ideas with me.

I am also grateful to Cesare Terracciano and Abdul Barakat for accepting to be my thesis' "rapporteurs", for taking the time to review and comment the present work.

Of course, this thesis would not have been possible without Onnik Agbulut and Matthieu Piel, who opened up their lab to me and never refused a scientific discussion. Not to mention members of their laboratories, respectively Pierre Joanne and Solène Boitard, as well as Nicolas Carpi and Emmanuel Terriac. Their technical knowledge was invaluable and they made me see cardiac differentiation and micropatterning (respectively), in ways I would never have imagined otherwise.

I would like to thank Jérôme Larghero, Valérie Vanneaux and all the members of the Cell Therapy team at the Saint-Louis Hospital, who really trained me in experimental stem cell biology, especially Valérie Vanneaux, Hélène Riesterer, Lionel Faivre, Hélène Boucher, Isabelle Cacciapuoti, Alexandre Parouchev, and Manuel Théry for his advice of microfabrication.

To all the members of the INSERM U970 team at the PARCC/HEGP who trained me and assisted me in performing the experiments described in this dissertation: Damelys Calderon, Hadhami Hamdi, Valérie Bellamy, Alain Bel, Mathieu Pieronne, Wardiya Afshar, Elodie Mouloungui, Nisa Renault, Isabelle Hédon, Julie Piquet, Adrien Lalot, Véronique Oberweiss, Marie-Cécile Périer.

To all the members of Ecole Normale Supérieure de Paris who trained me and assisted me in performing the experiments described in this dissertation: Yadong Tang, Diana Molino, Sandrine

Quignard, Jiangmei (Megan) Lian, Sisi Li, Wang Li, Jian (Olivier) Shi, Zhitao Han, Junjun Li, Naresh Kumar Mani, Anna Venancio Marques, Frédéric Bataille, Dominique Ho-Tin-Noé, Anne Hallopé, Nabil Garroum, Géraldine Hallais, Jacques Fattaccioli and Damien Baigl.

A special thanks to David Smadja at HEGP, Mathieu Pernot at Institut Langevin, as well as to Alba Marcellan at ESPCI for their help and guidance in fibrin-based assays and mechanical characterization.

To André Terzic, Marc Mercola, Karine Vauchez, Gabor Foldes and Michel Pucéat for their scientific and professional inputs.

To François Taddei from the CRI and Sophie Bernard from Université Paris Descartes, who gave me the opportunity to teach and to learn to teach. And, of course, to my students both from the FdV Bachelor Program 13' and from the BME Master Program 14' and 15', who had to patiently experiment my unorthodox and ever changing teaching methods.

To the group of Ecole Polytechnique's students I mentored during their PSC: Fanny Olivier, Hugo Soulat, Nora Faivre, Clémence Herzog, Gwendoline Tallec, Ricardo Furquim Pereira, Victor Ray. Thank you for your inputs and for your interest in crazy interdisciplinary projects.

I am deeply grateful to Kevin Kit Parker, Molly Stevens, Seung-Wuk Lee and their respective teams who cheerfully welcomed me before my PhD and initiated me to academic research and to the field of tissue engineering. A special mention to Ashutosh Agarwal for his friendship and mentorship and for always encouraging me to ask the right questions and think of the right experiments.

To Xavier Duportet, Camille Delebecque and Philippe Bouaziz, who unconsciously led me to start this PhD journey.

To Kévin Lhoste, for all the good times at the lab, at the CRI and outside.

To Kalthoum Ben M'Barek, friend and best co-PhD-student/colleague, for all the good times up at the mezzanine, down at the lab and outside, for all the support and cheering, and for all the open-minded discussions about Northern African cultures and so on.

To my family in law: Jean-François, Sylvie, Francine, Max, Nicolas and Caroline; and to my Parisian families for always helping me, supporting me and welcoming me so warmly: the Dekels; Gégé; the Masliahs, Soustiels and Sadocks; the Azoulays, Aboulkers, and Nahons.

To Coralie Villa and Juliette Dumoulin, who are always there for me regardless of the distance. Thanks for all the moments we lived since London and high school, respectively. Thanks in advance for all the future ones.

Thanks to my closest family: my regretted grand-fathers Papi Marc and Papi Soly; Mamie Marcelle, Tonton Joseph, Mamie Mady, Maman, Papa, Nat' and Jo', for whom neither my English nor my native French vocabulary will be sufficient to faithfully express my feelings of love, admiration and gratitude. Thanks for your education, for teaching me the values of our roots, traditions and legacy. Thanks for your unconditional and blind support regardless of my decisions, like my choice to pursue an academic career. Thanks for always pushing me beyond my limits. Thanks for our funny relationship to high-tech and for the DIY blood running in parts of the family.

Merci Papa, for teaching me how to balance "la rage de vaincre" with the pleasures of life like gastronomy and the arts.

Merci Maman, for instilling in me both creativity and rigor and for your selfless attentions.

Thanks to both for still loving me even if I don't call you often enough.

And to my beloved Sophie, who has accompanied me since the first year of the PhD, who lived with immense strength the best and worst moments of this journey. Thanks for having done your best to put yourself in my shoes; for having made my life as easy as possible for the sake of this PhD; for dealing with my lack of organization and for dealing with the struggle of our incompatible calendars; for cooking delicious macarons and fine dishes while I was away feeding stem cells during week-ends; for your organization skills; for keeping me from enslaving myself to my work; for always bringing me new perspectives on the world. And for all the things that would make this paragraph too personal in the context of this dissertation...

Main abbreviations

AFM: Atomic Force Microscopy

ATMP: Advanced Therapy Medicinal Product

BMP: Bone morphogenetic protein

BSA: Bovine Serum Albumine

CPC: Cardiac progenitor cells

EB: Embryoid Body (**mEB** for murine EB, **hEB** for human EB)

ECB: Engineered Cardiac Band

ECM: Extracellular matrix

EMA: European Medicines Agency

ESC: Embryonic stem cells (**mESC** for murine ESC, **hESC** for human ESC)

ESCd-CM: Embryonic stem cell-derived cardiomyocytes

FBS: Fetal Bovine Serum

FDA: Food and Drug Administration

FGF: Fibroblast growth factor

GAG: Glycosaminoglycan

GMP: Good Manufacturing Practice

HA: Hyaluronic acid

HMDS: Hexamethyldisilazane

iPSC: Induced pluripotent stem cells

μCP: Micro-contact printing

MSC: Mesenchymal stem cells

NRCM: Neonatal rat cardiomyocyte

PAA: Polyacrylamide

PBS: Phosphate Buffer Saline

PCP: Planar cell polarity

PDMS: Polydimethylsiloxane

PEG: Poly-ethylene glycol

PEG-DA: PEG-diacrylate

PFA: Paraformaldehyde

PLL-g-PEG: Poly-L-lysine grafted PEG

PSCd-CM: Pluripotent stem cell-derived cardiomyocytes

RGD: Argininyglycyl aspartic acid. Peptide of sequence L-Arginine (**R**)- Glycyl (**G**) – Aspartic acid (**D**)

RT: Room Temperature

SCD: Stem cell differentiation

SCD-CM: Stem cell-derived cardiomyocyte

SEM: Scanning Electron Microscopy

SSEA-1: Stage-specific embryonic antigen-1 (also referred to as **CD15**)

SWE: Shear Wave Elastography

TFM: Traction Force Microscopy

TMCS: Trimethyl chlorosilane

UV: Ultraviolet light

Wnt: (Wint) family of genes related to major developmental pathways. Wnt is a portmanteau word made of int and Wg, for “Wingless-related integration site”.

Y-27632: small molecule that inhibits the ROCK pathway.

YAP: Yes activation protein

Table of Contents

Abstract.....	iii
Résumé	iii
Acknowledgements - Remerciements	v
Main abbreviations	ix
Table of Figures and Movies	xv
List of Tables	xviii
Chapter 1 – Introduction.....	1
Cardiovascular diseases	2
Rationale of the ESCORT Clinical Trial.....	3
<i>Cell type</i>	4
<i>Scaffold type</i>	5
<i>Rationale</i>	5
Presentation of the thesis project	8
References	9
Chapter 2 – On the design of biomimetic materials for cardiac stem cell differentiation.....	11
Abstract.....	12
Introduction	13
<i>Rationale for cardiomyocyte production</i>	13
<i>Mechanical forces during cardiac development, systems biology and the main cardiac differentiation protocols</i>	13
Force transmission: Cell-Cell Interactions and Cell-ECM interactions	18
<i>Interactions in the developing embryo</i>	18
<i>Strategies for mimicking cell-cell communication and cell-ECM coupling</i>	19
Influence of substrate topography	20
<i>General overview</i>	20
<i>Influence of topography on SCD into mesodermal progenitors and cardiomyocytes: the importance of colony size</i>	22
<i>Influence of topography on sarcomere maturation and force generation of cardiomyocytes: the importance of anisotropy</i>	23
<i>Anisotropy in early differentiation and isotropy in ESCd-CM studies</i>	25
Influence of Tissue elasticity	25
<i>General overview</i>	25
<i>Influence of elasticity on mesodermal SCD</i>	27
<i>Influence of elasticity on cardiomyocyte sarcomere maturation</i>	28
Perspectives	30
<i>Influence of Stretching and Shearing:</i>	30

<i>Influence of electrical signals on the maturation of cardiomyocytes</i>	30
<i>Pharmacological and medical applications</i>	32
Conclusion	34
References	35
Chapter 3 – Safety, Regulatory and Ethical Issue of human studies	48
Introduction	49
Safety Issues	49
<i>Arrhythmias</i>	49
<i>Tumor Development</i>	50
<i>Rejection</i>	52
<i>Stent Restenosis/Thrombosis</i>	53
<i>Calcification</i>	53
Regulatory Issues	53
<i>Preclinical Studies</i>	53
<i>Cell Manufacturing</i>	54
<i>Release Criteria</i>	56
<i>Cell and Scaffold Combined Products</i>	58
Ethical Issues.....	59
Conclusion	61
References	62
Chapter 4 – From the clinics: Design of a Cardiac Patch for the ESCORT clinical trial	65
Introduction.....	66
<i>The ESCORT clinical trial</i>	66
<i>Design of a cardiac patch for clinical applications</i>	69
Material and methods.....	73
<i>Determination of fibrinogen and thrombin concentrations</i>	73
<i>Preparation of 3D Culture in fibrin gels</i>	73
<i>Immunohistology</i>	74
<i>Scanning Electron Microscopy (SEM)</i>	74
<i>Image analysis</i>	75
<i>Materials characterization</i>	75
Results.....	76
<i>Concentration of Evicel’s fibrinogen solutions</i>	76
<i>Structural characterization of fibrin patches</i>	77
<i>Mechanical characterization</i>	80
<i>Handling tests</i>	82
<i>Cell-laden fibrin patches</i>	83

<i>Manipulation during surgery</i>	84
<i>Effect of the patch on rats and sheep</i>	85
Conclusion and Discussion	86
<i>Perspectives</i>	87
References	89
Chapter 5 – From the clinics to the labs: development of new microfabricated platforms for the standardization of cardiomyocyte differentiation	92
Introduction	93
Materials and methods	94
<i>Stamp fabrication</i>	94
<i>Sacrificial coverslip microcontact printing</i>	94
<i>Polyacrylamide (PAA) gel fabrication</i>	95
<i>Cell Culture</i>	95
<i>Immunofluorescence</i>	96
<i>RT-qPCR</i>	96
<i>Statistical analysis</i>	97
<i>Movies</i>	97
Results	98
<i>Characterization of the substrates</i>	98
<i>Morphology of the colonies and cell density</i>	100
<i>Beating behavior of the colonies</i>	102
<i>Transcriptional analysis</i>	106
<i>Conclusion on the transcriptional analysis</i>	112
Discussion	113
<i>Limitations</i>	113
<i>Perspectives</i>	115
Conclusion	117
References	118
Supplementary Information	121
Chapter 6 – Back to the clinics: new design strategies for the fabrication of Engineering Cardiac Bands	131
Introduction	132
Materials & Methods	134
<i>Cell patterning on clinical fibrin hydrogels</i>	134
<i>Preparation of composite 3D scaffolds</i>	136
Results I: Soft micropatterning with the ESCORT protocol	138
<i>The choice of the substrate: BJ vs. FPBT</i>	138
<i>Patterning and stem cell culture</i>	141

<i>Initial Glass patterning success</i>	142
Results II: Proof-of-concept patterning strategies using clinical fibrin hydrogels	145
<i>First proof of concept for the transfer of patterned cells from PAA to clinical fibrin gels</i>	145
<i>Advanced proof of concept using an optimized geometry for single-material differentiation of hiPSCs into cardiomyocyte and subsequent transfer to clinical fibrin</i>	148
<i>Alternatives to cell transfer: direct ECM patterning on clinically-relevant hydrogels</i>	151
Results III: new blends of clinical materials	152
<i>Handling test</i>	154
<i>Histological profile</i>	155
<i>Mechanical properties</i>	156
<i>In vitro experiment</i>	157
<i>Conclusion on the new blends</i>	159
Conclusion and Perspectives	160
References	162
Supplementary Information	165
Chapter 7 – Conclusions and Perspectives	166
Summary	167
Perspectives	170
<i>Stem cell differentiation, biomaterials and cell-free cell therapy</i>	170
References	172
Abstract	174
Résumé	174

Table of Figures and Movies

Figure 1.1 Ischemic heart disease is the major risk factor of heart failure in high income countries worldwide.	2
Figure 1.2 The ideal cardiac patch.	3
Figure 1.3 Short summary of the differentiation protocol from hESCs to cardiovascular progenitor cells	5
Figure 1.4 The importance of scaffold parameters at every step of the fabrication process.	6
Figure 2.1 General strategy for differentiating PSCs into cardiomyocytes.	14
Figure 2.2 Important players involved in conventional cardiac differentiation protocols, and their interactions with physical factors (not published).....	17
Figure 2.3 Overview of popular techniques for controlling and characterizing materials and cells at the microscale.	21
Figure 4.1 Description of the cell production process in GMP conditions.....	69
Figure 4.2 Fibrin polymerization process	70
Figure 4.3 Mechanical characterization of fibrin hydrogels.....	75
Figure 4.4 Elasticity measurement with Shear Wave Elasticity on Aixplorer® Ultrasound System.....	76
Figure 4.5 Lot-to-lot variability in fibrinogen concentrations.....	77
Figure 4.6 Electron Micrographs of fibrin patches.	77
Figure 4.7 Fiber diameter as a function of fibrin composition	78
Figure 4.8 Confocal imaging of fluorescently labelled fibrin hydrogels	78
Figure 4.9 Photomicrographs of histological sections of fibrin patches, stained with Hematoxylin/Eosin stain.....	79
Figure 4.10 Variations in pore diameter (μm) as a function of patch concentrations (mg/mL-U/mL). .	79
Figure 4.11 Compressive testing results for fibrin hydrogels of increasing fibrinogen:thrombin concentrations.	80
Figure 4.12 SWE measurements of fibrin elasticity.	81
Figure 4.13 Representative images of the behavior of fibroblasts seeded within fibrin patches.	83
Figure 4.14 Shape and handling of the fibroblast-laden fibrin gels.....	84
Figure 4.15 Grafting of the patch on a sheep's heart	85
Figure 4.16 Grafting the patch on a rat's heart	85
Figure 5.1 Micropatterning ECM proteins on soft polyacrylamide hydrogels.....	95
Figure 5.2 Culture conditions and small molecule treatments for purely chemical-based cardiomyocyte differentiation.....	96
Figure 5.3 Example of beating patterns observed through movie analysis.	98
Figure 5.4 Characterization of the substrates.	99
Figure 5.5 Morphological analysis of the differentiated clusters.	100
Figure 5.6 General morphology of cell colonies at the end of differentiation.....	101
Figure 5.7 Percentage of beating spots as a function of time and spot diameter (A-i), time and elasticity (A-ii), and spot diameter and elasticity on days 12 (B-i) and 15 (B-ii).....	103

Figure 5.8 Beating frequency as a function of time and spot diameter (A-i), time and elasticity (A-ii), and spot diameter and elasticity at day 12 (B-i) and day 15 (B-ii).	104
Figure 5.9 Percentage of spots with circular contraction wave behavior, as a function of time (A), spot diameter (B) and elasticity (C).	105
Figure 5.10 Percentage of irregularly beating spots as a function of time, spot diameter and elasticity.	106
Figure 5.11 Gene expression in change fold versus undifferentiated hiPSC before seeding on micropatterns.	107
Figure 5.12 Clustergram of the relative expression profiles in different conditions of elasticity (brown), diameter (pink), and day (blue).	110
Figure 5.14 Classification of genetic expression variations depending on spot diameter and elasticity	112
Figure 5.15 Design of new platforms for higher-throughput assays.	116
Figure 6.1 Representative alginate structure: (A) chain conformation and (B) block distribution.	133
Figure 6.2 Representative structure of hyaluronic acid.	133
Figure 6.3 Comparative BMP-2 induction on BJ feeders or FPBT feeders.	139
Figure 6.4 Gene expression and purity analysis after specification on FPBT or BJ	140
Figure 6.5 Immunostaining attempts on patterns with inappropriate pattern cell density.	141
Figure 6.6 Effect of Y-27632 addition (A) and removal (B) from Nutristem® medium on hESCs seeded on spot patterns.	142
Figure 6.7 Immunostaining after BMP2 induction of hESCs on rigid spots.	143
Figure 6.8 qPCR analysis.	144
Figure 6.9 Example of patterning of BJ + hESCs on 10 kPa PAA substrates patterned with FN spots.	144
Figure 6.10 PAA to Fibrin patterned cell transfer.	145
Figure 6.11 Surface of PAA before and after transfer on fibrin patch	146
Figure 6.12 Surface of fibrin patches after transfer from PAA.	147
Figure 6.13 Fluorescent fibrinogen observation on 1 kPa PAA patterned with lines and seeded with BJ fibroblasts. (A) Epifluorescence. (B) LSCM of a cluster, (B-i) section, (B-ii) 3D reconstruction.	148
Figure 6.14 Beating patterns of engineered cardiac bands.	149
Figure 6.15 Proof-of-concept of a two-level fibrin patch made of parallel band of hiPSC-derived cardiomyocytes.	150
Figure 1.16 Evaluation of the stiffness of aggregated cardiac bands,	151
Figure 6.17 Confocal microscopy of the proof-of-concept fibrin micropatterning with lines of fibronectin + fibrinogen, after transfer from a 10-kPa polyacrylamide layer.	152
Figure 6.18 Cardiac muscular thin films constructed from micropatterned alginate substrates.	153
Figure 6.19 Histological sections of fibrin patches, stained with Hematoxylin/Eosin.	155
Figure 6.20 Histological sections of fibrin/alginate patches, stained with Hematoxylin/Eosin.	155
Figure 6.21 Histological sections of fibrin/hyaluronic acid patches, stained with Hematoxylin/Eosin.	156

Figure 6.22 Compressive test and SWE results for fibrin/alginate hydrogels.....	156
Figure 6.23 Compressive test and SWE results for fibrin/HA hydrogels.	157
Figure 6.24 Microscopic image of F20T4 seeded with hMSCs at Day 7. Scale bar: 200 μ m.....	158
Figure 6.25 Microscopic images of fibrin/Alginate seeded with hMSCs at Day 7.....	158
Figure 6.26 Microscopic images of fibrin/HA seeded with hMSCs at Day 7.....	158
Figure 6.27 Sheep surgery using a fibrin/HA patch loaded with CD15 ⁺ hESC-derived progenitors..	159
Supplementary Figure 5.1 qPCR's heat maps of clustered gene expression visualization grouped by diameters (x-axis) and elasticity (y-axis) [10^6 kPa represents glass coverslips].....	122
Supplementary Figure 5.2 Web diagram of gene expression for each condition of diameter and elasticity, day 12.....	123
Supplementary Figure 5.3 Web diagram of gene expression for each condition of diameter and elasticity, day 15.....	124
Supplementary Figure 5.4 p-value matrices corresponding to Figure 5.6 . Green represents significance.	126
Supplementary Figure 5.5 p-value matrices corresponding to Figure 5.7 . Green represents significance.	127
Supplementary Figure 5.6 p-value matrices corresponding to Figure 5.8 . Green represents significance.	128
Supplementary Figure 5.7 p-value matrices corresponding to Figure 5.9 . Green represents significance.	129
Supplementary Figure 5.8 p-value matrices corresponding to Figure 5.10 . Green represents significance.	130
Supplementary Movie 5.1 Representative movie of the analysis of a cystic cluster beating irregularly	121
Supplementary Movie 5.2 Representative movies of beating clusters in each condition	121
Supplementary Movie 5.3 Representative movies of circular beating	121
Supplementary Movie 6.1 Engineered Cardiac Bands, spontaneously beating on PAA substrates of variable stiffness	165
Supplementary Movie 6.2 Ultrasound imaging of a beating fibrin patch with 2 layers of cardiac bands	165
Supplementary Movie 6.3 Fibrin patch with 2 layers of cardiac bands, right after fibrin polymerization	165
Supplementary Movie 6.4 Shear Wave Elastography of free standing, clustered cardiac bands....	165

List of Tables

Table 3.1 Summary of major steps to be taken into account before submission to the Regulatory Authorities	54
Table 3.2 Main regulatory requirements for autologous and allogeneic cells.	56
Table 3.3 Major properties of cells that need to be characterized prior to a clinical use.....	57
Table 3.4 Main regulatory requirements for biomaterials alone or associated with cells (combined product)	59
Table 4.1 Literature survey of the use of fibrin for cardiovascular applications.	71
Table 4.2 Handling of patches as a function of fibrinogen and thrombin concentrations.	82
Table 5.1 Number of coverslips available for PCR extraction	97
Table 5.2 Total number of cluster images for movie analysis	97
Table 5.3 Classification of genetic markers depending on developmental stage or major tissue of predilection	109
Table 6.1 Specification yields after culture on BJ's or FPBT's feeders.	139
Table 6.2 Specification yields after culture on BJ or FPBT feeders.	140
Table 6.3 Handling of patches as a function of fibrinogen, thrombin and alginate concentrations. ...	154
Table 6.4 Handling of patches as a function of fibrinogen, thrombin and hyaluronic acid concentrations.	154
Supplementary Table 5.1 Primer sequences for qPCR experiments	125

Chapter 1 – Introduction

Important Note: The rationale for the PhD studies presented in this chapter is partly described in French in the following article [1]:

Farouz Y, Chen Y, Menasché P, Ino J, Atlan M, Le Visage C, Letourneur D: **Réparer les cœurs brisés et les vaisseaux abîmés**. *Biofutur* 2012:1–4.

Cardiovascular diseases

Cardiovascular diseases (CVD) are the main cause of mortality worldwide with more than 17.3 million death per year [2]. Taking the example of the United States (US), there were about 800,000 deaths due to CVD in the year of 2011, compared to less than 600,000 for all cancers together [3]. Cardiovascular diseases are various and include myocardial infarction, dilated cardiomyopathy, valvular heart diseases, hypertension (Figure 1.1). Not only cardiovascular diseases are of prime importance because of their implied mortality, but also because of the cost they represent for the Healthcare system as well as because of the shortage in manpower it generates. In 2011, this cost was estimated to about \$320 billion in the US [3] and to about \$863 billion worldwide [2].

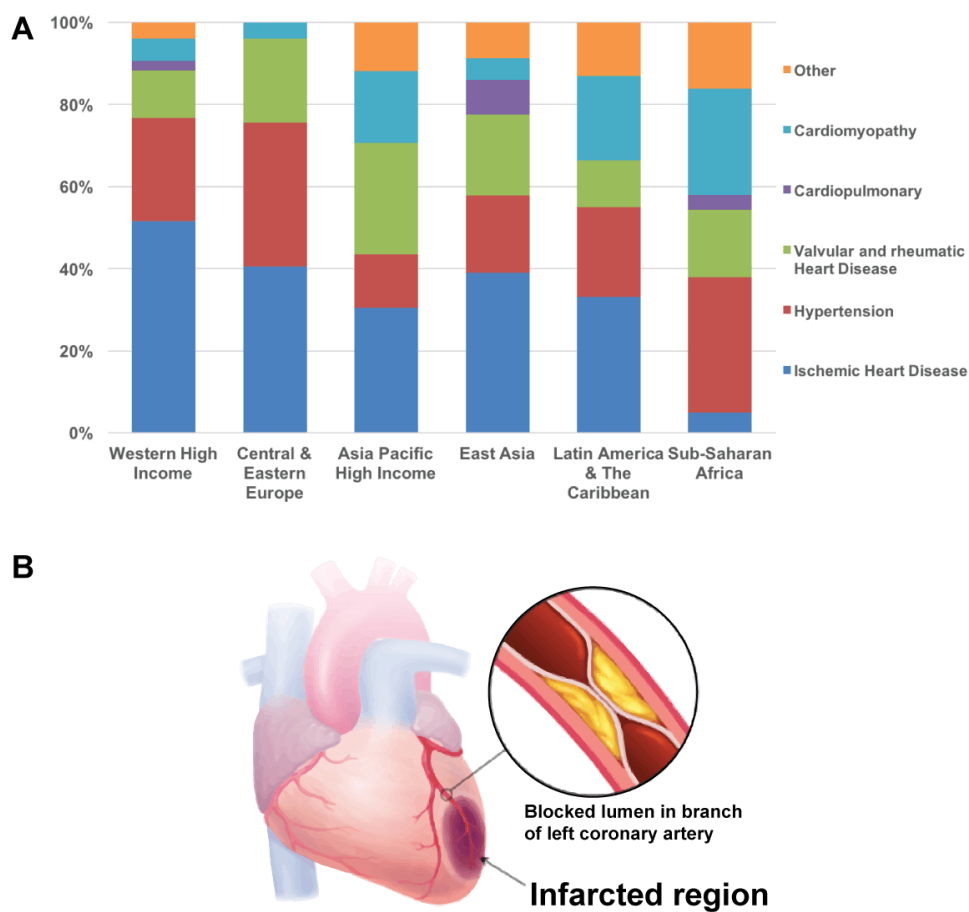


Figure 1.1 Ischemic heart disease is the major risk factor of heart failure in high income countries worldwide. (A) Age- and sex-adjusted relative contributions of different underlying risk factors of heart failure in six world regions (reproduced from [4]). (B) Schematic of the coronary occlusion leading to myocardial ischemia (adapted from NursingCrib.com).

One of the recurring consequences of such diseases is cardiac failure. Cardiac failure is defined as the inability of the heart to pump enough blood to the rest of the body, resulting in tiredness, coughing, water retention in lower limbs and dyspnea (shortness of breath). Once diagnosed, the 5-year survival rate from cardiac failure is only 50% [3]. There are many causes of cardiac failure, and their incidence strongly varies between countries. However, it appears

that cardiac failures usually results from ischemic heart diseases [4] (Figure 1.1-A), a problem caused by the obstruction of the coronary artery, leading to the death of the downstream cardiomyocytes that are no longer provided with nutrients and oxygen (Figure 1.1-B). Once these cells are dead, this part of the tissue cannot regenerate nor can it contract. Therefore, there is a tremendous loss in efficiency during heart contraction. In addition, scar tissue comprised mainly of collagen is formed in the infarcted area, resulting in increased stiffness and therefore, the healthy surrounding cells need to generate considerably more power to supply the body with blood. This increased activity leads to accelerated tiredness of the healthy cardiomyocyte, which eventually acquire an arrhythmogenic phenotype or even start to die.

Rationale of the ESCORT Clinical Trial

Many approaches have been considered in order to improve the function of the infarcted heart. Assisting devices can be implanted to stimulate cardiac pumping, but the best solution is still heart transplant, which is problematic due to the shortage of available hearts. Nowadays, cell therapy is considered as one of the most promising strategies to help regenerate the damaged heart. Indeed, replacing the dead cells with new cells would be a sustainable solution that corresponds best with physiological needs. Figure 1.2 shows a naïve representation of what could an ideal patch could look like in the close future, as imagine at the beginning of my PhD studies.

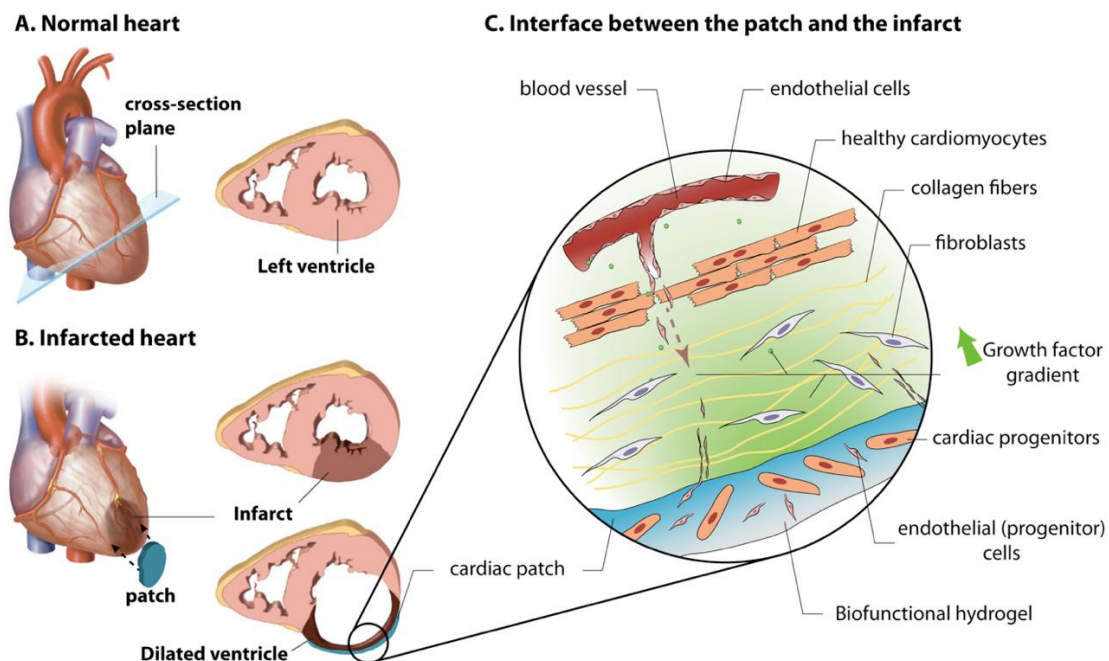


Figure 1.2 The ideal cardiac patch.

Global view and sections of a normal heart (A) and an infarcted heart (B) with the strategy for positioning the patch. The “ideal” patch (C) contains cardiac and endothelial progenitor cells. It delivers angiogenic factors and mechanically supports the dilating heart to ensure improved contractility, while waiting for grafted cells to have secreted their own extracellular matrix in the hope that they would replace the scar tissue made of stiff collagen and residual fibroblasts. Figure adapted from Th. Winslow’s artwork and Y. Farouz’ schematic published in [1].

Cell type

Many cell types have been considered as good candidates for the repopulation of the damaged heart. One would think that the best cells would be the exact same type as the ones that have died. This would include mainly cardiomyocytes, but also blood vessel cell types like endothelial cells or vascular smooth muscle cells. However, cardiomyocytes are very difficult to obtain because they can hardly be harvested from the patient's own body (and there would be a risk to get some damaged cells) and because they are already mature (meaning that they already established a well organized network of sarcomeres and formed gap junctions with their neighbors). Hence, it would be almost impossible to expand them and there would be a very low probability that they would be able to integrate in between the healthy cardiomyocytes of the patient's heart [5].

Another option is the use of myoblasts that can proliferate and then differentiate to form myotubes. These cells are interesting because, like cardiomyocytes, they become striated muscle cells. However, they lack of the ability to contract spontaneously and need an electrical stimulus in order to contract. This is not a problem a priori, but again their integration inside the already existing tissue is source of a lot of interrogations.

Therefore, recent studies have placed a lot of hopes in stem cells. Cells like mesenchymal stem cells or adipocyte-derived stem cells are not expected to replace the dead cells, thing that they can hardly do (although some laboratories claim they can) but instead would support the revascularization of the infarcted region by generating paracrine factors like VEGF, SDF-1 or PDGF. These growth factors will help the recruitment of new endothelial cells, smooth muscle cells and reduce apoptosis in the infarcted area [6, 7].

If adult stem cells can only act by paracrine stimulations, embryonic stem cells have a lot more potential, as they can actually differentiate into the three cardiac lineages: cardiomyocytes, endothelial cells and smooth muscle cells. The only concern when using embryonic stem cells would be their anarchical proliferation and their large panel of available commitments. To avoid these problems, we think the best solution is to differentiate these embryonic stem cells into cardiovascular progenitors (**Figure 1.3**), a type of cell that can only differentiate into one of the three cardiac cell types [8]. This early commitment decreases their proliferative capabilities, yet maintains their plasticity. It is this characteristic that we are looking for when considering the integration of the cells inside the host's tissue.

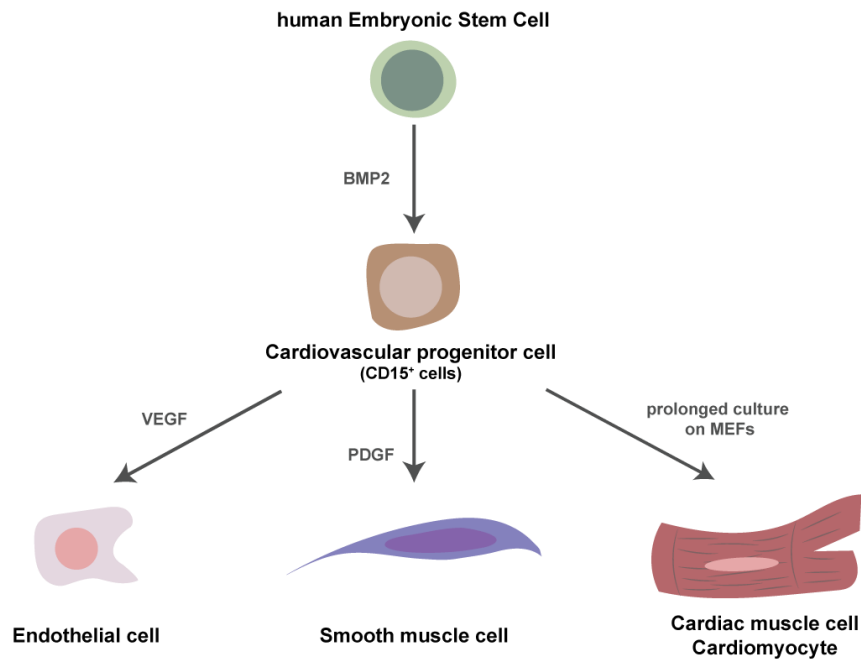


Figure 1.3 Short summary of the differentiation protocol from hESCs to cardiovascular progenitor cells as patented and published by Blin et al. [9]

Scaffold type

Clinical trials and other pre-clinical studies did not really meet the expectations mentioned above. Indeed, even though slight improvements in cardiac function were observed in terms of wall thickness, ejection fraction during the cardiac cycle, or in term of revascularization of the infarcted area, very low cell viability has been observed, as well as a very low retention of the cells inside the myocardium.

To address this problem, several teams including ours are designing new biomaterials to act as a vehicle for cell delivery and retention in the infarcted area [10, 11]. The ideal scaffold will be the one that would allow the cells to attach and maybe proliferate inside the patch, allowing them to generate a new extracellular matrix around them while the biomaterial is degrading or resorbing.

Rationale

Different cell types require different environments in order to develop appropriately and form a functional tissue. We want to start from human embryonic stem cells (Figure 1.4, step 1), to drive them to differentiate into cardiac progenitors (Figure 1.4, step 2), then we want to incorporate them in a scaffold (Figure 1.4, step 3) that would be grafted onto the myocardium (Figure 1.4, step 4) in order for them to integrate with the patient's tissue (Figure 1.4, step 5), forming new vessels as well as new contractile units. In each step of the project, different mechanical properties of materials are important, such as the elasticity for the stem cell differentiation, or the rate of degradability once the patch is inside the body. Also, mechanical stability has to be taken into consideration for surgical reasons, as a good patch will not only

be a patch that provides a physiological environment, but it will be a patch that would be easily manipulated inside the operating theater.

Furthermore, as cells change their phenotype about twice (from embryonic stem cells to cardiac progenitors to cardiac cells, see [Figure 1.3](#)), different environments need to be provided for each of these phenotypes. **Defining more clearly these two environments is the global aim of my PhD projects.**

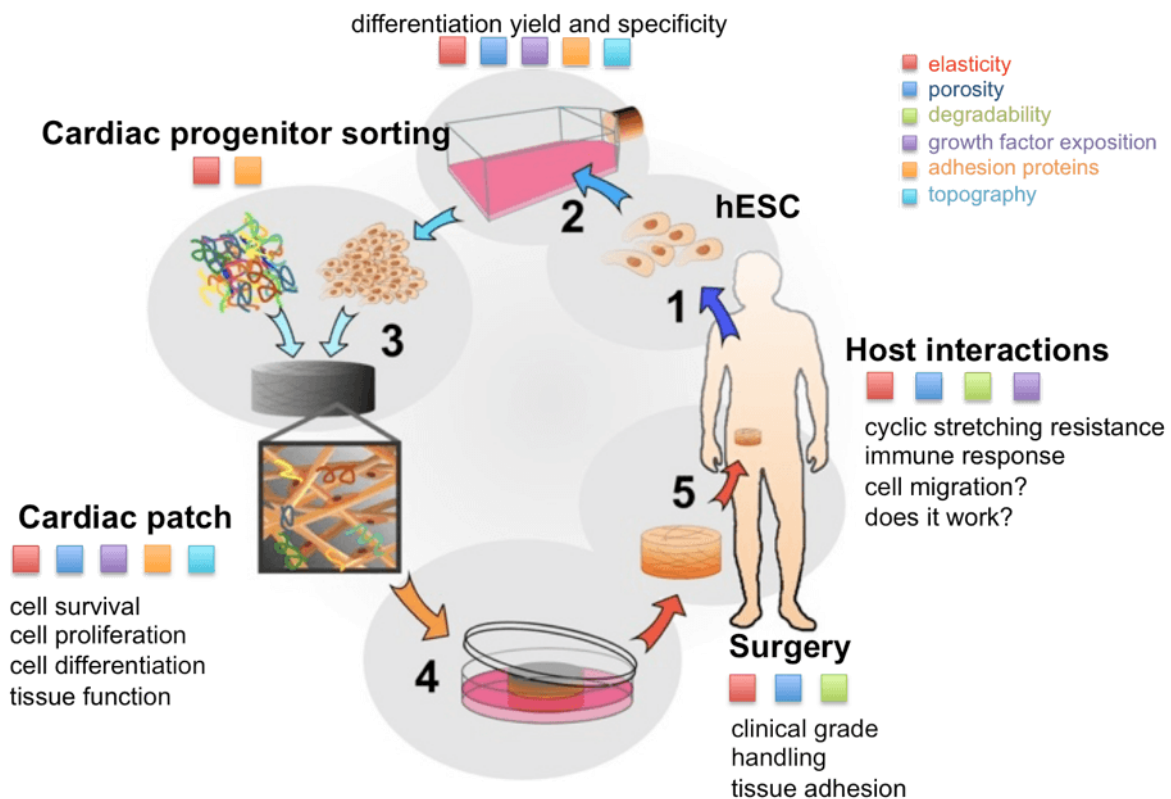


Figure 1.4 The importance of scaffold parameters at every step of the fabrication process. [Main image adapted from Julian George's PhD thesis]

Although differentiation has been deeply investigated by the use of developmental factors to induce cell maturation, it has been recently demonstrated that other properties like matrix elasticity, composition and structuration are of prime importance in the differentiation process. Culturing mesenchymal stem cells on surfaces with low stiffness (<1 kPa) led to their differentiation into neuron like cells, while increasing the stiffness led to their differentiation into skin cells (1 kPa), muscle cells (10 kPa) or bone cells (~100 kPa) [12]. Other independent studies showed that culturing embryonic cells on surfaces that were patterned with lines led to the formation of mature cardiomyocytes (see next chapter). Indeed, these cardiomyocytes formed anisotropic sarcomeres and formed gap junctions in order to maintain electrical coupling along the tissue [13-15]. Some studies also report variations in phenotypes

depending on the type of extracellular matrix protein the cells were seeded on. For instance, mimicking peptides like RGD (present in fibronectin or collagen, for instance) or YISGR (present in laminin) do not allow cells to form mature sarcomeric structures [16, 17].

As shown in [Figure 1.4](#), the next step toward the fabrication of a cardiac patch is the sorting of the cells. Sorting is a step that usually takes advantage of the differential affinity of cells for different adhesion proteins or substrates. The current technique is magnet-assisted cell sorting where antibodies are attached to magnetic beads. These antibodies are selective to the cell type we want to select or exclude. The current issues lie in the fact that we currently need to do positive sorting, meaning that the cells linked to the beads are the cells of interest. These beads, if not removed, can interfere with the good behavior of cells once inside the patch and then in the body.

The next step is the incorporation of the cells inside a patch. Again, many approaches have been considered. Patches can be made in two dimensions, where cells are seeded on top of the film. This method is very attractive because cells have been extensively studied in two-dimension and we know very well how to control their organization [18-20]. Also, it has the advantage of putting the cells directly in contact first with the culture medium and second with the host tissue. However, although we do not exclude such a strategy in the future, there are currently some clinical hurdles that would need to be overcome. First, having cells on a surface makes the patch handling much more complicated: the surgeon has to be very careful not to scratch the cells away, making sure that the right side is put in contact with the tissue. Second, the quantity of cells that we can seed on a surface is much lower than in a 3D gels, even though stacking 2D layers of cells is still an option to keep in mind.

In order to compensate for the cell mortality during the surgery, it is interesting to incorporate the cells in a three-dimensional matrix. It mimics better the natural cell environment, ease the manipulation of such a patch and increase the number of cells that can be delivered. However, it can be difficult to control the anisotropy and the porosity of the matrix and ensure its mechanical stability at the same time.

We plan on varying the composition of the fibrin precursors to alter the porosity of the fibrin gel, as well as to ensure good cell viability and manipulability. An important point will be the thickness of the construct, which will have to allow nutrients and oxygen to diffuse inside the patch.

Presentation of the thesis project

As described here, the physical characteristics of the biomaterial, like its elasticity, porosity, degradability, the biochemical characteristics of the biomaterial, like its growth factor composition, its adhesion proteins and their distribution, have a dramatic influence on the cell behavior, and this influence depends strongly on the cell type. The two main steps in this big project starting from hES culture and ending in the operating theater will therefore be investigated by taking into accounts these many parameters, but with very distinct points of view. First, we describe what is known regarding differentiation of stem cell into cardiomyocytes and how physical constraints play a role in it (Chapter 2). Second, we draw a picture of the practical challenges that arise when trying to translate biomaterials based stem cell therapies to the clinics (Chapter 3). From these observations, we came to the conclusion that the most urgent would be to make sure that hESC are a viable choice and thus, we focused on the fabrication of a patch made out of clinical components only. The cardiac patch had to be optimized with regards to clinical constraints in order to quickly receive an approval from the regulatory agencies to start clinical trials and get a first feedback from human patients (Chapter 4). Next, we take a step back and investigate how we could improve cardiac differentiation and finely control their final phenotype. Pluripotent stem cells will be studied with a rigorous set of conditions to determine the best microenvironment for their differentiation into cardiac progenitors (Chapter 5). Before taking another step back to look at the big picture of what we have achieved and what remains to do (Chapter 7), we propose strategies to design new ways to bridge the gap between cell culture and patch fabrication by taking advantage of the preferential adhesion of the cells onto ECM proteins, and we propose new blends of clinical materials that would allow modulating their mechanical properties while keeping their potential for fast clinical translation (Chapter 6).

References

1. Farouz Y, Chen Y, Menasché P, Ino J, Atlan M, Le Visage C, Letourneur D: **[Mending broken hearts and repairing damaged vessels] (French title: Réparer les cœurs brisés et les vaisseaux abîmés)**. *Biofutur* 2012:1–4.
2. Alwan A, Armstrong T, Bettcher D, Branca F: **Global Status Report on Noncommunicable Diseases 2010: Description of the Global Burden of NCDs, Their Risk Factors and Determinants**. World Health Organization; 2011.
3. Mozaffarian D, Benjamin EJ, Go AS, Arnett DK, Blaha MJ, Cushman M, de Ferranti S, Després J-P, Fullerton HJ, Howard VJ, Huffman MD, Judd SE, Kissela BM, Lackland DT, Lichtman JH, Lisabeth LD, Liu S, Mackey RH, Matchar DB, McGuire DK, Mohler ER, Moy CS, Muntner P, Mussolino ME, Nasir K, Neumar RW, Nichol G, Palaniappan L, Pandey DK, Reeves MJ, et al.: **Heart disease and stroke statistics–2015 update: a report from the American Heart Association**. *Circulation* 2015, **131**:e29–322.
4. Khatibzadeh S, Farzadfar F, Oliver J, Ezzati M, Moran A: **Worldwide risk factors for heart failure: A systematic review and pooled analysis**. *International Journal of Cardiology* 2013, **168**:1186–1194.
5. Ghafar-Zadeh E, Waldeisen JR, Lee LP: **Engineered approaches to the stem cell microenvironment for cardiac tissue regeneration**. *Lab Chip* 2011, **11**:3031–3048.
6. HAO X, Silva EA, MANSSONBROBERG A, GRINNEMO K, SIDDIQUI A, DELLGREN G, WARDELL E, BRODIN L, Mooney DJ, SYLVEN C: **Angiogenic effects of sequential release of VEGF-A165 and PDGF-BB with alginate hydrogels after myocardial infarction**. *Cardiovascular Research* 2007, **75**:178–185.
7. Yu J, Du KT, Fang Q, Gu Y, Mihardja SS: **The use of human mesenchymal stem cells encapsulated in RGD modified alginate microspheres in the repair of myocardial infarction in the rat**. *Biomaterials* 2010.
8. Blin G, Nury D, Stefanovic S, Neri T, Guillevic O, Brinon B, Bellamy V, Rücker-Martin C, Barbry P, Bel A, Bruneval P, Cowan C, Pouly J, Mitalipov S, Gouadon E, Binder P, Hagège A, Desnos M, Renaud J-F, Menasché P, Pucéat M: **A purified population of multipotent cardiovascular progenitors derived from primate pluripotent stem cells engrafts in postmyocardial infarcted nonhuman primates**. *J Clin Invest* 2010, **120**:1125–1139.
9. Blin G, Nury D, Stefanovic S, Neri T, Guillevic O, Brinon B, Bellamy V, Rücker-Martin C, Barbry P, Bel A, Bruneval P, Cowan C, Pouly J, Mitalipov S, Gouadon E, Binder P, Hagège A, Desnos M, Renaud J-F, Menasché P, Pucéat M: **A purified population of multipotent cardiovascular progenitors derived from primate pluripotent stem cells engrafts in postmyocardial infarcted nonhuman primates**. *J Clin Invest* 2010, **120**:1125–1139.
10. Hamdi H, Planat-Benard V, Bel A, Puymirat E, Geha R, Pidial L, Nematalla H, Bellamy V, Bouaziz P, Peyrard S, Casteilla L, Bruneval P, Hagège AA, Agbulut O, Menasché P: **Epicardial adipose stem cell sheets results in greater post-infarction survival than intramyocardial injections**. *Cardiovascular Research* 2011, **91**:483–491.
11. Le Visage C, Gournay O, Benguirat N, Hamidi S, Chaussumier L, Mougénot N, Flanders JA, Isnard R, Michel J-B, Hatem S: **Mesenchymal stem cell delivery into rat infarcted myocardium using a porous polysaccharide-based scaffold: a quantitative comparison with endocardial injection**. *Tissue Engineering : Part A* 2011, **18**:35–44.
12. Engler AJ, Sen S, Sweeney HL, Discher DE: **Matrix elasticity directs stem cell lineage specification**. *Cell* 2006, **126**:677–689.
13. Parker KK, Tan J, Chen CS, Tung L: **Myofibrillar architecture in engineered cardiac myocytes**. *Circulation Research* 2008, **103**:340–342.

14. Alford PW, Feinberg AW, Sheehy SP, Parker KK: **Biohybrid thin films for measuring contractility in engineered cardiovascular muscle.** *Biomaterials* 2010, **31**:3613–3621.
15. Kim D-H, Lipke EA, Kim P, Cheong R, Thompson S, Delannoy M, Suh K-Y, Tung L, Levchenko A: **Nanoscale cues regulate the structure and function of macroscopic cardiac tissue constructs.** *PNAS* 2010, **107**:565–570.
16. Shachar M, Tsur-Gang O, Dvir T, Leor J, Cohen S: **The effect of immobilized RGD peptide in alginate scaffolds on cardiac tissue engineering.** *Acta Biomaterialia* 2011, **7**:152–162.
17. Boateng SY: **RGD and YIGSR synthetic peptides facilitate identical cellular adhesion as laminin and fibronectin but alter the physiology of neonatal cardiac myocytes.** *AJP: Cell Physiology* 2004.
18. Takahashi H, Nakayama M, Shimizu T, Yamato M, Okano T: **Anisotropic cell sheets for constructing three-dimensional tissue with well-organized cell orientation.** *Biomaterials* 2011, **32**:8830–8838.
19. Williams C, Tsuda Y, Isenberg BC, Yamato M, Shimizu T, Okano T, Wong JY: **Aligned Cell Sheets Grown on Thermo-Responsive Substrates with Microcontact Printed Protein Patterns.** *Adv Mater* 2009, **21**:2161–2164.
20. Masuda S, Shimizu T, Yamato M, Okano T: **Cell sheet engineering for heart tissue repair.** *Advanced Drug Delivery Reviews* 2007, **60**:1–9.

Chapter 2 – On the design of biomimetic materials for cardiac stem cell differentiation

Important Note: Most of the content of this chapter has been published in Stem Cells in 2015 [1]: Farouz Y, Chen Y, Terzic A, Menasché P: **Concise review: growing hearts in the right place: on the design of biomimetic materials for cardiac stem cell differentiation.** *Stem Cells* 2015, **33**:1021–1035.

Abstract

Tissue engineering aims at recapitulating permissive conditions that enable cells to collaborate and form functional tissues. Applications range from human tissue modeling for diagnostic purposes to therapeutic solutions in regenerative medicine and surgery. Across this spectrum, human stem cells are the active ingredient, expandable virtually indefinitely and with the propensity to generate new tissue. Engaging lineage-specific differentiation requires a precise concerto of key spatial and temporal factors, such as soluble molecules and growth factors, but also physical and mechanical stimuli. These stimuli compete to modulate distinct developmental signaling pathways and ultimately affect the differentiation efficiency. The heart is a chemo-mechano-electrical biological system that behaves as both a sensor and an actuator. It can transduce electrical inputs to generate mechanical contraction and electrical wave propagation. Such a complex organ arises from multipart developmental events that interact with one another to self-regulate. Here, we overview the main events of heart development and the role of mechanical forces in modifying the microenvironment of the progenitor cells. We analyze the cascades regulating cardiac gene activation to illustrate how mechanotransduction is already involved in the most popular protocols for stem cell differentiation (SCD) into cardiomyocytes. We then review how forces are transmitted to embryonic stem cells (ESC) by cell-substrate or cell-cell communications, and how biomaterials can be designed to mimic these interactions and help reproduce key features of the developmental milieu. Putting this back in a clinical perspective, many challenges need to be overcome before biomaterials-based SCD protocols can be scaled up and marketed.

Introduction

Rationale for cardiomyocyte production

Beyond chemical signaling, mediated by soluble growth factors, providing the foundation for SCD protocols [2], there is growing evidence that environmental cues are also of prime importance in guiding differentiation events [3]. Indeed, it appears that the whole stem cell niche is important in determining cell fate. In addition to chemical factors (including transcription factors and other proteins), oxygenation [4], extracellular matrix (ECM) proteins [5-8], innervation, support cells [9, 10] and mechanical loading [11] are some of the key parameters that have been identified. In the heart, cardiac cells form anisotropic layers able to contract in response to electrical signals. Therefore, mechanical properties are thought to contribute to differentiation and further maturation during embryogenesis. Here we focus on the impact of the mechanical and topographical properties of materials used for cell culture on the differentiation of stem cells into cardiomyocytes. Adequate differentiation of stem cells into cardiomyocytes has significant medical applications offering the aptitude to recreate cardiac-like tissue for patient-specific *in vitro* drug toxicity assays [12, 13] as well as designing cell-based therapies for treatment of cardiac diseases [14-16]. Indeed, hopes were reinforced after historical observations on the benefits of human embryonic stem cell-derived cardiomyocytes (hESC-CM) on infarcted rat hearts [17] have been recently extended to non-human primate hearts [18, 19].

Mechanical forces during cardiac development, systems biology and the main cardiac differentiation protocols

With the formation of the four-chambered heart, the cellular arrangement of cells highly evolves from a cardiac crescent to a cardiac tube, followed by two looping events, the formation of the four chambers and finally septation (**Figure 2.1-A**). During these steps, differential growth occurs as well as increased blood flow and the initiation of electrical signals. Hence, cells are stretched, sheared, thereby resulting in different cell phenotypes at different stages of development [20, 21].

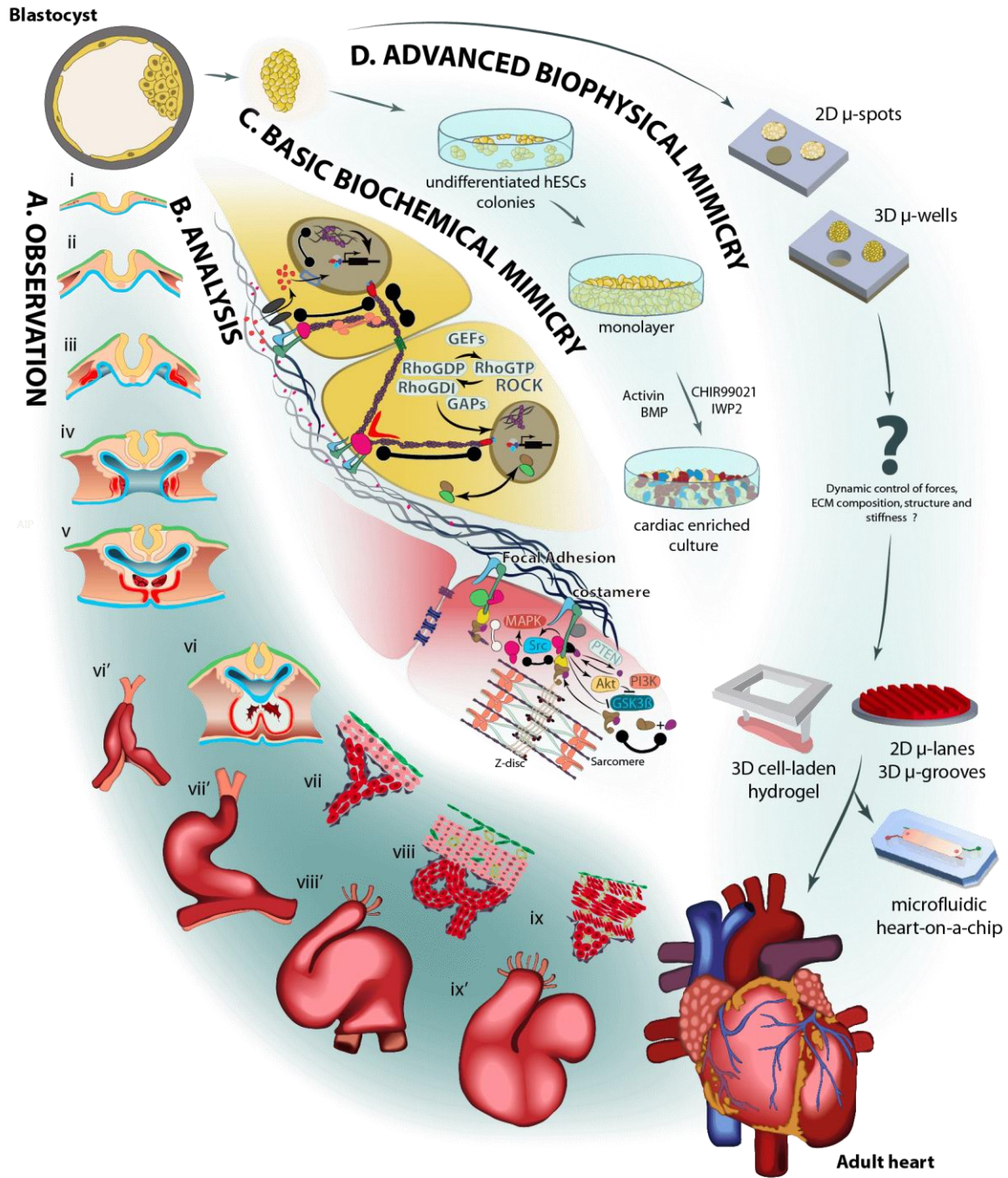
However, *in vitro* SCD is often realized only by activating signaling cascades mimicking the way they are activated during embryogenesis. This is achieved by using transcription factors [2], small molecules [2], or miRNAs [22, 23], often identified from high-throughput screenings [24-27].

The most used protocols involve modulation of developmental signaling pathway such as the canonical Wnt pathway [26, 28-32], the Wnt/PCP (non-canonical) pathway [33-36], TGF- β and

BMP pathways [37-40], and all their combinations [41]. These protocols are increasingly efficient and simpler than the original ones [42], and while the first versions relied on reagents that were either difficult to translate to the clinics or simply too expensive, a lot of effort is now made in order to create the simplest cocktails possible [43].

Figure 2.1 General strategy for differentiating PSCs into cardiomyocytes.

- A. **Observation** of the heart's developmental stages. After gastrulation and somite formation (i), the foregut arise and folding brings the two branches of splanchnic mesoderm together (ii-iv) before eventually merging (v) and forming the heart tube (vi, vi'). Cardiomyocytes are already beating and further differentiating but some keep proliferating (vii), cause the tube to start its C-loop (vii'). The S-loop (viii') causes the cardiomyocytes to stretch even more (viii) and when the four chambers are finally formed (ix'), they almost completed their elongation and differentiation (ix)
- B. **Analysis** of the relationships between external mechanical forces and gene expression. Although the main principles are similar, ESCs (top) and cardiomyocytes (bottom) have different mechanosensing architectures. ESCs connect together using E-cadherins and form round shaped colonies (cortical actomyosin network), while cardiomyocytes connect through N-cadherins, establish gap junctions for electrical signal transmission and express an important set of proteins for crystallization of actomyosin into highly anisotropic sarcomeric structures. Connections to the extracellular matrix are regulated via chemical (angiotensin II) or mechanical stimuli. Along with differentiation, tissues secrete different kind of ECM protein. For instance, the heart as a higher fibronectin:laminin ratio than the blastocyst.
- C. **Basic biochemical mimicry** can be achieved by culturing ESCs on petri dishes coated with ECM mixtures or mimics. Using sequential addition of cocktails of growth factors and/or small molecules, developmental signaling pathways are triggered and ESCs are directed toward cardiomyocyte differentiation.
- D. **Advanced biophysical mimicry** emerges through microfabrication techniques. 2D or 3D patterning of circular shapes allow for mimicking of the blastocyst structure (top) while patterning of lanes allow for mimicking aligned cardiac tissues (bottom).



Key

Ectoderm	Endothelial cells	Morphogenes	Actin	Integrin	FAK	Extracellular Matrix (±balanced Fibronectin:Laminin ratio)
Neural fold	Endocardiac cells	Nesprin	CAPZ	Talin	Paxillin	Extracellular Matrix (high Fibronectin:Laminin ratio)
Developing heart	Epicardiac cells	Filamin	α-Actinin	Melusin	ILK	Gap junctions (Cx43)
Pericardial coelom	Proliferating cardiomyocytes	Mechanosensitive ion channel	Myosin	p13	E-cadherin	N-cadherin
Mesoderm	Nuclear pore	Phospholipase	Titin	Vinculin		
Foregut	Differentiating cardiomyocyte	T-cap				
Endoderm						

While the two main pathways used in *in vitro* cardiac differentiation are the Wnt/ β -catenin pathway and the BMP pathway, it is becoming clearer that the common denominators are mechanosensing and calcium signaling (**Figure 2.2**). The Wnt/PCP pathway is responsible for convergence/extension of the gastrulating embryo [44-46] while the BMP pathway and smad genes activation is promoted by membrane mechanosensors [47] as well as calcium signaling [48]. Calcium is also responsible for stabilization of cell-cell interactions through N-cadherin [49]. As N-cadherins are ultimately coupled to β -catenin [50-52] and α -catenin, overpresence of N-cadherin contacts at the membrane can trigger overactivation of N-cadherin as well as inhibition of β -catenin translocation in the nucleus, which is equivalent to Wnt/ β -catenin inhibition or GSK3B overactivation [35, 53]. Another example of the importance of forces and calcium signaling is the establishment of the Left/Right axis, which precedes cardiac looping. Combining two models, it is thought that a right-to-left shear flow induces the generation of a gradient of growth factors, but also induces the bending of the primary cilia. Bending of the primary cilia will lead to the increase in calcium on the left side, cooperating with Nodal and BMP signaling to activate Pitx2 and trigger cardiac looping [21, 54, 55]. Finally, calcium is also one of the main actors of cardiac contraction, reestablishing the link between mechanical forces and calcium signaling (**Figure 2.1-B**).

Of importance, the Hippo pathway has also been found to be involved in cardiogenesis through the YAP/TAZ molecules [56], already known to act as mechanical transducers in tissue-growth servo-regulation pathways [57, 58]. Similarly, myocardial differentiation was observed by GSK3 β activation (i.e. Wnt/ β -Catenin inhibition) in a signaling cascade involving the insulin-like growth factor pathways, under control of the YAP/TAZ pathway [59]. This is no longer surprising under the light of a study by Azzolin et al., where Wnt inhibition is reinforced by the presence of YAP/TAZ in the beta-catenin destruction complex, while Wnt activation triggers both YAP/TAZ and beta-catenin release and nuclear translocation, a phenomenon responsible for the inhibition of mesendodermal differentiation[60]. More details on the relationship between Hippo, Wnt and stem cell differentiation can be found in recent reviews by Hao et al. and Varelas et al. [61, 62]. As further discussed later in this review, both the topography and the elasticity of the substrate influenced the fate of adult cardiac progenitor cells (CPC) through a YAP/TAZ-dependent mechanism [63]. Signaling studies on the relationship between the Hippo pathway, mechanotransduction and cardiogenesis have not been translated to efficient SCD protocols yet, but increased evidence of their intricate relationships can be found in other models, like for MSC differentiation [64] or neuronal differentiation from iPSCs [65].

In this review, we highlight the mechanotransduction effects in a hierarchical fashion, first by defining briefly how cells can sense forces, and then, zooming out on the physical forces generated by the cell-matrix interactions, the cell-cell interactions, aggregate mechanics, tissue mechanics and finally the heart development itself. At each scale, we will summarize current knowledge regarding the biophysics of development and maturation of cardiomyocytes, and which techniques are available to recapitulate these environmental properties in a modular bottom-up fashion.

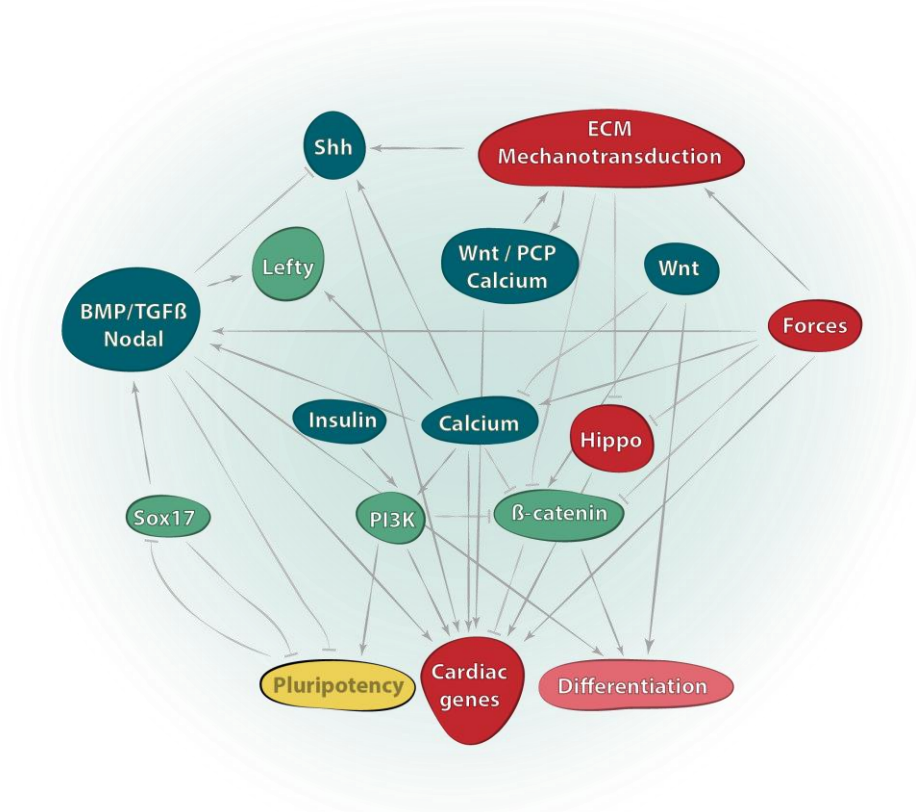


Figure 2.2 Important players involved in conventional cardiac differentiation protocols, and their interactions with physical factors (not published).

Debate 1: Murine vs. Human cells

Differentiation studies using murine models are very important in the field of developmental biology. Like other model species (the fruit fly, the xenopus or the zebra fish), they allowed identifying the main regulatory pathways that control embryonic development, with regard to both biological and mechanical behaviors. However, major differences exist between murine and human pluripotent cells. While murine ESCs (mESCs) can be cultivated on gelatin-coated petri dishes with the only addition of LIF (Leukemia Inhibitory Factor), human ESCs (hESCs) need a far more complex ECM coating (fibroblast feeder layer, Matrigel or vitronectin for non cellular materials). Another distinction is the timing of development and of expression of

membrane proteins. For instance, while induction of mesendodermal differentiation of mESC by BMP2 leads to CD15 negative cells, the same protocol on hESCs will give rise to a mesendodermal population of CD15 positive cells. Hence, the sorting will be reversed [18, 66].

Additionally, the beating rate of mature cardiomyocyte is completely different. While murine cells can be paced at more than 4Hz (240bpm), human cells prefer slower paces, of about 1-2Hz (60-120bpm). These interspecies differences thus need to be cautiously taken into consideration when trying to translate animal data into potential clinical applications. Still, in this review, many animal models will be referenced in an attempt to identify interesting mechanistic results or promising techniques that have not been translated to human cells yet.

Force transmission: Cell-Cell Interactions and Cell-ECM interactions

Interactions in the developing embryo

Before being able to adapt to different mechanical environments, cells need ways to sense the environment. Before compaction at the 8-cell stage, every single cell is only connected to its neighbor through cell-cell interactions, using proto E-cadherins and a few integrins [67, 68]. Upon cell compaction, cells increasingly express E-Cadherins and start secreting other types of cadherins [69], which can be seen as the first differentiation step before implantation of the embryo in utero, as cells self-sort by cadherin-type affinity. Later, cells start to secrete more and more ECM components, like collagen, vitronectin, tenascin, elastin, fibronectin, hyaluronic acid (HA) or laminin [70]. Cells then bind to these components through different mechanisms, for example by creating focal adhesion complexes through RGD-integrin interactions, or by other specific receptors (like CD44 for HA) [71].

By the end of development, cells can sense external forces either through cell-cell interactions, cell-ECM interactions, mechanosensitive ion channels or by directly sensing the force by wave propagation throughout the cell and toward the nucleus [71]. Hence, in order to manipulate the stem cell niche, the surface chemistry at the interface between the cell and the materials must reflect the integration of all the coupled mechanical signals before it reaches the cell membrane. Although not clearly demonstrated in the literature, one can think that if ECM proteins are too weakly bound to the materials, cells will not be able to generate the same amount of force, in similar ways as if it was linked to a soft material. Cells would then behave as if in suspension. Also, if ECM proteins are not abundant enough, integrin clusters and focal adhesions would be insufficient to form as efficiently as in a physiological context [72].

Cadherins and integrins are both linked to the cytosolic network of actomyosin. When the tension of this network is changed, a signaling cascade occurs, involving the Rho pathway, directly deforming the nucleus. These signals are then integrated within the nucleus leading to a differential gene expression and thus activating or repressing various developmental pathways [73, 74] (Figure 2.1-B).

Strategies for mimicking cell-cell communication and cell-ECM coupling

Providing cell-cell communication capabilities and cell-ECM coupling was the first strategy stem cell researchers have employed. In contrast to mESCs, one of the first attempts to culture what we call now hESCs showed that regular petri-dish treatments for cell adhesion allowed expansion but triggered spontaneous differentiation as early as the second passage [75]. These dishes are made adherent by exhibiting positively charged functional groups. Although cells can form adhesions, they do not recapitulate the signals given by different ECM components during embryogenesis. Additionally, the high brand-variability in terms of nanotopography and surface charge can have dramatic effects on cell behavior [76]. Because of their electrostatic properties, most of the ECM proteins can be adsorbed on the surface of tissue-culture-treated plates. Thomson et al. in 1998 [77], followed by Reubinoff et al. in 2000 [78], were the first to demonstrate that hESCs could be cultured for months provided that they were co-cultured on a layer of feeder cells. Later, feeder-free conditions were introduced by just coating a mixture of ECM proteins (Matrigel), or laminin on the surface of a petri dish [67] (Figure 2.1-C, top). However, it has been observed that ESCs behaved differently depending on the coating protein: vitronectin would enhance self-renewal and proliferation of pluripotent stem cells (PSC) while fibronectin, collagen IV or laminin would drive more easily the differentiation of the cells towards various lineages. In addition to ECM proteins, the use of recombinant cadherin coating to mimic cell-cell interactions occurring between feeders and ESCs has been reported [79].

Debate 2: Choice of the right ECM

The choice of the right ECM proteins for cardiac SCD is intricate. Different ECM proteins at different densities are present in cardiac tissues depending on the developmental stage [70]. Differentiating PSCs on Matrigel by an Activin A/BMP4 based protocol, Chan et al. observed *in vitro* time-dependent levels of HA and versican in the cell culture [5]. This evolving composition in ECM components not only affects the mechanical properties of the ECM but also many signaling cascades triggered by these two glycosaminoglycans (GAGs). Alternatively, Schenke-Layland et al. [80] made murine Embryonic Bodies (mEBs) on dishes either coated with collagen I, collagen IV, laminin or fibronectin, and evaluated mesodermal

and cardiovascular markers after culture in medium without any exogenous factor. They found that collagen IV induced significantly more mesendodermal cells (characterized by high Flk1 expression) than other ECM proteins. After sorting these precursors and seeding them again on the four coatings, cardiomyocytes appeared to be significantly more present on fibronectin-coated dishes. Also for mESC, Stary et al. reported that the protein SPARC acted in similar ways as BMP2 by increasing cardiomyogenesis in EB with clear upregulation of Nkx2.5 [81]. These studies highlight the fact that it might be questionable whether or not it is best to let the cells generate their own ECM components or designing biomaterials to use them as source polymers to control simultaneously stiffness dynamics and chemical signaling.

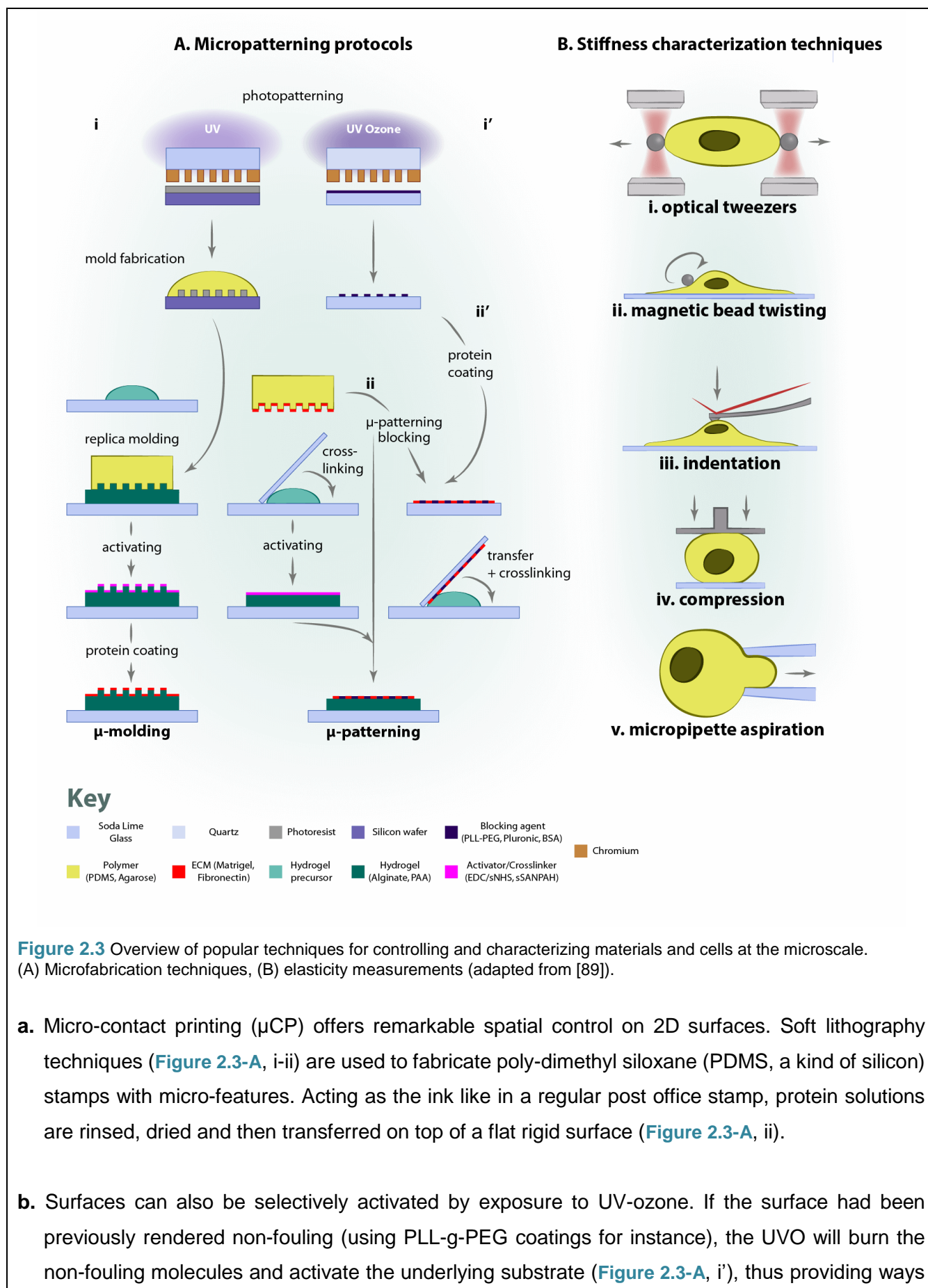
Influence of substrate topography

General overview

There is growing evidence that cell shape is an important parameter during heart development (Figure 2.1-A, vii-ix). Although cell proliferation may account for major mechanical events like asymmetric looping, it cannot explain the whole process, such as how the looping direction is controlled or why the growing four chambers are different from one another. Indeed, oriented growth may explain how any of the four chambers grow differently [82]. It has been reported that this kind of growth may be explained by mitotic spindle orientation [83], which can be directly correlated to cellular shape and more generally ECM distribution [84]. Another event, cardiac looping, is also highly influenced by the cell's geometrical shape. Studies in the chick have highlighted the fact that the cardiac tube starts looping not only by differential growth but mainly due to different morphologies of the cardiomyocytes at the outer curvature (elongated cells) as compared to the inner curvature (packed cuboidal cells) [85]. In the mature heart, cardiomyocytes are elongated and contract simultaneously in the direction of elongation. A specific aspect ratio has been correlated with healthy cardiomyocytes, and any variation to that aspect ratio may mimic features of the failing myocyte [86].

Technique Overview 1: Micro-patterning on flat hard substrates

There are multiple ways of controlling the distribution and topography of proteins on a substrate. Many of them have been adapted from Chen et al. first experiment of cell patterning [87] and rely on alternating regions of non-fouling coatings (or naturally non-fouling polymers), and ECM-like proteins. Consequently, cells cannot extend their focal adhesions beyond the regions coated with proteins:



to protein adsorption a posteriori (Figure 2.3-A, ii'). Bypassing the stamping step improves the resolution to sub-micrometer features and enables standard biology laboratories to develop micro-fabrication strategies without the need for dedicated nano-fabrication clean rooms [88]. Nevertheless, one of the limitations might be that UV-ozone lamps still are an important investment and still too few platforms for cell biology provide them.

Influence of topography on SCD into mesodermal progenitors and cardiomyocytes: the importance of colony size

The first step in deriving cardiomyocytes from ESCs *in vitro* is a step of specification. Like during embryogenesis, cells first differentiate into one of the three germ layers (namely ectoderm, mesoderm and endoderm, Figure 2.1-A, i). These three layers are more restricted in their fate and cardiomyocytes can only arise from mesodermal or mesendodermal cells. Peerani et al. showed that colony size mattered in driving this first specification [89]. They micro-contact printed Matrigel islands of varying diameters on glass coverslips and seeded them with ESCs without any exogenous inductive signals (Figure 2.1-D, top). By constraining the size of the aggregates, they showed that, after two days in culture, smaller aggregates (200µm in diameter) expressed more endodermal markers and had higher levels of BMP2 whereas bigger aggregates (1000-1200 µm in diameter) expressed more pluripotent markers. This was attributed to the modulation of the ratio of pSmad1 agonists over pSmad1 antagonists. Indeed, while pSmad1 antagonists increased with colony size, no correlation was found for pSmad1 agonists, thus leading to lower levels of agonists in smaller colonies when compared to pSmad1 antagonists. Later, they repeated the same experiment but adding Activin A and BMP2 in the culture medium to force mesendodermal differentiation [90]. This time, cells on smaller spots (200-400 µm in diameter) were found to express more endodermal markers (GSC, Sox17, Cer1) while bigger patterns (800-1200 µm) led to more mesodermal cells (T, KDR). To investigate further the hypothesis that colony size influences differentiation by changing cell number and thus local concentrations in proteins and chemical, they used micro-titer plates coated with Pluronic F-127 (a poloxamer used to create non-fouling regions on glass) to generate EBs by centrifugal aggregation [91, 92]. After sorting these cells for KDR, c-kit and cTnt (markers for early to late cardiomyocyte differentiation), they concluded that the largest number of cells was reached at an optimum of about 1000 cells per aggregate. Endodermal markers were predominantly found at the periphery of the aggregates, creating a higher ratio of endodermal cells over other cells for smaller aggregates (when calculating the surface:volume ratio).

Similar conclusions were drawn by Hwang et al. [93] after they cultured ESC on non-fouling micro-molded poly-ethylene glycol (PEG) wells of different diameter (from 150 to 450 µm).

Endothelial cells emerged from cells that had been cultured in small aggregates while cardiomyocytes emerged from cells cultured in bigger aggregates. Interestingly, they have been able to correlate these differences with modulation in Wnt5a and Wnt11, two important regulators of the non-canonical Wnt pathway.

Together, these four studies suggest that differential differentiation emerges from size-induced variations in the concentration of modulators of key signaling pathways involved in cardiogenesis (Nodal, BMP, Wnt). Although qualitatively consistent with each other, these studies were not performed with the same ranges of diameters, and in a similar experiment by Mohr et al., the greater relative number of cardiomyocytes was reached for 300 μm -diameter EBs [94].

An explanation could be that they neglected the impact of mechanotransduction. In these studies, radii of curvature are different depending on the spot size and therefore a surface tension emerges at the periphery of the colony whereas pressure is increasing inside the colony due to cell proliferation, as suggested by Nelson et al. [95]. Also, PEG microwells[93] might have been softer than gold-coated polystyrene wells [94].

At a completely different scale, Myers et al. compared six of the most popular differentiation protocols (all based on exogenous signals modulating either the BMP or the Wnt pathways) while constraining initial colony growth to 2-mm wide spots of Matrigel [96]. Clearly, micropatterning increased homogeneity in the yields of differentiation. Most importantly, this study highlighted the important discrepancies that can affect cardiac differentiation depending on the choice of the modulated pathway. Put together, these data emphasize the importance of controlling the size of cell aggregates to optimize the cardiomyocyte yield.

Influence of topography on sarcomere maturation and force generation of cardiomyocytes: the importance of anisotropy

Contact guidance and topographical effects on cardiomyocyte maturation has been studied in many ways. At the single cell level, *in vitro* studies on micropatterns [86, 97, 98] and *in silico* models of sarcomerogenesis [99] conducted by Parker's group suggested that a single cell will form more mature sarcomeres when its shape is constrained to a rectangle with an aspect ratio length:width of roughly 7:1. If the ratio is bigger, interdisc space will become bigger and cells will behave as a hypertrophied cardiomyocyte. If smaller (like in the case of circular patterns), sarcomeres will not be able to align in the same direction. They will be more randomly distributed within the cells, as characterized by orientation factors, and they will hence generate less force. At the multicellular level, they made the same observations regarding force generation (**Figure 2.1-D**, bottom). In this case, what mattered was less the aspect ratio than the elongated shape itself. If not all the cells were elongated in the same direction, the gap junctions were less well established and electromechanical coupling was

inefficient in the tissue. The force generated was then considerably smaller than for anisotropic tissues [100-102]. These results have also been confirmed in 3D collagen gels encapsulating neonatal rat cardiomyocytes (NRCMs) [103], thus confirming the importance of anisotropy itself. A recent study by Wang et al. highlights that in the case of ESC-derived cardiomyocytes (ESCd-CM), seeding cells on a topographically aligned substrate did not improve the maturation state of the cells. The improvements in term of electrical stability and reduction in induced reentrant arrhythmias were solely due to the spatial organization, as assessed by monophasic action potential measurements [104].

Technique Overview 2: Micro-patterning on soft materials and curable polymers

a. Stamps can be fabricated by soft lithography (for micrometer resolution) or by standard machining (micro-milling, 3D printer) for bigger features (**Figure 2.3-A, i**). Instead of transferring proteins, they can act as replica molds while a polymer or hydrogel polymerizes (**Figure 2.3-A, left**). Depending on the depth and spacing of the features, it provides the materials with quasi-2D microstructures (low spacing and height < 100 nm) or with real 3D-cues (larger spacing and height > 500 nm). Proteins are then coated uniformly, and thus cells will not constrain by adapting to changes in chemical signals, but by sensing local variations in topography [105]. If deep enough, these techniques can be adapted for miniaturization of culture wells for high-throughput screening on 3D aggregates [106, 107].

b. Coating proteins chemically on soft material is affected by the structural properties of the material itself, and protein surface density will vary as a function of local porosity. When using polyacrylamide (PAA), rather than using optochemical reactions to bind the proteins as in Engler et al. in 2006 [3], it has been recently suggested that simple transfer of proteins could be achieved by polymerizing a solution of acrylamide/bis-acrylamide sandwiched between a micropatterned surface and a glass coverslip [108] (**Figure 2.3-A right**), or simply using μ CP on polymerized PAA rendered adhesive with hydroxyl -OH groups [109] or with coupled streptavidin-acrylamide [110] (in this case, protein should be biotinylated prior to coating) (**Figure 2.3-A center**). Further studies are needed to confirm that these techniques overcome, as claimed, the artifact of the effect on cell mechanosensing of PAA's variation in porosity with regards to elasticity.

Many variations on this theme are proposed depending on the way the hydrogel of interest is polymerized, like photocuration for methacrylated or PEGDA-based hydrogels [111, 112]. Although many 3D-patterning techniques are emerging, their resolution still does not allow for single cell studies. We will briefly describe them in the *Debate 4*.

Anisotropy in early differentiation and isotropy in ESCd-CM studies

If many studies have shown similar results with NRCMs [113-119], ESCd-CMs [113, 118] or extracted CPCs [120], there is little evidence of any effect of anisotropy of the ECM proteins on earlier stages of mesodermal differentiation [121, 122]. It could be interesting to know at which stage of development cells are able to sense lines of proteins and start aligning. This switch could correspond to the loss or the gain of a phenotype, like, one might suggest, the vanishing of the primary cilium, an important mechanosensing feature involved in cardiogenesis [123]. Cardiomyocytes could also start aligning because fibroblasts first aligned and hence anisotropically secreted ECM proteins, driving the orientation of other cells [124-126]. Nevertheless, anisotropy is involved in many morphogenetic events and for instance, researchers recently reported that the culture of human PSCs (hPSCs) on nanogrooved surfaces led to rapid differentiation of the cells into neurons [127]. In a completely different approach, it was found that reprogramming of fibroblasts into induced PSCs (iPSCs) was enhanced on grooved substrates due to increased acetylation and methylation of histone H3 [128]. This phenomenon could imply that anisotropy would act as a global inducer of epigenetic modifications leading to increased genetic sensitivity to differentiation/reprogramming protocols.

As for culturing beating cardiomyocytes on circular spots, experiments reported above do not really encourage it in that it would rather mimic pathological behaviors than physiological ones. However, in light of the high-throughput drug-screening platform designed by Serena et al. [129], one can argue that circular micro-tissues of cardiomyocytes might still give precious information on the relative behavior of cells subjected to different kinds of drugs.

Influence of Tissue elasticity

General overview

As cells are differentiating, their phenotype considerably changes, i.e., not only their cytosolic composition is affected (resulting in a different stiffness by polymerization of the cytoskeleton), but their proliferation rate as well. Regions of differential growth can be observed, leading to different compressive or tensional forces applied to their neighbors. The composite material that is the cell environment considerably changes - the overall stiffness changes as well as the stretching forces. At the same time, cells are rearranged by affinity due to the different expression and amounts of cadherins. Mimicking these dynamic changes of highly non-linear materials is obviously very challenging but simple models of constant linear elasticity have shown important results on SCD.

Not only the cell-cell interactions but also the cell-ECM interactions play a large role in cardiac differentiation and maturation. Particularly, the cardiac jelly, which interfaces the endocardium and the myocardium, is composed of GAGs (such as HA), proteoglycans and proteins (such as fibronectin, collagen or laminin). Based on the properties of GAGs to osmotically attract water, the cardiac jelly acquires a compressive strength and the internal pressure it generates on the myofibrillar architecture of the myocardium is thought to drive cardiac chamber expansion [21].

Technique Overview 3: Measurement of tissues elasticity in the developing and adult muscle

In order to mimic the mechanical properties of cardiac tissues, it is important to be able to have precise measurements from tissue samples at different stages of the development. The difficulty relies on defining precisely the “substrate”: is the tissue in its whole, only the ECM or the ECM plus the support cells? And if we deplete the tissue from their cells, what are the effects of the decellularisation techniques on the mechanical properties of the tissue? Many laboratories have tried doing such measurements, either using Atomic Force Microscopy (AFM) or standard rheology or tensile/compression testing. Moreover, elastic anisotropy (different stiffness in orthogonal directions) has been identified for cardiac tissue but is rarely considered as a requirement for biomimetic cardiac constructs in the literature [130]. Furthermore, measuring the stiffness of a material will not mean much if the bonding force with the coated ECM protein is too weak [131].

In the field of tissue engineering, the measure most reported for characterization a material's elasticity is the Young's modulus. However, depending on the technique used, it can be indirectly derived from more or less complex mathematical extrapolations of other mechanical characteristics.

a. Nanoscale elasticity can be measured by magnetic/optical tweezers. Nanobeads are constrained in a magnetic field and attached to the material. The material is then pulled away from the beads and the force needed to maintain the bead inside the field is measured (Figure 2.3-B, i). Similar setups can use twisting of the beads to measure shear elasticity (Figure 2.3-B, ii).

b. Nanoscale and microscale elasticity can also be measured by AFM in contact mode (Figure 2.3-B, iii). The cantilever tip is modeled as a pyramidal or spherical tip in herzian contact with the material. Measuring the deformation upon nanoindentation is directly related to the Young's modulus and the Poisson ratio of the material.

c. Microscale elasticity of cells or materials can be measured by micrograph analysis of deformation upon an applied force. Cells and materials can be squished between plates (Figure 2.3-B, iv), or aspirated through micropipettes (Figure 2.3-B, v).

d. Mesoscale elasticity (cell aggregates, hydrogel microspheres) can be measured by micropipette aspiration (**Figure 2.3-B**, v) as well as microrheology. In microrheology, fluorescent nanobeads displaced inside the tissue or material are optically tracked and statistical analysis of their random motion can be related to a measure of elasticity.

e. Mesoscale indentation can also be performed with simple handmade setups by measuring the deformation of a weight or small tip on the material or by hooking a small weight under the material to measure the implied deformation.

f. Bulk elasticity of macroscale materials is often measured by standard mechanical engineering testing machine, like the Instron. It can be set to apply uniaxial or biaxial strain in tension or compression on the tissues.

Influence of elasticity on mesodermal SCD

In cardiac repair, it has initially been thought that the use of striated muscle, be it skeletal muscle or cardiac, would be sufficient for engraftment and contraction inside the infarcted heart. They have quite similar mechanical properties and one can think that the properties of the matrix will feature a roughly similar elasticity. When Engler and Discher first reported that matrix elasticity had a great influence on stem cell differentiation [3], they showed they had been able to make MSCs differentiate into myoblast-like cells on polyacrylamide gels of about 10 kPa in elasticity. From then on, material design studies for cardiac patches report measurements of the elastic properties of their materials in order to show that they closely match native heart muscle [105, 130, 132-135].

However, no strong evidence has been shown yet during the entire process of cardiac differentiation and experiments are often performed only after exposition to exogenous differentiation chemicals. Culturing pre-implantation stage embryos on 2D PDMS substrates of varying stiffness resulted in significantly greater frequency of development from the 2-cell stage to the hatching blastocyst stage, as compared to cultures in standard petri dishes [136]. Sun et al. linked higher levels of Oct4 expression to higher stiffness when seeding hESCs on 2D PDMS micropillars but did not really look at the whole panel of genes expressed by the three germ layers [137].

As explained in *Debate 1*, many differences can emerge when switching from a mouse model to human cells. But as importantly, researchers recently started to point out that the influence of elasticity on SCD varies depending on the dimensionality (2D or 3D) of the materials [138]. Indeed, the distribution of ECM cues are completely different and affect the response of the membrane receptors (integrins for instance). It has been reported that cells in 2D tend to form more stress fibers than in 3D, which could prevent cardiomyocytes from forming mature sarcomeres [139]. Also, if high stiffness allows cell to generate high traction forces in 2D, it is not true in 3D where high stiffness can prevent the cell from moving around

and force it to stay round. Interestingly, Zoldan et al. performed a strong investigation on the effect of elasticity on early specification in the three germ layers by encapsulating hESC into 3D polymers [140]. As suspected before, there is a strong correlation between the material's stiffness and germ layer differentiation. Surprisingly, the ranges of measured elasticity are several orders of magnitude higher than in the other studies afore-mentioned. Also, few details are given on the impact of the surface chemistry of the various polymers used in this study.

One study, nevertheless, has been able to correlate cardiac differentiation to matrix stiffness, through the regulation of YAP/TAZ expression [63]. Using Sca1+ adult CPCs seeded on polyacrylamide gels of controllable stiffness, the authors have showed that the control CPCs differentiated best into cardiomyocytes on gels of 10kPa in elasticity, while YAP-silenced CPCs would not differentiate at all into cardiomyocytes under the same conditions.

Influence of elasticity on cardiomyocyte sarcomere maturation

Sarcomere maturation is probably the most studied effect among mechanical properties. By isolating cardiac cells at different developmental stages of the mouse embryo, Engler et al. have been able to establish a relationship between the variation in elasticity and the developmental stage of the heart [132]. Interestingly, it has been shown that embryonic cardiomyocytes beat best on substrates where the rigidity matches the embryonic tissue rigidity. These cardiomyocytes were only able to form mature sarcomeres on PAA gels of about 10kPa. On softer gels, sarcomeres were less spaced and not fully organized whereas on stiffer gels, sarcomeres were not present at all and some sarcomeric proteins were completely diffuse in the cytoplasm. This result was also confirmed for NRCMs [141] as well as for ESCd-CMs [133, 142], although Hazeltine et al. found that the intermediate stiffness supporting best ESCd-CM differentiation from a progenitor stage would be around 50 kPa [142]. Previous studies on the differentiation of adipose stem cells into myotubes had already shown that pathological tissue stiffness led to reduced differentiation whereas tissue-like elasticity led to optimal maturation and striation formation of the myotubes [143].

Not surprisingly, it has been shown that depending on the type of extracellular element that was linked to the hydrogel, there could be different cellular responses to stiffness. Cardiomyocytes have been able to grow mature sarcomeres on HA-based gels of less than 500 Pa whereas it was only achieved at around 10 kPa with fibronectin-coated PAA gels [144]. This starts to show the limits of considering the Young's modulus as the principal mechanical parameter influencing cell phenotype. It is thought that the HA signaling cascade could bypass the mechanotransduction pathway and direct sarcomerogenesis. One explanation could be that in this case, HA does not convey its message through mechanical signaling but rather

through chemical interaction with the CD44 receptors [145]. However, it was also shown that the dynamic properties of HA gels are actually important in the cell response. Whereas PAA has a static elastic behavior, HA gels show time-dependent stiffening and thus can go from about 1 kPa to almost 10 kPa depending on its fabrication process [146]. This phenomenon was also observed in 3D fibrin cultures of myoblasts, where the fibrin gel, initially softer than 5kPa, exhibited a stiffness of 15 kPa after several days [138].

This highlights the fact that static mechanical signals alone cannot act as a replacement of chemical induction of differentiation. Both signals are complementary and will act synergistically in a time-dependent manner. Furthermore, the point of introducing mechanical compliance and mechanical stimuli in cell culture is to avoid mixed signals. As cells sense their mechanical environment, adding pro-myogenic soluble factors can be hindered by the pro-osteogenic mechanical signals of the rigid petri dish.

Debate 3: Elasticity vs. viscosity and porosity

If current techniques of microfabrication are increasingly simple, a few biases arise from the technique itself. Trappmann et al. recently suggested that depending on the polymer (they compared PAA and PDMS), the results shown initially by Engler and Discher could not be reproduced in the case of PDMS [131]. This could be explained by a difference in porosity and tethering of the ECM proteins to the synthetic polymer. Soft PAA gels (that led to neuronal differentiation) were highly porous and the ECM density at their surface was considerably lower than on stiffer gels, but these problems were not observed for PDMS, which has a more constant porosity. To further complexify this issue, a new study addressing the problem of porosity in soft polyacrylamide gels has refuted the hypothesis that tethering had biased the observation of differential fates depending on elasticity [147]. Yet, it is unclear whether tethering of ECM is the only source of this difference as very soft PDMS made out of big ratio of the PDMS base and curing agent can exhibit significant viscous behaviors. The balance between the viscous modulus and the elastic modulus of this kind of soft PDMS directly influenced the cell's migration properties [148]. Although other types of PDMS have been reported as good candidates for traction force studies in purely elastic conditions [149, 150], there is no doubt that further studies will underpin the importance of viscosity during guided differentiation of ESCs into cardiomyocytes.

Perspectives

Influence of Stretching and Shearing:

In addition to designing biomimetic materials for stem cell culture and differentiation, other mechanical stimuli can be dynamically applied to the cells. While shearing is considered to be of prime importance in vascular remodeling, cyclic stretching and static strains mimic more faithfully the mechanical behavior of muscle tissues. The effect of stretching on signaling pathways has been reported in review by Brandon et al. [151]. When subjected to static stretching, ESCs and iPSCs increased their markers of (cardio-) myogenic differentiation [152]. Although many setups exist for stretching cells (in 2D or 3D), like magnetic stretcher, manual stretcher or vacuum stretching [151], the results are usually consistent.

As for the cardiac cells, it has not been shown that stretching PSCs would act synergistically with chemical factors for the induction of cardiac differentiation. In this particular case, it has only been shown that either NRCM, endogenous CPC, or stem cell-derived cardiomyocytes (SCd-CM) had better contractility and sarcomere maturation when subjected to cyclic stretching [153, 154]. Cyclic stretching enhanced their alignment and favored gap junction formation for a better electromechanical coupling. Not only can stretching improve the alignment of cells, but also of the 3D matrix that surrounds the cells. When static strain was applied on a polymerizing gel of fibrin, the nanofibers of the mesh tended to align in the stretching direction [138, 155, 156]. A global review on some other physical signals that can affect cardiac differentiation protocols can be found in the review by Ghafar-Zadeh et al. [157].

Influence of electrical signals on the maturation of cardiomyocytes

Many efforts have been made to develop either conductive scaffolds or electrically stimulated systems for recreating the cardiomyocyte's natural environment [158-161]. In these articles, emphasis is put on trying to mimic a healthy environment to avoid the appearance of diseased phenotypes. The changes that have been demonstrated using these many proof-of-concept materials are more related to phenotypic changes in already mature cardiomyocytes, rather than to specification, differentiation or maturation events in cardiovascular progenitors or PSCs. One of the main improvements observed by electrical stimulation is an increase in connexin43 (Cx43) expression. This is a phenotypic change that considerably improves cardiac contraction as compared to standard *in vitro* controls (without electrical stimulation).

The goal of these new materials and systems is either to help implanted cardiomyocytes to integrate better with the host's cardiomyocytes or to drive pathological cardiomyocytes to regain a healthier phenotype by expressing more Cx43. Future studies involving the culture

of immature cardiogenic cells or even PSC using these materials will be needed to address questions like the relationship of cardiac progenitor phenotype and the establishment of electrical currents in the developing heart.

Debatable 4: 2D vs. 3D culture

2D models helped understand the signaling cascades in mechanotransduction, but this is still far from reality and adding a third dimension should be the next step. However, although 2D soft and patterned materials can now be prepared in a relatively high scale, 3D techniques are still cost-prohibitive, time-consuming and poorly resolved. Multi-photon technologies allow for 3D patterning by *in situ* chemical bonding of proteins to the backbone materials [162], as well as for the localized cell encapsulation by polymerization of photosensitive materials [163]. If these techniques can be quite slow, complex microfluidic systems have been designed for high-throughput and digitally-tunable fabrication of 3D-patterned cell-laden fibers and sheets [164, 165]. Yet, the impact on PSC viability, pluripotency, and differentiation potential remains to be addressed.

Another pitfall would be to expect the same effects than previously shown on 2D substrates on 3D substrates from the same material or a material with similar mechanical properties. Indeed, the distribution (and production) of membrane receptors will be completely rearranged. Additionally, embedding cells in a 3D matrix will paradoxically decrease the number of degrees of freedom of the cell system. While 2D substrates allow cells to move freely on the topside, 3D materials constrain the cell in all directions. The stress distribution will be completely different. This is even more true when considering the integration of MMP-degradable sites inside 3D scaffolds, as it has been shown that it would induce, at least in MSCs, traction forces different from those seen in non degradable materials, thus leading to different fates [166].

As for *in vivo* cardiomyogenesis and embryogenesis, cells are arranged either in 3D or in 2D assemblies depending on the developmental stage. At first, cells are clustered in 3D but soon form the three germinal layers, which can be roughly modeled in 2D. Later on, gastrulation leads to the primitive streak formation and the mesodermal cells that will become the heart form 3D structures again. But after cardiac looping and the beginning of the formation of the four chambers, cardiomyocytes are stretched and eventually define the final myocardium. Although three dimensional in theory, ultrasounds and diffusion tensor magnetic resonance imaging (MRI) studies have highlighted the fact that the myocardium is composed of layers of anisotropic cardiomyocytes oriented with a variable angle from the endocardium to the epicardium. Therefore, the myocardium can also be described as a monolayer of aligned cells wrapped around the ventricle with varying angles. In that case, one could argue that 2D

models are better. Nevertheless, the question remains whether the best strategy would be to create a 3D scaffold and push it to self-organize into a multi-layered structure of aligned cells (like what happens during cardiogenesis [167]) or to force the cells to align on multiple layers before stacking them (as proposed by Takahashi [168] et al. for the design of cardiac patches [169]). In both cases though, the limits of oxygen and nutrient diffusion will have to be overcome in order for the construct to be viable, and this is particularly relevant to cells embedded in its core.

Comments on nanofibers

Nanofibers have been extensively used to show the importance of surface roughness and hydrophilicity in maintaining pluripotency in PSC cultures. They are often cited as a simple way to have mesh-like topographies or substrates with aligned fibers [170]. Also, new techniques demonstrate the possibility to overcome the slow speed, high variability [171, 172] and high cost of electrospinning [173]. However, generating fibers only allows for two kinds of patterns: random fibers and aligned fibers. Whenever different shapes are needed, electrospinning has still quite a poor resolution [174] and needs to be combined with the most popular techniques described here above [175, 176].

Pharmacological and medical applications

In this review, we have seen that two parameters, substrate elasticity and ECM protein patterns, had a strong influence on sarcomerogenesis and cardiac maturation. Recent advances in materials design have led to the possibility of studying the synergetic effect of both properties [105, 108-110, 135] and it appears that appropriate stiffness (around 10 kPa) and aspect ratio (7:1) enabled optimal sarcomeric organization and optimal contractility both at the single cell level but also at the cell pair level [135]. This study highlights the fact that cell-cell coupling also results from a balance of forces influenced by the environment.

Whether the end goal of producing striated muscle cells is to develop toxicopharmacological assays [12, 13, 177-180] or regenerative solutions [19, 181-183] does not change the fact that cells would have to behave like in a healthy muscle. The fabrication of scaffolds for regenerative medicine has the same requirements than when mimicking developmental mechanics, but with additional constraints. First, in the case of surgical applications, structural integrity of the patch is of prime importance. Although cell sheets are a tempting option due to their fully natural composition and their promising results in cardiac failure [168, 184-186], they were found to be quite fragile and hard to handle. Second, to our knowledge, there is still no work reported on the combined influence of the materials properties described here on earlier mesodermal induction and cardiac differentiation. One can suggest that ESCs or iPSCs will behave like MSCs and differentiate into cardiomyocytes at around

10kPa. However, studies reported above suggest that cell density will have an important impact as well. This complexity needs to be addressed when determining the whole range of materials that need to be used from the extraction, reprogramming or thawing of stem cells to the patch fabrication. On one hand, scaffold-free techniques would ideally emerge and give rise to bioreactors that act directly on the 3D stem cell aggregate by providing chemical, mechanical and electrical stimulations to produce highly pure cardiomyocytes. These techniques would naturally overcome additional constraints related to the “memory” a cell can have of its previous mechanical environments, which, as described by Yang et al. [187], can affect cell's fate in a given physical environment. On the other hand, it might be more realistic in a nearer future to develop multiphasic culture systems: one biomaterial-based bioreactor for early commitment of ESC, then a second biomaterial-based bioreactor onto which cells would be transferred for cardiac maturation (in parallel to the production of endothelial and smooth muscle cells) and eventually, the three cell types would be mixed in a third bioreactor prior to implantation onto the failing myocardium [188-190]. Notwithstanding the complexity of streamlining the translational process for adapting these approaches to wide-scale clinical applications, a key and yet unsettled issue is that one still ignores whether highly mature cardiomyocytes integrate better or not than earlier progenitor cells in the host myocardium.

In a nutshell, the ideal scaffold for differentiation and maturation will likely be a scaffold that can diffuse some key growth factors, like BMP2 or Wnt inhibitors, have the appropriate stiffness and be coated with adhesion molecules that can trigger mechanosensitive events, such as ECM protein or GAGs, or, when considering upscale of these processes, short mimicking peptides. These elements would have to be patterned to direct oriented proliferation and spreading of the differentiating cardiomyocytes. Such materials have been partially reported by Agarwal, Farouz et al. when they showed that NRCM could adhere, align and spread on soft micropatterned calcium-alginate scaffolds functionalized with fibronectin. These muscular thin films showed enhanced contraction when stimulated electrically as compared to isotropic equivalents. Thus, using these kinds of scaffold for ESC differentiation could be the beginning of new standardized culturing conditions for cardiac differentiation [105].

Conclusion

Whether mechanical forces arise by activation of pathways resulting in varied cytoskeleton behavior or developmental pathways are modulated in response to cytoskeletal modifications promoted by mechanical forces is unclear. It can be seen as a “chicken and the egg” kind of question and undermining one or the other component can dramatically affect the outcome of the experiments to be performed.

A few efforts have been made toward the establishment of a global interactome of cardiopoiesis [191-194] and this kind of approach keeps being expected by cardiovascular researchers [195]. Additionally, *in silico* models are increasingly efficient in predicting cardiogenic events during development [196].

Combining the latest high-throughput and high-content technologies [26, 197] to the techniques described here in the design of micro-patterned stiffness-controlled materials will eventually unravel many of the mysteries of cardiac development and provide invaluable information for the establishment of robust analytical models [198] and reliable patient-specific therapies.

References

1. Farouz Y, Chen Y, Terzic A, Menasché P: **Concise review: growing hearts in the right place: on the design of biomimetic materials for cardiac stem cell differentiation.** *Stem Cells* 2015, **33**:1021–1035.
2. Mummery CL, Zhang J, Ng ES, Elliott DA, Elefanty AG, Kamp TJ: **Differentiation of human embryonic stem cells and induced pluripotent stem cells to cardiomyocytes: a methods overview.** *Circulation Research* 2012, **111**:344–358.
3. Engler AJ, Sen S, Sweeney HL, Discher DE: **Matrix elasticity directs stem cell lineage specification.** *Cell* 2006, **126**:677–689.
4. Radisic M, Park H, Chen F, Salazar-Lazzaro JE, Wang Y, Dennis R, Langer R, Freed LE, Vunjak-Novakovic G: **Biomimetic approach to cardiac tissue engineering: oxygen carriers and channeled scaffolds.** *Tissue Engineering* 2006, **12**:2077–2091.
5. Chan CK, Rolle MW, Potter-Perigo S, Braun KR, Van Biber BP, Laflamme MA, Murry CE, Wight TN: **Differentiation of cardiomyocytes from human embryonic stem cells is accompanied by changes in the extracellular matrix production of versican and hyaluronan.** *J Cell Biochem* 2010, **111**:585–596.
6. Tan G, Shim WS, Gu Y, Qian L, Chung YY, Lim SY, Yong P, Sim E, Wong P: **Differential effect of myocardial matrix and integrins on cardiac differentiation of human mesenchymal stem cells.** *Differentiation* 2010, **79**:260–271.
7. Schenke-Layland K, Angelis E, Rhodes KE, Heydarkhan-Hagvall S, Mikkola HK, Maclellan WR: **Collagen IV induces trophoectoderm differentiation of mouse embryonic stem cells.** *Stem Cells* 2007, **25**:1529–1538.
8. Zhang J, Klos M, Wilson GF, Herman AM, Lian X, Raval KK, Barron MR, Hou L, Soerens AG, Yu J, Palecek SP, Lyons GE, Thomson JA, Herron TJ, Jalife J, Kamp TJ: **Extracellular matrix promotes highly efficient cardiac differentiation of human pluripotent stem cells: the matrix sandwich method.** *Circulation Research* 2012, **111**:1125–1136.
9. Uosaki H, Andersen P, Shenje LT, Fernandez L, Christiansen SL, Kwon C: **Direct Contact with Endoderm-Like Cells Efficiently Induces Cardiac Progenitors from Mouse and Human Pluripotent Stem Cells.** *PLoS ONE* 2012, **7**:e46413.
10. Brown K, Doss MX, Legros S, Artus J, Hadjantonakis A-K, Foley AC: **eXtraembryonic ENdoderm (XEN) Stem Cells Produce Factors that Activate Heart Formation.** *PLoS ONE* 2010, **5**:e13446.
11. Shimko VF, Claycomb WC: **Effect of mechanical loading on three-dimensional cultures of embryonic stem cell-derived cardiomyocytes.** *Tissue Engineering : Part A* 2008, **14**:49–58.
12. Hansen A, Eder A, Bönstrup M, Flato M, Mewe M, Schaaf S, Aksehirliglu B, Schwoerer AP, Schwörer A, Uebeler J, Eschenhagen T: **Development of a drug screening platform based on engineered heart tissue.** *Circulation Research* 2010, **107**:35–44.
13. Grosberg A, Alford PW, McCain ML, Parker KK: **Ensembles of engineered cardiac tissues for physiological and pharmacological study: heart on a chip.** *Lab Chip* 2011, **11**:4165–4173.
14. Garbern JC, Lee RT: **Cardiac stem cell therapy and the promise of heart regeneration.** *Cell Stem Cell* 2013, **12**:689–698.
15. Menasché P: **Embryonic stem cells pace the heart.** *Nature Biotechnology* 2004, **22**:1237–1238.

16. Menasché P: **Stem cells for clinical use in cardiovascular medicine: current limitations and future perspectives.** *Thromb Haemost* 2005, **94**:697–701.
17. Laflamme MA, Chen KY, Naumova AV, Muskheli V, Fugate JA, Dupras SK, Reinecke H, Xu C, Hassanipour M, Police S, O'Sullivan C, Collins L, Chen Y, Minami E, Gill EA, Ueno S, Yuan C, Gold J, Murry CE: **Cardiomyocytes derived from human embryonic stem cells in pro-survival factors enhance function of infarcted rat hearts.** *Nature Biotechnology* 2007, **25**:1015–1024.
18. Blin G, Nury D, Stefanovic S, Neri T, Guillevic O, Brinon B, Bellamy V, Rücker-Martin C, Barbry P, Bel A, Bruneval P, Cowan C, Pouly J, Mitalipov S, Gouadon E, Binder P, Hagège A, Desnos M, Renaud J-F, Menasché P, Pucéat M: **A purified population of multipotent cardiovascular progenitors derived from primate pluripotent stem cells engrafts in postmyocardial infarcted nonhuman primates.** *J Clin Invest* 2010, **120**:1125–1139.
19. Chong JJH, Yang X, Don CW, Minami E, Liu Y-W, Weyers JJ, Mahoney WM, Van Biber B, Palpant NJ, Gantz JA, Fugate JA, Muskheli V, Gough GM, Vogel KW, Astley CA, Hotchkiss CE, Baldessari A, Pabon L, Reinecke H, Gill EA, Nelson V, Kiem H-P, Laflamme MA, Murry CE: **Human embryonic-stem-cell-derived cardiomyocytes regenerate non-human primate hearts.** *Nature* 2014:1–17.
20. Kirby ML, Waldo K: *Cardiac Development.* Oxford University Press; 2007.
21. Rosenthal N, Harvey RP: *Heart Development and Regeneration.* Academic Press, Boston; 2010.
22. Malizia AP, Wang D-Z: **MicroRNAs in cardiomyocyte development.** *WIREs Syst Biol Med* 2011, **3**:183–190.
23. Lee S-Y, Ham O, Cha M-J, Song B-W, Choi E, Kim I-K, Chang W, Lim S, Lee CY, Park J-H, Lee J, Bae Y, Seo H-H, Choi E, Jang Y, Hwang K-C: **The promotion of cardiogenic differentiation of hMSCs by targeting epidermal growth factor receptor using microRNA-133a.** *Biomaterials* 2013, **34**:92–99.
24. Eulalio A, Mano M, Dal Ferro M, Zentilin L, Sinagra G, Zacchigna S, Giacca M: **Functional screening identifies miRNAs inducing cardiac regeneration.** *Nature* 2012, **492**:376–381.
25. Nazareth EJP, Ostblom JEE, Lückner PB, Shukla S, Alvarez MM, Oh SKW, Yin T, Zandstra PW: **High-throughput fingerprinting of human pluripotent stem cell fate responses and lineage bias.** *Nature Methods* 2013, **10**:1225–1231.
26. Willems E, Spiering S, Davidovics H, Lanier M, Xia Z, Dawson M, Cashman J, Mercola M: **Small-molecule inhibitors of the Wnt pathway potently promote cardiomyocytes from human embryonic stem cell-derived mesoderm.** *Circulation Research* 2011, **109**:360–364.
27. Gan L, Schwengberg S, Denecke B: **MicroRNA Profiling during Cardiomyocyte-Specific Differentiation of Murine Embryonic Stem Cells Based on Two Different miRNA Array Platforms.** *PLoS ONE* 2011, **6**:e25809.
28. Lian X, Hsiao C, Wilson G, Zhu K, Hazeltine LB, Azarin SM, Raval KK, Zhang J, Kamp TJ, Palecek SP: **Robust cardiomyocyte differentiation from human pluripotent stem cells via temporal modulation of canonical Wnt signaling.** *PNAS* 2012, **109**:E1848–57.
29. Lian X, Zhang J, Azarin SM, Zhu K, Hazeltine LB, Bao X, Hsiao C, Kamp TJ, Palecek SP: **Directed cardiomyocyte differentiation from human pluripotent stem cells by modulating Wnt/β-catenin signaling under fully defined conditions.** *Nature Protocols* 2013, **8**:162–175.
30. Ni TT, Rellinger EJ, Mukherjee A, Xie S, Stephens L, Thorne CA, Kim K, Hu J, Lee E, Marnett L, Hatzopoulos AK, Zhong TP: **Discovering small molecules that promote cardiomyocyte generation by modulating Wnt signaling.** *Chemistry & Biology* 2011, **18**:1658–1668.
31. Nakamura T, Sano M, Songyang Z, Schneider MD: **A Wnt- and β-catenin-dependent pathway for mammalian cardiac myogenesis.** *PNAS* 2003, **100**:5834–5839.

32. Minami I, Yamada K, Otsuji TG, Yamamoto T, Shen Y, Otsuka S, Kadota S, Morone N, Barve M, Asai Y, Tenkova-Heuser T, Heuser JE, Uesugi M, Aiba K, Nakatsuji N: **A small molecule that promotes cardiac differentiation of human pluripotent stem cells under defined, cytokine- and xeno-free conditions.** *Cell Reports* 2012, **2**:1448–1460.
33. He Z, Li H, Zuo S, Pasha Z, Wang Y, Yang Y, Jiang W, Ashraf M, Xu M: **Transduction of Wnt11 promotes mesenchymal stem cell transdifferentiation into cardiac phenotypes.** *Stem Cells Dev* 2011, **20**:1771–1778.
34. Panáková D, Werdich AA, MacRae CA: **Wnt11 patterns a myocardial electrical gradient through regulation of the L-type Ca²⁺ channel.** *Nature* 2010, **466**:874–878.
35. Nagy II, Railo A, Rapila R, Hast T, Sormunen R, Tavi P, Räsänen J, Vainio SJ: **Wnt-11 signalling controls ventricular myocardium development by patterning N-cadherin and β -catenin expression.** *Cardiovascular Research* 2010, **85**:100–109.
36. Deb A, Davis BH, Guo J, Ni A, Huang J, Zhang Z, Mu H, Dzau VJ: **SFRP2 regulates cardiomyogenic differentiation by inhibiting a positive transcriptional autofeedback loop of Wnt3a.** *Stem Cells* 2008, **26**:35–44.
37. Pucéat M: **TGF β in the differentiation of embryonic stem cells.** *Cardiovascular Research* 2007, **74**:256–261.
38. Kattman SJ, Witty AD, Gagliardi M, Dubois NC, Niapour M, Hotta A, Ellis J, Keller G: **Stage-specific optimization of activin/nodal and BMP signaling promotes cardiac differentiation of mouse and human pluripotent stem cell lines.** *Cell Stem Cell* 2011, **8**:228–240.
39. Leschik J, Stefanovic S, Brinon B, Pucéat M: **Cardiac commitment of primate embryonic stem cells.** *Nature Protocols* 2008, **3**:1381–1387.
40. de Pater E, Ciampricotti M, Priller F, Veerkamp J, Strate I, Smith K, Lagendijk AK, Schilling TF, Herzog W, Abdelilah-Seyfried S, Hammerschmidt M, Bakkers J: **Bmp signaling exerts opposite effects on cardiac differentiation.** *Circulation Research* 2012, **110**:578–587.
41. Weng Z, Kong C-W, Ren L, Karakikes I, Geng L, He J, Chow MZY, Mok CF, Keung W, Chow H, Leung AYH, Hajar RJ, Li RA, Chan CW: **A simple, cost-effective but highly efficient system for deriving ventricular cardiomyocytes from human pluripotent stem cells.** *Stem Cells Dev* 2014, **23**:1704–1716.
42. Yang L, Soonpaa MH, Adler ED, Roepke TK, Kattman SJ, Kennedy M, Henckaerts E, Bonham K, Abbott GW, Linden RM, Field LJ, Keller GM: **Human cardiovascular progenitor cells develop from a KDR⁺ embryonic-stem-cell-derived population.** *Nature* 2008, **453**:524–528.
43. Burridge PW, Matsa E, Shukla P, Lin ZC, Churko JM, Ebert AD, Lan F, Diecke S, Huber B, Mordwinkin NM, Plews JR, Abilez OJ, Cui B, Gold JD, Wu JC: **Chemically defined generation of human cardiomyocytes.** *Nature Methods* 2014, **11**:855–860.
44. Amin N, Vincan E: **The Wnt signaling pathways and cell adhesion.** *Front Biosci* 2012.
45. Tanegashima K, Zhao H, Dawid IB: **WGEF activates Rho in the Wnt-PCP pathway and controls convergent extension in *Xenopus* gastrulation.** *EMBO J* 2008, **27**:606–617.
46. Wallingford JB: **Planar cell polarity and the developmental control of cell behavior in vertebrate embryos.** *Annu Rev Cell Dev Biol* 2012, **28**:627–653.
47. Kopf J, Petersen A, Duda GN, Knaus P: **BMP2 and mechanical loading cooperatively regulate immediate early signalling events in the BMP pathway.** *BMC Biol* 2012, **10**:37.
48. Peiris D, Pacheco I, Spencer C, MacLeod RJ: **The extracellular calcium-sensing receptor reciprocally regulates the secretion of BMP-2 and the BMP antagonist Noggin in colonic**

myofibroblasts. *Am J Physiol Gastrointest Liver Physiol* 2007, **292**:G753–66.

49. Kim SA, Tai C-Y, Mok L-P, Mosser EA, Schuman EM: **Calcium-dependent dynamics of cadherin interactions at cell-cell junctions.** *PNAS* 2011, **108**:9857–9862.

50. Kinney MA, Sargent CY, McDevitt TC: **Temporal modulation of β -catenin signaling by multicellular aggregation kinetics impacts embryonic stem cell cardiomyogenesis.** *Stem Cells Dev* 2013, **22**:2665–2677.

51. Brembeck FH, Rosário M, Birchmeier W: **Balancing cell adhesion and Wnt signaling, the key role of β -catenin.** *Current Opinion in Genetics & Development* 2006, **16**:51–59.

52. Lickert H, Kutsch S, Kanzler B, Tamai Y, Taketo MM: **Formation of Multiple Hearts in Mice following Deletion of β -catenin in the Embryonic Endoderm.** *Developmental Cell* 2002, **3**:171–181.

53. Imanaka-Yoshida K, Knudsen KA, Linask KK: **N-cadherin is required for the differentiation and initial myofibrillogenesis of chick cardiomyocytes.** *Cell Motil Cytoskeleton* 1998, **39**:52–62.

54. Ibañes M, Izpisua Belmonte JC: **Left–right axis determination.** *WIREs Syst Biol Med* 2009, **1**:210–219.

55. Mammoto T, Ingber DE: **Mechanical control of tissue and organ development.** *Development* 2010, **137**:1407–1420.

56. Xin M, Kim Y, Sutherland LB, Murakami M, Qi X, McAnally J, Porrello ER, Mahmoud AI, Tan W, Shelton JM, Richardson JA, Sadek HA, Bassel-Duby R, Olson EN: **Hippo pathway effector Yap promotes cardiac regeneration.** *PNAS* 2013, **110**:13839–13844.

57. Dupont S, Morsut L, Aragona M, Enzo E, Giulitti S, Cordenonsi M, Zanconato F, Le Digabel J, Forcato M, Bicciato S, Elvassore N, Piccolo S: **Role of YAP/TAZ in mechanotransduction.** *Nature* 2011, **474**:179–183.

58. Gaspar P, Tapon N: **The local environment: actin architecture and Hippo signalling.** *Current Opinion in Cell Biology* 2014, **31**:74–83.

59. Xin M, Kim Y, Sutherland LB, Qi X, McAnally J, Schwartz RJ, Richardson JA, Bassel-Duby R, Olson EN: **Regulation of insulin-like growth factor signaling by Yap governs cardiomyocyte proliferation and embryonic heart size.** *Sci Signal* 2011, **4**:ra70.

60. Beyer TA, Weiss A, Khomchuk Y, Huang K, Ogunjimi AA, Varelas X, Wrana JL: **Switch Enhancers Interpret TGF- β and Hippo Signaling to Control Cell Fate in Human Embryonic Stem Cells.** *Cell Reports* 2013, **5**:1611–1624.

61. Hao J, Zhang Y, Wang Y, Ye R, Qiu J, Zhao Z, Li J: **Role of extracellular matrix and YAP/TAZ in cell fate determination.** *Cell Signal* 2014, **26**:186–191.

62. Varelas X: **The Hippo pathway effectors TAZ and YAP in development, homeostasis and disease.** *Development* 2014, **141**:1614–1626.

63. Mosqueira D, Pagliari S, Uto K, Ebara M, Romanazzo S, Escobedo-Lucea C, Nakanishi J, Taniguchi A, Franzese O, Di Nardo P, Goumans MJ, Traversa E, Pinto-do-Ó P, Aoyagi T, Forte G: **Hippo pathway effectors control cardiac progenitor cell fate by acting as dynamic sensors of substrate mechanics and nanostructure.** *ACS Nano* 2014, **8**:2033–2047.

64. Halder G, Dupont S, Piccolo S: **Transduction of mechanical and cytoskeletal cues by YAP and TAZ.** *Nat Rev Mol Cell Biol* 2012, **13**:591–600.

65. Sun Y, Yong KMA, Villa-Diaz LG, Zhang X, Chen W, Philson R, Weng S, Xu H, Krebsbach PH, Fu J: **Hippo/YAP-mediated rigidity-dependent motor neuron differentiation of human pluripotent**

stem cells. *Nature Materials* 2014, **13**:599–604.

66. Vallée J-P, Hauwel M, Lepetit-Coiffé M, Bei W, Montet-Abou K, Meda P, Gardier S, Zammaretti P, Kraehenbuehl TP, Herrmann F, Hubbell JA, Jaconi ME: **Embryonic stem cell-based cardiopatches improve cardiac function in infarcted rats.** *Stem Cells Translational Medicine* 2012, **1**:248–260.

67. Xu C, Inokuma MS, Denham J, Golds K, Kundu P, Gold JD, Carpenter MK: **Feeder-free growth of undifferentiated human embryonic stem cells.** *Nature Biotechnology* 2001, **19**:971–974.

68. Tsai Z-Y, Singh S, Yu S-L, Chou C-H, Li SS-L: **A feeder-free culture using autogeneic conditioned medium for undifferentiated growth of human embryonic stem cells: comparative expression profiles of mRNAs, microRNAs and proteins among different feeders and conditioned media.** *BMC Cell Biol* 2010, **11**:76.

69. Kan NG, Stemmler MP, Junghans D, Kanzler B, de Vries WN, Dominis M, Kemler R: **Gene replacement reveals a specific role for E-cadherin in the formation of a functional trophectoderm.** *Development* 2007, **134**:31–41.

70. Damsky C, Sutherland A, Fisher S: **Extracellular Matrix-5 - Adhesive Interactions in Early Mammalian Embryogenesis, Implantation, and Placentation.** *The FASEB Journal* 1993, **7**:1320–1329.

71. Kolahi KS, Mofrad MRK: **Mechanotransduction: a major regulator of homeostasis and development.** *WIREs Syst Biol Med* 2010, **2**:625–639.

72. Massia SP, MASSIA S, Hubbell JA, Hubbell JA: **An RGD spacing of 440 nm is sufficient for integrin $\alpha_v\beta_3$ -mediated fibroblast spreading and 140 nm for focal contact and stress fiber formation.** *J Cell Biol* 1991, **114**:1089–1100.

73. Bhadriraju K, Yang M, Alom Ruiz S, Pirone D, Tan J, Chen CS: **Activation of ROCK by RhoA is regulated by cell adhesion, shape, and cytoskeletal tension.** *Experimental Cell Research* 2007, **313**:3616–3623.

74. McBeath R, Pirone DM, Nelson CM, Bhadriraju K, Chen CS: **Cell shape, cytoskeletal tension, and RhoA regulate stem cell lineage commitment.** *Developmental Cell* 2004, **6**:483–495.

75. Bongso A, Fong CY, Ng SC, Ratnam S: **Isolation and Culture of Inner Cell Mass Cells From Human Blastocysts.** *Human Reproduction* 1994, **9**:2110–2117.

76. Zeiger AS, Hinton B, Van Vliet KJ: **Why the dish makes a difference: quantitative comparison of polystyrene culture surfaces.** *Acta Biomaterialia* 2013, **9**:7354–7361.

77. Thomson JA, Itskovitz-Eldor J, Shapiro SS, Waknitz MA, Swiergiel JJ, Marshall VS, Jones JM: **Embryonic Stem Cell Lines Derived from Human Blastocysts.** *Science* 1998, **282**:1145–1147.

78. Reubinoff BE, Pera MF, Fong CY, Trounson A, Bongso A: **Embryonic stem cell lines from human blastocysts: somatic differentiation in vitro.** *Nature Biotechnology* 2000, **18**:399–404.

79. Lambert M, Padilla F, Mège RM: **Immobilized dimers of N-cadherin-Fc chimera mimic cadherin-mediated cell contact formation: contribution of both outside-in and inside-out signals.** *Journal of Cell Science* 2000, **113**:2207–2219.

80. Schenke-Layland K, Nsair A, Van Handel B, Angelis E, Gluck JM, Votteler M, Goldhaber JI, Mikkola HK, Kahn M, Maclellan WR: **Recapitulation of the embryonic cardiovascular progenitor cell niche.** *Biomaterials* 2011, **32**:2748–2756.

81. Stary M, Pastener W, Summer A, Hrdina A, Eger A, Weitzer G: **Parietal endoderm secreted SPARC promotes early cardiomyogenesis in vitro.** *Experimental Cell Research* 2005, **310**:331–343.

82. Meilhac SM: **Oriented clonal cell growth in the developing mouse myocardium underlies cardiac morphogenesis.** *The Journal of Cell Biology* 2004, **164**:97–109.
83. Strauss B, Adams RJ, Papalopulu N: **A default mechanism of spindle orientation based on cell shape is sufficient to generate cell fate diversity in polarised Xenopus blastomeres.** *Development* 2006, **133**:3883–3893.
84. Théry M, Racine V, Pépin A, Piel M, CHEN Y, Sibarita J-B, Bornens M: **The extracellular matrix guides the orientation of the cell division axis.** *Nat Cell Biol* 2005, **7**:947–953.
85. Auman HJ, Coleman H, Riley HE, Olale F, Tsai HJ: **Functional modulation of cardiac form through regionally confined cell shape changes.** *PLoS Biol* 2007.
86. Geisse NA, Sheehy SP, Parker KK: **Control of myocyte remodeling in vitro with engineered substrates.** *In Vitro CellDevBiol-Animal* 2009, **45**:343–350.
87. Chen CS, Mrksich M, Huang S, Whitesides GM, Ingber DE: **Micropatterned surfaces for control of cell shape, position, and function.** *Biotechnol Progress* 1998, **14**:356–363.
88. Vignaud T, Ennomani H, Théry M: **Polyacrylamide hydrogel micropatterning.** *Methods Cell Biol* 2014, **120**:93–116.
89. Peerani R, Rao BM, Bauwens CL, Yin T, Wood GA, Nagy A, Kumacheva E, Zandstra PW: **Niche-mediated control of human embryonic stem cell self-renewal and differentiation.** *EMBO J* 2007, **26**:4744–4755.
90. Lee LH, Peerani R, Ungrin M, Joshi C, Kumacheva E, Zandstra P: **Micropatterning of human embryonic stem cells dissects the mesoderm and endoderm lineages.** *Stem Cell Research* 2009, **2**:155–162.
91. Ungrin MD, Joshi C, Nica A, Bauwens C, Zandstra PW: **Reproducible, ultra high-throughput formation of multicellular organization from single cell suspension-derived human embryonic stem cell aggregates.** *PLoS ONE* 2008.
92. Bauwens CL, Song H, Thavandiran N, Ungrin M, Massé S, Nanthakumar K, Seguin C, Zandstra PW: **Geometric control of cardiomyogenic induction in human pluripotent stem cells.** *Tissue Engineering : Part A* 2011, **17**:1901–1909.
93. Hwang Y-S, Chung BG, Ortmann D, Hattori N, Moeller H-C, Khademhosseini A: **Microwell-mediated control of embryoid body size regulates embryonic stem cell fate via differential expression of WNT5a and WNT11.** *PNAS* 2009, **106**:16978–16983.
94. Mohr JC, Zhang J, Azarin SM, Soerens AG, de Pablo JJ, Thomson JA, Lyons GE, Palecek SP, Kamp TJ: **The microwell control of embryoid body size in order to regulate cardiac differentiation of human embryonic stem cells.** *Biomaterials* 2010, **31**:1885–1893.
95. Nelson CM, Jean RP, Tan JL, Liu WF, Sniadecki NJ, Spector AA, Chen CS: **Emergent patterns of growth controlled by multicellular form and mechanics.** *Proceedings of the National Academy of Sciences* 2005, **102**:11594–11599.
96. Myers FB, Silver JS, Zhuge Y, Beygui RE, Zarins CK, Lee LP, Abilez OJ: **Robust pluripotent stem cell expansion and cardiomyocyte differentiation via geometric patterning.** *Integr Biol* 2013, **5**:1495–1506.
97. Parker KK, Tan J, Chen CS, Tung L: **Myofibrillar architecture in engineered cardiac myocytes.** *Circulation Research* 2008, **103**:340–342.
98. Bray M-A, Sheehy SP, Parker KK: **Sarcomere alignment is regulated by myocyte shape.** *Cell Motil Cytoskeleton* 2008, **65**:641–651.

99. Grosberg A, Kuo P-L, Guo C-L, Geisse NA, Bray M-A, Adams WJ, Sheehy SP, Parker KK: **Self-organization of muscle cell structure and function.** *PLoS Comput Biol* 2011, **7**:e1001088.
100. Alford PW, Feinberg AW, Sheehy SP, Parker KK: **Biohybrid thin films for measuring contractility in engineered cardiovascular muscle.** *Biomaterials* 2010, **31**:3613–3621.
101. Feinberg AW, Alford PW, Jin H, Ripplinger CM, Werdich AA, Sheehy SP, Grosberg A, Parker KK: **Controlling the contractile strength of engineered cardiac muscle by hierarchical tissue architecture.** *Biomaterials* 2012, **33**:5732–5741.
102. Feinberg AW, Feigel A, Shevkoplyas SS, Sheehy S, Whitesides GM, Parker KK: **Muscular thin films for building actuators and powering devices.** *Science* 2007, **317**:1366–1370.
103. van Spreeuwel ACC, Bax NAM, Bastiaens AJ, Foolen J, Loerakker S, Borochoin M, van der Schaft DWJ, Chen CS, Baaijens FPT, Bouten CVC: **The influence of matrix (an)isotropy on cardiomyocyte contraction in engineered cardiac microtissues.** *Integr Biol (Camb)* 2014, **6**:422–429.
104. Wang J, Chen A, Lieu DK, Karakikes I, Chen G, Keung W, Chan CW, Hajjar RJ, Costa KD, Khine M, Li RA: **Effect of engineered anisotropy on the susceptibility of human pluripotent stem cell-derived ventricular cardiomyocytes to arrhythmias.** *Biomaterials* 2013, **34**:8878–8886.
105. Agarwal A, Farouz Y, Nesmith AP, Deravi LF, McCain ML, Parker KK: **Micropatterning Alginate Substrates for in vitro Cardiovascular Muscle on a Chip.** *Adv Funct Mater* 2013, **23**:3738–3746.
106. Cimetta E, Sirabella D, Yeager K, Davidson K, Simon J, Moon RT, Vunjak-Novakovic G: **Microfluidic bioreactor for dynamic regulation of early mesodermal commitment in human pluripotent stem cells.** *Lab Chip* 2013, **13**:355–364.
107. Khademhosseini A, Ferreira L, Blumling J, Yeh J, Karp JM, Fukuda J, Langer R: **Co-culture of human embryonic stem cells with murine embryonic fibroblasts on microwell-patterned substrates.** *Biomaterials* 2006, **27**:5968–5977.
108. Tang X, Ali MY, Saif MTA: **A Novel Technique for Micro-patterning Proteins and Cells on Polyacrylamide Gels.** *Soft Matter* 2012, **8**:7197–7206.
109. Grevesse T, Versaevel M, Circelli G, Desprez S, Gabriele S: **A simple route to functionalize polyacrylamide hydrogels for the independent tuning of mechanotransduction cues.** *Lab Chip* 2013, **13**:777–780.
110. Hynd MR, Frampton JP, Burnham M-R, Martin DL, Dowell-Mesfin NM, Turner JN, Shain W: **Functionalized hydrogel surfaces for the patterning of multiple biomolecules.** *J Biomed Mater Res* 2007, **81**:347–354.
111. Jeon O, Alsberg E: **Regulation of Stem Cell Fate in a Three-Dimensional Micropatterned Dual-Crosslinked Hydrogel System.** *Adv Funct Mater* 2013, **23**:4765–4775.
112. Annabi N, Tsang K, Mithieux SM, Nikkhah M, Ameri A, Khademhosseini A, Weiss AS: **Highly Elastic Micropatterned Hydrogel for Engineering Functional Cardiac Tissue.** *Adv Funct Mater* 2013, **23**:4950–4959.
113. Luna JI, Ciriza J, Garcia-Ojeda ME, Kong M, Herren A, Lieu DK, Li RA, Fowlkes CC, Khine M, McCloskey KE: **Multiscale biomimetic topography for the alignment of neonatal and embryonic stem cell-derived heart cells.** *Tissue Engineering Part C: Methods* 2011, **17**:579–588.
114. Kim D-H, Lipke EA, Kim P, Cheong R, Thompson S, Delannoy M, Suh K-Y, Tung L, Levchenko A: **Nanoscale cues regulate the structure and function of macroscopic cardiac tissue constructs.** *PNAS* 2010, **107**:565–570.
115. Bursac N, Parker KK, Iravanian S, Tung L: **Cardiomyocyte Cultures With Controlled Macroscopic Anisotropy A Model for Functional Electrophysiological Studies of Cardiac**

Muscle. *Circulation Research* 2002, **91**:e45–e54.

116. Badie N, Bursac N: **Novel micropatterned cardiac cell cultures with realistic ventricular microstructure.** *Biophysical Journal* 2009, **96**:3873–3885.

117. Bian W, Juhas M, Pfeiler TW, Bursac N: **Local tissue geometry determines contractile force generation of engineered muscle networks.** *Tissue Engineering : Part A* 2012, **18**:957–967.

118. Parrag IC, Zandstra PW, Woodhouse KA: **Fiber alignment and coculture with fibroblasts improves the differentiated phenotype of murine embryonic stem cell-derived cardiomyocytes for cardiac tissue engineering.** *Biotechnol Bioeng* 2012, **109**:813–822.

119. Orlova Y, Magome N, Liu L, CHEN Y, Agladze K: **Electrospun nanofibers as a tool for architecture control in engineered cardiac tissue.** *Biomaterials* 2011, **32**:5615–5624.

120. Kim D-H, Kshitiz, Smith RR, Kim P, Ahn EH, Kim HN, Marbán E, Suh K-Y, Levchenko A: **Nanopatterned cardiac cell patches promote stem cell niche formation and myocardial regeneration.** *Integr Biol* 2012, **4**:1019–1033.

121. Massumi M, Abasi M, Babaloo H, Terraf P, Safi M, Saeed M, Barzin J, Zandi M, Soleimani M: **The effect of topography on differentiation fates of matrigel-coated mouse embryonic stem cells cultured on PLGA nanofibrous scaffolds.** *Tissue Engineering : Part A* 2012, **18**:609–620.

122. Chen A, Lieu DK, Freschauf L, Lew V, Sharma H, Wang J, Nguyen D, Karakikes I, Hajjar RJ, Gopinathan A, Botvinick E, Fowlkes CC, Li RA, Khine M: **Shrink-film configurable multiscale wrinkles for functional alignment of human embryonic stem cells and their cardiac derivatives.** *Adv Mater* 2011, **23**:5785–5791.

123. Clement CA, Kristensen SG, Møllgård K, Pazour GJ, Yoder BK, Larsen LA, Christensen ST: **The primary cilium coordinates early cardiogenesis and hedgehog signaling in cardiomyocyte differentiation.** *Journal of Cell Science* 2009, **122**:3070–3082.

124. Radisic M, Park H, Martens TP, Salazar-Lazaro JE, Geng W, Wang Y, Langer R, Freed LE, Vunjak-Novakovic G: **Pre-treatment of synthetic elastomeric scaffolds by cardiac fibroblasts improves engineered heart tissue.** *J Biomed Mater Res* 2008, **86**:713–724.

125. Ieda M, Tsuchihashi T, Ivey KN, Ross RS, Hong T-T, Shaw RM, Srivastava D: **Cardiac fibroblasts regulate myocardial proliferation through $\beta 1$ integrin signaling.** *Developmental Cell* 2009, **16**:233–244.

126. Liau B, Christoforou N, Leong KW, Bursac N: **Pluripotent stem cell-derived cardiac tissue patch with advanced structure and function.** *Biomaterials* 2011, **32**:9180–9187.

127. Lee MR, Kwon KW, Jung H, Kim HN, Suh KY, Kim K, Kim K-S: **Direct differentiation of human embryonic stem cells into selective neurons on nanoscale ridge/groove pattern arrays.** *Biomaterials* 2010, **31**:4360–4366.

128. Downing TL, Soto J, Morez C, Houssin T, Fritz A, Yuan F, Chu J, Patel S, Schaffer DV, Li S: **Biophysical regulation of epigenetic state and cell reprogramming.** *Nature Materials* 2013, **12**:1154–1162.

129. Serena E, Cimetta E, Zatti S, Zaglia T, Zagallo M, Keller G, Elvassore N: **Micro-Arrayed Human Embryonic Stem Cells-Derived Cardiomyocytes for In Vitro Functional Assay.** *PLoS ONE* 2012, **7**:e48483.

130. Engelmayr GC, Cheng M, Bettinger CJ, Borenstein JT, Langer R, Freed LE: **Accordion-like honeycombs for tissue engineering of cardiac anisotropy.** *Nature Materials* 2008, **7**:1003–1010.

131. Trappmann B, Gautrot JE, Connelly JT, Strange DGT, Li Y, Oyen ML, Cohen Stuart MA, Boehm H, Li B, Vogel V, Spatz JP, Watt FM, Huck WTS: **Extracellular-matrix tethering regulates stem-cell**

fate. *Nature Materials* 2012, **11**:642–649.

132. Engler AJ, Carag-Krieger C, Johnson CP, Raab M, Tang H-Y, Speicher DW, Sanger JW, Sanger JM, Discher DE: **Embryonic cardiomyocytes beat best on a matrix with heart-like elasticity: scar-like rigidity inhibits beating.** *Journal of Cell Science* 2008, **121**:3794–3802.

133. Jacot JG, Kita-Matsuo H, Wei KA, Chen HSV, Omens JH, Mercola M, McCulloch AD: **Cardiac myocyte force development during differentiation and maturation.** *Annals of the New York Academy of Sciences* 2010, **1188**:121–127.

134. Jacot JG, McCulloch AD, Omens JH: **Substrate stiffness affects the functional maturation of neonatal rat ventricular myocytes.** *Biophysical Journal* 2008, **95**:3479–3487.

135. McCain ML, Lee H, Aratyn-Schaus Y, Kléber AG, Parker KK: **Cooperative coupling of cell-matrix and cell-cell adhesions in cardiac muscle.** *PNAS* 2012, **109**:9881–9886.

136. Kolahi KS, Donjacour A, Liu X, Lin W, Simbulan RK, Bloise E, Maltepe E, Rinaudo P: **Effect of Substrate Stiffness on Early Mouse Embryo Development.** *PLoS ONE* 2012, **7**:e41717.

137. Sun Y, Villa-Diaz LG, Lam RHW, Chen W, Krebsbach PH, Fu J: **Mechanics Regulates Fate Decisions of Human Embryonic Stem Cells.** *PLoS ONE* 2012, **7**:e37178.

138. Chiron S, Tomczak C, Duperray A, Lainé J, Bonne G: **Complex interactions between human myoblasts and the surrounding 3D fibrin-based matrix.** *PLoS ONE* 2012.

139. Legant WR, Miller JS, Blakely BL, Cohen DM, Genin GM, Chen CS: **Measurement of mechanical tractions exerted by cells in three-dimensional matrices.** *Nature Methods* 2010, **7**:969–971.

140. Zoldan J, Lytton-Jean AKR, Karagiannis ED, Deiorio-Haggar K, Bellan LM, Langer R, Anderson DG: **Directing human embryonic stem cell differentiation by non-viral delivery of siRNA in 3D culture.** *Biomaterials* 2011, **32**:7793–7800.

141. Bhana B, Iyer RK, Chen WLK, Zhao R, Sider KL, Likhitpanichkul M, Simmons CA, Radisic M: **Influence of substrate stiffness on the phenotype of heart cells.** *Biotechnol Bioeng* 2010, **105**:1148–1160.

142. Hazeltine LB, Badur MG, Lian X, Das A, Han W, Palecek SP: **Temporal impact of substrate mechanics on differentiation of human embryonic stem cells to cardiomyocytes.** *Acta Biomaterialia* 2014, **10**:604–612.

143. Engler AJ, Griffin MA, Sen S, Bönnemann CG, Sweeney HL, Discher DE: **Myotubes differentiate optimally on substrates with tissue-like stiffness: pathological implications for soft or stiff microenvironments.** *J Cell Biol* 2004, **166**:877–887.

144. Chopra A, Chopra A, Lin V, McCollough A, McCollough A, Atzet S, Atzet SK, Prestwich GD, Wechsler AS, Murray ME, Oake SA, Kresh JY, Janmey PA: **Reprogramming cardiomyocyte mechanosensing by crosstalk between integrins and hyaluronic acid receptors.** *Journal of Biomechanics* 2012, **45**:824–831.

145. Chopra A, Murray ME, Mendez MG, Raz-Ben Aroush D, Galie PA, Marcinkiewicz C, Prestwich GD, Chen CS, Kresh JY, Janmey PA: **Augmentation of integrin-mediated mechanotransduction by hyaluronic acid.** *Biomaterials* 2014, **35**:71–82.

146. Young JL, Engler AJ: **Hydrogels with time-dependent material properties enhance cardiomyocyte differentiation in vitro.** *Biomaterials* 2011, **32**:1002–1009.

147. Wen JH, Vincent LG, Fuhrmann A, Choi YS, Hribar KC, Taylor-Weiner H, Chen S, Engler AJ: **Interplay of matrix stiffness and protein tethering in stem cell differentiation.** *Nature Materials* 2014, **13**:979–987.

148. Murrell M, Kamm R, Matsudaira P: **Substrate viscosity enhances correlation in epithelial sheet movement.** *Biophysical Journal* 2011, **101**:297–306.
149. Mertz AF, Che Y, Banerjee S, Goldstein JM, Rosowski KA, Revilla SF, Niessen CM, Marchetti MC, Dufresne ER, Horsley V: **Cadherin-based intercellular adhesions organize epithelial cell-matrix traction forces.** *PNAS* 2013, **110**:842–847.
150. Mertz AF, Banerjee S, Che Y, German GK, Xu Y: **Scaling of traction forces with the size of cohesive cell colonies.** *Phys Rev Lett* 2012.
151. Riehl BD, Park J-H, Kwon IK, Lim JY: **Mechanical stretching for tissue engineering: two-dimensional and three-dimensional constructs.** *Tissue Engineering Part B: Reviews* 2012, **18**:288–300.
152. Schmelter M, Ateghang B, Helmig S, Wartenberg M, Sauer H: **Embryonic stem cells utilize reactive oxygen species as transducers of mechanical strain-induced cardiovascular differentiation.** *The FASEB Journal* 2006, **20**:1182–1184.
153. Gwak S-J, Bhang SH, Kim I-K, Kim S-S, Cho S-W, Jeon O, Yoo KJ, Putnam AJ, Kim B-S: **The effect of cyclic strain on embryonic stem cell-derived cardiomyocytes.** *Biomaterials* 2008, **29**:844–856.
154. Zhang T, Wan LQ, Xiong Z, Marsano A, Maidhof R, Park M, Yan Y, Vunjak-Novakovic G: **Channelled scaffolds for engineering myocardium with mechanical stimulation.** *J Tissue Eng Regen M* 2011, **6**:748–756.
155. Matsumoto T, Sasaki J-I, Alsberg E, Egusa H, Yatani H, Sohmura T: **Three-Dimensional Cell and Tissue Patterning in a Strained Fibrin Gel System.** *PLoS ONE* 2007, **2**:e1211.
156. Boublik J, Park H, Radisic M, Tognana E, Chen F, Pei M, Vunjak-Novakovic G, Freed LE: **Mechanical properties and remodeling of hybrid cardiac constructs made from heart cells, fibrin, and biodegradable, elastomeric knitted fabric.** *Tissue Engineering* 2005, **11**:1122–1132.
157. Ghafar-Zadeh E, Waldeisen JR, Lee LP: **Engineered approaches to the stem cell microenvironment for cardiac tissue regeneration.** *Lab Chip* 2011, **11**:3031–3048.
158. Radisic M, Marsano A, Maidhof R, Wang Y, Vunjak-Novakovic G: **Cardiac tissue engineering using perfusion bioreactor systems.** *Nature Protocols* 2008, **3**:719–738.
159. You J-OO, Rafat M, Ye GJC, Auguste DT: **Nanoengineering the Heart: Conductive Scaffolds Enhance Connexin 43 Expression.** *Nano Lett* 2011:110803085826058.
160. Dvir T, Timko BP, Brigham MD, Naik SR, Karajanagi SS, Levy O, Jin H, Parker KK, Langer R, Kohane DS: **Nanowired three-dimensional cardiac patches.** *Nature Nanotech* 2011, **6**:720–725.
161. Shin SR, Jung SM, Zalabany M, Kim K, Zorlutuna P, Kim SB, Nikkhah M, Khabiry M, Azize M, Kong J, Wan K-T, Palacios T, Dokmeci MR, Bae H, Tang XS, Khademhosseini A: **Carbon-Nanotube-Embedded Hydrogel Sheets for Engineering Cardiac Constructs and Bioactuators.** *ACS Nano* 2013, **7**:2369–2380.
162. Wylie RG, Ahsan S, Aizawa Y, Maxwell KL, Morshead CM, Shoichet MS: **Spatially controlled simultaneous patterning of multiple growth factors in three-dimensional hydrogels.** *Nature Materials* 2011, **10**:799–806.
163. Chueh B-H, Zheng Y, Torisawa Y-S, Hsiao AY, Ge C, Hsiong S, Huebsch N, Franceschi R, Mooney DJ, Takayama S: **Patterning alginate hydrogels using light-directed release of caged calcium in a microfluidic device.** *Biomed Microdevices* 2010, **12**:145–151.
164. Kang E, Jeong GS, Choi YY, Lee KH, Khademhosseini A, Lee S-H: **Digitally tunable physicochemical coding of material composition and topography in continuous microfibres.**

Nature Materials 2011, **10**:877–883.

165. Onoe H, Okitsu T, Itou A, Kato-Negishi M, Gojo R, Kiriya D, Sato K, Miura S, Iwanaga S, Kuribayashi-Shigetomi K, Matsunaga YT, Shimoyama Y, Takeuchi S: **Metre-long cell-laden microfibres exhibit tissue morphologies and functions.** *Nature Materials* 2013, **12**:584–590.

166. Khetan S, Guvendiren M, Legant WR, Cohen DM, Chen CS, Burdick JA: **Degradation-mediated cellular traction directs stem cell fate in covalently crosslinked three-dimensional hydrogels.** *Nature Materials* 2013, **12**:458–465.

167. Sedmera D, Pexieder T, Vuillemin M, Thompson RP, Anderson RH: **Developmental patterning of the myocardium.** *Anat Rec* 2000, **258**:319–337.

168. Takahashi H, Takahashi H, Shimizu T, Shimizu T, Nakayama M, Nakayama M, Yamato M, Yamato M, Okano T, Okano T: **The use of anisotropic cell sheets to control orientation during the self-organization of 3D muscle tissue.** *Biomaterials* 2013, **34**:7372–7380.

169. Takahashi H, Nakayama M, Shimizu T, Yamato M, Okano T: **Anisotropic cell sheets for constructing three-dimensional tissue with well-organized cell orientation.** *Biomaterials* 2011, **32**:8830–8838.

170. Li D, Wang Y, Xia Y: **Electrospinning Nanofibers as Uniaxially Aligned Arrays and Layer-by-Layer Stacked Films.** *Adv Mater* 2004, **16**:361–366.

171. Badrossamay MR, McIlwee HA, Goss JA, Parker KK: **Nanofiber assembly by rotary jet-spinning.** *Nano Lett* 2010, **10**:2257–2261.

172. Wang L, Shi J, Liu L, Secret E, CHEN Y: **Fabrication of polymer fiber scaffolds by centrifugal spinning for cell culture studies.** *Microelectronic Engineering* 2011.

173. Alamein MA, Stephens S, Liu Q, Skabo S, Warnke PH: **Mass production of nanofibrous extracellular matrix with controlled 3D morphology for large-scale soft tissue regeneration.** *Tissue Engineering Part C: Methods* 2013, **19**:458–472.

174. Lee J, Lee SY, Jang J, Jeong YH, Cho D-WW: **Fabrication of Patterned Nanofibrous Mats Using Direct-Write Electrospinning.** *Langmuir* 2012:120427135255000.

175. Sundararaghavan HG, Metter RB, Burdick JA: **Electrospun fibrous scaffolds with multiscale and photopatterned porosity.** *Macromol Biosci* 2010, **10**:265–270.

176. Liu J, Shi J, Secret E, Wang L, Zhang H: **Parametric optimization of micro-contact printing based thermal transfer of electrospun nanofibers.** *Microelectronic Engineering* 2010.

177. Agarwal A, Goss JA, Cho A, McCain ML, Parker KK: **Microfluidic heart on a chip for higher throughput pharmacological studies.** *Lab Chip* 2013, **13**:3599–3608.

178. Grosberg A, Nesmith AP, Goss JA, Brigham MD, McCain ML, Parker KK: **Muscle on a chip: in vitro contractility assays for smooth and striated muscle.** *J Pharmacol Toxicol Methods* 2012, **65**:126–135.

179. Schaaf S, Shibamiya A, Mewe M, Eder A, Stöhr A, Hirt MN, Rau T, Zimmermann W-H, Conradi L, Eschenhagen T, Hansen A: **Human engineered heart tissue as a versatile tool in basic research and preclinical toxicology.** *PLoS ONE* 2011, **6**:e26397.

180. Wang G, McCain ML, Yang L, He A, Pasqualini FS, Agarwal A, Yuan H, Jiang D, Zhang D, Zangi L, Geva J, Roberts AE, Ma Q, Ding J, Chen J, Wang D-Z, Li K, Wang J, Wanders RJA, Kulik W, Vaz FM, Laflamme MA, Murry CE, Chien KR, Kelley RI, Church GM, Parker KK, Pu WT: **Modeling the mitochondrial cardiomyopathy of Barth syndrome with induced pluripotent stem cell and heart-on-chip technologies.** *Nat Med* 2014, **20**:616–623.

181. Shiba Y, Fernandes S, Zhu W-Z, Filice D, Muskheli V, Kim J, Palpant NJ, Gantz J, Moyes KW, Reinecke H, Van Biber B, Dardas T, Mignone JL, Izawa A, Hanna R, Viswanathan M, Gold JD, Kotlikoff MI, Sarvazyan N, Kay MW, Murry CE, Laflamme MA: **Human ES-cell-derived cardiomyocytes electrically couple and suppress arrhythmias in injured hearts.** *Nature* 2012, **489**:322–325.
182. Stevens KR, Pabon L, Muskheli V, Murry CE: **Scaffold-free human cardiac tissue patch created from embryonic stem cells.** *Tissue Engineering : Part A* 2009, **15**:1211–1222.
183. Zimmermann W-H, Didié M, Döker S, Melnychenko I, Naito H, Rogge C, Tiburcy M, Eschenhagen T: **Heart muscle engineering: an update on cardiac muscle replacement therapy.** *Cardiovascular Research* 2006, **71**:419–429.
184. Hamdi H, Planat-Benard V, Bel A, Puymirat E, Geha R, Pidial L, Nematalla H, Bellamy V, Bouaziz P, Peyrard S, Casteilla L, Bruneval P, Hagège AA, Agbulut O, Menasché P: **Epicardial adipose stem cell sheets results in greater post-infarction survival than intramyocardial injections.** *Cardiovascular Research* 2011, **91**:483–491.
185. Bel A, Planat-Bernard V, Saito A, Bonnevie L, Bellamy V, Sabbah L, Bellabas L, Brinon B, Vanneaux V, Pradeau P, Peyrard S, Larghero J, Pouly J, Binder P, Garcia S, Shimizu T, Sawa Y, Okano T, Bruneval P, Desnos M, Hagège AA, Casteilla L, Pucéat M, Menasché P: **Composite cell sheets: a further step toward safe and effective myocardial regeneration by cardiac progenitors derived from embryonic stem cells.** *Circulation* 2010, **122**:S118–23.
186. Matsuura K, Haraguchi Y, Shimizu T: **Cell sheet transplantation for heart tissue repair.** *Journal of Controlled Release* 2013.
187. Yang C, Tibbitt MW, Basta L, Anseth KS: **Mechanical memory and dosing influence stem cell fate.** *Nature Materials* 2014, **13**:645–652.
188. Menasché P, Vanneaux V, Fabreguettes J-R, Bel A, Tosca L, Garcia S, Bellamy V, Farouz Y, Pouly J, Damour O, Périer M-C, Desnos M, Hagège A, Agbulut O, Bruneval P, Tachdjian G, Trouvin J-H, Larghero J: **Towards a clinical use of human embryonic stem cell-derived cardiac progenitors: a translational experience.** *European Heart Journal* 2014.
189. Farouz Y, Chen Y, Menasché P, Ino J, Atlan M, Le Visage C, Letourneur D: **[Mending broken hearts and repairing damaged vessels] (French title: Réparer les cœurs brisés et les vaisseaux abîmés).** *Biofutur* 2012:1–4.
190. Bellamy V, Vanneaux V, Bel A, Nematalla H, Boitard SE, Farouz Y, Joanne P, Périer M-C, Robidel E, Mandet C, Hagège A, Bruneval P, Larghero J, Agbulut O, Menasché P: **Long-term functional benefits of human embryonic stem cell-derived cardiac progenitors embedded into a fibrin scaffold.** *Journal of Heart and Lung Transplantation* 2014:1–10.
191. Faustino RS, Terzic A: **Interactome of a cardiopoietic precursor.** *J of Cardiovasc Trans Res* 2008, **1**:120–126.
192. Faustino RS, Chiriak A, Niederlander NJ, Nelson TJ, Behfar A, Mishra PK, Macura S, Michalak M, Terzic A, Perez-Terzic C: **Decoded calreticulin-deficient embryonic stem cell transcriptome resolves latent cardiophenotype.** *Stem Cells* 2010, **28**:1281–1291.
193. Faustino RS, Behfar A, Perez-Terzic C, Terzic A: **Genomic chart guiding embryonic stem cell cardiopoiesis.** *Genome Biol* 2008, **9**:R6.
194. Behfar A, Faustino RS, Arrell DK, Dzeja PP, Perez-Terzic C, Terzic A: **Guided stem cell cardiopoiesis: discovery and translation.** *Journal of Molecular and Cellular Cardiology* 2008, **45**:523–529.
195. Young DA, DeQuach JA, Christman KL: **Human cardiomyogenesis and the need for systems biology analysis.** *WIREs Syst Biol Med* 2011, **3**:666–680.

196. Gould RA, Aboulmouna LM, Varner JD, Butcher JT: **Hierarchical approaches for systems modeling in cardiac development.** *WIREs Syst Biol Med* 2013, **5**:289–305.
197. Colas AR, McKeithan WL, Cunningham TJ, Bushway PJ, Garmire LX, Duester G, Subramaniam S, Mercola M: **Whole-genome microRNA screening identifies let-7 and mir-18 as regulators of germ layer formation during early embryogenesis.** *Genes & Development* 2012, **26**:2567–2579.
198. Underhill GH: **Stem cell bioengineering at the interface of systems-based models and high-throughput platforms.** *WIREs Syst Biol Med* 2012, **4**:525–545.

Chapter 3 – Safety, Regulatory and Ethical Issue of human studies

Important Note: this chapter has been written by Yohan Farouz, Mathilde Cossé, Nisa Renault and Philippe Menasché and was published in the following book [1]:
Suuronen EJ, Ruel M: Biomaterials for Cardiac Regeneration. *Springer* 2015.

Introduction

To get approval for initiating a stem cell clinical trial is becoming increasingly difficult because of the stringency of regulatory guidelines. The first section of this chapter presents an outline of the major issues which should be kept in mind by investigators from the very early onset of the program so as to frame it in such a way that it may satisfactorily comply with the multiple constraints, thereby avoiding a waste of time, efforts, and money. While the regulators legitimately require proof of efficacy of the stem cell product and mechanistic insights before granting approval for a human study, their main concern still pertains to safety, particularly for first-in-man interventions. The next section of this chapter briefly summarizes the main cell-related complications that have happened or remain of concern, and which need to be addressed by a risk plan analysis. Finally, stem cells pose unique ethical problems, particularly when one is dealing with human pluripotent stem cells and some general considerations surrounding this ethical debate are presented in the last part of the chapter.

Safety Issues

Overall, the safety record of stem cell trials has been excellent [2]. The incidence of adverse events observed in treated patients has usually not been different from that of control groups. Only two complications have raised specific concerns: arrhythmias and tumor development. They are expanded accordingly in the sections below.

Arrhythmias

Concerns about arrhythmic events have been raised from the very beginning of our skeletal myoblast trials where some patients experienced this complication (which was never lethal). A possible explanation which had been provided was that failure of engrafted myoblasts to express connexin-43 resulted in their isolation, thereby setting the stage for reentries. Indeed, several factors can contribute to the arrhythmogenicity of stem cells, including the immaturity of electrical phenotypes of the transplanted cells and poor cell–cell coupling [3]. Even ESC-derived cardiomyocytes fail to consistently couple with host cardiomyocytes in a guinea pig chronic infarct model [4], and recent data from Murry's group [5] using a nonhuman primate model of myocardial infarction have reported an early high incidence of arrhythmias. The mechanism of these episodes is likely multifactorial, but highlights the fact that cardiac-lineage commitment does not automatically result in a coordinated electrical integration. Furthermore, two mechanisms not directly related to the cells themselves deserve special consideration: the first is the underlying substrate since patients with heart failure are prone to develop arrhythmias, as demonstrated by the occurrence of these events in the placebo-treated patients of the myoblast transplantation (MAGIC) trial [6]. The second mechanism pertains to

the mode of cell delivery. In most cases, cells are injected directly into the myocardium in several areas; these multiple intramyocardial punctures induce inflammation and result in isolated clusters which may slow conduction of electrical impulses and set the stage for reentries; this hypothesis is actually supported by the observation that cells injected into the myocardium cause more arrhythmias than when they are delivered through the systemic route [7]. The additional finding that the epicardial delivery of a cell-loaded patch is also less arrhythmogenic than when the same cells are directly injected into the myocardium [8] strengthens the role of the cell delivery modalities in the pathogenesis of arrhythmias. Finally, if allogeneic cells are to be used, a possible immune rejection and the attendant inflammation can further contribute to this complication. In practice, conservatory preventive measures may include a pulse of periprocedural anti-inflammatory drugs (a 24-h corticosteroid-based regimen was used in our myoblast trials), the limitation of multiple myocardial punctures (through the endocardium or transepically) and the implantation of an automatic defibrillator, which may in any case be indicated or even be already in place given the extent of the left ventricular dysfunction in heart failure patients eligible for stem cell therapy. Conversely, genetic engineering of the cells to force them to over-express connexin-43 is conceptually attractive and has been experimentally successful [9], (but this approach adds so many additional layers of technical and regulatory complexity that it is unlikely to ever reach the level of clinical applications.

Tumor Development

This concern was initially relevant to culture-expanded MSCs, which can acquire genetic abnormalities and even undergo malignant transformation. However, MSCs currently tested in a huge number of clinical trials, extending well beyond the field of cardiology, usually undergo only a limited number of passages and the outcomes of these trials have failed to document an oncologic risk [10].

Concerns about tumorigenesis are clearly greater with the use of pluripotent stem cells because their fundamental properties (self-renewal and pluripotency) are intrinsically linked to a tumorigenic potential. It is well established that both ESCs and iPSCs can become genetically unstable during in vitro propagation [11], and although some cells may respond to these abnormalities by undergoing apoptosis, others can gain a selective growth advantage [12] and generate teratomas (which are benign tumors but can be harmful through their compressive effects as they grow) or their malignant variety (teratocarcinoma). Obviously, for therapeutic applications, these cells will not be used in their originally undifferentiated state, but rather are exposed to specific cues to drive their fate towards a given lineage prior to transplantation. The risk, however, is that the ultimate lineage-committed population may

remain, even at a low degree, contaminated by a fraction of pluripotent cells prone to uncontrolled proliferation.

In practice, mitigation of the oncogenic risk requires three main categories of measures. First, it is critical to purify the differentiated cell population as much as possible to “purge” it from its unspecified components. Currently, selection based on flow cytometry is not compatible with clinical standards (although a device may be under development). Enrichment for the target lineage-committed cells has therefore to rely on immunomagnetic sorting using relevant surface markers. In our experience with ESC-derived cardiac progenitors, we have found that stage-specific embryonic antigen-1 (SSEA-1) could be used for labeling cells that have entered a differentiation pathway [13], and thus the collected SSEA-1-positive cell yield is the one used for transplantation. We acknowledge, however, that alternate and possibly more robust purification strategies need to be investigated. They could be based on a negative-type of selection, targeting markers of still pluripotent stem cells like SSEA-5 [14] or lectins [15] or the selective elimination of residual undifferentiated cells by metabolic interventions [16], cytotoxic antibodies [17] or genotoxic drugs [18].

Second, the purified population should be extensively screened *in vitro* for genetic abnormalities which might have arisen during the expansion/specification steps. As part of the translational process which led to approval for our human phase I trial of ESC-derived cardiac progenitor transplantation in patients with severe heart failure, we have used a combinatorial approach including karyotype, oligonucleotide based-array comparative genomic hybridization and fluorescent *in situ* hybridization focusing on chromosomes known to be particularly unstable, as each of these methods provides a different and complementary set of information.

Third, the teratogenic potential of the cells should finally be assessed using one of the different tests that are available [19], of which injection of cells in severely immunodeficient mice is the most widely used. In our preclinical studies, we have used this mouse model and tried to sensitize the occurrence of teratomas by subcutaneous injections of cells mixed with Matrigel [20]. We have also transplanted nonhuman primate ESCs into infarcted primates [13] since this allogeneic setting could be more predictive of the tumorigenic risk than data collected in xenograft models [21]. In fact, we have never observed teratomas in either model following transplantation of the “purified” SSEA-1-positive cell population. For the clinical protocol, the purity rate, which is one of the release criteria, has been set at 95 % and it is noteworthy that when the SSEA-1-*negative* fraction collected at the completion of sorting was injected *alone* at high doses in immunodeficient mice, it also failed to be teratogenic. The transcriptomic analysis of this population showed that it still expressed pluripotency genes to various

degrees, but likely not a level exceeding the threshold above which teratomas could develop [22].

It should finally be emphasized that iPSCs share with ESCs this oncogenic risk since they undergo the same type of expansion once they have been brought back to an undifferentiated state. It has even be reported that they could be more tumorigenic than ESCs [23] because of some additional tumorigenic factors like preexisting somatic mutations in the parent cells, genomic insertion of transgenes or genetic instability associated with the global hypomethylation state resulting from the induction of pluripotency [12].

In summary, the oncogenic risk of pluripotent cells cannot be ignored. It is therefore mandatory to fully inform the patients about it, but also to reduce it through the combination of safety measures mentioned above. They are likely more clinically relevant than genetically engineered cells with suicide genes that can be activated in vivo to eliminate transduced ESCs that have escaped growth control [24], since this approach raises other mechanistic and regulatory issues. Additional precautions include the exclusion of patients with an increased risk of cancer because of a comorbidity, the limitation of immunosuppression (justified if, on the basis of the paracrine hypothesis, the main target is optimization of early cell retention to give cells enough time to release their protective factors rather than long-term engraftment) and a regular monitoring of these stem cell recipients. It is also possible that failure of the cells to engraft in the long-term provides a natural fail-safe protective mechanism.

Rejection

This complication is obviously relevant to the use of allogeneic/xenogeneic cells only. As a separate chapter of this book is devoted to the immunological issues associated with cell and biomaterial therapies, this paragraph will be limited to two brief comments. First, only immunosuppressive drugs have been used so far in clinical studies entailing transplantation of non-autologous cells, but protocols have largely be empirical as many unknown factors persist like the nature of the most effective drugs, their optimal dosage and the specific interactions they may have with stem cells, independently of their immunosuppressive properties [25]. Second, as alluded to above, it is increasingly believed that transplanted cells do not act by generating new myocardial tissue by themselves, but rather foster endogenous repair pathways through the release of an array of factors [26]. In this setting, what may be critical is to optimize their early residency in the transplanted tissue, long enough for them to release the bioactive molecules underlying their protective effects. In this context, their expected clearance over time should not necessarily compromise the benefits of the transplantation as long as endogenous paracrine signaling has been appropriately turned on and remains long-acting. The exact time frame during which cells need to be present is not precisely known but, based on literature data, the time mismatch between the fast clearance

of the cells and the sustained maintenance of functional benefits suggests that the “operational” time window is probably short, in the order of a few weeks at most. It will be important to better quantify this time window as it directly impacts the duration of any immunosuppression regimen which, if shortened, will correspondingly minimize the drug side-effects and favorably shift the risk-to-benefit ratio. Induction of immune tolerance for a relatively limited period of time could also become an attractive alternative to pharmacologic immunosuppression.

Stent Restenosis/Thrombosis

There are no data to support that intra-coronary applications of bone marrow- or adipose tissue-derived cells increase the incidence of in-stent restenosis or thrombosis.

Calcification

One experimental observation of intramyocardial calcification has been reported following transplantation of bone marrow-derived cells [27], but this isolated case described long ago looks anecdotal and has never been confirmed by the follow-up clinical studies of stem cell recipients.

Regulatory Issues

To successfully translate bench-scale methods to a manufacturing process complying with the current Good Manufacturing Practices (GMP), a dialogue should be initiated from the very beginning of any clinically targeted program to clearly identify what is allowed, what can be tolerated in the setting of a limited phase I trial (but would no longer be accepted for a larger-scale phase II/III study) and what is strictly forbidden. The guidelines of the European and US agencies are publicly available on the respective websites of the European Medicines Agency (EMA) and the US Food and Drug Administration (FDA), and their enumeration would be tedious. We will then limit our comments to some general guidelines that may be helpful to avoid waste of time and money and streamline the translational process leading to the initial application for trial approval.

Preclinical Studies

Renowned statistician George E. P. Box’s statement that “All models are wrong but some are useful” is quite relevant. Most stem cell studies have been performed in rodents which are actually useful for screening purposes and, if mice are used, for mechanistic gain-of-function and loss-of function studies, enabled by the availability of transgenic strains. However, the physiology of rodents markedly diverges from that of humans (which is best exemplified by the differences in heart rates), and thus the regulators now commonly request additional large

animal studies. Although pig, sheep, and even nonhuman primates cannot fully duplicate the complex patterns of human diseases, they may yet be useful for: (1) establishing dose–effect relationships; (2) assessing function and tracking cell fate with front-edge imaging technologies under clinically relevant scale conditions; (3) testing delivery devices; and (4) allowing for more extended observation periods, which is relevant to the long-term assessment of safety of cell-based therapeutics. To be reliable, however, these animal studies should be conducted according to the same principles which govern clinical trials, particularly sample size calculations, randomization, blinding, and choice of appropriate controls [28]. This is mandatory to improve the predictive value of animal data. **Table 3.1** presents a summarized road-map of studies which may be required before submitting an application for an initial clinical trial. Each component of the roadmap has, however, to be tailored to the specific composition of the cell product, its manufacturing process, presumed mechanism of action and anticipated mode of delivery as well as the target disease.

<i>In vitro</i> studies
<ul style="list-style-type: none"> • Cell genotype and phenotype, including epigenetic changes potentially induced by differentiation/culture conditions • Optimal culture conditions • Electrophysiological properties • Resistance to stress/protective effects of interventions targeted at improving cell viability • Composition of the secretome
Small animal studies
<ul style="list-style-type: none"> • Comparative studies of different cell types (function, engraftment rate, phenotype, effects on angiogenesis, fibrosis, apoptosis, recruitment of endogenous progenitor/stem cells) • Dose-effect relationships • Screening of biomaterials if used alone or combined with cells (safety, inflammatory, and immune responses, effects on the local microenvironment) • Mechanistic studies (gain-of-function and loss-of-function transgenic models)
Large animal studies
<ul style="list-style-type: none"> • Validation of cell efficacy under clinically relevant scale-up in species physiologically closer to humans • Assessment of best routes/techniques of delivery with collection of biodistribution data • Extension of follow-up for efficacy (transient vs. sustained benefits) and safety (ectopic seeding of cells in remote off-target organs) studies

Table 3.1 Summary of major steps to be taken into account before submission to the Regulatory Authorities

Cell Manufacturing

The source of the cells, the results of infectious disease screening and details about the collection method (mobilization, surgery, leukapheresis, devices like those used for liposuction of adipose tissue-derived stem cells) must be documented. Further cell processing (isolation, scale-up, optimized enzymatic dissociation and, whenever required, cryopreservation, storage and thawing) needs to be performed in GMP-approved facilities. The regulators are much concerned about the full traceability record and quality controls for

all raw materials (reagents, media) and efforts should thus be made from the beginning to get as much information as possible from the suppliers, which is not always easy. In contrast to a common thought, the use of animal-derived products is not (yet) completely prohibited; for example, fetal calf serum is tolerated provided the serum is irradiated and calves originate from a transmissible spongiform encephalopathy-free country. However, because of bio-safety concerns, there is an increasing trend to eliminate xenogeneic components as well as feeder cells when they are required (for example, for growing pluripotent stem cells) and to culture cells onto synthetic matrices and in fully defined chemical media (from this standpoint, human platelet lysate has been promoted as a substitute for fetal calf serum with the additional advantage that it may feature less variability from one batch to the other). Of note, the exact composition of these defined media is usually proprietary information of the company, which will not be transmitted to the investigators but can be communicated to the regulatory agency under a confidentiality agreement. In addition, different growth factors often have to supplement the media at one step of the procedure. They should ideally be GMP-grade products, which is not yet the case for many of them; at least, their characteristics (origin, mode of processing, type of sterilization, post-production quality controls) should be carefully documented, preferably under the form of a company-issued Master File. Furthermore, as part of a general trend to standardize procedures, minimize risks of contamination associated with frequent changing of media, improve consistency, reproducibility, and production yield of the cell product, and reduce costs, current time-consuming and labor-consuming manual handling of cells in open flasks will increasingly be replaced by fully automated systems incorporated in closed bioreactors [29]. A specific issue is raised by the techniques that may be required for selecting a given subset of cells within a heterogeneous population. As previously mentioned, enrichment for a cell fraction (for example, CD34+ or CD133+ progenitors from a bone marrow harvest or cardiac lineage-committed progenitor cells derived from ESC) has to primarily rely on immunomagnetic sorting. While some microbead-coupled antibodies approved for clinical use are available, such is not the case for others targeted at some specific surface markers which may be relevant to a particular indication. The regulators may then tolerate a “research grade” antibody for a limited phase I trial provided a maximum of microbiological data are provided. However, for a larger-scale study, antibodies will be required to be upgraded to a “clinical” level. This implies starting from the hybridoma, setting up master and working cell banks, going through controlled purification procedures and finally performing a full set of functional assays and microbiological controls to ensure that the final product has the required affinity for the target surface antigen and is free from contamination by adventitious agents (microbial or viral). The time required for completing the whole process and the cost of such a development should not be underscored. The whole manufacturing process should be controlled by a robust quality management system allowing

to monitor quality parameters at each processing step to ensure that the final product will meet the preset specifications with regard to stability, functionality and safety (absence of aberrant culture-induced changes, absence of contamination, and in the case where pluripotent stem cells have been the starting material, a high purity rate providing the greatest guarantee against a tumorigenic potential). Although the development of cell therapy products is governed by common principles on manufacturing and quality control plans, specificities exist in relation with the origin of the cells (**Table 3.2**). Furthermore, when cells are not intended to be used immediately but undergo an initial storage in cell banks, each of these banks (Master Cell Bank and Working Cell Bank) needs to be extensively qualified to adequately establish the safety, purity, biological activity, and stability of the cells. In particular, the impact of the freezing and thawing steps as well as the effects of cryoprotectants should be evaluated. In all cases, labeling, storage, and transport conditions also need to be extensively characterized and validated.

Cell types	Requirements
All (autologous and allogeneic)	<ul style="list-style-type: none"> • Cell source • Mobilization protocol • Collection or recovery method • Donor screening and testing
Autologous	<ul style="list-style-type: none"> • Assessment of the potential risk of propagation of pathogenic agents that may be present in the donor due to manufacturing process. • Precautions to prevent the spread of viruses and other adventitious agents to persons other than the autologous recipient
Allogeneic	<ul style="list-style-type: none"> • Screening and testing for HIV-1, HIV-2, hepatitis B virus (HBV, surface and core antigens), hepatitis C virus (HCV), <i>Treponema pallidum</i> (syphilis) and CJD (screening only) • Documentation of tests used, description of the type of serological, diagnostic and clinical history data obtained from the donor • Typing for polymorphisms and human leukocyte antigens (HLA) matching, where appropriate • If cord blood or other maternally derived tissues, testing and screening performed on birth mothers

Table 3.2 Main regulatory requirements for autologous and allogeneic cells.

Adapted from the Content and Review of Chemistry, Manufacturing, and Control (CMC) Information for Human Gene Therapy Investigational New Drug Applications (INDs) (<http://www.fda.gov/cber/guidelines.htm>)

Release Criteria

These are an important component of the regulatory requirements. Some of them, like cell counting, viability, sterility, or identity (based on the expeditious flow cytometry-based assessment of the relevant surface markers on an aliquot of the final cell product) can be performed in a straightforward fashion. Conversely, demonstration of potency is more challenging as it implies measuring a biological activity which is linked to the biological

property of interest. This requires the investigator to perform functional assays both in vitro (such as gene expression profiling) and in vivo (animal testing), in which case readouts will lag behind the time of cell delivery and, whenever the product has a short half-life, will require surrogate assays which may be acceptable as long as they are reliable and sensitive enough. These hurdles emphasize the several advantages of using banked allogeneic cells: off-the-shelf immediate availability; possibility of an extensive functional, genetic and microbiological qualification prior to use; elimination of the batch-to-batch variability intrinsic to patient-specific products; and availability of fully documented quality controls at the time of batch release. The drawback of allogeneic cells is rejection. However, as stated above, this may not be a roadblock if reliance on the paracrine hypothesis leads to privilege cell engraftment during a relatively limited period of time post-transplantation with a correspondingly short immunosuppressive regimen. Like for tumors, clearance of the cells could even be looked at a natural fail-safe mechanism preventing the occurrence of potentially delayed cell-induced complications. **Table 3.3** presents a summary of the major release criteria which are usually required by the Regulatory Authorities before a specific batch can be used for human use.

Identity	
<ul style="list-style-type: none"> • Expression of specific markers indicative of cell type, pluripotency, lineage commitment, and/or assays of functionality • Characterization of the profile of the final product if heterogeneous cell population (mRNA-based markers, if used, should be validated by corresponding protein marker expression) 	
Purity	
<ul style="list-style-type: none"> • Minimisation of undesirable non-cellular impurities or cell debris • Demonstration of product consistency (previous development and selection of appropriate in-process controls and release tests) 	
Potency^a	
Functional tests and/or marker-based assays showing correlation with the intended therapeutic effect:	
<ul style="list-style-type: none"> • In vitro and/or in vivo tests • Release of a biologically relevant substance • Formation of extracellular matrix • Demonstration of differentiation • Interactions with immune cells, migration 	
Tumorigenicity and genomic stability	
<ul style="list-style-type: none"> • Cytogenetic analysis (Karyotype, FISH, CGH-arrays) • Telomerase activity • Proliferative capacity • Senescence 	
Stability	
Description of a stability protocol	Measure of product sterility, identity, purity, quality, potency
In-process stability testing	Analyses carried out pre-freeze and post-thaw
Final product stability testing (under proposed shipping conditions)	Product integrity, sterility, and potency

^aGuidance for Industry Potency Tests for Cellular and Gene Therapy Products, <http://www.fda.gov/BiologicsBloodVaccines/GuidanceComplianceRegulatoryInformation/Guidances/default.htm>

Table 3.3 Major properties of cells that need to be characterized prior to a clinical use

Cell and Scaffold Combined Products

Of note, cells (as well as tissue-engineered products, i.e., products which may contain “biomolecules, biomaterials, chemical substances, scaffolds, or matrices”) belong to the category of biologics now covered in Europe under the general term of Advanced Therapy Medicinal Products (ATMP). If, however, cells are to be combined with a scaffold, the latter will fall under the medical device regulation and will thus be evaluated according to tissue engineering-specific requirements (biocompatibility, description of the manufacturing process and characterization of its residuals, sterility, toxicity). For the combination product, cell seeding onto the material needs to be documented (dose response, cell growth, cell functions, cell– scaffold interactions) and the final cell/scaffold product will then have to undergo extensive in vitro and in vivo testing specifically assessing safety, potency, durability, cell fate, structure and biomaterial decomposition products. In particular, it is relevant to assess to what extent the device may impact the biologic with regard to genotypic/phenotypic changes, survival of cells within the scaffold, possible protection against immune responses or adventitious agents and, on the other hand, to equally assess to what extent the biologic may impact the device such as changes in rate of breakdown of biodegradable materials or any other biocompatibility issues. Some specific regulatory steps are summarized in [Table 3.4](#) but the readers interested in having a broader view of the regulatory framework are invited to look at the websites of the European and US Agencies, particularly the Reflection paper on classification of Advanced Therapy Medicinal Products issued by the EMA (http://www.ema.europa.eu/ema/index.jsp?curl=pages/regulation/general/general_content_000296.jsp&mid=WC0b01ac058007f4bc) and the FDA-issued draft guidance entitled “Considerations for the Design of Early-Phase Clinical Trials of Cellular and Gene Therapy Products”

(<http://www.fda.gov/BiologicsBloodVaccines/CellularGeneTherapyProducts/default.htm>).

At the end, the investigators’ decision to proceed to a clinical trial and its ultimate approval by the regulatory authorities remain largely based on the classical risk-to- benefit ratio. Diseases for which there are still unmet medical needs clearly remain the priority targets of new interventions, including those entailing the use of stem cells. We acknowledge, however, that it may be occasionally challenging to find the right balance between a permissive attitude aimed at not depriving severely sick patients from a potentially efficacious therapy even though uncertainties may persist regarding mechanism of action or validation of preclinical models and a more conservative attitude dictated by the willingness to avoid exposing the patients to the risks inherent to any novel intervention. Finally, it is worth mentioning that a current important area of research aims at leveraging data on the paracrine effects of the cells by assessing whether their transplantation can be replaced by the administration of the sole

secretome with equivalent outcomes. As shown by the definition given above, such cell-derived biologics would still fall under the regulatory framework of the ATMP, but this approach is nevertheless attractive because it might streamline the manufacturing process and improve cost-effectiveness. The same holds true for acellular biomimetic materials intended to duplicate the stimulating effects of cells on host-associated repair mechanisms [30, 31].

Parameter	Requirements
Cells	<ul style="list-style-type: none"> • Characterization (similar to cell therapy products)
Scaffold	<ul style="list-style-type: none"> • Composition • Degradation profile • Biomechanical performance • Biocompatibility (with respect to host response to the scaffold and to the cell components of the product)
Biological responsiveness	<ul style="list-style-type: none"> • Proof-of-concept studies using morphological and functional end points
Dose response	
Durability of the response	
Safety	<ul style="list-style-type: none"> • Tumorigenicity • Altered tissue function at the delivery site • Inappropriate cellular differentiation • Inflammatory infiltrates • Immune response • Ectopic tissue formation due to cell migration

Table 3.4 Main regulatory requirements for biomaterials alone or associated with cells (combined product)

Ethical Issues

The objective of this section is not to discuss the general ethical issues which surround research on human tissues or the design and conduct of clinical trials, which fall under the general principles issued in the Declaration of Helsinki (<http://www.wma.net/en/20activities/10ethics/10helsinki/index.html>). We would rather like to highlight two issues that more specifically pertain to the use of stem cells.

The first issue is related to the procurement of the cells and, as such, fundamentally differs depending on their origin. When cells are harvested from the patient, there are practically no ethical issues and only the risk-to-benefit ratio of the intended clinical trial needs to be considered. The problem is obviously completely different for human ESCs. The legislation in this area greatly varies from one country to another and reflects the diversity of political positions which is, to a large extent, driven by religious considerations. Banning this research has indeed been the long-standing fight of the pro-life lobbies. Their arguments should be respected as long as they do not tend to be justified by erroneous scientific statements. The

most commonly used of these arguments is that these cells are tumorigenic. Definitely they are, if they were to be used in their pluripotent, undifferentiated state. However, the opponents of ESC research pretend to ignore that nobody has ever thought of using them without a prior step of lineage commitment and a subsequent phase of purification intended to discard the potentially residual “contaminating” cells, as discussed in the previous sections. Another commonly heard argument is that despite the huge amount of money which has been devoted to ESC research, nothing has yet come out in terms of improvement of patient outcomes. Again, those who disseminate these statements pretend to ignore that clinical trials entailing transplantation of human ESCs have just started, that there are still few of them (currently limited to the spinal cord, retinal diseases and heart failure) and that it will necessarily take time before any conclusion regarding efficacy can be drawn. The third argument which has been repeatedly brought up is that the availability of iPSC has made ESC research obsolete. The best counter-argument has come from Yamanaka (father of the iPSC) himself in a paper whose title “New advances in iPS cell research do not obviate the need for human embryonic stem cells” speaks for itself [32], and which strongly supports the cross-fertilization between these two areas of research and thus the absolute requirement to pursue their development “hand in hand.”

Finally, it should be reiterated that these cells are derived from leftover embryos conceived in the setting of in vitro fertilization, once the fully informed parents have given up a parental project. As the alternate option would then be the simple destruction of these supernumerary embryos, it is really debatable that their use for research and, possibly, therapeutic applications, is ethically condemnable. At the opposite, there is a wide consensus that the intentional creation of embryos for research would be ethically unacceptable but the huge number of cryofrozen embryos which are already stored and thus potentially available for scientific and/or medical purposes makes such an approach largely irrelevant.

A second specific ethical concern is related to the design of clinical trials and, more specifically, to the choice of the control groups. Here, scientific rigor may come in opposition with the respect of ethical principles. This is best exemplified by studies entailing intracoronary infusion of autologous bone marrow-derived cells following successful percutaneously induced revascularization of the culprit artery. One can question whether it is ethical to impose the patients with the discomfort and risks (even if they are limited) of a sham iliac crest puncture followed by a repeat intra-coronary catheterization for delivery of a placebo medium. On the contrary, one can argue that such a stringent design is important to minimize biases in interpretation of outcomes. In our own initial experience with skeletal myoblasts, we have been committed to perform a muscular biopsy and in-scar injections in all randomized patients, which implied that those assigned to the control group eventually received the myoblast-free suspension medium[6]. This strategy proved useful to document, for example, that after 6

months, there was no significant differences in arrhythmic events (as documented by recordings of the automatic defibrillators implanted in all patients) between the myoblast-treated and untreated cohorts. To avoid any “loss of chance,” one possible option when harvested cells are not re injected because of the allocation of the patient to the control group is to cryopreserve the cells and, once the trial is completed, to deliver them in a minimally invasive fashion (whenever feasible) if the outcome has been positive. However, this requires a detailed characterization of the cryopreservation procedures which may not have been initially planned as well as additional quality checks to ensure that thawed cells remain functionally competent. Clearly, such a “study within the study” may represent a significant burden in terms of time, efforts, and budget. In practice, the dilemma is often resolved by the local Ethical Review Boards whose variable permissiveness is actually reflected by the large variability in the nature of the “control” groups, which range from the absence of any intervention (standard of care) to the delivery of placebo and active treatments without any possibility of distinguishing them so as to ensure a rigorous double blinding [33].

Conclusion

In conclusion, stem cells and other biologics in therapy pose a unique set of technical, regulatory, and ethical challenges. It is critical not to expose patients to the unavoidably unknown risks of any novel therapy. However, it would be equally unfair to deny them the possibility of even a relief if it can be provided by a treatment targeting diseases for which there is still an unmet medical need. The main driver thus remains a balanced estimate of the risk-to-benefit ratio which can be optimized by a tight and permanent cross talk between scientists, clinicians, engineers, regulators, and trialists. Furthermore, given the magnitude of the technical and regulatory challenges associated with stem cell therapy, it is clear that whereas phase I studies can still be academia-driven, the same is no longer possible for larger Phase II/III trials which require the involvement of industry. In turn, this does not only imply a possible control over intellectual property but also the setup of a cost-effective manufacturing process. As such, the company incentives on the one hand, and the safety, regulatory, and ethical guidelines on the other hand, join together under the form of the “KISS” (Keep it Safe and Simple) principle that should govern clinically targeted stem cell programs.

References

1. Suuronen EJ, Ruel M: **Biomaterials for Cardiac Regeneration**. Springer 2015.
2. Fischer SA, Brunskill SJ, Doree C, Mathur A, Taggart DP, Martin-Rendon E: **Stem cell therapy for chronic ischaemic heart disease and congestive heart failure (Review)**. *The Cochrane Collaboration* 2014;1–170.
3. Liu Y, Tse H-F: **The proarrhythmic risk of cell therapy for cardiovascular diseases**. *Expert Rev Cardiovasc Ther* 2011, **9**:1593–1601.
4. Shiba Y, Filice D, Fernandes S, Minami E, Dupras SK, Biber BV, Trinh P, Hirota Y, Gold JD, Viswanathan M, Laflamme MA: **Electrical Integration of Human Embryonic Stem Cell-Derived Cardiomyocytes in a Guinea Pig Chronic Infarct Model**. *Journal of Cardiovascular Pharmacology and Therapeutics* 2014.
5. Chong JJH, Yang X, Don CW, Minami E, Liu Y-W, Weyers JJ, Mahoney WM, Van Biber B, Cook SM, Palpant NJ, Gantz JA, Fugate JA, Muskheli V, Gough GM, Vogel KW, Astley CA, Hotchkiss CE, Baldessari A, Pabon L, Reinecke H, Gill EA, Nelson V, Kiem H-P, Laflamme MA, Murry CE: **Human embryonic-stem-cell-derived cardiomyocytes regenerate non-human primate hearts**. *Nature* 2014, **510**:273–277.
6. Menasche P, Alfieri O, Janssens S, McKenna W, Reichenspurner H, Trinquart L, Vilquin JT, Marolleau JP, Seymour B, Larghero J, Lake S, Chatellier G, Solomon S, Desnos M, Hagege AA: **The Myoblast Autologous Grafting in Ischemic Cardiomyopathy (MAGIC) Trial: First Randomized Placebo-Controlled Study of Myoblast Transplantation**. *Circulation* 2008, **117**:1189–1200.
7. Fukushima S, Varela-Carver A, Copen SR, Yamahara K, Felkin LE, Lee J, Barton PJR, Terracciano CMN, Yacoub MH, Suzuki K: **Direct Intramyocardial But Not Intracoronary Injection of Bone Marrow Cells Induces Ventricular Arrhythmias in a Rat Chronic Ischemic Heart Failure Model**. *Circulation* 2007, **115**:2254–2261.
8. Terajima Y, Shimizu T, Tsuruyama S, Sekine H, Ishii H, Yamazaki K, Hagiwara N, Okano T: **Autologous Skeletal Myoblast Sheet Therapy for Porcine Myocardial Infarction Without Increasing Risk of Arrhythmia**. *cell med* 2014, **6**:99–109.
9. Abraham MR, Henrikson CA, Tung L, Chang MG, Aon M, Tian X, Li RA, ORourke B, Marban E: **Antiarrhythmic Engineering of Skeletal Myoblasts for Cardiac Transplantation**. *Circulation Research* 2005, **97**:159–167.
10. Hatzistergos KE, Blum A, Ince TA, Grichnik JM, Hare JM: **What Is the Oncologic Risk of Stem Cell Treatment for Heart Disease?** *Circulation Research* 2011, **108**:1300–1303.
11. Ben-David U, Benvenisty N: **The tumorigenicity of human embryonic and induced pluripotent stem cells**. *Nature Publishing Group* 2011, **11**:268–277.
12. Lee AS, Tang C, Rao MS, Weissman IL, Wu JC: **Tumorigenicity as a clinical hurdle for pluripotent stem cell therapies**. *Nat Med* 2013, **19**:998–1004.
13. Blin G, Nury D, Stefanovic S, Neri T, Guillevic O, Brinon B, Bellamy V, Rücker-Martin C, Barbry P, Bel A, Bruneval P, Cowan C, Pouly J, Mitalipov S, Gouadon E, Binder P, Hagege A, Desnos M, Renaud J-F, Menasché P, Pucéat M: **A purified population of multipotent cardiovascular progenitors derived from primate pluripotent stem cells engrafts in postmyocardial infarcted nonhuman primates**. *J Clin Invest* 2010, **120**:1125–1139.
14. Tang C, Lee AS, Volkmer J-P, Sahoo D, Nag D, Mosley AR, Inlay MA, Ardehali R, Chavez SL, Pera RAR, Behr B, Wu JC, Weissman IL, Drukker M: **An antibody against sseA-5 glycan on human**

pluripotent stem cells enables removal of teratoma-forming cells. *Nature Biotechnology* 2011, **29**:829–834.

15. Wang Y-C, Nakagawa M, Garitaonandia I, Slavin I, Altun G, Lacharite RM, Nazor KL, Tran HT, Lynch CL, Leonardo TR, Liu Y, Peterson SE, Laurent LC, Yamanaka S, Loring JF: **Specific lectin biomarkers for isolation of human pluripotent stem cells identified through array-based glycomic analysis.** *Cell Res* 2011, **21**:1551–1563.

16. Tohyama S, Hattori F, Sano M, Hishiki T, Nagahata Y, Matsuura T, Hashimoto H, Suzuki T, Yamashita H, Satoh Y, Egashira T, Seki T, Muraoka N, Yamakawa H, Ohgino Y, Tanaka T, Yoichi M, Yuasa S, Murata M, Suematsu M, Fukuda K: **Distinct Metabolic Flow Enables Large-Scale Purification of Mouse and Human Pluripotent Stem Cell-Derived Cardiomyocytes.** *Stem Cell* 2013, **12**:127–137.

17. Tan HL, Fong WJ, Lee EH, Yap M, Choo A: **mAb 84, a Cytotoxic Antibody that Kills Undifferentiated Human Embryonic Stem Cells via Oncosis.** *Stem Cells* 2009, **27**:1792–1801.

18. Smith AJ, Nelson NG, Oommen S, Hartjes KA, Folmes CD, Terzic A, Nelson TJ: **Apoptotic susceptibility to DNA damage of pluripotent stem cells facilitates pharmacologic purging of teratoma risk.** *Stem Cells Translational Medicine* 2012, **1**:709–718.

19. Kuroda T, Yasuda S, Sato Y: **Tumorigenicity studies for human pluripotent stem cell-derived products.** *Biological & pharmaceutical bulletin* 2012.

20. Prokhorova TA, Harkness LM, Frandsen U, Ditzel N, Schröder HD, Burns JS, Kassem M: **Teratoma Formation by Human Embryonic Stem Cells Is Site Dependent and Enhanced by the Presence of Matrigel.** *Stem Cells Dev* 2009, **18**:47–54.

21. Cunningham JJ, Ulbright TM, Pera MF, Looijenga LHJ: **Lessons from human teratomas to guide development of safe stem cell therapies.** *Nature Biotechnology* 2012, **30**:848–856.

22. Menasché P, Vanneaux V, Fabreguettes J-R, Bel A, Tosca L, Garcia S, Bellamy V, Farouz Y, Pouly J, Damour O, Périer M-C, Desnos M, Hagège A, Agbulut O, Bruneval P, Tachdjian G, Trouvin J-H, Larghero J: **Towards a clinical use of human embryonic stem cell-derived cardiac progenitors: a translational experience.** *European Heart Journal* 2014.

23. Gutierrez-Aranda I, Ramos-Mejia V, Bueno C, Munoz-Lopez M, Real PJ, Mácia A, Sanchez L, Ligeró G, Garcia-Parez JL, Menendez P: **Human Induced Pluripotent Stem Cells Develop Teratoma More Efficiently and Faster Than Human Embryonic Stem Cells Regardless the Site of Injection.** *Stem Cells* 2010, **28**:1568–1570.

24. Jung J, Hackett NR, Pergolizzi RG, Pierre-Destine L, Krause A, Crystal RG: **Ablation of Tumor-Derived Stem Cells Transplanted to the Central Nervous System by Genetic Modification of Embryonic Stem Cells with a Suicide Gene.** *Human Gene Therapy* 2007, **18**:1182–1192.

25. Jansen of Lorkeers SJ, Hart E, Tang XL, Chamuleau MED, Doevendans PA, Bolli R, Chamuleau SAJ: **Cyclosporin in Cell Therapy for Cardiac Regeneration.** *J of Cardiovasc Trans Res* 2014.

26. Garbern JC, Lee RT: **Cardiac stem cell therapy and the promise of heart regeneration.** *Cell Stem Cell* 2013, **12**:689–698.

27. Yoon YS, Park JS, Tkebuchava T, Luedman C, Losordo DW: **Unexpected Severe Calcification After Transplantation of Bone Marrow Cells in Acute Myocardial Infarction.** *Circulation* 2004, **109**:3154–3157.

28. van der Worp HB, Howells DW, Sena ES, Porritt MJ, Rewell S, O'Collins V, Macleod MR: **Can Animal Models of Disease Reliably Inform Human Studies?** *Plos Med* 2010, **7**:e1000245.

29. Abbasalizadeh S, Baharvand H: **Technological progress and challenges towards cGMP manufacturing of human pluripotent stem cells based therapeutic products for allogeneic and**

autologous cell therapies. *Biotechnology Advances* 2013, **31**:1600–1623.

30. Matsumura G, Isayama N, Matsuda S, Taki K, Sakamoto Y, Ikada Y, Yamazaki K: **Long-term results of cell-free biodegradable scaffolds for in situ tissue engineering of pulmonary artery in a canine model.** *Biomaterials* 2013, **34**:6422–6428.

31. Sicari BM, Rubin JP, Dearth CL, Wolf MT, Ambrosio F, Boninger M, Turner NJ, Weber DJ, Simpson TW, Wyse A, Brown EHP, Dziki JL, Fisher LE, Brown S, Badylak SF: **An Acellular Biologic Scaffold Promotes Skeletal Muscle Formation in Mice and Humans with Volumetric Muscle Loss.** *Science Translational Medicine* 2014, **6**:234ra58–234ra58.

32. Hyun I, Hochedlinger K, Jaenisch R, Yamanaka S: **New Advances in iPS Cell Research Do Not Obviate the Need for Human Embryonic Stem Cells.** *Cell Stem Cell* 2007, **1**:367–368.

33. Wöhrle J, Merkle N, Mailänder V, Nusser T, Schauwecker P, Scheidt von F, Schwarz K, Bommer M, Wiesneth M, Schrezenmeier H, Hombach V: **Results of intracoronary stem cell therapy after acute myocardial infarction.** *Am J Cardiol* 2010, **105**:804–812.

Chapter 4 – From the clinics: Design of a Cardiac Patch for the ESCORT clinical trial

Introduction

Materials have been implanted in human bodies for thousands of years already. Some are harmful, some are not. However, hESCs have been discovered and harvested only very recently and very little is known on the damages they can cause to the body. Therefore, although they raise a lot of hope, it is critical to ensure that they can be tested rapidly in human, in order to determine as fast as possible whether they constitute a viable solution or a threat. In this project, we bore in mind that the safety would be the main concern, and for this reason, there was no need to start designing a new biomaterial from scratch, i.e. a biomaterial that would need to pass all the safety tests from *in vitro* assays to preclinical studies before being available in the clinics. The fact the hESCs are so controversial adds to the urgency to demonstrate or infirm their benefits. First, we need a clinical biomaterial to make sure that the cells are safe. Second, we need to define the specifications that would have to meet new biomaterials for fostering the cellular therapeutic effects. And only then can we think of a perfect patch for the treatment of congestive heart failure.

The ESCORT clinical trial

In 2010, Blin et al. identified a population of cardiovascular progenitors that could be easily purified before injections into the hearts of diseased animals [1]. After purification by immunospecific magnetic sorting, the remaining cells demonstrated the ability to differentiate into either contractile cardiomyocytes, or vascular cells, such as endothelial cells and smooth muscle cells. In addition, it was shown that these cells had completely lost their ability to form teratomas, making them good candidates for clinical trials. Last but not least, these cells were able to engraft into the heart of non-human primates, creating great hope in the scientific community.

While the results were really encouraging from a research point of view, translating this discovery to the clinics was yet another challenge. As described in [Figure 4.1](#), the generation of these cardiac progenitors necessitated to be adapted in many ways to ensure GMP compliance [2].

Choice of the cell line

The cell line had to be carefully chosen. Since not all hESCs are equal, some may respond better to cardiogenic growth factors than others [3]. The selected line is called I6 and comes from the Technion Institute (Haifa, Israel), with the approval of Prof. J. Itskovitz and M. Amit to proceed to clinical trials.

Choice of the culture conditions for hESC amplification

The culture conditions need to be fixed to generate a bank of pluripotent hESC. To maintain their pluripotency, hESCs need very specific chemical and physical signals. Some chemical signals were already available through commercial culture media, but others and the physical signals could, at the time, only be generated using either a layer of support cells (called the feeder cells), or a mixture of extracellular components extracted from cancerous mice. The latter, commonly called Matrigel, is obviously not approved clinically and thus the choice was naturally oriented towards the feeder cells. These cells, fibroblasts, are extracted from human foreskin tissues, then amplified (cell bank from Edouard Henriot Hospital, Lyon, France), and ultimately irradiated to stop their proliferation. Because they will not proliferate, they will not compete with hESCs and thus can support hESC adhesion, self-renewal, and maintenance of pluripotency by providing cell-cell adhesion clues, by secreting growth factors and extracellular components.

Choice of the conditions for Detachment, Conservation, Thawing and Specification

After reaching confluency, hESCs are likely to start losing their pluripotency and start behaving erratically if left in culture. Either the required number of cells has been reached for banking (at passage p38, in GMP conditions, by Mabgene, Alès, France), or cells need to be amplified further, after having been cautiously split into many different dishes (for clinical preparation). For the clinics, Collagenase IV was chosen (NB6, GMP grade, from Coger), for being an enzyme acting only on the extracellular matrix and not on the cells themselves, thus reducing the risks of damaging the therapeutic agents. Also, keeping hESCs in aggregates was crucial for their survival and the maintenance of their pluripotency. Conservation can then be achieved by supplementing the culture medium with 10% DMSO, a chemical that slows down ice formation to avoid the apparition of crystals that could potentially rupture the cell membrane and induce cytolysis. Note that while some chemicals like the Rock inhibitor Y-27632, regulating cytoskeleton's mechanics, have been found to dramatically improve viability after cryopreservation and during seeding, they were not included in the protocol because to date, no clinical trial has shown their safety.

As a result, there is an average loss of 50% of the cryopreserved cells after thawing. These cells are first re-amplified for about two weeks, in order to let them recover from the stress of cryopreservation and to reach the required amount of cells to be included in the cardiac patch. Once enough cells have been generated (at passage P41), the specification consists only in adding a growth factor, BMP2, responsible for pushing cells toward a mesendodermal lineage. Luckily, this protein is already produced and approved in the clinics, in the treatment of bone

defects, in combination with a collagen network that serves as scaffold (Inductos[®], Wyeth pharmaceuticals, now part of Pfizer, New York, NY). Unfortunately, the feeder cells were found to inhibit the specification by secreting TGF-Beta, a factor known to be important in pluripotency maintenance and also for neuronal differentiation. Therefore, BMP2 also had to be administered with a supplement of SU-5402, an inhibitor of the TGF-Beta signaling pathway.

Cell sorting and choice of the dose

After four days of specification, where medium was changed everyday to freshen up the BMP2, cells are ready to be collected and sorted depending on their surface markers. There are many different cell populations in the mixture, from potentially undifferentiated cells to cells of other lineages than the cardiovascular mesendoderm. Consequently, positive cell sorting was found to be the best option to select the cardiac progenitors, even considering the damages that could cause immune-magnetic labeling. Antibodies were produced in GMP facilities (Miltenyi, Teterow, Germany) and functionalized to magnetic beads. These antibodies can only bind to very specific membrane markers, such as CD15 (also named SSEA-1) in our case. After collecting these cells, a small amount is then fluorescently labeled in order to quantify, using flow cytometry, the proportion of impurities (non cardiovascular/mesendodermal cells) in the positive fraction, as well as the amount of dead cells and even the proportion of lost cells (CD15⁺ cells found in the negative fraction).

Ten million cells were chosen to be delivered. This value was the result of theoretical calculations with a focus on patient's safety. As a result, an under-evaluated doses was preferred in this first step. It was assumed that above 1,000 residual undifferentiated cells per milligram of tissue, tumoral clusters could emerge [4, 5]. For a 400-g heart with one fourth of the tissue being infarcted, we would reach 10 millions of grafted cells per 100 grams of covered tissue, or 100 cells/mg of tissue. After 2 divisions, this value will reach 400 cells/mg, and, in the worse-case scenario where 10% of the CD15⁺ fraction would correspond to undifferentiated cells, we would observe an average of 40 undifferentiated cells per mg of tissue. This value is thus well below the threshold of 1,000 cells/mg defined here above.

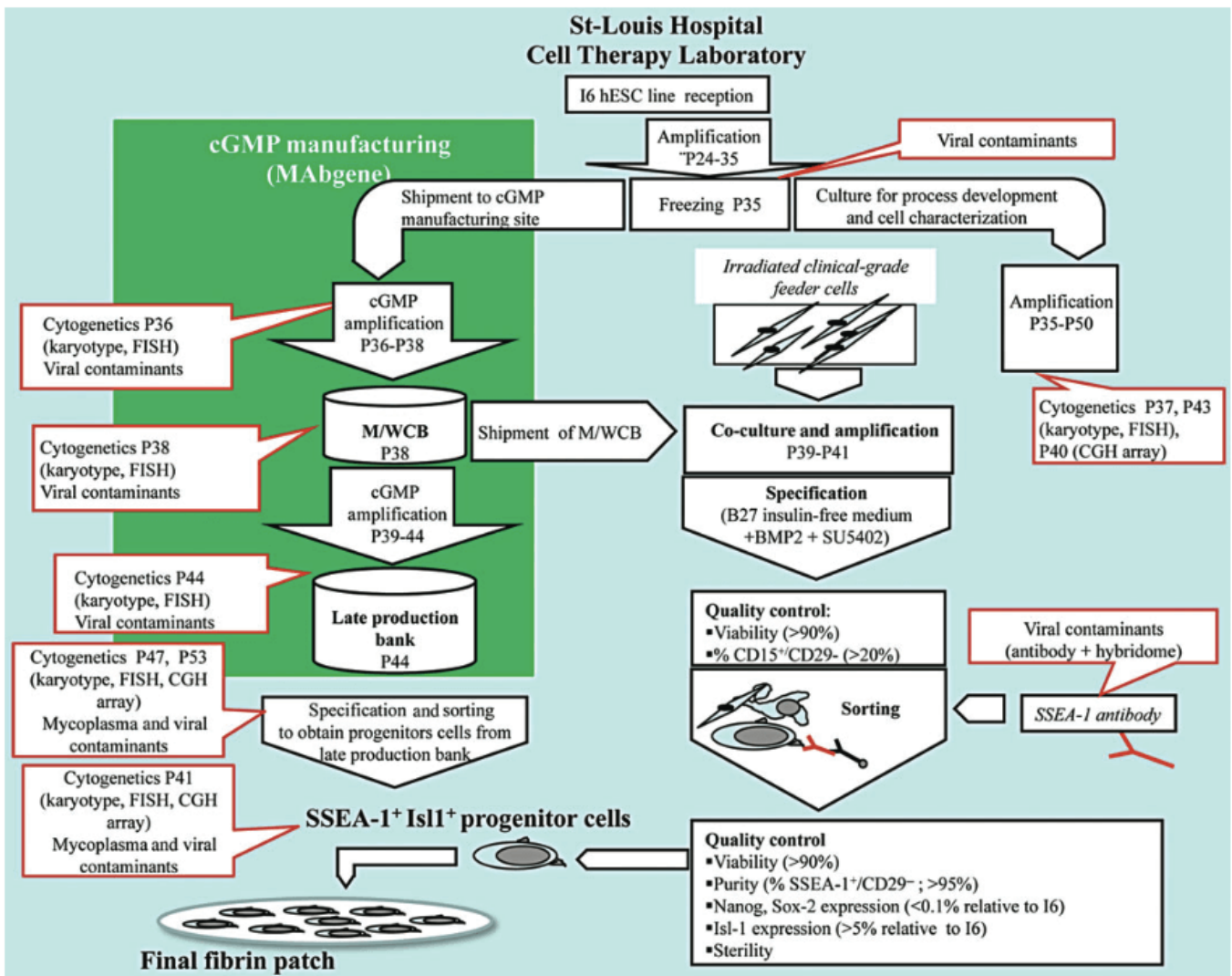


Figure 4.1 Description of the cell production process in GMP conditions
Adopted from Menasché et al. 2014 [2]

Design of a cardiac patch for clinical applications

As the reader would have already convinced himself, this protocol is already very complex and bringing it up to GMP specifications took years. The next step was to find a way to deliver the cells onto the heart. Many clinical materials had already been tried with other kinds of cells with limited success, and many criteria for optimal cell survival and retention, and even easy surgery and handling, had not been met [4-8]. In that context, fibrin emerged as a potential candidate for it had already shown success in rats and most importantly was available in a clinically approved formulation: Evicef®.

Fibrin

Among natural biomaterials, fibrin is a central one in scaffold design. Even if absent from the extra-cellular matrix, it is present during the wound healing process as the primary component of blood clot and as a scaffold to promote wound repair. Fibrin (factor Ia) is formed from the

interaction between fibrinogen (factor I) and thrombin, in the presence of Ca^{2+} , and is then polymerized [9] (Figure 4.2). Once polymerized, the structure of fibrin presents pores that block some biological components and allow others to go through. Fibrin also promotes cell adhesion and proliferation [10]. Even though it is highly flexible and not much brittle, its mechanical properties remain limited [11].

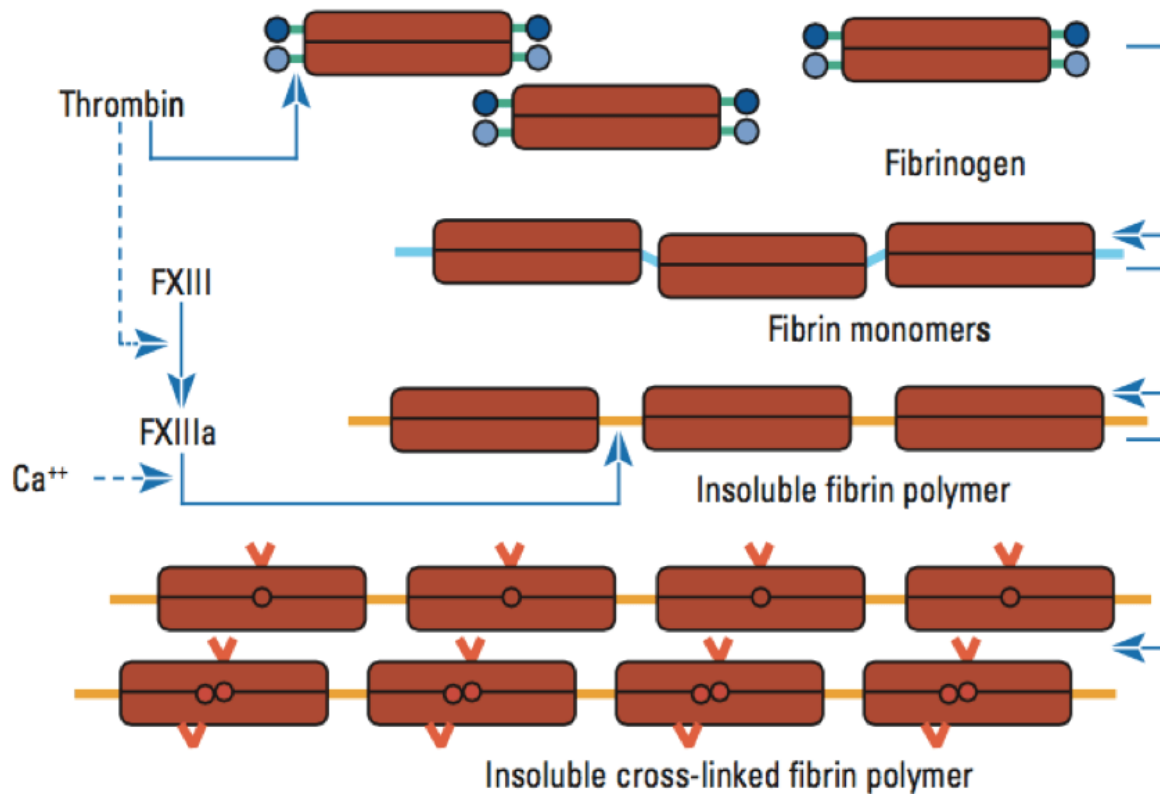


Figure 4.2 Fibrin polymerization process

As an already clinically approved material for the incorporation of cardiac progenitors, we decided to make scaffolds based on fibrin sealant formulations. We chose the brand Evicel[®] for it does not contain aprotinin, a protein that stabilizes fibrin polymerization. In spite of its efficacy in reducing post-operative bleeding, aprotinin was withdrawn from many pharmaceutical markets worldwide after safety concerns had been raised by results from the BART clinical trial in 2008 [12]. While recent studies are generating new debates on the real benefits of aprotinin for antifibrinolytic treatments, questioning the advantages and drawbacks of its main replacement, tranexamic acid [13-15], it was safer to avoid taking the risk of delaying further the start of our clinical trial.

The literature from pre-clinical biomedical research groups has a lot of references regarding the fabrication of cardiac tissues with fibrin [16-19], sometimes using chemical-grade bovine fibrin, sometimes using clinical grade human fibrin, either with or without aprotinin, factor XIIIa and other additives (see Table 4.1 for references).

	Fibrinogen (mg/mL)	Thrombin (UI/mL)	Young's modulus (kPa)	Reference	Method
Evicel	140	2000	38	[20-22]	Tensile Testing
Tisseel	87 (+ aprotinin)	512	15	[20, 21]	Tensile Testing
Huang: Tisseel	87 (+ aprotinin)	512	15?		
Huang: Standard	95	500	27	[23]	Hang up loads
Liu	100	400			
Godier-Furmémont	40	200			
Huang	95	50	9.5	[23]	Hang up loads
Huang	95	10	5.3	[23]	Hang up loads
Xiong	25	75			
Huang	9.5	50	5.7	[23]	Hang up loads
Vallée	10	40			
Rowe	2	2	10	[24]	Tensile testing
	2	0.2	10		
	2	0.02	19		
	2	0.002	29		

Table 4.1 Literature survey of the use of fibrin for cardiovascular applications.

Yet, no study has been done with hESC-derived cardiac progenitors and their behavior in such a cardiac patch.

Mechanical characterization

As described in Chapter 2, there are many ways to characterize the mechanical properties of materials, and the choice of the protocol depends on the application of the material and the environment destined to interact with it. While in chapter 2, we have only described techniques for assessing the mechanical properties at the cellular level, there exist solutions for evaluating the performance of a material at the macroscopic scale, which we thought would be more relevant for our cardiac patch in a clinical setting.

The problem in measuring elasticity is that it requires a perfect knowledge of other parameters of the sample to be tested, such as its thickness and its geometrical shape, and sometimes, parameters such as the viscosity of the materials.

For compressive testing using an apparatus like Instron machines, one requirement is absolute flatness of the cylinder-shaped sample. If the sample is not flat, compressive forces are not applied uniformly on the sample, causing differential deformation and possible sample slipping.

Also, for very soft materials and especially hydrogels, one has to make sure that the sample does not deform under its own weight, which would bias the measure. Soft formulations of our fibrin patches were found to be too soft to handle their own weight.

For tensile testing, similar problems can emerge such as a precise measurement of the thickness of the sample, and the ability to mold it in a bone-like structure that fits in the machine. Fibrin was found to be too deformable and yet too resistant to be cut out with a cutting die without being torn apart and damaged.

Many people [23-28] found ways to characterize fibrin gels in the literature (Table 4.1), but not only all these solutions are disputable, but they also are all different from each other and from measurements of the mechanical properties of heart tissues [29-31], [32, 33].

And even the characteristics of heart tissues are rarely determined *in vivo* when the tissue is still fully functional, but rather *in vitro*, where post-mortem stiffening and processing techniques may have altered their mechanical properties.

Therefore, we sought a way to characterize the gels that would be relevant in a clinical setup. The idea behind it would be to become able to determine the characteristics of a healthy tissue versus a diseased tissue in terms of its elasticity, and to compare it to the elasticity of our engineered cardiac patches.

While previous collaborations with the Langevin Institute had already led to the demonstration that ultrasounds could be used to dynamically measure contraction forces *in vivo* [32, 33], it had never been shown that we could use this technique to measure the elasticity of materials destined to the fabrication of cardiac patches or cellular cultures.

Shear Wave Elastography (SWE) is a very powerful technique that was first developed as a non invasive tool for the diagnosis of breast cancer. Because it allows a measure of the elasticity of tissues in real time, the observation of a very stiff ball in mammary gland would be the sign of a developing tumor.

Here, we used this technique because it allowed non destructive characterization of the Young's modulus of our materials, without any requirements in terms of geometry, thickness, or possible analytical troubles such as the determination of the point of contact of a tip of the AFM cantilever.

However, this technique has a very narrow range of applications, which happened to fit perfectly in our study. While new models can be developed taking the sound propagation speed in other media (such as PDMS, for example), the (commercially available) clinical version of the SWE only uses mathematical models using the velocity of sound in water, as it is the main component of bodily tissues. The range of stiffness that it can discriminate without any loss of precision corresponds to the range of stiffness found in soft biological tissues (excluding bones), i.e. from a little less than 1 kPa to about 200 kPa. Finally, the observed sample needs to be echogenic, meaning that the generated ultrasonic waves can bounce

back to the probe. For this to be possible, there has to exist particles the size of at least half the wavelength of the signal generated by the ultrasonic probe.

While most bodily tissues meet these characteristics, due to the presence of many imperfections and cells as the echogenic particles, it was not the case of our cell-free samples.

The solution was therefore to add particles, enough to make the entire hydrogel echogenic with a good signal-to-noise ratio, and not too many not to bias the measure of the hydrogel's elasticity.

In this chapter, we detail the results of the preliminary investigations that led to the establishment of the final protocol for the fabrication and use of a fibrin patch loaded with hESC-derived cardiac progenitors in an attempt to get the green light from the regulatory authorities to proceed to clinical trials.

Material and methods

Determination of fibrinogen and thrombin concentrations

A solution of fibrinogen from the Evicel[®] package was diluted 10 folds in NaCl and then subjected to a Von Clauss clot formation assay. Briefly, the diluted fibrinogen solution is placed at 37°C, to which is added an excess thrombin solution followed by a calcium solution. Clotting time was recorded with $t=0s$ corresponding to addition of calcium. Clotting was considered complete when the optical density had reached a certain threshold. Clotting curves were then compared to a calibration curve constructed using a reference plasma solution and the final fibrinogen concentration was derived by simple interpolation.

Thrombin's concentration is measured by its activity for clot formation. Therefore, any parameter that can affect the activity of thrombin, such as freeze-thaw cycles, conservation temperature, etc., will bias the "concentration" initially determined. Hence, we chose to fix an arbitrary value to thrombin concentration, corresponding to the center of the concentration range provided by the manufacturer, i.e. 1000 U/mL for an official range between 800 and 1200 U/mL.

Preparation of 3D Culture in fibrin gels

An aqueous solution of agarose 2% v/v was overlaid on the bottom of each well of a 24-well plate, so as to avoid important adhesion of patches. A 5 mg/mL fibrinogen solution (diluted from the Evicel's vial) was mixed with suspended cells, and a volume of 150 μ L was poured in each well. Thereafter, a 1 U/ml thrombin solution (diluted from the Evicel's vial) was

overlaid on top of the fibrinogen solution at a ratio of 1:1 v/v, and mixed by swirling and tilting the plate. Gels were incubated for 45 minutes at 37°C and 5% CO₂.

The structure of the fibrin gel was then modulated by varying fibrin volumes and initial fibrinogen concentrations at a constant fibrinogen:thrombin ratio (5 milligrams of fibrinogen per 1 unit of thrombin). In the rest of the present document, samples are referred to using their fibrinogen:thrombin concentrations, “F” standing for the fibrinogen concentration in mg/mL and “T” standing for the thrombin concentration in U/mL. For the qualitative assessment of fibrin handling and stability, patches were polymerized into 24-multiwell plates with α -MEM as the culture medium.

Immunohistology

After polymerization, patches were embedded in Tissue-Tek OCT compound Mounting Media, and cut into 10- μ m-thick sagittal sections using a cryostat. A selected set of sections was mounted on microscope slides. After 24 hours, they were rinsed with ethanol 70% and washed with Phosphate Buffer Saline (PBS).

The sections were then stained with Hematoxylin for a few seconds, and then rinsed with ddH₂O. Next, they were counterstained with Eosin for 5 minutes, and then rinsed with ddH₂O. A solution of 60% Warm glycerol was added and slides were covered with glass coverslips.

Scanning Electron Microscopy (SEM)

After polymerization of the patches, 1 mL of glutaraldehyde was added into each well for 2 hours at room temperature (RT). Then, patches were washed twice with PBS for 15 minutes and water was progressively removed by replacing the PBS solution with an ethanol/PBS solution of increasing ethanol concentration. More precisely, the concentrations v/v of ethanol were 25%, 35%, 50%, 60%, 70%, 80%, 90% and finally the solution was replaced by pure ethanol. Each incubation lasted 15 min.

Ethanol was then progressively removed and replaced by hexamethyldisilazane (HMDS) using a similar procedure with solutions of HMDS 33%, 67%, and 100% v/v in ethanol. Samples were transferred into multi-well plates covered with aluminum foil in order to avoid attachment of the samples to the bottom of the dish. After the HMDS had fully evaporated, all samples were sputter-coated with 10 nm of gold and imaged using a Scanning Electron Microscope under full vacuum.

Image analysis

Pore sizes were quantified by measurement of the pore diameter of H&E-stained fibrin cross-sections using Image J software (NIH, MD, USA) ($n = 3$). At least 10 pores were assessed in each sample. *Manual measurements* refer to handmade delimitations of the pores, while *automatic measurements* denote the use of Image J plugins for particle counting after the images had been filtered using binary thresholds.

Materials characterization

Compressive test

The Young's modulus in compression was derived from stress-strain curves obtained using an Instron 5565 mechanical apparatus (Instron, Norwick, MA), equipped with a 10 N load cell (**Figure 4.3-A**). Briefly, fibrin pieces were formed in flat-bottomed syringes to have a controlled geometry. The height of cylinders was measured and placed in the apparatus and the strain was recorded at different loads. The Young's modulus in compression was calculated as the slope of the stress-strain curve, at the beginning of the deformation, where the stress-strain curve can be assumed to be linear.

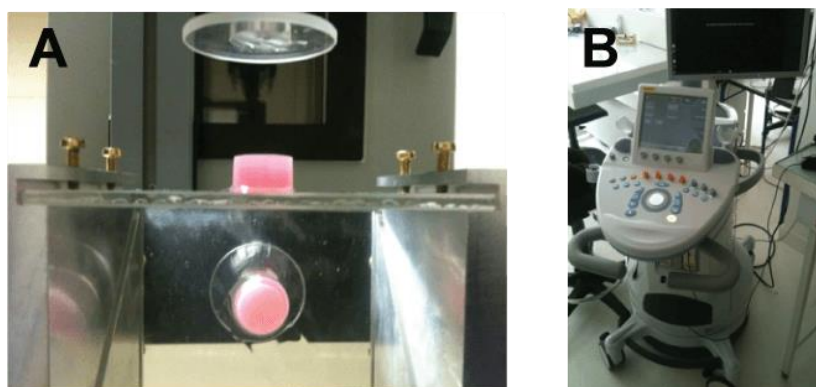


Figure 4.3 Mechanical characterization of fibrin hydrogels

(A) procedure on Instron device for compressive testing. The upper surface will compress the hydrogel (in pink) at a controlled speed and resistance is recorded at the same time. (B) Aixplorer® Ultrasound imaging system

Shear Wave Elastography (SWE) – Aixplorer® Ultrasound Imaging

SWE is an adaptation of standard ultrasound imaging techniques (**Figure 4.3-B**) provides in real-time a quantitative map of soft tissue's shear modulus (**Figure 4.4**) by tracking remotely induced shear waves at high spatial and temporal resolution. To our knowledge, this method has already shown success in breast cancer diagnosis but had never been exploited in the field of tissue engineering and biomaterial design. As hydrogels were transparent to ultrasounds we added agarose powder during the

preparation. Hydrogels required no specific geometry but cylinders appeared to be more practical. Hydrogels were prepared the same way as for compressive tests.

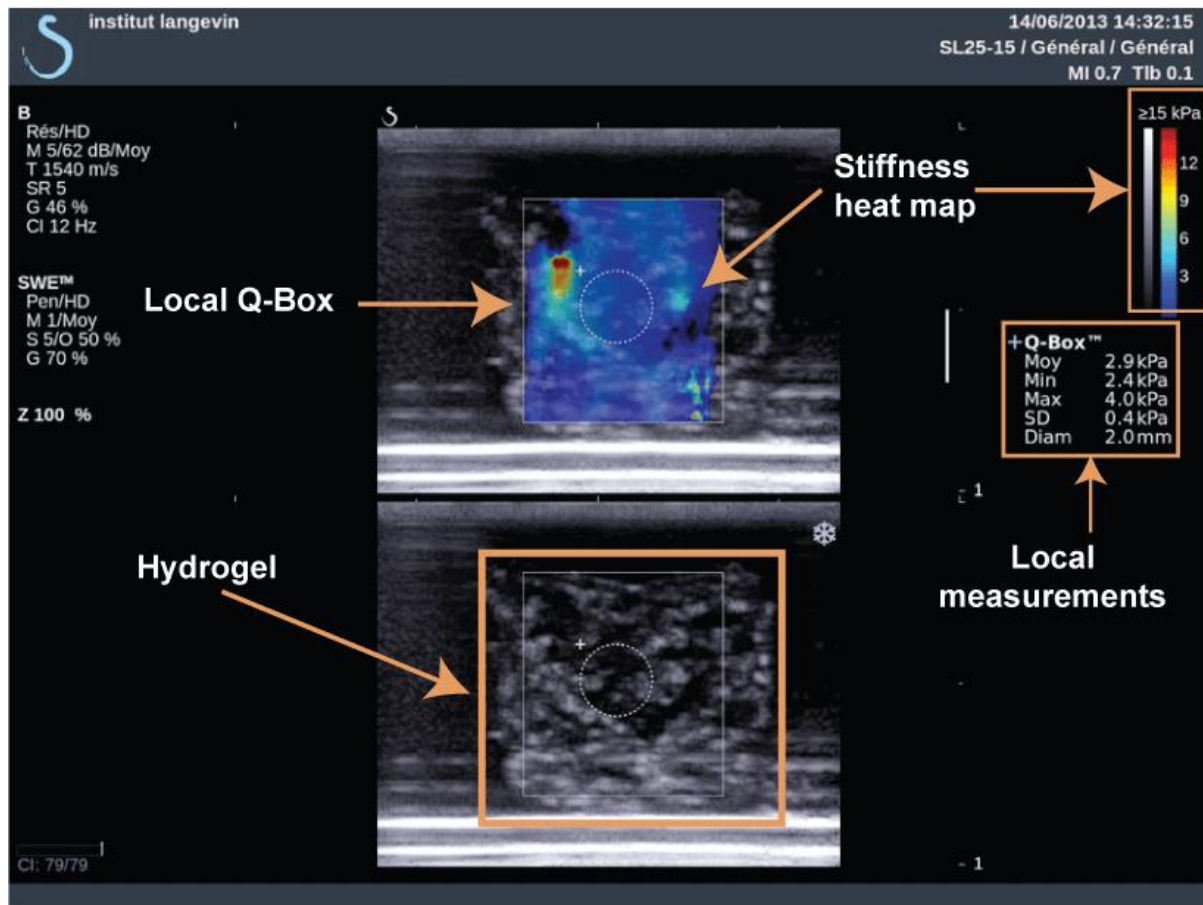


Figure 4.4 Elasticity measurement with Shear Wave Elasticity on Aixplorer® Ultrasound System [example for F20T4HA2.5 (see Chapter 6)]

Results

Concentration of Evicel's fibrinogen solutions

Biological materials are often very difficult to purify and depending on their application, they might not require a very precise control of their concentration. This is the case of the surgical glue commercialized under the name Evicel®. Indeed, the manufacturer's specifications reads a fibrinogen concentration ranging between 50 mg/mL and 90 mg/mL, which is a very broad interval. As lot to lot variability from patch to patch could lead to dramatic variations in the outcome of the future patients, we routinely assessed the real concentration in fibrinogen, since this data could not even be provided by the manufacturer itself (Figure 4.5). Results were highly heterogeneous, with a higher frequency for concentrations between 50 and 55 mg/mL.

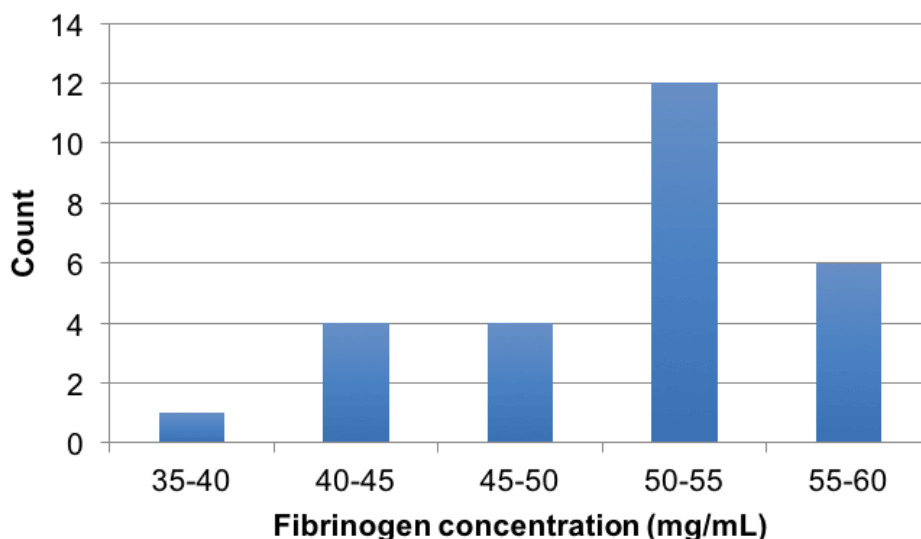


Figure 4.5 Lot-to-lot variability in fibrinogen concentrations

Structural characterization of fibrin patches

At the nanoscopic level, we observed a woven network of homogeneously distributed and randomly oriented fibers (Figure 4.6). Qualitatively, unlike other groups had previously reported, there was no visible difference between our conditions, neither in terms of fiber diameter nor in terms of fiber spacing (i.e. overall porosity).

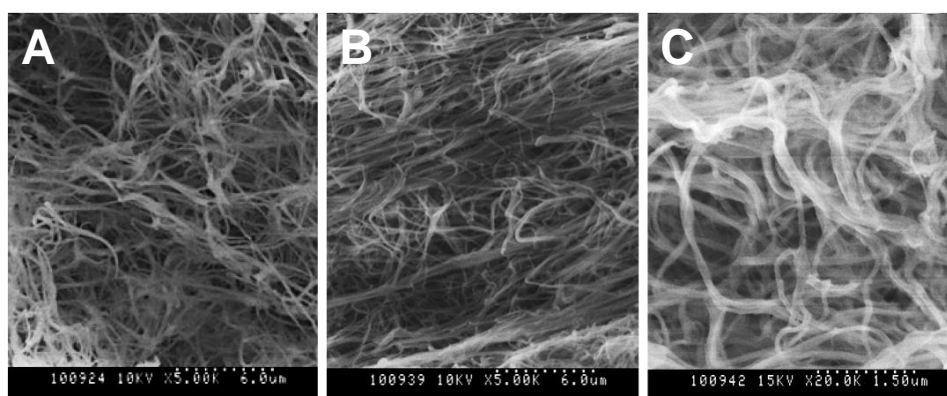


Figure 4.6 Electron Micrographs of fibrin patches.

(A) Patch with 5 mg/mL of fibrinogen and 1 U/mL of thrombin. (B) Patch with 10 mg/mL of fibrinogen and 2 U/mL of thrombin. (C) Zoom in the structure of patch A.

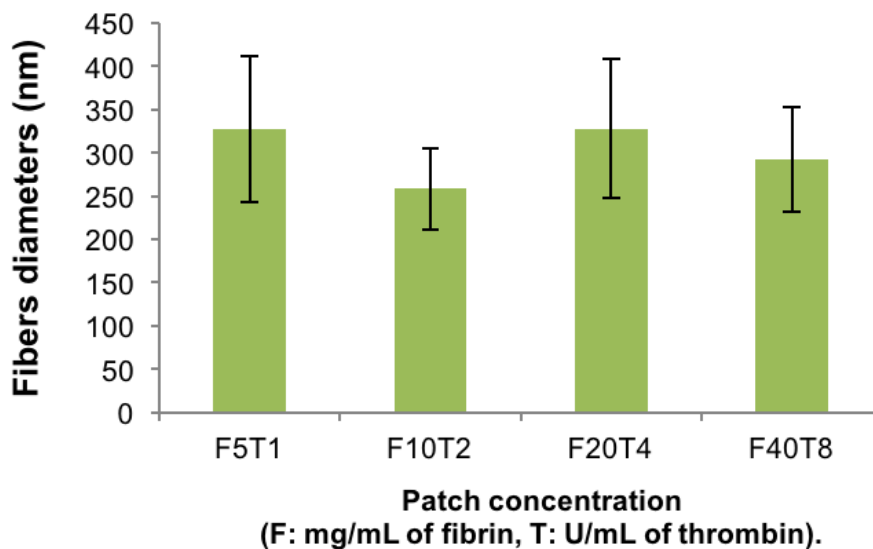


Figure 4.7 Fiber diameter as a function of fibrin composition

After quantification (**Figure 4.7**), fiber diameters for F5T1 was about 327 nm, and decreased for F10T2 with a value of 258 nm. Similarly, when the concentration was doubled to F20T4, there was no difference in fiber diameters with a value of 328 nm. Finally, at the highest concentration of fibrinogen and thrombin F40T8, there was also no difference in fiber diameters with a value of 292 nm. This could be explained by the processing conditions needed for a hydrogel to be imaged under an old SEM without variable pressure. Despite our attempts to use confocal microscopy on fibrin hydrogels made of Evicel[®] supplemented in fluorescently labelled fibrinogen (**Figure 4.8**), it was not possible to acquire images with sufficient resolution to perform better *in situ* quantifications.

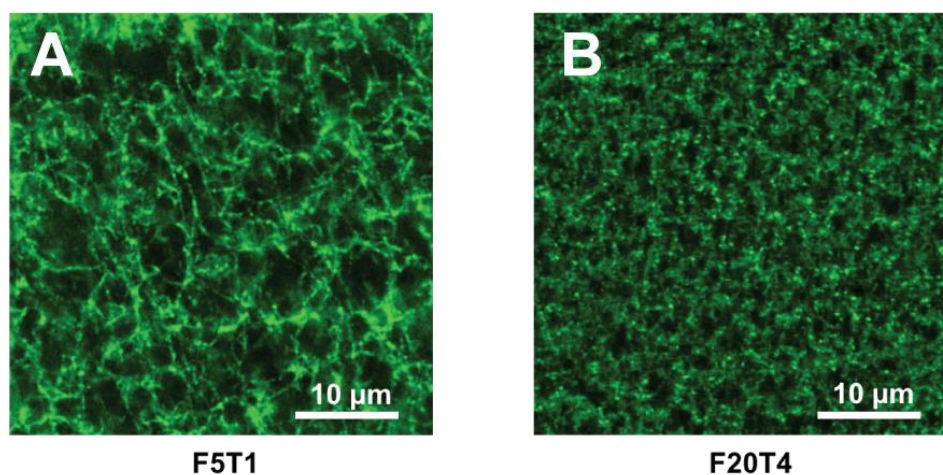


Figure 4.8 Confocal imaging of fluorescently labelled fibrin hydrogels

At the microscopic level, histological sections revealed bright pores clearly distinguishable from dark purple clusters of fibrin fibers (**Figure 4.9**).

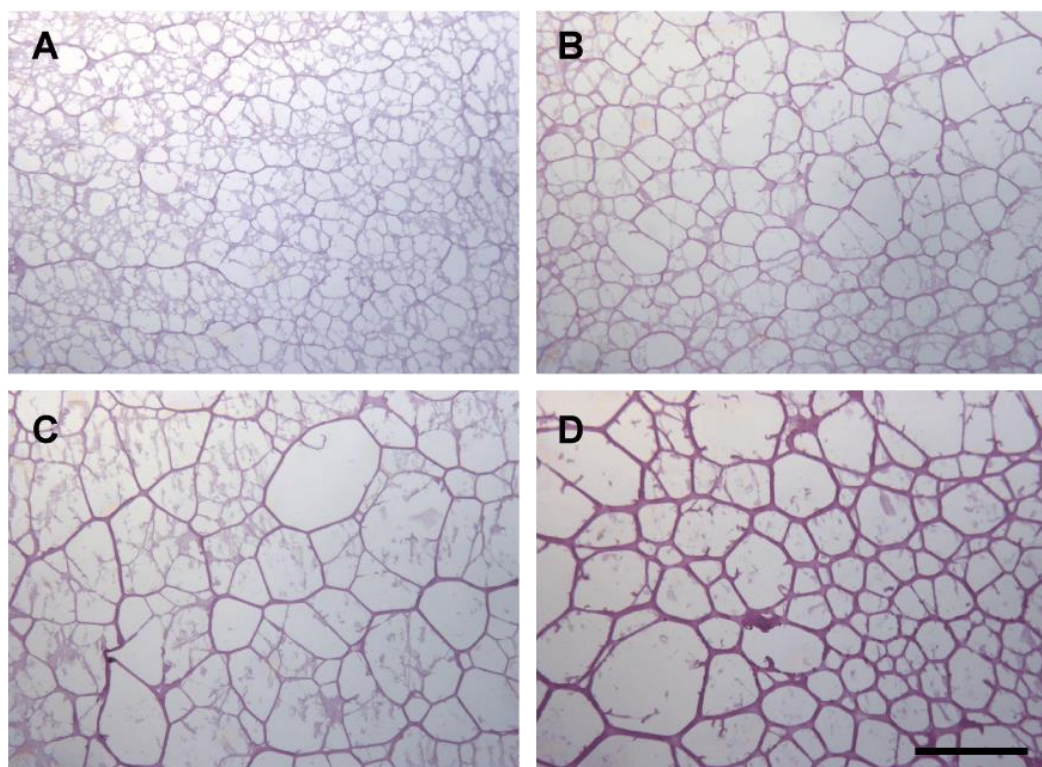


Figure 4.9 Photomicrographs of histological sections of fibrin patches, stained with Hematoxylin/Eosin stain. **(A)** Patch with 5 mg/mL of fibrinogen and 1 U/mL of thrombin. **(B)** Patch with 10 mg/mL of fibrinogen and 2 U/mL of thrombin. **(C)** Patch with 20 mg/mL of fibrinogen and 4 U/mL of thrombin. **(D)** Patch with 40 mg/mL of fibrinogen and 8 U/mL of thrombin. Scale bar: 200 μm

Qualitatively, pore size seemed to increase with fibrinogen (and thus, thrombin) concentration. Furthermore, fibers seemed, in this case, to have a larger diameter with increasing fibrinogen concentrations. Interestingly, these microscopic observations were hardly interpretable in the light of what had been previously seen at the nanoscale. Indeed, the pores that were visible in cryosections (**Figure 4.9**) did not seem to correspond to the porosity observed for confocal images (**Figure 4.8**).

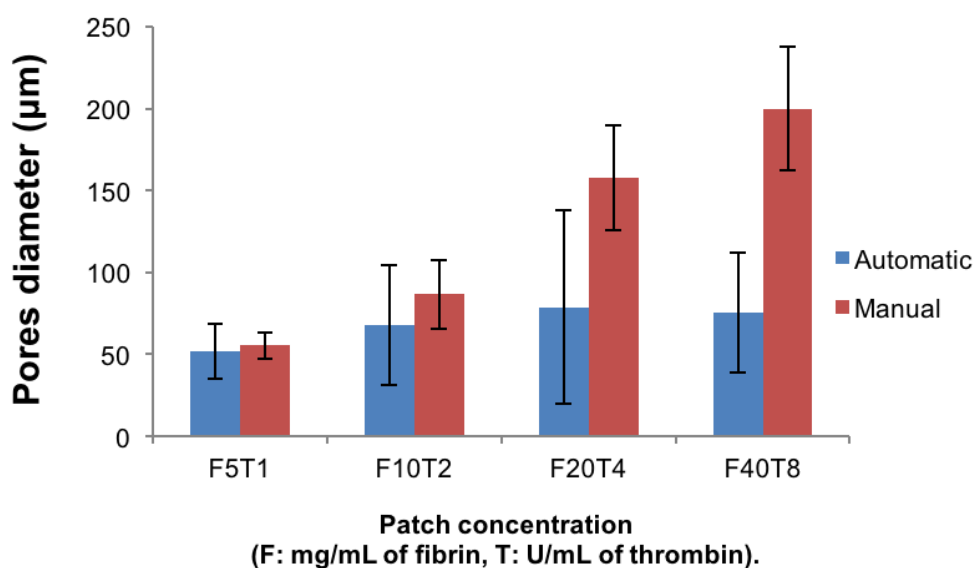


Figure 4.10 Variations in pore diameter (μm) as a function of patch concentrations (mg/mL-U/mL).

Quantitatively, after manual measurements (Figure 4.10, blue histogram), there was a linear increase in pore diameter with increasing concentration of fibrinogen. Indeed, the fibrin pore diameter for F5T1 was about 55 μm , and increased for F10T2 with a value of 86 μm . When the concentration was doubled to F20T4, fibrin pore size increased to 158 μm . Finally, the biggest pore diameter was about 200 μm , which corresponded to the highest concentration in fibrinogen and thrombin F40T8. Therefore, fibrinogen exerts a clear dose dependent effect on the diameter of fibrin pores (Figure 4.10).

Surprisingly however, automatic measurements gave different results (Figure 4.10, red bars). Indeed, the lowest value of diameters was found for F5T1 with a value of 52 μm whereas the highest value was found for F20T4, and was 79 μm , with error bars of the same order of magnitude as the means. While a similar qualitative increase was observed, this was not enough to be interpreted rigorously. Yet, it might shed some light on the reasons why nanoscopic observations are clearly different from microscopic observations. In fact, one explanation of the bad performance of the automated method could be, in addition to inhomogeneous lighting problems, the presence of very thin and small fibers or fibrin aggregates (especially visible on Figure 4.10-A and Figure 4.10-C) that seemed to form a sub-network within the bigger network. We can hypothesize that these smaller fibers do match those revealed by SEM and Confocal imaging, while bigger fibers might result from their aggregation due to various mechanical constraints. While bigger fibers are more mechanically stable, small individual ones are weaker and probably removed from the samples during the cryo-sectioning and staining steps, leaving behind microscopic pores.

Mechanical characterization

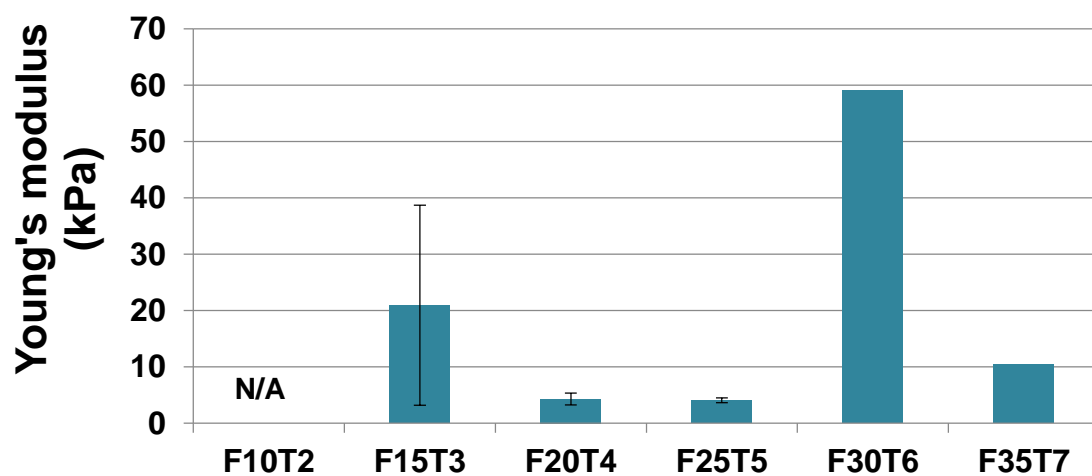


Figure 4.11 Compressive testing results for fibrin hydrogels of increasing fibrinogen:thrombin concentrations.

On one hand, compressive tests showed high variability both between replicates of the same condition and between condition themselves. Even though structural analysis had shown an homogeneity in the evolution of the fibrin network from low concentrations of fibrinogen to higher concentrations, the compressive results, taken independently, could have suggested a complete decorrelation between fibrinogen and thrombin concentrations and elastic modulus, where concentrations as low as 15 mg/mL fibrinogen would result in an average Young's modulus above 20 kPa (with a SEM of more than 15 kPa) and F25T5 patches, composed of 25 mg/mL fibrinogen, would have an elasticity lower than 5 kPa (Figure 4.11). Additionally, the patches with the lowest concentrations of fibrinogen:thrombin happened to be too soft to withstand their own weight and to allow precise compressive testing. As described earlier, this could be explained by technical hurdles and the very high manufacturing constraints that may limit and distort the results.

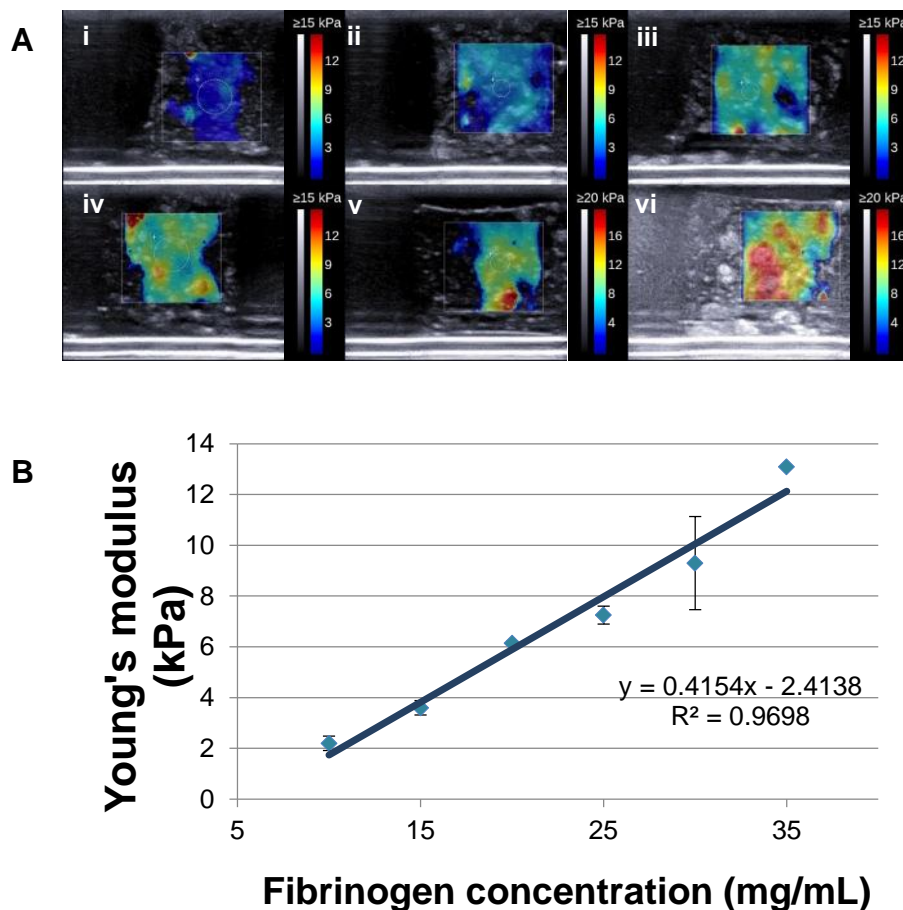


Figure 4.12 SWE measurements of fibrin elasticity.

(A) Representative images of B-modes superimposed with elasticity heat maps for the 6 concentrations tested, from the lowest F10T2 (A-i) to the highest F35T7 (A-vi); (B) Variations and linear fitting of the patch's elastic modulus depending on fibrinogen concentrations.

On the other hand, SWE measurements (Figure 4.12) showed homogeneous results with lower variability, suggesting an increase in stiffness with the increase of the fibrinogen and

thrombin concentrations. These data concord with both confocal and brightfield micrograph. Indeed, although unquantifiable, the pores observed *in situ* were wider for formulations of low fibrinogen (Figure 4.8-A) than for their more concentrated counterparts (Figure 4.8-B). This higher porosity would eventually results in weaker mechanical properties for F5T1. As for sections of patches, the presence of very thick fibers resulting from aggregation of smaller fibers would have undoubtedly strenghtened the hydrogel at higher concentrations in fibrinogen and thrombin (Figure 4.9). Additionally, there was a linear correlation ($R^2=0.97$, Figure 4.12-B) between elasticity and fibrinogen concentration. This observation will allow us to interpolate with confidence the elasticity of scaffolds with different fibrinogen compositions that might be needed in the future.

Handling tests

We then determined the most appropriate patch volume and reduced its size as much as we could to limit nutrient and oxygen diffusion problems but keeping in mind that the surgeon has to be able to handle the patch without breaking it during the surgery. For the handling test of fibrin patches, four different volumes were tested for each concentration: 50 μL , 100 μL , 200 μL and 300 μL .

Concentrations F [mg/mL] – T [U/mL]	Medium	Volume (μL)	Pinch grip	Retention	Re- spreading	Number of samples
F40T8	αMEM	50	+	-	-	n=3
	αMEM	100	+	+	-	n=3
	αMEM	200	+	+	+	n=3
	αMEM	300	+	+	+	n=3
F20T4	αMEM	50	-	-	-	n=3
	αMEM	100	+	-	-	n=3
	αMEM	200	+	-	+	n=3
	αMEM	300	+	+	+	n=3
F10T2	αMEM	50	-	-	-	n=3
	αMEM	100	+	-	-	n=3
	αMEM	200	+	-	+	n=3
	αMEM	300	+	+	+	n=3
F5T1	αMEM	50	-	-	-	n=3
	αMEM	100	+	-	-	n=2
	αMEM	200	+	-	-	n=3

Table 4.2 Handling of patches as a function of fibrinogen and thrombin concentrations.

“Pinch grip” corresponds to the ability to seize the patch using standard flat teetted tweezers. “Retention” denotes whether the patch immediately folds on itself or retains its circular shape. “re-spreading” refers to the ability of the patch to spread back to its original shape when deposited back in the conservation solution.

Results presented in Table 4.2 suggest that 300 μL of fibrin was necessary for an optimal handling of the hydrogel. However, there was no qualitative difference in handling between the four concentrations. While the optimal volume was considered to be 300 μL for patches destined to be grafted on rats, upscaling our system for sheep and thus for humans made us realize that an even thicker patch (up to 1-mm thick) was needed for better surgical performances.

Cell-laden fibrin patches

We then focused on how to make the patch usable in the operating theater. We defined ways to keep it under tension for 24 hours (until implantation) and to avoid patch contraction due to adhesion-mediated cellular tension. Even before detaching the patch from its substrate, it was possible to observe the important traction exerted by test cell lines (here NIH-3T3 fibroblasts) inside the fibrin patch (**Figure 4.13, B-D**). Immediately after cell trypsinization and fibrin polymerization, cells had kept their round shape (**Figure 4.13-A**), yet after a few hours, it was not possible to distinguish between fibroblast's cellular extensions and thickened fibrin fibers (**Figure 4.13-B**), confirming reported analyses that fibrin is highly remodeled by its host cells to the point where fibers can eventually be re-oriented [34]. Again, as compared to histological analyses of cellularized patches [35], looking at fluorescently conjugated fibrin patches under a confocal microscope (**Figure 4.13, C-D**) revealed both the nano-pores in between fibrin's nanofibers and the micro-/meso- pores generated by cellular traction (or other external stress). It also revealed the formation of thicker fibers, as suggested by stronger fluorescence intensity.

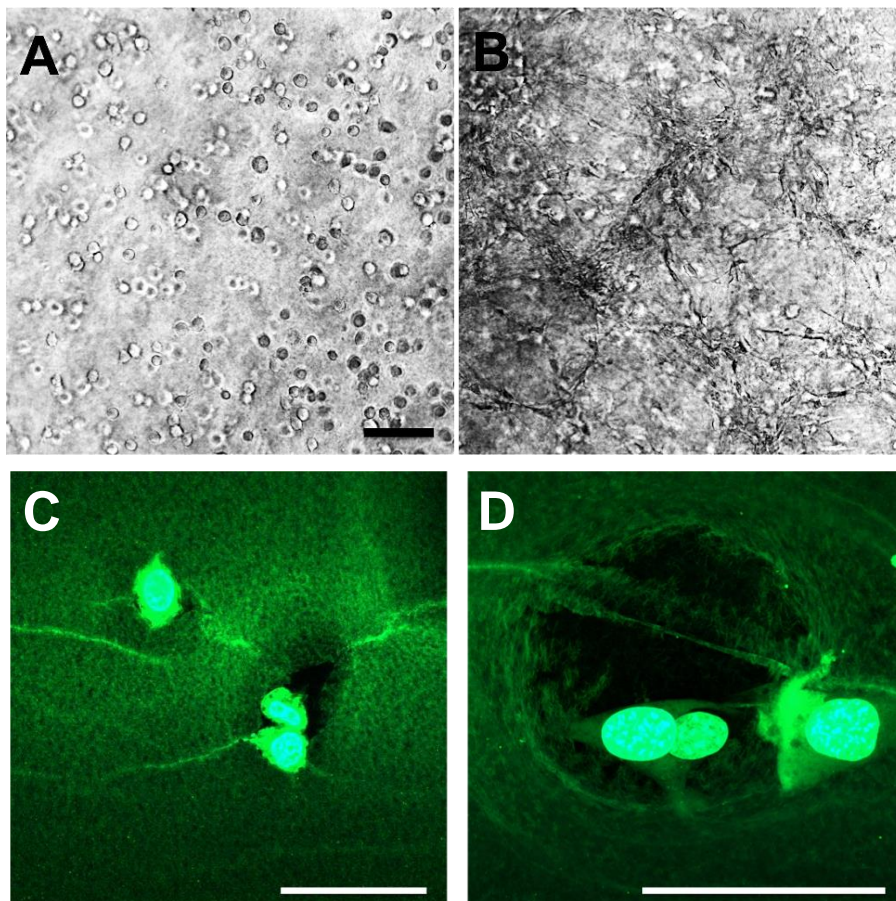


Figure 4.13 Representative images of the behavior of fibroblasts seeded within fibrin patches. (A-B) Phase contrast image of fibroblasts in F20T4 fibrin patches (A) at t=0 (B) at t=20h (scale bar: 100 μ m). (C-D) 3D projections of confocal images of fibroblasts in F20T4 fluorescently conjugated fibrin patches after 4 hours in culture. Note how fibroblasts are pulling on the fibrin, generating holes and thickening some fibers. Scale bar: 50 μ m.

Furthermore, after observing this phenomenon on a patch made with cardiac progenitors (data not shown), *in vitro* tests with murine fibroblasts confirmed that patch's surface area significantly decreased over time if left without constraints in culture medium (Figure 4.14 A and B). However, having no adhesion between the patch and the culture dish would allow surgeons to easily take the patch out with no risk of rupture. Therefore, we defined a trade-off where the bottom of the dish is coated with agarose to remove adhesions with the fibrin gel, while the wall of the well remain untreated, allowing the hydrogel to be maintained under tension for as long as the patch is not removed nor are adhesion forces compensated (Figure 4.14 C-E). Consequently, fibroblasts could adhere and spread in the patch without shrinking it.

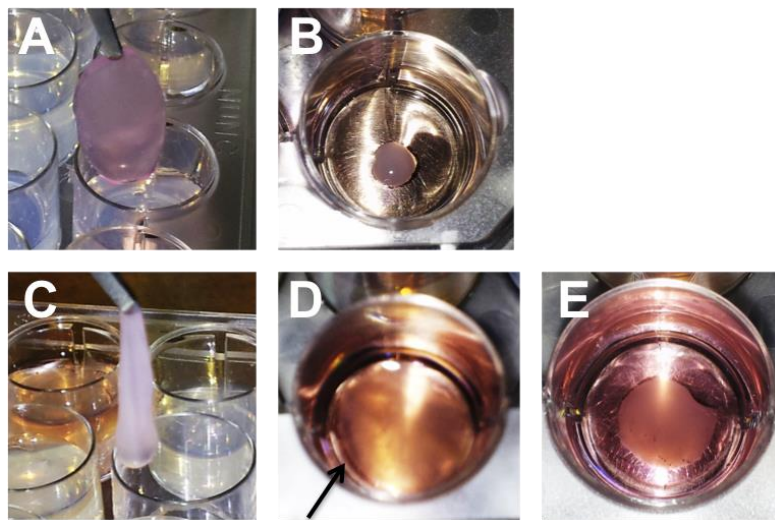


Figure 4.14 Shape and handling of the fibroblast-laden fibrin gels (A) After unmolding at $t=0$ (B) Unmolded for 20h (C-D) After unmolding at $t=20h$ (E) Unmolded for 30min after the 20h.

Manipulation during surgery

When deposited on the surface of the epicardium, first patches would slip on the sides of the sheep's heart and had to be sutured. However, after a few optimization steps, we now have a patch of about 1-mm thickness that looks reasonably thin (even though it is still thicker than the admitted diffusion limit of 200 μm), that can be handled easily (patch unfolds itself on the heart), that sticks to the epicardium and that does not contract after 24 hours of incubation *in vitro* (before surgery). One of the interesting techniques developed during surgery is the use of the pericardium of the sheep as a “kangaroo pouch” (Figure 4.15). This flap allows maintaining the patch on the infarcted area, and, as pericardial cells are adipose tissue cells, we are confident that this pouch will act as a source of paracrine factors that will further recruit autologous endothelial cells to help form a new vasculature inside the patch and the infarcted regions.

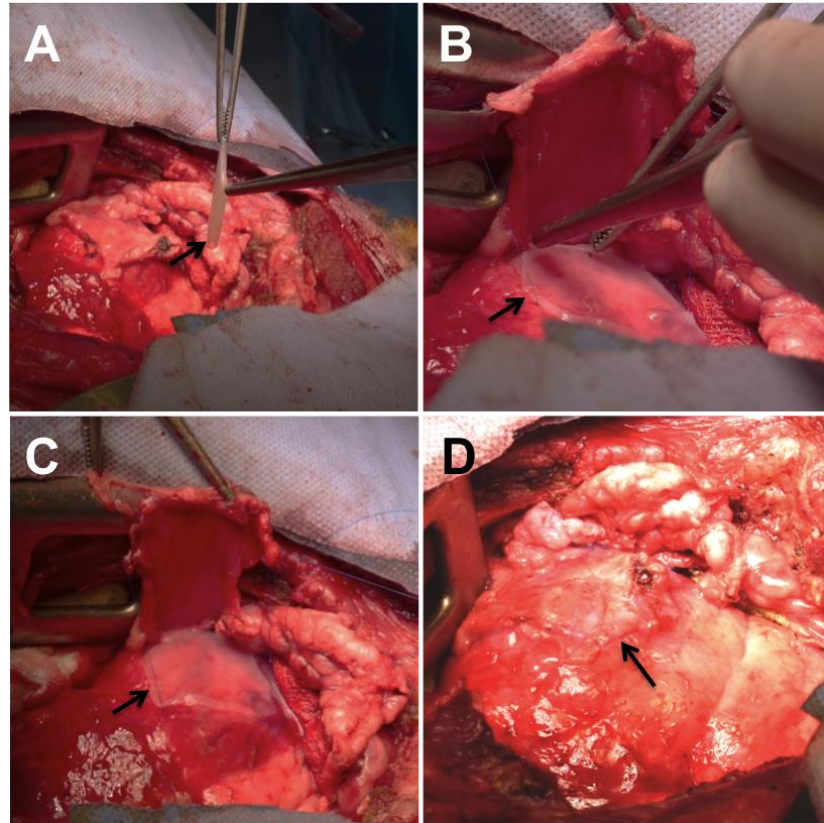


Figure 4.15 Grafting of the patch on a sheep's heart. (A) Handling of the patch with tweezers (B-C) Placing the patch between the epicardium and the kangaroo-like pericardium pouch (D) Suturing the pericardium.

Effect of the patch on rats and sheep

Such patches have then been more thoroughly tested on rats (**Figure 4.16**) and sheep (**Figure 4.15**), and analyses have been reported by Bellamy et al. for the long term outcome of treated rats [35] and by Menasché et al. for the lessons learnt during this 10-year long journey until the authorization to proceed to clinical trial by the regulatory authorities [2].

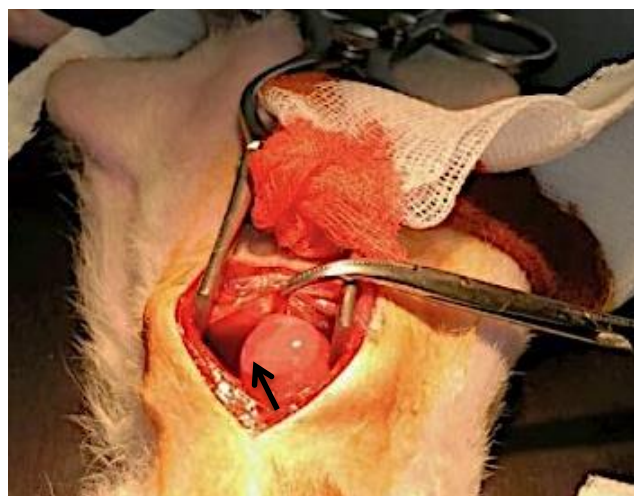


Figure 4.16 Grafting the patch on a rat's heart

Conclusion and Discussion

The aim of this study was to determine the appropriate conditions needed to retain hESCs-derived cardiovascular progenitors inside a fibrin hydrogel for the treatment of congestive heart failure.

After having defined standard methods to quantify fibrinogen concentration in the commercially available fibrin sealant Evicel[®], structural studies were performed in absence of cells to qualitatively assess the optimal volume and concentration to obtain sustainable patches, and then to quantify the pore size inside each patch. Measurements of pore diameters were performed first manually, based on the measurement of 10 pores by patch. These measures have permitted to show that there was an increase in pore size, when the concentration of thrombin and fibrinogen were increased, while keeping the same ratio 5:1 fibrinogen:thrombin (mg/mL : UI/mL). Surprisingly, the automatic and manual techniques did not lead to the same conclusion. The automatic technique gave a global value of pore size from 50 to 80 μm . This could be due to the larger distribution of pores analyzed for one patch, with a less accurate discrimination between the two networks resulting from a hierarchical organization of fibrin's hydrogels: (i) the nanoscopic natural network, formed during polymerization, and (ii) the meso-scopic aggregation of fibers, probably resulting from external stimuli. While measurements of nanoscopic fiber diameter did not give much information regarding the optimal concentration in fibrinogen, the comparison of these values to those of ECM fibers such as collagen and elastin (around 30-300 nm) places fibrin hydrogels among the scaffolds of highest fiber thickness.

Two techniques have been used to assess the mechanical properties of fibrin patches. One more traditional technique on one hand: macroscopic compression testing, using an Instron device with a 10 N load cell. And a far younger one, specially designed for the clinics, on the other hand: shear wave elastography, taking advantage of the attenuation rate of high-frequency ultrasound propagation velocity when penetrating soft tissues. This technique permits to have access to local elasticity measures, when conventional compressive test gives only a global elasticity of the material. Our base material, fibrin, showed a progressive increase in stiffness, from about 2 kPa to 12 kPa with increasing concentrations of fibrinogen and thrombin, from F5T1 to F40T8, respectively. This linear trend may be explained by the fluorescent and histological profiles of these networks. As the real natural pore size is progressively reduced with increasing concentrations, fibers tend to aggregate and both components (dense network and apparition of thick fibers) might act synergistically to form a more rigid network.

Some studies have shown that a good retention inside scaffolds seems to be necessary for promoting hESCs differentiation and preventing loss due to cell mobility (either by passive diffusion or elimination or by active cellular motion) into surrounding tissues [36]. This leads to the conclusion that narrower pores are better at retaining cells inside the fibrin, like those represented in F5T1 patches. Nevertheless, the ideal patch should allow cells to be integrated with the scar tissue or with the healthy tissue at its closest vicinity, and then to repopulate, to revascularize and eventually to replace the necrotic tissue. Considering that scenario, too much retention could be prejudicial for cell migration. Based on our multiple qualitative and quantitative assays of fibrin patches, the optimal size of pores of fibrin gels seemed to be about 100 to 200 μm in diameter. This range matched with the structure of F20T4 patches, that presented an average pore diameter of 158 μm . With regards to stiffness, this formulation had a Young's modulus of about 6.2 kPa. While this is soft compared to a healthy adult myocardium, it lands in the range of fetal heart tissues, as reported by Engler et al. [30].

In order to make sure that the fibrin concentration selected was really efficient for cell encapsulation, cell-laden fibrin patches have been implanted *in vivo*. After sacrifice, the presence of the patch, its vascularization and the presence or remaining CD15⁺ progenitor cells have been assessed in the hearts of treated animals. Also, the evaluation of cardiac function showed improvements at shorter terms for sheep and in the long term for bigger cohorts of rats. The comparison between the histological profiles and the functional improvements suggested that the benefits would in fact result from paracrine signals, with both the patch and the cells disappearing in a 3-week time frame. Nevertheless, as the goal of the phase I clinical trial is only to demonstrate safety, the first patient has now been treated since October 2014 and a first case report has recently been published [37], showing with loads of caution the promising benefits of the cardiac patch on the treated patient.

Perspectives

Because we chose not to use aprotinin in the composition of the fibrin hydrogels, it was natural to observe a rapid degradation of the cardiac patch after implantation either in rats, sheep or even humans. However, recent findings showed that polymerization of fibrin gels in presence of a genetically modified recombinant aprotinin led to dramatic improvements in the degradation rates of the fibrin patch [38]. By combining this modified aprotinin with VEGF, a growth factor involved in the differentiation or the recruitment of endothelial cells, they could promote a long lasting vascularization of the region where fibrin was injected. This is an important step in the field of tissue engineering, where one of the major hurdles is the vascularization of the constructs in order to avoid premature cell death *in vitro* or *in vivo*. Furthermore, even though we did not discuss it in details here because of important

controversies (see Anderson et al. and subsequent replies [39]), cell injections are still considered the best strategy by some groups [40] who are considering clinical trials. Another recent study also reported that small changes in injection techniques, such as aggregating hPSC-derived cardiomyocytes into big clusters prior to injection, could promote a real engraftment of the delivered cells with the host myocardium, while superficial epicardial grafting of a large flap of clustered hESC-derived cardiomyocytes prevented their integration in the host myocardium due to the presence of an interfacial layer of cells that isolated the deposited patch [41]. Consequently, if paracrine-induced regeneration is already a considerable step and is undoubtedly worth further investigation (especially regarding microvesicles, as discussed at the end of this dissertation), there is growing evidence that what we described as our ideal patch, with generation and delivery of new contractile units, is not out of reach in a not-so-far future. We are confident that optimizing the cardiomyocyte and vascular progenitor production step as well as the patch fabrication and delivery steps would help prove or infirm this utopic hypothesis.

References

1. Blin G, Nury D, Stefanovic S, Neri T, Guillevic O, Brinon B, Bellamy V, Rücker-Martin C, Barbry P, Bel A, Bruneval P, Cowan C, Pouly J, Mitalipov S, Gouadon E, Binder P, Hagège A, Desnos M, Renaud J-F, Menasché P, Pucéat M: **A purified population of multipotent cardiovascular progenitors derived from primate pluripotent stem cells engrafts in postmyocardial infarcted nonhuman primates.** *J Clin Invest* 2010, **120**:1125–1139.
2. Menasché P, Vanneaux V, Fabreguettes J-R, Bel A, Tosca L, Garcia S, Bellamy V, Farouz Y, Pouly J, Damour O, Périer M-C, Desnos M, Hagège A, Agbulut O, Bruneval P, Tachdjian G, Trouvin J-H, Larghero J: **Towards a clinical use of human embryonic stem cell-derived cardiac progenitors: a translational experience.** *European Heart Journal* 2014.
3. Gallo P, Condorelli G: **Human embryonic stem cell-derived cardiomyocytes: inducing strategies.** *Regenerative Medicine* 2006, **1**:183–194.
4. Menasché P, Alfieri O, Janssens S, McKenna W, Reichenspurner H, Trinquart L, Vilquin JT, Marolleau JP, Seymour B, Larghero J, Lake S, Chatellier G, Solomon S, Desnos M, Hagege AA: **The Myoblast Autologous Grafting in Ischemic Cardiomyopathy (MAGIC) Trial: First Randomized Placebo-Controlled Study of Myoblast Transplantation.** *Circulation* 2008, **117**:1189–1200.
5. HAMDHI H: **Amélioration de la thérapie cellulaire par greffes de biomatériaux cellularisés dans un modèle d'ischémie myocardique chez le rat.** *PhD Thesis* 2012:1–138.
6. Hamdi H, Furuta A, Bellamy V, Bel A, Puymirat E, Peyrard S, Agbulut O, Menasché P: **Cell Delivery: Intramyocardial Injections or Epicardial Deposition? A Head-to-Head Comparison.** *ATS* 2009, **87**:1196–1203.
7. Hamdi H, Planat-Benard V, Bel A, Puymirat E, Geha R, Pidial L, Nematalla H, Bellamy V, Bouaziz P, Peyrard S, Casteilla L, Bruneval P, Hagège AA, Agbulut O, Menasché P: **Epicardial adipose stem cell sheets results in greater post-infarction survival than intramyocardial injections.** *Cardiovascular Research* 2011, **91**:483–491.
8. Araña M, Gavira JJ, Peña E, González A, Abizanda G, Cilla M, Pérez MM, Albiasu E, Aguado N, Casado M, López B, González S, Soriano M, Moreno C, Merino J, García-Verdugo JM, Díez J, Doblaré M, Pelacho B, Prosper F: **Biomaterials.** *Biomaterials* 2014, **35**:143–151.
9. Laurens N, Koolwijk P, de Maat MPM: **Fibrin structure and wound healing.** *J Thromb Haemost* 2006, **4**:932–939.
10. Barsotti MC, Magera A, Armani C, Chiellini F, Felice F, Dinucci D, Piras AM, Minnocci A, Solaro R, Soldani G, Balbarini A, Di Stefano R: **Fibrin acts as biomimetic niche inducing both differentiation and stem cell marker expression of early human endothelial progenitor cells.** *Cell Proliferation* 2010, **44**:33–48.
11. Yang CL, Chen HW, Wang TC, Wang YJ: **A novel fibrin gel derived from hyaluronic acid-grafted fibrinogen.** *Biomed Mater* 2011, **6**:025009–12.
12. Fergusson DA, Hébert PC, Mazer CD, Frenes S, MacAdams C, Murkin JM, Teoh K, Duke PC, Arellano R, Blajchman MA, Bussières JS, Côté D, Karski J, Martineau R, Robblee JA, Rodger M, Wells G, Clinch J, Pretorius R, BART Investigators: **A comparison of aprotinin and lysine analogues in high-risk cardiac surgery.** *N Engl J Med* 2008, **358**:2319–2331.
13. Sander M, Spies CD, Martiny V, Rosenthal C, Wernecke K-D, Heymann von C: **Mortality associated with administration of high-dose tranexamic acid and aprotinin in primary open-heart procedures: a retrospective analysis.** *Crit Care* 2010, **14**:R148.
14. Lin C-Y, Shuhaiber JH, Loyola H, Liu H, del Nido P, DiNardo JA, Pigula FA: **The Safety and Efficacy of Antifibrinolytic Therapy in Neonatal Cardiac Surgery.** *PLoS ONE* 2015, **10**:e0126514–

11.

15. Jakobsen C-J, Søndergaard F, Hjortdal VE, Johnsen SP: **Use of aprotinin in cardiac surgery: effectiveness and safety in a population-based study.** *Eur J Cardiothorac Surg* 2009, **36**:863–868.

16. Badie N, Bursac N: **Novel micropatterned cardiac cell cultures with realistic ventricular microstructure.** *Biophysical Journal* 2009, **96**:3873–3885.

17. Ho W, Tawil B, Dunn JCY, Wu BM: **The Behavior of Human Mesenchymal Stem Cells in 3D Fibrin Clots: Dependence on Fibrinogen Concentration and Clot Structure.** *Tissue Engineering* 2006, **12**:1587–1595.

18. Zimmermann W-HH, Melnychenko I, Eschenhagen T: **Engineered heart tissue for regeneration of diseased hearts.** *Biomaterials* 2004, **25**:1639–1647.

19. Zimmermann W-HH, Melnychenko I, Wasmeier G, Didié M, Naito H, Nixdorff U, Hess A, Budinsky L, Brune K, Michaelis B, Dhein S, Schwörer A, Ehmke H, Eschenhagen T: **Engineered heart tissue grafts improve systolic and diastolic function in infarcted rat hearts.** *Nat Med* 2006, **12**:452–458.

20. Dhillon S: **Fibrin sealant (evicel® [quixil®/crosseal™]): a review of its use as supportive treatment for haemostasis in surgery.** *Drugs* 2011, **71**:1893–1915.

21. Hickerson WL, Nur I, Meidler R: **A comparison of the mechanical, kinetic, and biochemical properties of fibrin clots formed with two different fibrin sealants.** *Blood Coagulation & Fibrinolysis* 2011, **22**:19–23.

22. Velada JL, Hollingsbee DA, Menzies AR, Cornwell R, Dodd RA: **Reproducibility of the mechanical properties of Vivostat system patient-derived fibrin sealant.** *Biomaterials* 2002, **23**:2249–2254.

23. Huang NF, Chu J, Lee RJ, Li S: **Biophysical and chemical effects of fibrin on mesenchymal stromal cell gene expression.** *Acta Biomaterialia* 2010, **6**:3947–3956.

24. Rowe SL, Lee S, Stegemann JP: **Influence of thrombin concentration on the mechanical and morphological properties of cell-seeded fibrin hydrogels.** *Acta Biomaterialia* 2007, **3**:59–67.

25. Liu J, Hu Q, Wang Z, Xu C, Wang X, Gong G, Mansoor A, Lee J, Hou M, Zeng L, Zhang JR, Jerosch-Herold M, Guo T, Bache RJ, Zhang J: **Autologous stem cell transplantation for myocardial repair.** *AJP: Heart and Circulatory Physiology* 2004, **287**:H501–11.

26. Godier-Furnémont AFG, Martens TP, Koeckert MS, Wan L, Parks J, Arai K, Zhang G, Hudson B, Homma S, Vunjak-Novakovic G: **Composite scaffold provides a cell delivery platform for cardiovascular repair.** *PNAS* 2011, **108**:7974–7979.

27. Xiong Q, Hill KL, Li Q, Suntharalingam P, Mansoor A, Wang X, Jameel MN, Zhang P, Swingen C, Kaufman DS: **A Fibrin Patch-Based Enhanced Delivery of Human Embryonic Stem Cell-Derived Vascular Cell Transplantation in a Porcine Model of Postinfarction Left Ventricular Remodeling.** *Stem Cells* 2011, **29**:367–375.

28. Vallée J-P, Hauwel M, Lepetit-Coiffé M, Bei W, Montet-Abou K, Meda P, Gardier S, Zammaretti P, Kraehenbuehl TP, Herrmann F, Hubbell JA, Jaconi ME: **Embryonic stem cell-based cardiopatches improve cardiac function in infarcted rats.** *Stem Cells Translational Medicine* 2012, **1**:248–260.

29. Engelmayer GC, Cheng M, Bettinger CJ, Borenstein JT, Langer R, Freed LE: **Accordion-like honeycombs for tissue engineering of cardiac anisotropy.** *Nature Materials* 2008, **7**:1003–1010.

30. Engler AJ, Carag-Krieger C, Johnson CP, Raab M, Tang H-Y, Speicher DW, Sanger JW, Sanger JM, Discher DE: **Embryonic cardiomyocytes beat best on a matrix with heart-like elasticity: scar-like rigidity inhibits beating.** *Journal of Cell Science* 2008, **121**:3794–3802.

31. Young JL, Engler AJ: **Hydrogels with time-dependent material properties enhance cardiomyocyte differentiation in vitro.** *Biomaterials* 2011, **32**:1002–1009.
32. Wei-Ning Lee, Pernot M, Couade M, Messas E, Bruneval P, Bel A, Hagege AA, Fink M, Tanter M: **Mapping Myocardial Fiber Orientation Using Echocardiography-Based Shear Wave Imaging.** *IEEE Trans Med Imaging*, **31**:554–562.
33. Pernot M, Couade M, Mateo P, Crozatier B, Fischmeister R, Tanter M: **Real-time assessment of myocardial contractility using shear wave imaging.** *Journal of the American College of Cardiology* 2011, **58**:65–72.
34. Chiron S, Tomczak C, Duperray A, Lainé J, Bonne G: **Complex interactions between human myoblasts and the surrounding 3D fibrin-based matrix.** *PLoS ONE* 2012.
35. Bellamy V, Vanneaux V, Bel A, Nemetalla H, Boitard SE, Farouz Y, Joanne P, Périer M-C, Robidel E, Mandet C, Hagege A, Bruneval P, Larghero J, Agbulut O, Menasché P: **Long-term functional benefits of human embryonic stem cell-derived cardiac progenitors embedded into a fibrin scaffold.** *Journal of Heart and Lung Transplantation* 2014:1–10.
36. Willerth SM, Rader A, Sakiyama-Elbert SE: **The effect of controlled growth factor delivery on embryonic stem cell differentiation inside fibrin scaffolds.** *Stem Cell Research* 2008, **1**:205–218.
37. Menasche P, Vanneaux V, Hagege A, Bel A, Cholley B, Cacciapuoti I, Parouchev A, Benhamouda N, Tachdjian G, Tosca L, Trouvin JH, Fabreguettes JR, Bellamy V, Guillemain R, Suberbielle Boissel C, Tartour E, Desnos M, Larghero J: **Human embryonic stem cell-derived cardiac progenitors for severe heart failure treatment: first clinical case report.** *European Heart Journal* 2015:1–7.
38. Sacchi V, Mittermayr R, Hartinger J, Martino MM, Lorentz KM, Wolbank S, Hofmann A, Largo RA, Marschall JS, Groppa E, Gianni-Barrera R, Ehrbar M, Hubbell JA, Redl H, Banfi A: **Long-lasting fibrin matrices ensure stable and functional angiogenesis by highly tunable, sustained delivery of recombinant VEGF164.** *Proceedings of the National Academy of Sciences* 2014, **111**:6952–6957.
39. Anderson ME, Goldhaber J, Houser SR, Puceat M, Sussman MA: **Embryonic Stem Cell-Derived Cardiac Myocytes Are Not Ready for Human Trials.** *Circulation Research* 2014, **115**:335–338.
40. Chong JJH, Yang X, Don CW, Minami E, Liu Y-W, Weyers JJ, Mahoney WM, Van Biber B, Cook SM, Palpant NJ, Gantz JA, Fugate JA, Muskheli V, Gough GM, Vogel KW, Astley CA, Hotchkiss CE, Baldessari A, Pabon L, Reinecke H, Gill EA, Nelson V, Kiem H-P, Laflamme MA, Murry CE: **Human embryonic-stem-cell-derived cardiomyocytes regenerate non-human primate hearts.** *Nature* 2014, **510**:273–277.
41. Gerbin KA, Yang X, Murry CE, Coulombe KLK: **Enhanced Electrical Integration of Engineered Human Myocardium via Intramyocardial versus Epicardial Delivery in Infarcted Rat Hearts.** *PLoS ONE* 2015, **10**:e0131446–20.

Chapter 5 – From the clinics to the labs: development of new microfabricated platforms for the standardization of cardiomyocyte differentiation

Introduction

While cardiovascular diseases do not cease to progress worldwide, no new drug has been marketed in the last 10 years. Not only the important cost for developing a new drug and testing it on models such as cell cultures, small and big animals has been discouraging. But also, the status of gold standard of afore mentioned models have become more and more questionable. At the same time, cell therapy has emerged as a bankable alternative with a simple hypothesis: there is probably no need to screen for new, complex drugs if we can harvest the healing and regenerating properties of the body itself. As a matter of fact, the human body possess many types of cells that can help regenerate or heal organs. As a result, being able to harvest and produce large quantities of these cells with a good yield is probably one of the biggest challenges to date. Not only would it help making banks for future cell therapies, but using tissue engineering techniques, these cells can help form micro-tissues able to mimic the physiological or pathological behavior of certain organs more reliably than common culture dishes or even animals, small or big.

From the pioneering work of Laflamme and colleagues [1], protocols have been refined to take into consideration the production costs of these cells as well as the risks (and hence the regulatory requirements) for patient's health [2-4]. Laboratories worldwide have been moving from growth factors-based differentiation protocols to small molecules in xeno-free cell culture media. While they start to be very efficient, they are performed in conditions that have been shown to affect the differentiation stage itself. Engler and colleagues reported in 2006 that the fate of MSCs could be altered by cultivating them on substrate of different elasticity [5]. Since then, it has been established that cell fate is highly dependent on substrate stiffness, culture dimension (2D or 3D), ECM protein type and density, as well as ECM organization [6]. Placing cells in the wrong environment can lead to counterproductive effects that are not to be neglected when considering both clinical and pharmaceutical applications. In an attempt to create standardized culture methods for cardiomyocytes differentiation, a few groups have already proposed either circular geometries (in the case of 2D cultures) or spherical geometries (in the case of 3D cultures). However, optimal dimensions and protocols were very different from group to group, and microfabrication was either used for very practical reasons [7], or used to address more foundational questions, be it the effect of local concentrations of growth factors [8] or to study the formation of cardiac micro-chambers from pluripotent cellular monolayers [9].

Here we study two parameters of the cell environment that can be controlled to make reliable and high-throughput differentiation of embryonic or induced pluripotent stem cells: the elasticity of the substrate, and the cellular confinement (materialized by the ECM spot size). While many protocols have been published regarding microfabrication techniques on soft

materials as reviewed earlier in this document [6], they proved inappropriate for the differentiation of hESCs or hiPSCs in an environment as close to the clinics as possible. Indeed, most studies questioned very short-ranged phenomena related to cytoskeletal architecture and the related mechanotransduction pathways [10, 11]. The cells of interest were rarely human and did not require the absence of antibiotics to behave healthily.

These challenges led us to go back to a completely non-clinical *in vitro* model, rather than pursuing in trying to use clinical resources to study a fundamental phenomenon. Consequently, we removed all the uncertainties that arose from restricting our options to clinically acceptable solutions. Instead of using feeder cells, we preferred Matrigel and recombinant vitronectin fragments. Rather than using a growth factor-based differentiation protocol, we used small molecules to modulate developmental signaling pathways. Last but not least, hESCs were replaced by commercially available hiPSCs, for obvious practical reasons. Here, we present the effects of substrate elasticity and confinement on cardiac differentiation. As a conclusion, we will discuss how, after having used a model environment to isolate the effect of our two parameters of interest, elasticity and topographical confinement, we can adapt the proposed model protocol either to the clinical needs or to higher-throughput protocols for pharmacotoxicology screening.

Materials and methods

Stamp fabrication

Poly-dimethylsiloxane (PDMS) stamps were fabricated using standard photolithography techniques. Briefly, a chromium mask was exposed using a μ PG 101[®] and then developed and etched. Silicon wafers were cleaned with acetone and isopropanol, dried and plasma cleaned. Then, negative or positive photoresist was spun coated onto the wafer, baked, and exposed through the chromium mask using broadband ultraviolet (UV) light. The wafer was then post-baked, developed, dried and silanized using gaseous trimethylchlorosilane (TMCS). PDMS was prepared at a 10:1 base to curing agent ratio, poured on the silicon wafer, degassed and cured for 2 hours at 80 °C. Then, stamps were cut out of the PDMS and stored in a sealed box at room temperature (RT).

Sacrificial coverslip microcontact printing

A mixture of 178 μ g/mL of Matrigel, 50 μ g of fibronectin and 15 μ g/mL of Alexa-fluor-647-conjugated fibrinogen was prepared in PBS. The PDMS stamps were covered with a small amount of this mixture and left at 4 °C for 45 min.

Glass coverslips were cleaned with ethanol and plasma treated for 30 seconds.

After 45 min, the protein solution was carefully collected. Then, the stamp was quickly rinsed in Ethanol and in ddH₂O. The stamp was completely dried and rapidly transferred on the glass coverslip. After ensuring full contact between the microstructures and the glass, the stamp was allowed to sit for 10 min, then removed. Micropatterned coverslips were then transferred in the multi-well plate and covered with a solution of Bovine Serum Albumine (BSA) 5% in PBS for the duration of the quality control by fluorescent microscopy.

Polyacrylamide (PAA) gel fabrication

Supporting glass coverslips were cleaned with ethanol and plasma treated for 3 min. Then, they were covered for 10 min by a solution of 2% Silyl Methacrylate, 1% acetic acid in ethanol. The coverslips were then rinsed twice, dried and stored at 80°C for at least 1 hour.

A solution of Acrylamide/Bis-Acrylamide 19:1 (BioRad®) was diluted in PBS to reach various concentrations (3.5%, 5.5% and 9.5%) depending on the expected stiffness. Tetramethylethylene diamide (TEMED) and ammonium persulfate (APS) 10% were rapidly added to the Acrylamide solution at a ratio of 3:500 v/v activator:acrylamide. The mixture was thoroughly mixed by agitation and then pipetted up and down multiple times before being applied on the silanized coverslips. The liquid solution was quickly covered with the patterned coverslip, avoiding any bubble formation. Remaining PAA was kept as a control of the good gelation.

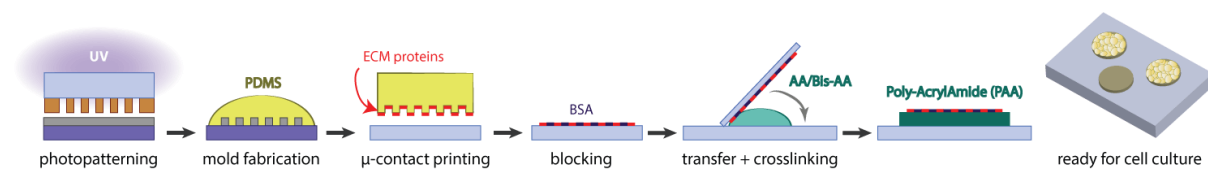


Figure 5.1 Micropatterning ECM proteins on soft polyacrylamide hydrogels.

Instead of using regular petri-dishes coated with Matrigel or vitronectin, we used microfabricated coverslips made of PAA with varying elasticity, covered with a micropatterned mixture of Matrigel and Fibronectin, and blocked with BSA.

The coverslips were left 30 min at RT, then placed 5 min at 37 °C in a humid chamber, transferred in PBS and kept 5 more minutes at 37 °C. Still in PBS, the top coverslip was then carefully removed and discarded using sharp tweezers with bent tips (**Figure 5.1**).

Extensive washing with PBS was performed and the coverslips could be stored a few days in BSA at 4 °C before use. On the day of the experiment, coverslips were left at RT to equilibrate, then washed once with PBS, submerged in complete Essential 8® medium and stored in the cell incubator while the cells were being prepared.

Cell Culture

Human iPS cells from Life Technologies® were cultured on Matrigel-coated dishes in Essential 8® medium. Medium was changed every day. When cells had reached confluency, they were detached with Versene® (0.05% EDTA), resuspended in Essential 8® supplemented with 10

μM Y-27632 and counted. Cells were seeded between passages 15 and 25 at a density of 50,000 cells/well of a 12-well plate, i.e. at about 14,000 cells/cm². The seeding volume was 1 mL so as to be able to shake relatively strongly the plate to spread the cells on the entire surface. This step is considered as t=D-2.5.

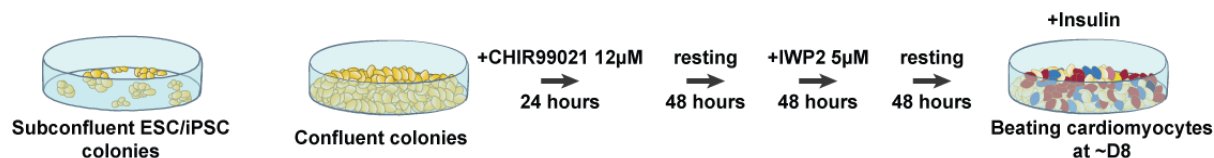


Figure 5.2 Culture conditions and small molecule treatments for purely chemical-based cardiomyocyte differentiation.

Cell culture media, small molecules and the timing of the differentiation protocol are described in details in Lian et al.[4]. After being maintained in 2 days in Essential 8 Medium, cells are then exposed to CHIR99021, medium alone, IWP2, medium alone, and then medium supplemented with insulin.

After 6 hours of incubation (with regular observation and shaking to avoid inhomogeneous sedimentation), 1 mL of Essential 8[®] without any rock inhibitor was added. On the next day, half of the medium was replaced twice at a 6-hour interval so as to reach a concentration of 1.25 μM Y-27632. On D-0.5, half the medium was replaced again. On D0, the medium was replaced by 2 mL of RPMI with B27 Minus Insulin, supplemented with 12 μM CHIR-99021 to inhibit the GSK3- β pathway. From this moment on, the exact protocol of Lian et al. was followed until D13 or later (**Figure 5.2**), when samples were processed for further analysis [4].

Immunofluorescence

Samples were washed with PBS and fixed with a solution of 3.7% Paraformaldehyde (PFA) and 0.05% TritonX-100 for 15-20 min. After fixation, the samples were washed again and placed on drops of a solution of primary antibodies. After 45 min, samples were washed and then placed on drops of secondary antibodies for another 45 min. They were then washed again and stored at 4 °C before preliminary observation and mounting (FluoroShield[®] has been used as preservation agent).

RT-qPCR

For RNA extractions and RT-qPCR, patterns with a single spot size were used. Coverslips were washed with PBS and cells were then resuspended and dissociated in Trizol[®] reagent. The RNA was then extracted using standard phase separation protocols, and DNA and proteins were discarded. The RNA was then reverse transcribed using RevertAid[®] First Strand cDNA Synthesis Kit from Life Technologies using random oligonucleotides. Quantitative PCR was performed at the PCR platform of the Institut du Cerveau et de la Moëlle épinière (ICM) on 1,536-well plates, with the primers described in **Supplementary Table 5.1**.

Statistical analysis

Experiments were repeated not only in terms of number of spots that were patterned on the coverslip, but at least 3 times with different lots of patterned gels. Whenever possible, the different lots were seeded with the same cell passage.

	D12	D15	D12	D15	D12	D15	D12	D15	D12	D15
Glass	1	3	2	3	3	3	3	3	3	3
100 kPa	2	1	2	2	2	1	2	3	2	3
10 kPa	2	2	2	2	1	2	1	3	2	2
1 kPa	2	0	0	1	1	1	2	1	2	1
	800 μm		1600 μm		1600 μm		2000 μm		4000 μm	

Table 5.1 Number of coverslips available for PCR extraction

	D12	D15	D12	D15	D12	D15	D12	D15	D12	D15
Glass	33	25	17	26	21	30	38	45	7	13
100 kPa	28	15	40	31	26	11	31	28	4	5
10 kPa	44	21	38	35	11	15	30	23	6	5
1 kPa	22	0	0	16	11	3	11	7	7	1
	800 μm		1600 μm		1600 μm		2000 μm		4000 μm	

Table 5.2 Total number of cluster images for movie analysis

Data are represented using mean \pm STD. For movie analysis, student t-tests is used to compare conditions together. Significance is displayed using one, two or three stars depending on whether the p-value was < 0.1 , < 0.05 or < 0.01 .

Movies



<https://goo.gl/y2kTf0>

Movies of contracting clusters were filmed using a CMOS Camera from ThorLabs® at a frame rate of 20 fps for 10 s. They were then processed using a custom made software written in Processing (**Supplementary Movie 5.1**).

Briefly, RGB frames were filtered using a binary mask on a selected Region of Interest (ROI) so that white pixel density would vary simultaneously with cell contraction, allowing measuring their beating rate. Additionally, the beating area was measured, together with Boolean parameters such as whether the clusters were cystic, detached from the substrate, presenting a ball, not beating at all, beating in circular waves or irregularly (**Figure 5.3**). Some movies were removed from the analysis when noise had been too important to extract these parameters. All the data were saved in a Simple Query Language (SQL) table and accessed later on using a custom made software developed in Processing language.

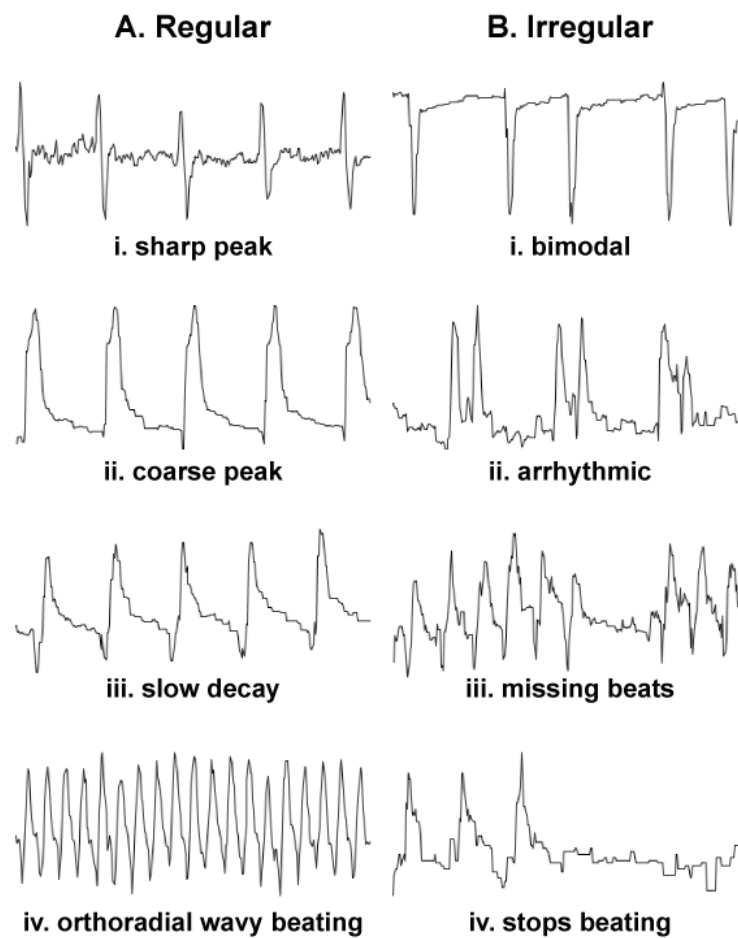


Figure 5.3 Example of beating patterns observed through movie analysis.

(A) Regular patterns, with either i) very fast contraction, ii) slow contraction or iii) slow relaxation. Iv) Some orthoradial waves ("circular" contractions) have been observed in some cases. (B) Irregular contractions, showing either i) a bimodal behavior, ii) an arrhythmic pattern, iii) missing beats, or iv) cell clusters that would stop beating. Total duration for each representative pattern is 10 s.

Results

Characterization of the substrates

In order to make measurements that could be later on linked to clinical observations, we chose to perform mechanical testing using Shear Wave Elastography (SWE)s, a non-invasive technique developed primarily to quickly diagnose tumor, but whose interest in cardiovascular diseases is constantly growing. We have been able to make gels ranging from 1 kPa to 150 kPa just by changing the concentration of a 19:1 solution of acrylamide/bis-acrylamide (**Figure 5.4-A**). Around 3.5%, the stiffness approached 1 kPa while above 10%, the Young's modulus approached 150 kPa.

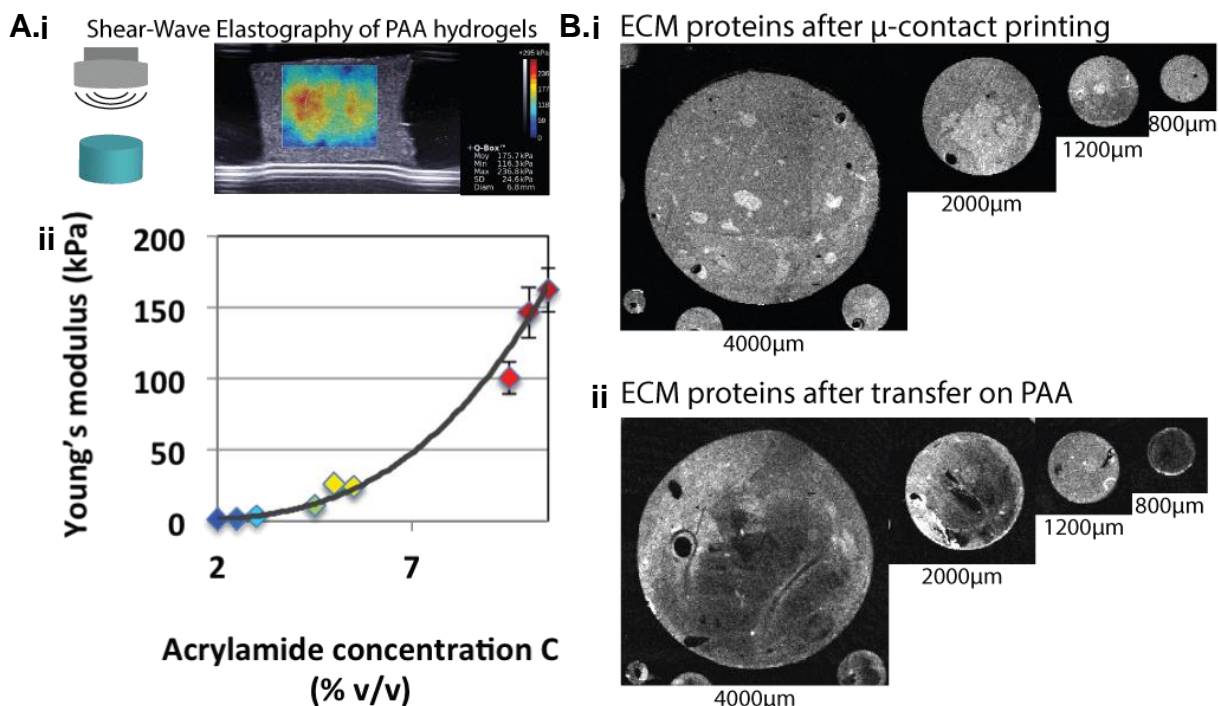


Figure 5.4 Characterization of the substrates.

(A) The Young's modulus of the PAA substrates have been derived from Shear Wave Elastography data. (A-i) Representative picture of the superimposition of echographic visualization and (A-ii) SWE elasticity mapping. (B) Quality of the micropatterning on glass (B-i) and after transfer/molding on PAA (B-ii).

Quality of patterning was systematically assessed by mixing a small amount of fluorescent fibrinogen solution together with a Matrigel/FN solution. Since it appeared that fluorescence decreased between the first patterning step and the transfer on PAA, we chose to double the initial concentration compared to the producer's recommendations (**Figure 5.4-B**). Surprisingly, we observed that the transfer was not as good when the volume of PAA was too high, and this effect was even more pronounced for low concentrations of Acrylamide/Bis-Acrylamide. Additionally, blocking the coverslips with BSA right after the first patterning step was critical to allow for clean unmolding of the PAA after it had polymerized.

While the samples could not be stored in PBS at 4 °C for a long time without contamination happening, we found that maintaining the coverslip in the solution of 5% BSA supplemented with 0.01% NaN_3 led to a good preservation without contamination for weeks. In this way, after washing the coverslips, cell viability was normal, while any attempt to supplement the solution of Acrylamide/Bis-Acrylamide with NaN_3 had led to high cell mortality at seeding, even after several washing steps.

Morphology of the colonies and cell density

The controlled microenvironment allowed for reproducible conditions of differentiation. On each coverslip, we could observe similar organization from spot to spot, with only few variations.

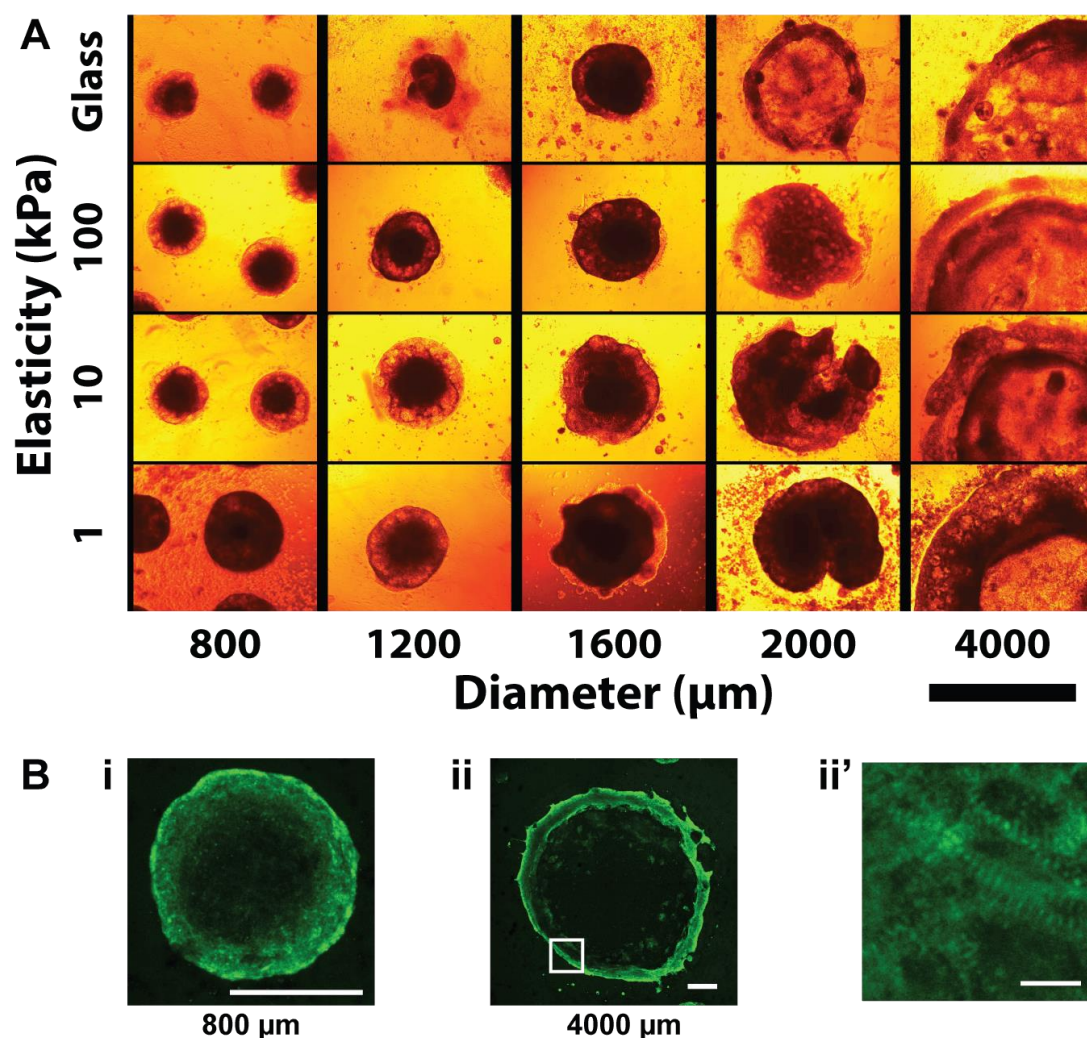


Figure 5.5 Morphological analysis of the differentiated clusters. (A) Snapshots of bright field movie recordings. For each conditions, we can distinguish a cystic beating ring and a non beating central region, either very dense (low diameters) or very flat (high diameters). Scale bar: 2 mm (B) Alpha-actinin immunofluorescent micrograph of spots of 800 μm diameter (B-i) and 4,000 μm (B-ii) with a zoom in the inset (B-ii'). Scale bar: 500μm. Inset scale bar: 10 μm

At the time of the removal of the pluripotency medium, cells were covering the surface of the spot and formed monolayers of epithelial colonies such as those observed in regular iPSC cultures. However, the initial density was different depending on the substrate's elasticity (data not shown). For soft substrates, colonies were spread and formed a bigger dome in the **z** direction. The cell density also seemed smaller. On glass, cells were proliferating more quickly, with a dense flat monolayer at the center (with very small cell volume) and, from time to time, a denser ring at the periphery. Overgrowth would lead to detachment of the colony,

which would hang out in the medium like a crepe. During the 24 hours of GSK3- β inhibition, no significant change has been observed regarding the morphology of the colonies. However, as soon as the CHIR-99021 had been removed, cells started to go out of the epithelial layer and individual migratory cells could be observed.



<https://qoo.gl/KphCqb>

By day 3, the organization of the colony had reached a point that barely changed during the rest of the experiment, with similar morphologies as depicted on **Figure 5.5**. On small spots, colonies formed a dome-like or spherical structure, with the presence of some cysts. For bigger spots, less cysts were observed, but rings were already present at the periphery of the colony, confirming previous observations of Myers et al. 2013 that constrained differentiation reliably led to the apparition of ring of contractions regardless of the differentiation protocol [7]. From 2000 μm to 4000 μm , rings formed as soon as day 3-4, and appeared to be the regions where cells could beat later in the differentiation (**Figure 5.5-A**, xiii to xx, schematic **Figure 5.6-D** and **Supplementary Movie 5.2**).

Although by the end of the differentiation, contractions had caused the cellular clusters to detach from the spots, the final surface area remained, on average, close to the initial one (**Figure 5.6-A**). The thickness of the ring, regardless of the elasticity, depended linearly with the spot diameter, with a correlation factor R^2 of 0.98 (**Figure 5.6-B**). Nevertheless, albeit non statistically significant, rings appeared bigger with decreasing elasticity (**Figure 5.6-C**).

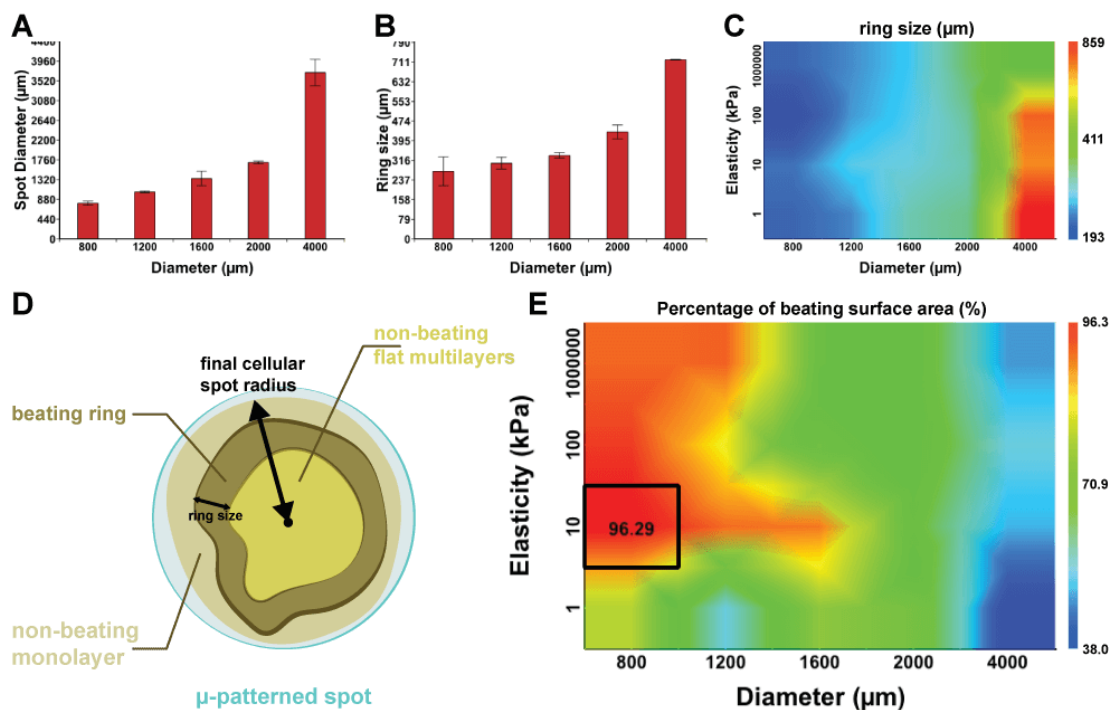


Figure 5.6 General morphology of cell colonies at the end of differentiation.

(A) Diameter of the colony as a function of the initial ECM spot diameter. (B) Size of the beating ring as a function of spot diameter, as depicted in (D). (C) Heatmap of the size of the beating ring as a function of both elasticity and diameter. (D) Schematic of the general morphology of the colony, with a beating ring close to the periphery surrounded by a thin monolayer and surrounding a denser region of flat non beating cells. (E) Ratio of the beating surface area over the total area of the colony. [p-values are summarized in **Supplementary Figure 5.4**]

Consequently, a semi-quantitative approach was used to evaluate an approximate yield of cardiomyocyte differentiation, with the following assumptions (**Figure 5.6-D-E**). First, we considered that no cardiomyocyte was present in the non-beating areas, which had been confirmed in preliminary stains (**Figure 5.5-B**). Second, we neglected the 3D architecture of the ring. With these hypotheses, we calculated the ratio between the surface area of the spot that was actually occupied by cells and the surface area of the beating clusters. Since we found a linear relationship between ring thickness and spot diameter, it was not surprising to find that the smaller the spot, the better the ratio. Even though the ratio was maximal for the condition “800 μm – 10 kPa”, no significant correlation could be established regarding the impact of the elasticity.

Beating behavior of the colonies

Apparition of beating cells

Beating could be observed as soon as day 6 of the differentiation protocol, i.e. 24 hours after removal of the IWP-2. The apparition of beating seemed more related to whether the clusters were well attached to the substrate rather than the elasticity itself. Indeed, beating usually started on very soft substrates, but glass coverslips that had imperfect regions showed early beating as well. In addition, small aggregates that formed outside of the coverslip started beating quite early too, indicating that 3D organization and detachment are necessary conditions for early establishment of contractions. However, it was repeatedly observed that there was an optimal spot size for which beating started first, between 1200 and 1600 μm , but additional experiments would be needed in order to confirm this qualitative statement.

As for the total percentage of beating colonies per condition (**Figure 5.7**), it could be noted that there was almost 100% beating colonies on large patterns, above 2000 μm , while smaller diameters were only beating in between 60% and 100% of the colonies on day 12, and this percentage dropped below 50% on day 15 (**Figure 5.7**). Of importance, **Figure 5.7-A** shows that elasticity changes was related to high variations in beating percentages as a function of time. It was observed that beating percentage was systematically dropping on days 10 and 13 for samples of lower elasticity. As these two days actually correspond to medium changes, we suggest that this is in fact an artifact related to perturbations that happen during this process, such as a decrease in temperature, and a renewal of medium contents. However, even though movie acquisition was always performed after medium change and temperature stabilization, it is uncertain whether it is the stress related to the old medium or the stress related by the medium change operation itself that caused such an irregularity in the beating

patterns. Yet, regardless of the cause, we can already conclude that it affects more strongly the colonies on softer patterns, below 100 kPa.

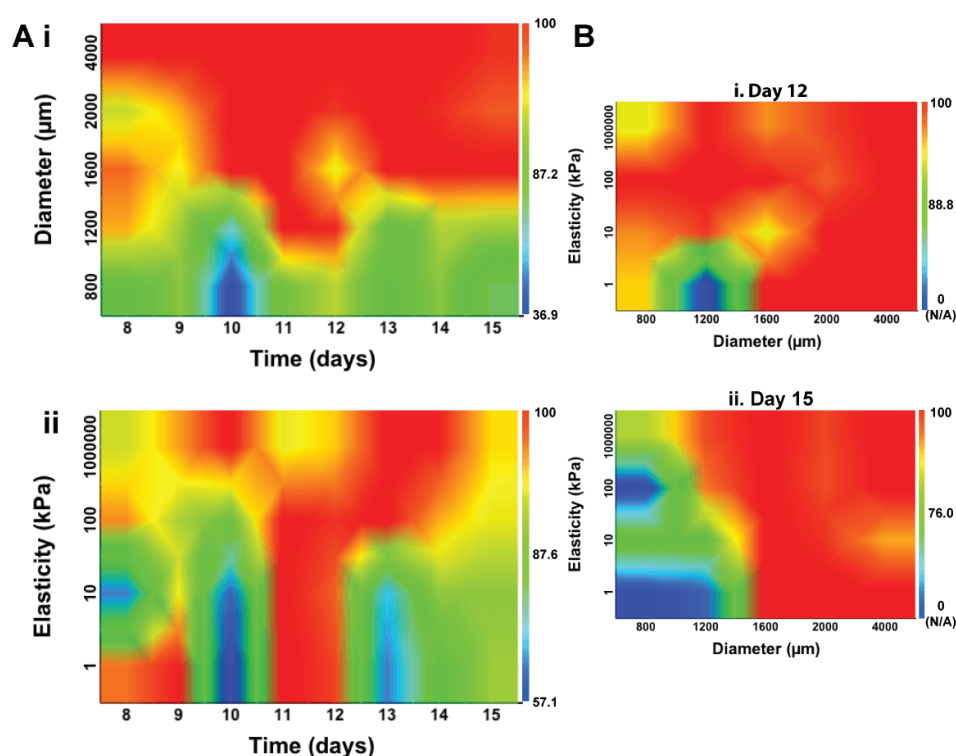


Figure 5.7 Percentage of beating spots as a function of time and spot diameter (A-i), time and elasticity (A-ii), and spot diameter and elasticity on days 12 (B-i) and 15 (B-ii). [p-values are summarized in [Supplementary Figure 5.5](#)]

The first beating days



<https://goo.gl/98Yxt1>

From day 6 to day 8-9, all the colonies started beating with increasing frequency. Remarkably, small spot diameters led to more uniformly beating colonies, while, above 2000 µm, the beating ring did not show strong, synchronous contraction of all the cells at the same time, but rather the propagation of a contraction wave initiated in only one region ([Supplementary Movie 5.3](#)). These patterns of "circular beating" were orthoradial, while regular synchronous contraction occurred radially ([Supplementary Movie 5.2](#)). Also, these auto-stimulated colonies beat may have contributed to the significantly faster pace on large patterns, compared to the average of the regularly beating colonies, as shown in [Figure 5.8-Bi](#), at day 12.

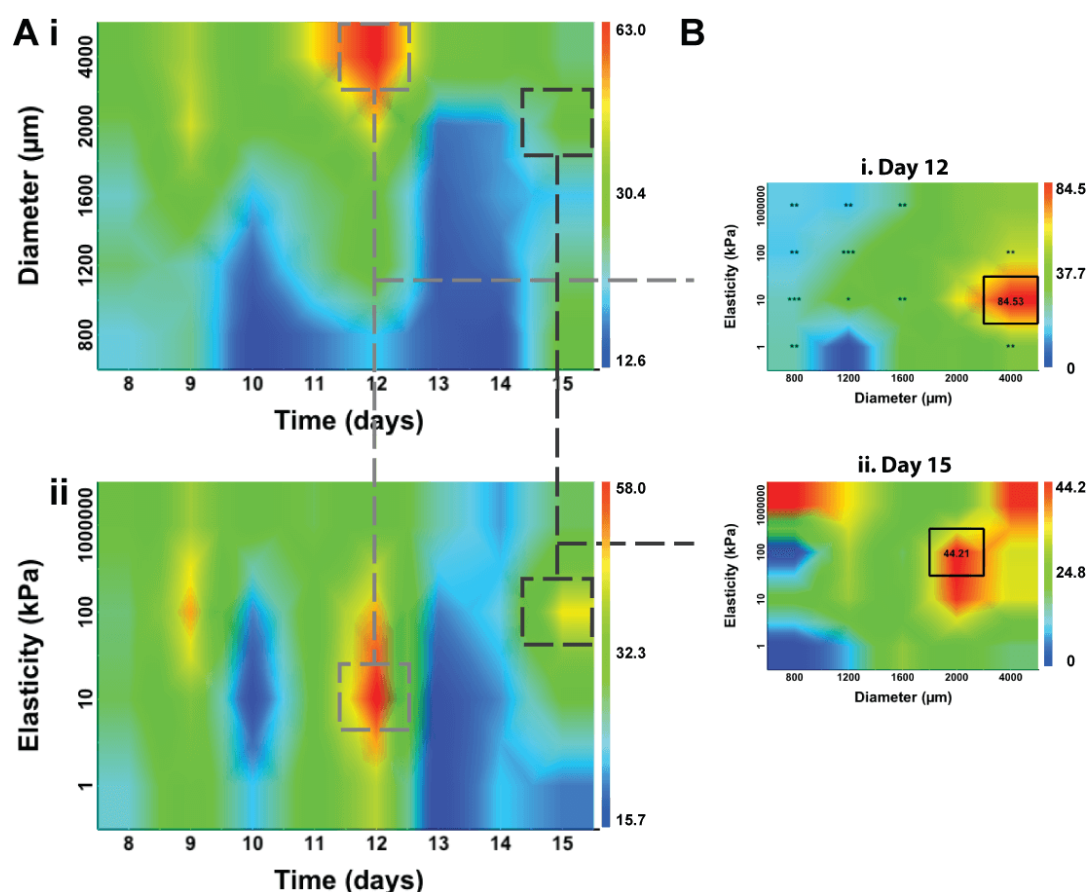


Figure 5.8 Beating frequency as a function of time and spot diameter (A-i), time and elasticity (A-ii), and spot diameter and elasticity at day 12 (B-i) and day 15 (B-ii). [p-values are presented in [Supplementary Figure 5.6](#)]

Stabilization over time

Especially after the addition of insulin, colonies started beating more strongly in all conditions. However, the beating rate started decreasing over time, after day 12 ([Figure 5.8](#)). On soft substrates, the frequency was higher (52 bpm) during the first days, and dropped under 15 bpm after day 12 while the difference was less marked on hard substrates, with a rate of 30 bpm at first and a stabilization around 20 bpm ([Supplementary Movie 5.2](#)). Conversely, spots of higher diameter showed a very high beating frequency in the early days, mainly due to the high proportion of “circular-beat” rings ([Figure 5.9](#) and [Supplementary Movie 5.3](#)), while very small spots showed very slow contraction with a less important decrease after day 12.

Variability decreases with spot diameter and does not depend much on elasticity

When considering higher-scale applications, it is important to assess the variability of the experiment. One of the main problem of regular culture dish differentiation protocol is their high variability for small changes in cell density. Peerani et al. [8] as well as Myers et al. [7]

already showed that it is important to homogenize the density in order to have reproducible results. In a regular petri dishes, there will always be regions of higher density, and experience have led us to conclude that the important parameter is cell density.

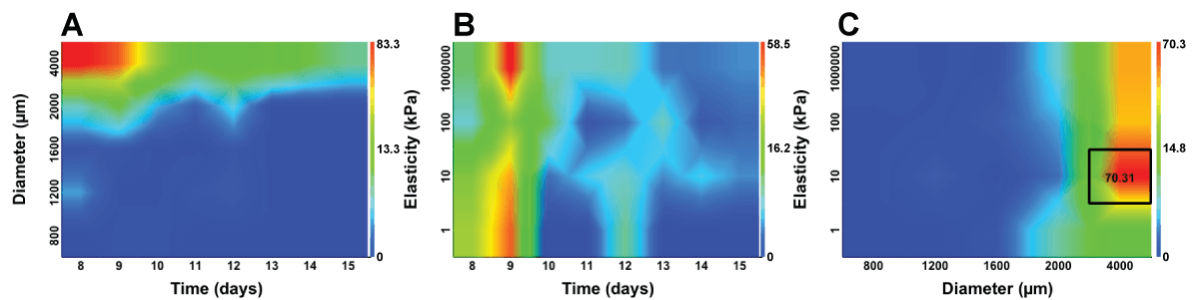


Figure 5.9 Percentage of spots with circular contraction wave behavior, as a function of time (A), spot diameter (B) and elasticity (C).

[p-values are summarized in [Supplementary Figure 5.7](#)]

Here, we show that not only colonies stabilize their beating rate over time, but we observe that there is less and less variability between different colonies in term of beating rate. While spot diameters above 1200 μm still show the highest degree of variability, all the colonies of lower spot diameter behave similarly after day 12.

With regards to the elasticity, although the variability decreases after day 12, there is no real difference between the conditions.

In addition to colony-to-colony variability, we also looked at the proportion of colonies that exhibited non synchronous or non periodic beating patterns. Only after day 14 could we observe variations in irregular beating behavior with a reasonably low standard deviation ([Figure 5.10-A](#)). On day 11 ([Figure 5.10-C](#)), when irregular colonies were most observed (about 20%) and with the highest standard deviation, the most irregular regions were found in wide and soft patterns (diameter of 4000 μm and elasticity of 1 kPa) or hard and intermediate spot sizes. Yet on day 15, even though the highest rate had reached 35% ([Figure 5.10-D](#)), this was largely compensated by all the other formulations, since the average only reached 7.2% of irregularly beating colonies.

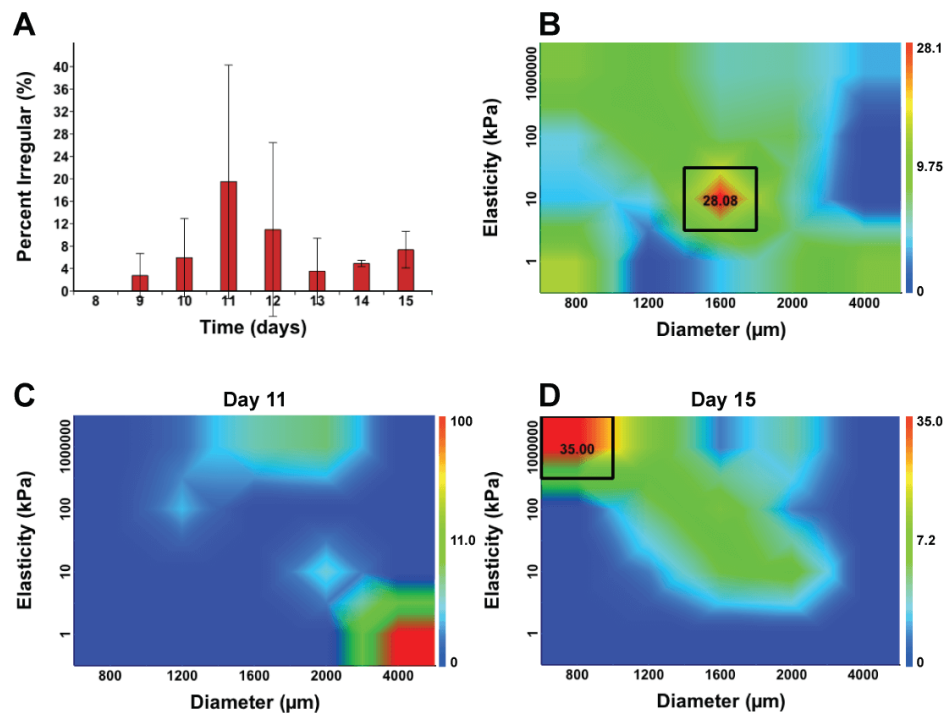


Figure 5.10 Percentage of irregularly beating spots as a function of time, spot diameter and elasticity. [p-values are summarized in [Supplementary Figure 5.8](#)]

Transcriptional analysis

General Transcriptional characterization

We first grouped all the conditions together and compared them to expression levels of undifferentiated hiPSCs isolated before cell seeding at D-2.5 ([Figure 5.11](#)).

As mentioned in the introduction, one of the key parameters that need to be controlled when processing pluripotent stem cells for clinical application is the risk of teratoma formation. Therefore, it is of prime importance to verify that all the pluripotency genes are well down regulated in differentiated cells as compared to naïve hPSCs.

Then, the second question that needs to be addressed is the approximate stage of development reached by the cells, i.e. whether they will behave more like the early mesoderm, the cardiac mesoderm or more like fetal cardiac cells and even neonatal cardiac cells. While some research groups are targeting the latest differentiation stages possible, it is clearly uncertain whether better integration in the host myocardium will be achieved with more mature cardiomyocytes or more plastic early progenitors. As for pharmacotoxicological assays, the more mature the better.

Third, even though it is similar to assessing maturity, it can be important to determine whether cardiomyocytes have more an atrial or a ventricular phenotype. Indeed, it had been previously reported that genes associated with atrial phenotypes are similar to those expressed in the immature fetal heart [12-15].

Finally, vascularization is key to promote the integration and survival of the cells of interest. More independently, we wanted to verify if the softness or the substrates would promote neurogenic or osteogenic differentiation, as reported by Engler and Discher, but with Mesenchymal Stem Cells [5]. Although the main difference was that we modulated the Wnt/ β -catenin signaling pathway to trigger cardiomyocyte differentiation, it has to be noted that neurons are often a side product of uncontrolled, spontaneous differentiation of pluripotent stem cells, and, on the other side, it is well documented that BMP2, albeit at significantly higher doses, can promote osteogenic differentiation [16-19].

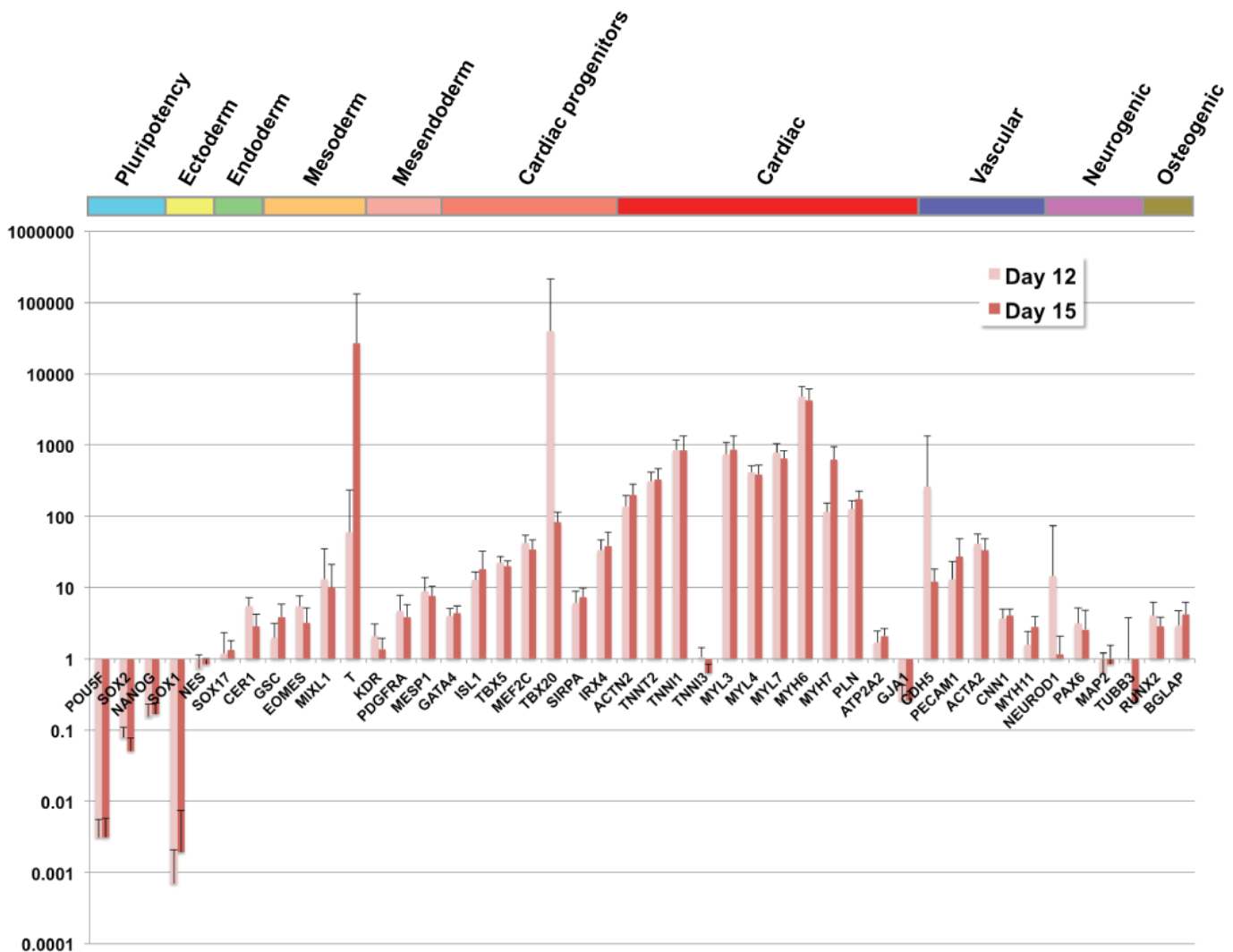


Figure 5.11 Gene expression in change fold versus undifferentiated hiPSC before seeding on micropatterns.

Pluripotency and non-mesodermal markers

The most downregulated genes associated with pluripotency were Oct4 and Sox2 (150 and 20 times less expressed, respectively) whereas Nanog was only downregulated more than 5 times, on average. This is surprising since Nanog is considered to be one of the pluripotency genes that are repressed the earliest, while Oct4 is more persistent, especially in the mesodermal lineage.

As for the three germ lineages, ectoderm related genes were the most downregulated. It is important to notice that the fact that ectoderm genes are not present cannot be correlated with the presence or absence of cells that usually originate from it. In fact, early neurogenic markers such as NeuroD1 and Pax6 were overexpressed on average, but with an important variability from condition to condition. Nonetheless, advanced neuronal markers like β -Tubulin III (TUBB3) were generally downregulated, which is consistent with published literature, where axonal extension (and hence overexpression of TUBB3) is reported to start relatively late, often after the two first weeks of differentiation.

Endoderm-related genes were still slightly expressed even after 12 or 15 days, highlighting the fact that differentiation always gives rise to relatively heterogeneous cell populations. As reported by Warmflash et al., stem cell differentiation on spot patterns can lead to a concentric organization of the cells on the spots, with more ectodermal cells on the outside, mesodermal cells in the middle and endodermal cells at the center [20]. Therefore, what we previously reported as the “non-beating” central areas might in fact be cells from the endodermal lineage.

Mesodermal, early cardiac progenitors and cardiac markers

When looking at the expression profile, the main trend that emerge is a slight overexpression of mesodermal and mesendodermal genes, a bigger overexpression of early cardiovascular progenitors and a dramatically more important overexpression of fetal cardiac markers.

Strikingly, two markers stand out in the expression profile: Brachyury and TBX20. On average, Brachyury was overexpressed more than a hundred folds on day 12, and plummeted to more than 10000-fold expression as compared to naïve pluripotent stem cells. Conversely, Tbx20 expression dropped from more than 10000x to about 100x expression. This is hardly explainable other than by an artifact of the PCR, that is still under investigation.

Atrial vs Ventricular and markers of maturity

It is well known that in humans (and not necessarily in rodents), markers of fetal cardiomyocytes correlates with markers of the adult atria. Ventricular markers appear later in the development. Myosin heavy and light chains belong to the best studied markers as their isoforms give myosins very distinct physical and mechanical properties, such as the ability to generate faster or slower contractions. For light chains, MYL2 and MYL3 correspond to more mature and ventricular phenotypes, while MYL4 and MYL7 correspond to atrial or immature phenotypes. As for the heavy chains, the ratio between MYH6 and MYH7 is often regarded as a good characteristic of immaturity. The lower the ratio, the more mature the phenotype of cardiomyocytes. Here, we observed a very clear trend across all conditions: MYH7 was significantly higher on Day 15 than on Day 12. This increase reveals that on day 15, cells are already a step closer to neonatal cardiomyocytes, rather than the clearly fetal phenotype observed on Day 12.

However, day-15 cardiomyocytes were clearly not as mature as would be neonatal cardiomyocytes, as shown by the relative expression of calcium handling markers such as Serca2 (ATP2A2) and Pln for intercellular calcium management, and Connexin43, the major protein involved in gap junctions and intercellular calcium communications. Indeed, while PLN was clearly overexpressed, ATP2A2 was only increased by less than 5 folds and GJA1 was even less expressed than naïve pluripotent stem cells. This characteristic pattern of immature cardiomyocytes was confirmed by the high overexpression of TNNI1, a slow non cardiac-specific isoform of troponin I that is transiently expressed in fetal hearts, and the basal expression of TNNI3, a fast and cardiac-specific isoform of troponin I that appears only post-partum [13].

Taken together, these results show that on average, cardiomyocytes had a phenotype that was quite mature from a fetal point of view, but still younger than neonatal cardiomyocytes.

Groups	Gene List
Pluripotency	OCT4, NANOG, SOX2
Ectoderm	SOX1, NES
Endoderm	SOX17, CER1
Mesoderm	MIXL1, T, GSC, EOMES
Mesendoderm	MESP1, KDR, PDGFRa
Early cardiac progenitors	MEF2C, TBX5, TBX20, ISL1, GATA4, NKX2.5
Cardiac progenitors	NKX2.5, GATA4, SIRPA, IRX4
Cardiac	TNNT2, TNNI1, TNNI3, ACTN2, MYL2, MYL3, MYL4, MYL7, MYH6, MYH7, ATP2A2, PLN, GJA1
Atrial Immature	MYL4, MYL7, MYH6
Ventricular Mature	TNNI1, MYL7, MYH6, MYL4
	MYL2, MYH7, IRX4
	ATP2A2, PLN, TNNI3, GJA1, MYL2, MYH7, MYL3, ACTN2, MYH11
Vascular	CDH5, PECAM1, ACTA2, CNN1, MYH11
Neurogenic	NEUROD1, PAX6, MAP2, TUBB3
Osteogenic	RUNX2, BGLAP

Table 5.3 Classification of genetic markers depending on developmental stage or major tissue of predilection

Vascular cell lineages

When looking at endothelial and smooth muscle cell markers, it appeared that all of our markers (CDH5, PECAM1 for endothelial cells, CNN1, ACTA2 and MYH11 for vascular smooth muscle cells) were upregulated both at day 12 and 15, but with less relative amplitude regarding smooth muscle cell markers. While PECAM1 and ACTA2 had similar profiles, CDH5 seemed more heterogeneous across conditions, and CNN1 and MYH11 were only upregulated by less than 10 folds.

Neuronal and osteogenic markers

Neuronal markers seemed highly variable and not much overexpressed compared to pluripotent stem cells. However, consistent with the fact

osteogenic cells and muscle cells originate both from the mesoderm and as a result of Wnt inhibition and BMP activation, we found that early osteogenic markers such as BGLAP (osteocalcin) and RUNX2 (CBA1) were both significantly upregulated more than 5 folds. This could be a parameter of prime importance when looking for the optimal condition for clinical applications, since we might want to minimize the amount osteogenic progenitor cells.

Relative transcriptional variations between conditions

We went further and tried to really characterize the phenotype of each and every condition of elasticity and diameter we had tested. Nonetheless, instead of isolating our results for day 12 from our results for day 15, we were curious to see whether the modulation of the physical environment would allow controlling the cardiovascular phenotype earlier than day 15. We wondered if compared to uniformly coated polystyrene petri-dishes (approximated here by the condition with 4000- μm wide spots on glass coverslips), there was a way to generate the most mature cardiomyocytes faster. Hence, we pooled both results from day 12 and day 15 and performed a hierarchical cluster analysis (Figure 5.12) of the gene expression profile, after grouping genes in functional families (Table 5.3) for easier interpretation.

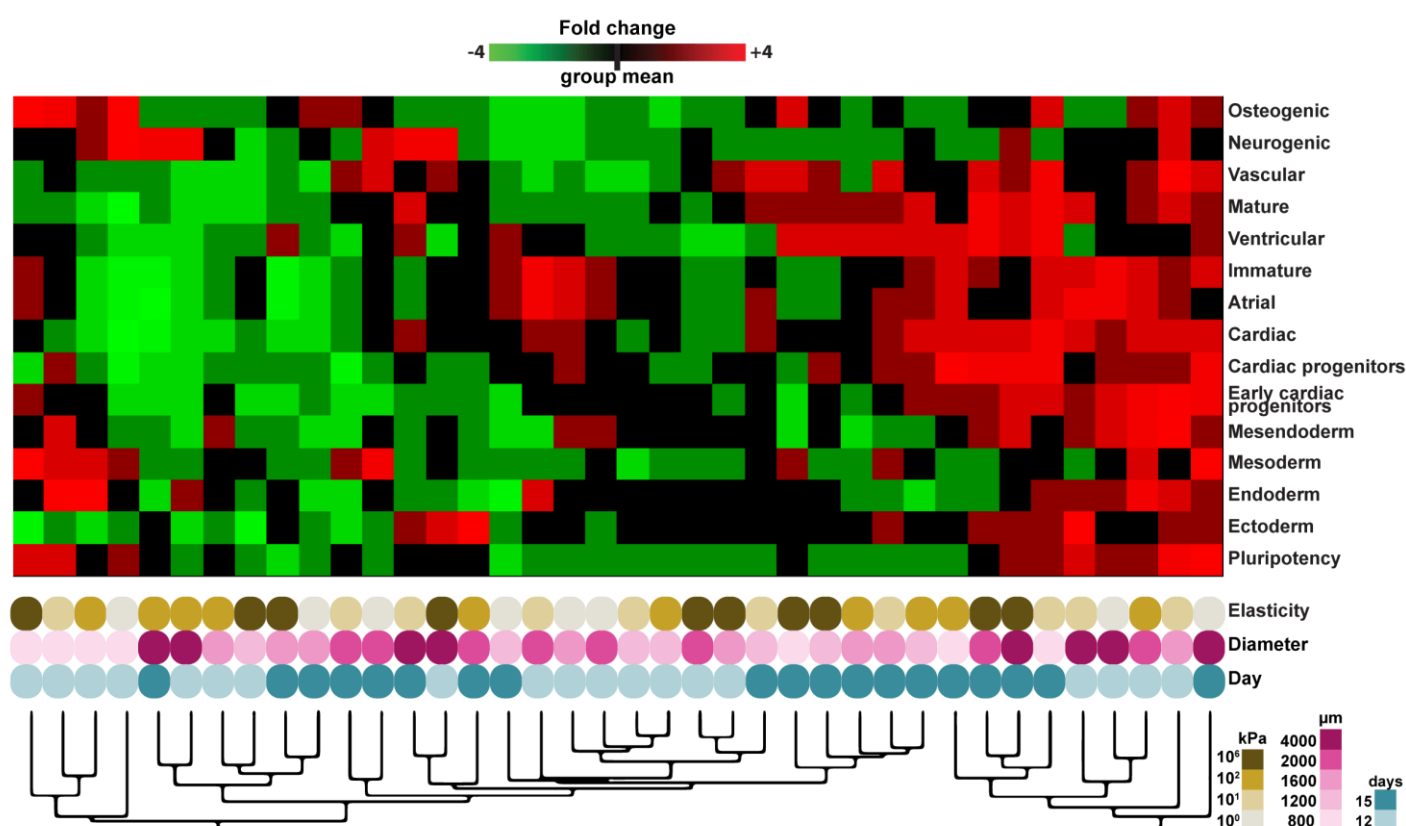


Figure 5.12 Clustergram of the relative expression profiles in different conditions of elasticity (brown), diameter (pink), and day (blue).

Expressions are compared to the overall group mean, and a threshold of ± 4 -fold has been chosen for the heat map generation and for clustering [10^6 kPa represents Glass coverslips]

Interestingly, we found that there were high variations between conditions and that the newly isolated clusters of conditions sometimes grouped samples from both day 12 and day 15. From the clustering, we visually identified three groups of prime interest, regarding cardiac markers: a first group with clear predominance of early cardiac and atrial markers and lower expression of mesoderm or mature markers; a second group with below average expression of mesodermal, early cardiovascular and immature cardiac markers but very high expression of more mature cardiac markers; and a third group of high overexpression of all cardiac and

mesodermal markers. In the following description, we will refer to the different conditions using “E” as a prefix for the elastic modulus in kPa and “D” for the diameter in μm .

A specific population of immature cardiac cells

The first population mentioned above grouped mainly conditions of low elasticity and low/intermediate diameter, such as E1-D1200 at day 15, E10-D2000, E1-D1600 and E1-D2000 at day 12, and, to a lesser extent, E10-D800 and E100-D800 at day 12. Since these conditions were found at day 12, we wondered how they had evolved at day 15.

At day 15, E10-D2000 expressed more mesodermal and vascular genes, together with more markers of mature cardiomyocytes. However, when compared only to conditions at day 15, there were still less than average expression of mature cardiomyocytes. E1-D1600 also shifted to the left side of the clustergram, with less than average expression of all cardiac and pre-cardiovascular markers but higher expression of osteogenic markers. E1-D2000 on the other hand, expressed more average marker of both immature and mature cardiomyocytes but with a strong increase in mesodermal and vascular markers.

Taken together, these results show that while immature cardiac markers emerge faster and more specifically in smaller and softer substrates, these culture conditions seem more unstable and likely to diverge over extended time in culture.

A specific population of mature cardiac cells

The second population was found exclusively at day 15 and mostly on hard and intermediate spot sizes. It included Glass-D800, Glass-D1200, E100-D1600, and, to a lesser extent, E10-D1600 and E100-D1200.

At day 12, Glass-D800 was already showing signs of over average expression of immature cardiomyocyte and average expression of mature and ventricular cardiomyocytes. On the opposite, Glass-D1200 showed lower expression of all genes but those specific to atrial and immature cardiomyocytes. However, when compared only to conditions of similar age, it showed a higher than average expression of ventricular markers, both at day 12 and day 15. Further apart in the tree, E100-D1600 showed average expression of endoderm and ectoderm and at the same time, average expression of mesendoderm, early cardiac progenitors and immature or atrial cardiomyocytes. Albeit its closest neighbor, E10-D1600, on the other hand, belonged to the far right side of the clustergram at day 12, with an overexpression of almost all the studied groups, with a slight “preference” for early cardiac progenitor markers. This is the signature of a very heterogeneous population.

We hypothesize that a mixed population of cells with few cardiac progenitors existed at day 12, and by day 15, many of these cells had differentiated toward a more mature phenotype of cardiomyocytes.

Mixed populations of cardiac precursors

On the right side of the clustergram were grouped populations with the highest expression of all genetic groups. However, two subpopulations can be distinguished: one with more ventricular and mature markers, represented by conditions Glass-D2000, Glass-D4000 and E10-D800 at day 15, and one with more atrial and immature markers, represented by conditions E10-D4000, E1-D4000, E100-D2000 and E10-D1600 at day 12. When looking at the evolution of the latter conditions, we found that at day 15, E10-D4000 had a profile characteristic of mature cardiomyocytes with an overexpression of neurogenic markers, whereas E100-D2000 evolved toward an average profile in all advanced cardiac and vascular markers, with lower than average expression of early markers, neurogenic and osteogenic markers. Additionally, E1-D4000 continued representing a very heterogeneous population where all markers were overexpressed compared to the average signature. Finally, E10-D4000 matured toward a more ventricular phenotype, while conserving an average expression of earlier progenitor markers, and with an overexpression of neuronal markers.

Conclusion on the transcriptional analysis

Even though the significance of this transcriptional study has to be further assessed with more precise metrics, some trends can already be extracted from the above remarks. As a rule of thumb, it appears that soft substrates seem to promote faster differentiation and faster apparition of cardiac markers, at the expense of stability. Wide patterns seem to promote the maintenance and maturation of cardiac progenitors. The combination of elasticity and confinement resulted in the following effects: hard and small substrates led to a slower but more ventricular specific differentiation, hard and wide substrates led to slow and heterogeneous differentiation toward cardiovascular lineages, whereas soft and wide preserved pluripotency and promoted at the same time cardiac progenitor differentiation and the apparition of neuronal markers and soft and small spots showed signs of fast differentiation toward cardiovascular progenitors, slowly maturing toward ventricular cardiomyocytes (Figure 5.13).

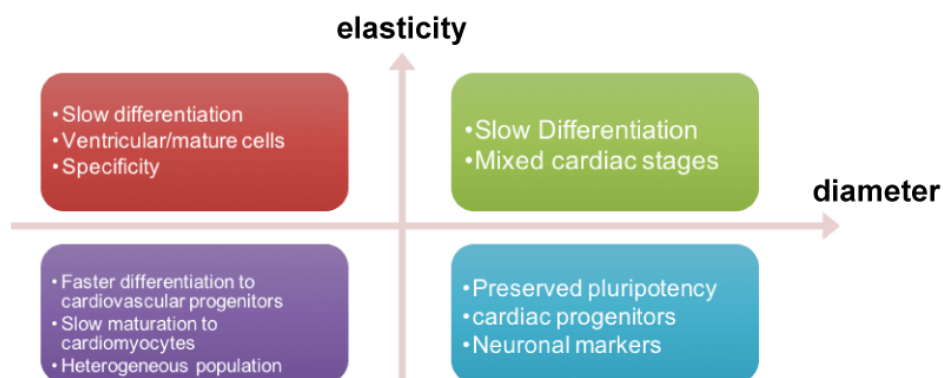


Figure 5.13 Classification of genetic expression variations depending on spot diameter and elasticity

Discussion

In this study, we evaluated the importance of physical parameters of the cellular environment on the differentiation of human iPSCs into cardiomyocytes, using a well-known small molecule based protocol. By modulating the elasticity and the maximal diameter available for hiPSC adhesion, we found out that many functional and epigenetic parameters of the derived cardiomyocytes could be controlled in a more reliable way. Differentiation on average spot size and small elasticity led to the earliest apparition of beating clusters as well as the highest yield of cardiomyocyte production. Generally, the fact that the cells had been confined helped stabilize and homogenize the beating behavior of the cells in the colony, if we consider that 4,000 μm already models the behavior of cells in a small petri dish. Generally, less anomalies like circular contraction propagation were observed on smaller spot sizes but larger spots had the best percentage of beating clusters. This is to be taken very cautiously as the number of clusters of large diameter was significantly lower than on smaller spots.

Even though the role of elasticity remains unclear when assessing functional parameters, genetic expression suggested new differentiation patterns distributed in roughly 4 classes, as summarized in [Figure 5.13](#). However, in the light of experimental considerations, it seems like polyacrylamide substrates, and thus soft substrates, have permitted a faster differentiation as well as better micropatterning quality and sustainability. Additionally, it allowed for the selection of slightly purer populations of immature cardiomyocytes.

Limitations

Experimental limitations

As there were many parameters involved in this study, it is hard to evaluate them independently of the others, and we can highlight a few limitations in the interpretation of the results.

For instance, the initial cell density is crucial for the differentiation to work well, as it has already been reported in many protocols [4, 8, 21, 22]. Therefore, here, we chose one unique density that was found to work well in standard culture conditions (Matrigel-coated polystyrene petri dishes, without any microfabricated sample). But researchers also previously reported the fact that cells adhere and proliferate more slowly on soft substrates than on glass substrate. This means that between $D=-2^-$ and $D=-2^+$ (after cell adhesion), there was already less cells on softer substrates. And because of the slow proliferation rate, there was even less cells at D_0 , which could have biased the experiment. Not only is the Hippo pathway (an important regulator of cell proliferation) closely interacting with ECM-mechanotransduction pathways [23] and with the Wnt/ β -catenin pathway [24], but it has been observed that it played also an important role

in BMP-triggered neuronal differentiation on soft substrates [25] as well as in cardiac development [26-33]. Consequently, it would be interesting to modulate cell density and proliferation rates in defined ways to study these signaling pathways at different stages of the cardiomyocyte differentiation.

Another important point could be the total surface area available for cell adhesion in the cell culture well. For a constant volumetric cell density, we should have had a constant surface area of ECM proteins to promote similar amount of cellular adhesion. However, because of the micro-patterning technique used here, namely micro-contact printing with PDMS stamps, we were restrained in the choice of pitch size between spots, in an attempt to maximize the accuracy and the amount of ECM deposition. Indeed, highly spaced PDMS pillars are much more delicate to handle, as small variations in impression forces can generate bending of the PDMS between the pillars, thus transferring ECM components in between spots. This problem, combined to other experimental considerations such as petri-dish dimensions, cell culture volumes and many others prevented from designing coverslips with exactly identical total surface areas of ECM components.

In order to make definitive conclusions regarding these experiments, additional assays would need to be performed such as optical mapping of calcium wave propagation, force microscopy assays using traction force microscopy (TFM), muscular thin films or engineered heart microtissues, and eventually patch clamping for action potential morphological characterization, preferentially using quality metrics described by Sheehy and colleagues in order to standardize the evaluation of hPSC-derived cardiomyocytes [34]. Because contracting rings often detached from the substrate, TFM could not be performed. Yet, other assays would require cellular dissociation and reseeding into new dishes. Characterizing beating patterns can be very imprecise when considering experimental perturbations such as medium change (as shown on [Figure 5.7](#) and [Figure 5.8](#), medium change always resulted in alteration of the beating patterns). Also, spontaneous contractions can be very irregular in vitro, and even neonatal cardiomyocytes (in rats) show high variability in beating patterns (personal experience). Thus, electrical field stimulation would help address questions regarding pace capture, i.e. the capability of cardiomyocytes to synchronize their depolarization.

Although our video processing technique revealed different beating patterns, from fast *dirac*-shaped pulses to slowly relaxing peaks, it would be premature to conclude on a potential correlation with one cardiac chamber or the other. Especially since Du et al. reported electrophysiological chamber type classifications could be biased by cell culture parameters such as cell density [35].

Furthermore, immunolocalization would allow for more precise spatial characterization of protein expression and cytoskeletal organization, such as sarcomere maturation into widely spaced Z-band striations or gap junction organization. If immunostaining was difficult to achieve using the most common protocols available, there is no doubt that multi-photon microscopy combined with fixation techniques of growing popularity like CLARITY [36] would remove the hurdles of imaging thick and opaque microtissues such as those that resulted from our differentiation protocol.

Finally, even if RT-qPCR provided precious information on the diversity of the cell populations resulting from our differentiation protocol, it does not provide a clear and quantitative answer regarding the yield of cardiomyocytes and the phenotypes of individual populations within a condition. Indeed, it is yet impossible to know whether many cells expressed a small amount of a given cardiac mRNA or if very few cells expressed high amount of the same mRNA.

Which positive control?

The question of the positive control is of prime importance in order to determine whether micropatterning techniques can really lead to improved culture protocols for clinical applications, as compared to traditional methods. Ideally, one would want to investigate whether the mechanical properties of the substrate can drive the differentiation of hiPSCs into cardiomyocytes without the need for small chemicals. Unfortunately, the definition itself of a “small molecule” makes it impossible to isolate the basal culture medium composition from what can be considered as “extra small molecule”. For instance, we observed that while RPMI+B27+CHIR-99021 was able to trigger an epithelial-to-mesenchymal transition (EMT) leading to the generation of cardiac precursors, the removal of CHIR-99021 from the culture medium was not able to maintain a good cell viability when cells were still pluripotent. For these reasons, we chose to perform a published protocol [4] based on the modulation of the Wnt/ β -catenin pathway by small molecules in all conditions of confinement and elasticity. As a result, the positive control would be the regular well, which, under minor approximations detailed here, can also be seen as a big spot on glass coverslips.

Perspectives

Microfabrication on soft substrate can be time consuming when the number of conditions is increased. Furthermore, cell culture medium volumes as well as cell amplification have to be dramatically increased. Common 12-well or 6-well differentiation protocols can then become tedious and expensive and therefore, we looked for ways to reduce the culture dimensions while conserving the ability to incorporate soft, micropatterned substrates. We first considered

the fabrication of PDMS chambers by superimposing two layers of punched PDMS sealed on glass. The first layer (Figure 5.14-A), of wider diameter, would accept the micropatterned hydrogel. The second layer, of smaller diameter (Figure 5.14-B), would act as a culture well. To avoid leakages, the two layers would then be sealed using PDMS glue, or fast curing siloxanes similar to those used in dentistry. Then, the entire structure can be covered either with glass or with a thin sheet of PDMS, to avoid medium evaporation.

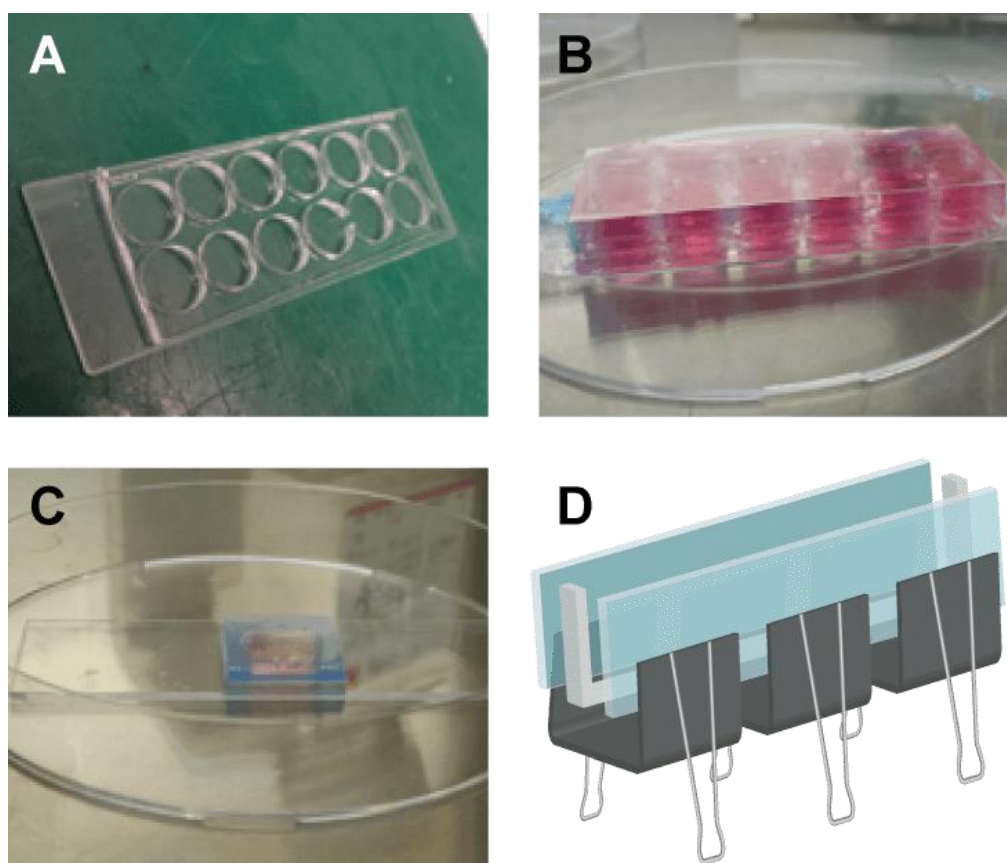


Figure 5.14 Design of new platforms for higher-throughput assays.

(A) First layer of PDMS bonded on a glass slide, with small wells (9-mm diameter, 2-mm thickness). (B) Final construct with a second layer of PDMS (7-mm diameter, 3-mm thickness), holding the PAA gels and supplemented with cells and culture medium. (C) New design using double-sided tape to stick the PDMS microwell (2-mm thickness, 1.5-cm side length) on top of the covalently attached thin PAA hydrogel. The top of the construct is covered by a 350- μ m thick PDMS membrane punched with 8 holes for bubble-less medium injection. (D) Home-made molds for making PDMS, PAA or even alginate and fibrin slabs with similar dimensions as standard glass slides. Office clipboards hold the slides in close contact with the Plexiglas U-shaped spacer.

Yet, as we previously mentioned, the transfer of micropatterns from glass to polyacrylamide seems to be dependent on the volume of polyacrylamide that is sandwiched. We observed that for thick slabs of polyacrylamide of as low as 2-mm, only residual transfer had been achieved. This intriguing question would be worth addressing, but meanwhile, we propose a new design that allows direct polymerization (and ECM transfer) of very thin (100 μ m) layers of polyacrylamide on thick glass slides (previously silanized to exhibit acrylate groups). Then, individual wells can be created by punching out PDMS wells and sticking them to double-faced

tape commonly available at Thermo Fischer for performing low volume immunostaining or qPCR (**Figure 5.14-C**). In both cases, the thickness of the PDMS slabs can be finely controlled using common techniques for the preparation of polymers prior to tensile testing (**Figure 5.14-D**). In our hands, both 2mm-thick slabs and membranes as thin as 350 μm could be produced to make the different parts of the device.

Conclusion

Here, we demonstrated the feasibility of cardiomyocyte stem cell differentiation from hiPSCs using small molecules together with new micropatterned soft substrates made of Matrigel-FN coated polyacrylamide. We show that these culture conditions can be screened using multiple read-outs such as cardiac function (movie analyses of beating patterns), cellular architecture (immunofluorescence) or genetic expression (RT-qPCR). While the most mature and ventricular genetic profiles had been observed for wide patterns on rigid glass coverslips, these conditions would in fact correlate with lower *yields* of beating cells than samples with a smaller diameter (800 μm) and a lower elasticity (10 kPa), due to the toric organization of the cells. In **Supplementary Figure 5.2** and **Supplementary Figure 5.3**, we provide charts for helping deciders choosing the optimal condition depending on their use, and finally, we propose strategies for upscaling this technique to make sure that they benefit to the fields of regenerative medicine, by allowing high volume production of cardiomyocytes or cardiomyocyte-secreted exosomes, and of pharmacotoxicology, by allowing the fabrication of standardized human organs-on-a-chip.

References

1. Laflamme MA, Chen KY, Naumova AV, Muskheli V, Fugate JA, Dupras SK, Reinecke H, Xu C, Hassanipour M, Police S, O'Sullivan C, Collins L, Chen Y, Minami E, Gill EA, Ueno S, Yuan C, Gold J, Murry CE: **Cardiomyocytes derived from human embryonic stem cells in pro-survival factors enhance function of infarcted rat hearts.** *Nature Biotechnology* 2007, **25**:1015–1024.
2. Weng Z, Kong C-W, Ren L, Karakikes I, Geng L, He J, Chow MZY, Mok CF, Keung W, Chow H, Leung AYH, Hajjar RJ, Li RA, Chan CW: **A simple, cost-effective but highly efficient system for deriving ventricular cardiomyocytes from human pluripotent stem cells.** *Stem Cells Dev* 2014, **23**:1704–1716.
3. BurrIDGE PW, Matsa E, Shukla P, Lin ZC, Churko JM, Ebert AD, Lan F, Diecke S, Huber B, Mordwinkin NM, Plews JR, Abilez OJ, Cui B, Gold JD, Wu JC: **Chemically defined generation of human cardiomyocytes.** *Nature Methods* 2014, **11**:855–860.
4. Lian X, Zhang J, Azarin SM, Zhu K, Hazeltine LB, Bao X, Hsiao C, Kamp TJ, Palecek SP: **Directed cardiomyocyte differentiation from human pluripotent stem cells by modulating Wnt/ β -catenin signaling under fully defined conditions.** *Nature Protocols* 2013, **8**:162–175.
5. Engler AJ, Sen S, Sweeney HL, Discher DE: **Matrix elasticity directs stem cell lineage specification.** *Cell* 2006, **126**:677–689.
6. Farouz Y, Chen Y, Terzic A, Menasché P: **Concise review: growing hearts in the right place: on the design of biomimetic materials for cardiac stem cell differentiation.** *Stem Cells* 2015, **33**:1021–1035.
7. Myers FB, Silver JS, Zhuge Y, Beygui RE, Zarins CK, Lee LP, Abilez OJ: **Robust pluripotent stem cell expansion and cardiomyocyte differentiation via geometric patterning.** *Integr Biol* 2013, **5**:1495–1506.
8. Peerani R, Rao BM, Bauwens C, Yin T, Wood GA, Nagy A, Kumacheva E, Zandstra PW: **Niche-mediated control of human embryonic stem cell self-renewal and differentiation.** *EMBO J* 2007, **26**:4744–4755.
9. Ma Z, Wang J, Loskill P, Huebsch N, Koo S, Svedlund FL, Marks NC, Hua EW, Grigoropoulos CP, Conklin BR, Healy KE: **Self-organizing human cardiac microchambers mediated by geometric confinement.** *Nature Communications* 2015, **6**:7413.
10. Tang X, Ali MY, Saif MTA: **A Novel Technique for Micro-patterning Proteins and Cells on Polyacrylamide Gels.** *Soft Matter* 2012, **8**:7197–7206.
11. Deforet M, Hakim V, Yevick HG, Duclos G, Silberzan P: **Emergence of collective modes and tri-dimensional structures from epithelial confinement.** *Nature Communications* 2014, **5**:3747.
12. Veerman CC, Kosmidis G, Mummery CL, Casini S, Verkerk AO, Bellin M: **Immaturity of Human Stem-Cell-Derived Cardiomyocytes in Culture: Fatal Flaw or Soluble Problem?** *Stem Cells Dev* 2015:150225071411000–18.
13. Bedada FB, Chan SS-K, Metzger SK, Zhang L, Zhang J, Garry DJ, Kamp TJ, Kyba M, Metzger JM: **Acquisition of a Quantitative, Stoichiometrically Conserved Ratiometric Marker of Maturation Status in Stem Cell-Derived Cardiac Myocytes.** *Stem Cell Reports* 2014, **3**:594–605.
14. Schwan, Campbell S: **Prospects for In Vitro Myofilament Maturation in Stem Cell-Derived Cardiac Myocytes.** *BMI* 2015:91–13.
15. Birket MJ, Mummery CL: **Pluripotent stem cell derived cardiovascular progenitors – A developmental perspective.** *Developmental Biology* 2015, **400**:169–179.

16. Han Q, Zhang B, Chen B, Dai J, Xu J, Wang C, Wang Z: **Evaluation of a bioactive bone-inducing material consisting of collagen scaffolds and collagen-binding BMP2.** *J Biomed Mater Res* 2013.
17. Dolatshahi-Pirouz A, Nikkhah M, Gaharwar AK, Hashmi B, Guermani E, Aliabadi H, Camci-Unal G, Ferrante T, Foss M, Ingber DE, Khademhosseini A: **A combinatorial cell-laden gel microarray for inducing osteogenic differentiation of human mesenchymal stem cells.** *Sci Rep* 2014, **4**.
18. Wang Y-K, Cohen DM, Wozniak MA, Yang MT, Gao L, Eyckmans J, Chen CS: **Bone Morphogenetic Protein-2-Induced Signaling and Osteogenesis Is Regulated by Cell Shape, RhoA/ROCK, and Cytoskeletal Tension.** *Stem Cells Dev* 2012, **21**:1176–1186.
19. Kilian KA, Bugarija B, Lahn BT, Mrksich M: **Geometric cues for directing the differentiation of mesenchymal stem cells.** *PNAS* 2010, **107**:4872–4877.
20. Warmflash A, Sorre B, Etoc F, Siggia ED, Brivanlou AH: **A method to recapitulate early embryonic spatial patterning in human embryonic stem cells.** *Nature Methods* 2014, **11**:847–854.
21. Zhang J, Klos M, Wilson GF, Herman AM, Lian X, Raval KK, Barron MR, Hou L, Soerens AG, Yu J, Palecek SP, Lyons GE, Thomson JA, Herron TJ, Jalife J, Kamp TJ: **Extracellular matrix promotes highly efficient cardiac differentiation of human pluripotent stem cells: the matrix sandwich method.** *Circulation Research* 2012, **111**:1125–1136.
22. Blin G, Nury D, Stefanovic S, Neri T, Guillevic O, Brinon B, Bellamy V, Rücker-Martin C, Barbry P, Bel A, Bruneval P, Cowan C, Pouly J, Mitalipov S, Gouadon E, Binder P, Hagège A, Desnos M, Renaud J-F, Menasché P, Pucéat M: **A purified population of multipotent cardiovascular progenitors derived from primate pluripotent stem cells engrafts in postmyocardial infarcted nonhuman primates.** *J Clin Invest* 2010, **120**:1125–1139.
23. Halder G, Dupont S, Piccolo S: **Transduction of mechanical and cytoskeletal cues by YAP and TAZ.** *Nat Rev Mol Cell Biol* 2012, **13**:591–600.
24. Azzolin L, Zanconato F, Bresolin S, Forcato M, Basso G, Bicciato S, Cordenonsi M, Piccolo S: **Role of TAZ as Mediator of Wnt Signaling.** *Cell* 2012, **151**:1443–1456.
25. Sun Y, Yong KMA, Villa-Diaz LG, Zhang X, Chen W, Philson R, Weng S, Xu H, Krebsbach PH, Fu J: **Hippo/YAP-mediated rigidity-dependent motor neuron differentiation of human pluripotent stem cells.** *Nature Materials* 2014, **13**:599–604.
26. Mosqueira D, Pagliari S, Uto K, Ebara M, Romanazzo S, Escobedo-Lucea C, Nakanishi J, Taniguchi A, Franzese O, Di Nardo P, Goumans MJ, Traversa E, Pinto-do-Ó P, Aoyagi T, Forte G: **Hippo pathway effectors control cardiac progenitor cell fate by acting as dynamic sensors of substrate mechanics and nanostructure.** *ACS Nano* 2014, **8**:2033–2047.
27. Xin M, Kim Y, Sutherland LB, Murakami M, Qi X, McAnally J, Porrello ER, Mahmoud AI, Tan W, Shelton JM, Richardson JA, Sadek HA, Bassel-Duby R, Olson EN: **Hippo pathway effector Yap promotes cardiac regeneration.** *PNAS* 2013, **110**:13839–13844.
28. Xin M, Kim Y, Sutherland LB, Qi X, McAnally J, Schwartz RJ, Richardson JA, Bassel-Duby R, Olson EN: **Regulation of insulin-like growth factor signaling by Yap governs cardiomyocyte proliferation and embryonic heart size.** *Sci Signal* 2011, **4**:ra70.
29. Porrello ER, Olson EN: **A Neonatal Blueprint for Cardiac Regeneration.** *Stem Cell Research* 2014:1–52.
30. Omatsu-Kanbe M, Nishino Y, Nozuchi N, Sugihara H, Matsuura H: **Prion protein- and cardiac troponin T-marked interstitial cells from the adult myocardium spontaneously develop into beating cardiomyocytes.** *Sci Rep* 2014, **4**:7301.
31. Hidaka K, Shirai M, Lee J-K, Wakayama T, Kodama I, Schneider MD, Morisaki T: **The cellular**

prion protein identifies bipotential cardiomyogenic progenitors. *Circulation Research* 2010, **106**:111–119.

32. Lin Z, Zhou P, Gise von A, Gu F, Ma Q, Chen J, Guo H, van Gorp PR, Wang DZ, Pu WT: **Pi3kcb Links Hippo-YAP and PI3K-AKT Signaling Pathways to Promote Cardiomyocyte Proliferation and Survival.** *Circulation Research* 2014:CIRCRESAHA.114.304457.

33. Wang Y, Hu G, Liu F, Wang X, Wu M, Schwarz JJ, Zhou J: **Deletion of yes-associated protein (YAP) specifically in cardiac and vascular smooth muscle cells reveals a crucial role for YAP in mouse cardiovascular development.** *Circulation Research* 2014, **114**:957–965.

34. Sheehy SP, Pasqualini F, Grosberg A, Park SJ, Aratyn-Schaus Y, Parker KK: **Quality Metrics for Stem Cell-Derived Cardiac Myocytes.** *Stem Cell Reports* 2014, **2**:282–294.

35. Du DTM, Hellen N, Kane C, Terracciano CMN: **Action Potential Morphology of Human Induced Pluripotent Stem Cell-Derived Cardiomyocytes Does Not Predict Cardiac Chamber Specificity and Is Dependent on Cell Density.** *Biophysj* 2015, **108**:1–4.

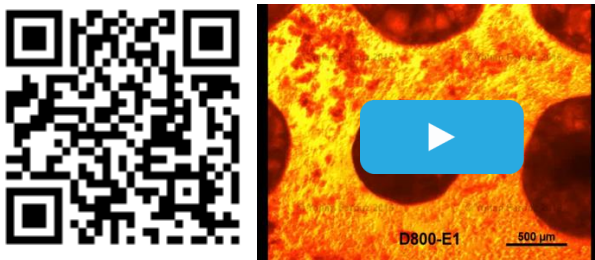
36. Tomer R, Ye L, Hsueh B, Deisseroth K: **Advanced CLARITY for rapid and high-resolution imaging of intact tissues.** *Nature Protocols* 2014, **9**:1682–1697.

Supplementary Information

Supplementary Movie 5.1 Representative movie of the analysis of a cystic cluster beating irregularly (click on any image, flash the QR code or go to the following address: <https://goo.gl/y2kTf0>)

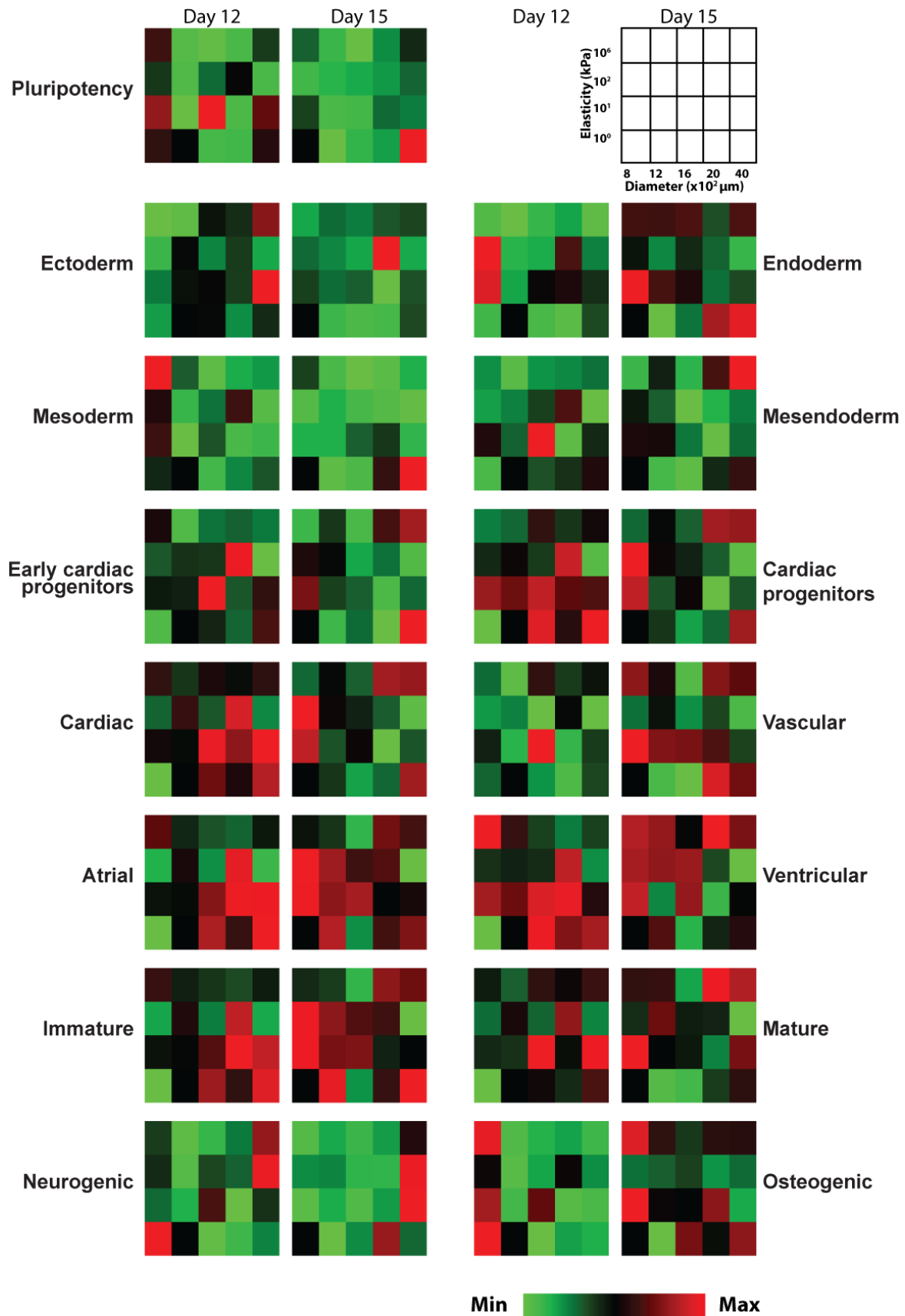


Supplementary Movie 5.2 Representative movies of beating clusters in each condition (click on any image, flash the QR code or go to the following address: <https://goo.gl/KphCgb>)

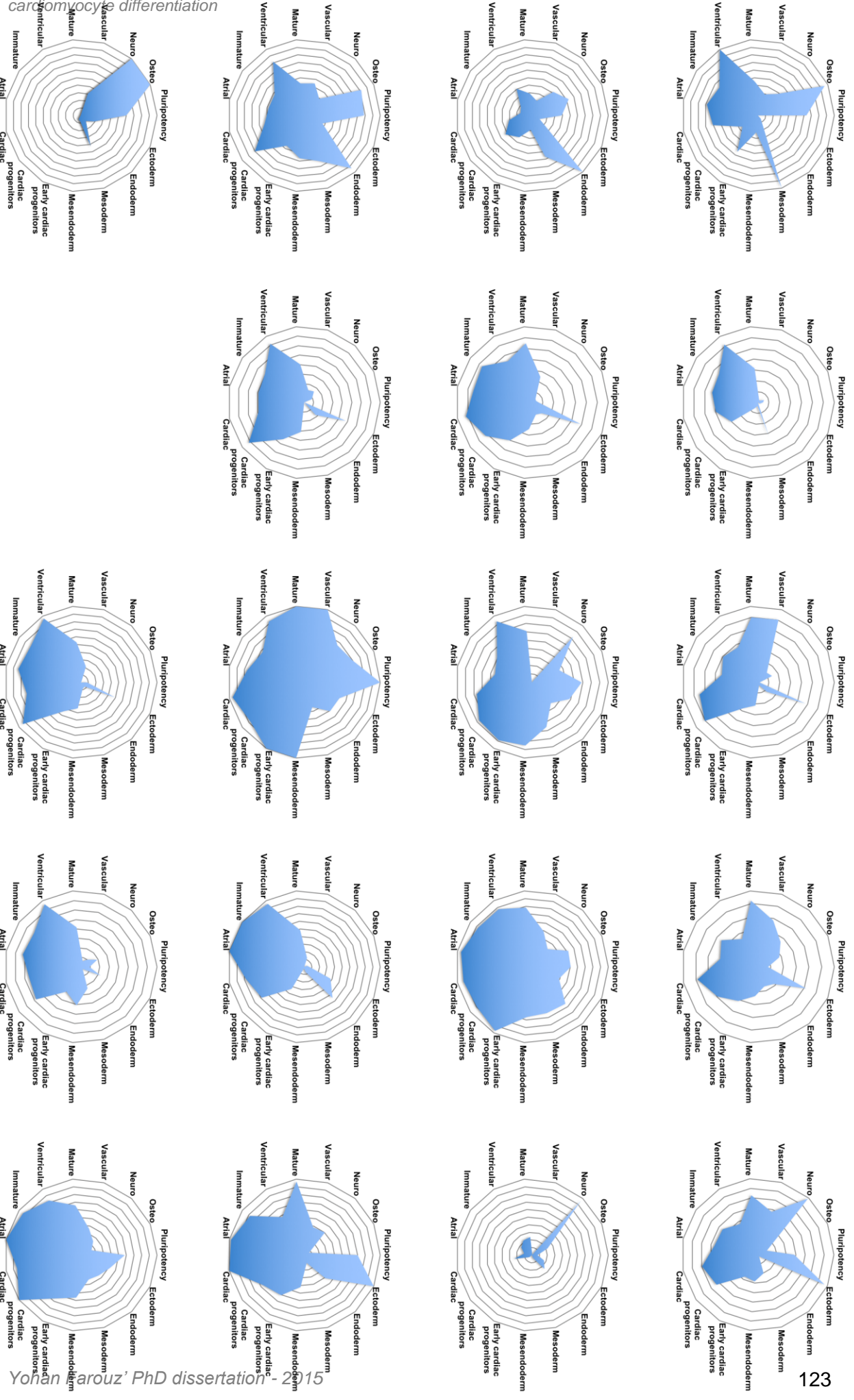


Supplementary Movie 5.3 Representative movies of circular beating (click on any image, flash the QR code or go to the following address: <https://goo.gl/98Yxt1>)

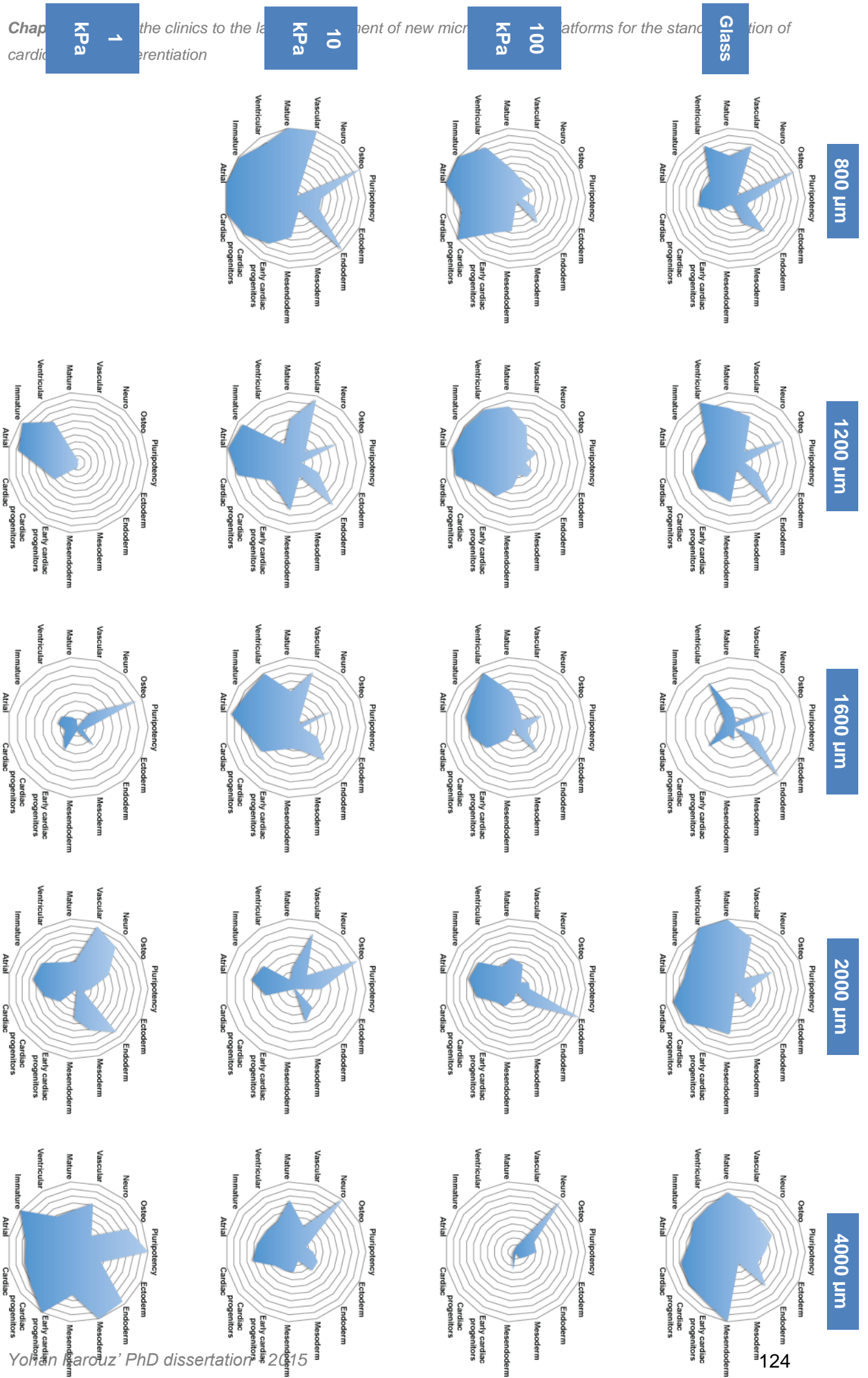




Supplementary Figure 5.1 qPCR's heat maps of clustered gene expression visualization grouped by diameters (x-axis) and elasticity (y-axis) [10⁶ kPa represents glass coverslips]



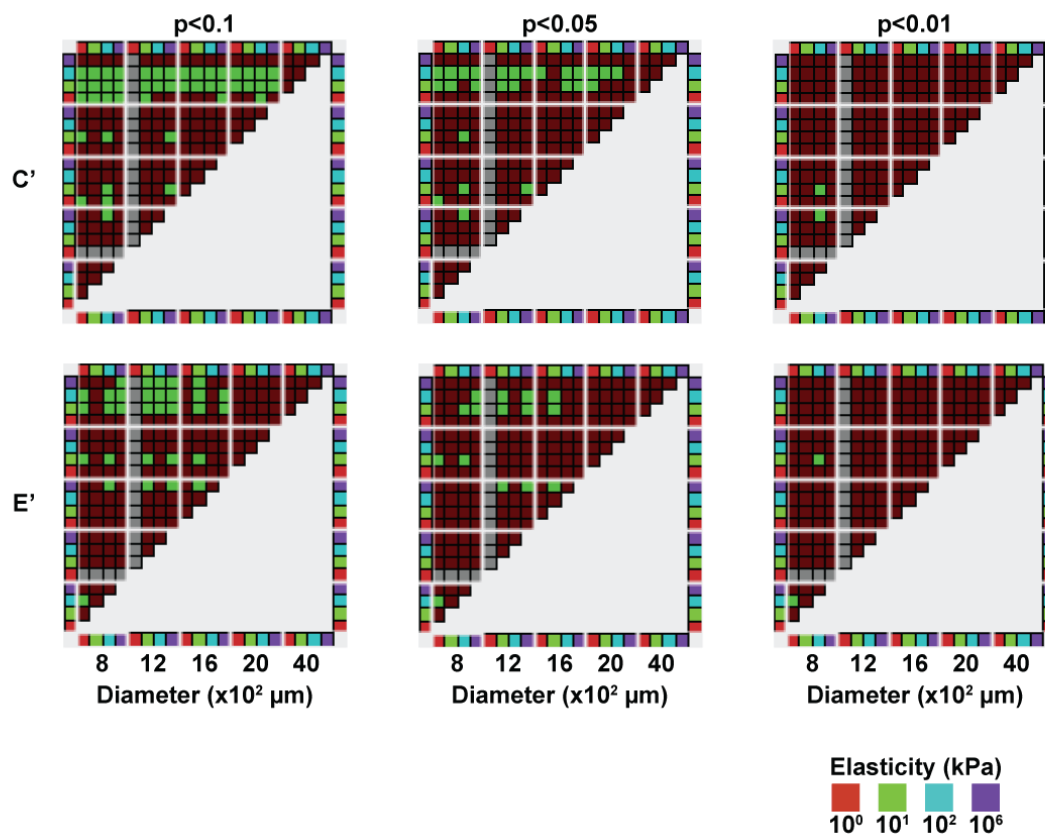
Supplementary Figure 5.2 Web diagram of gene expression for each condition of diameter and elasticity, day 12



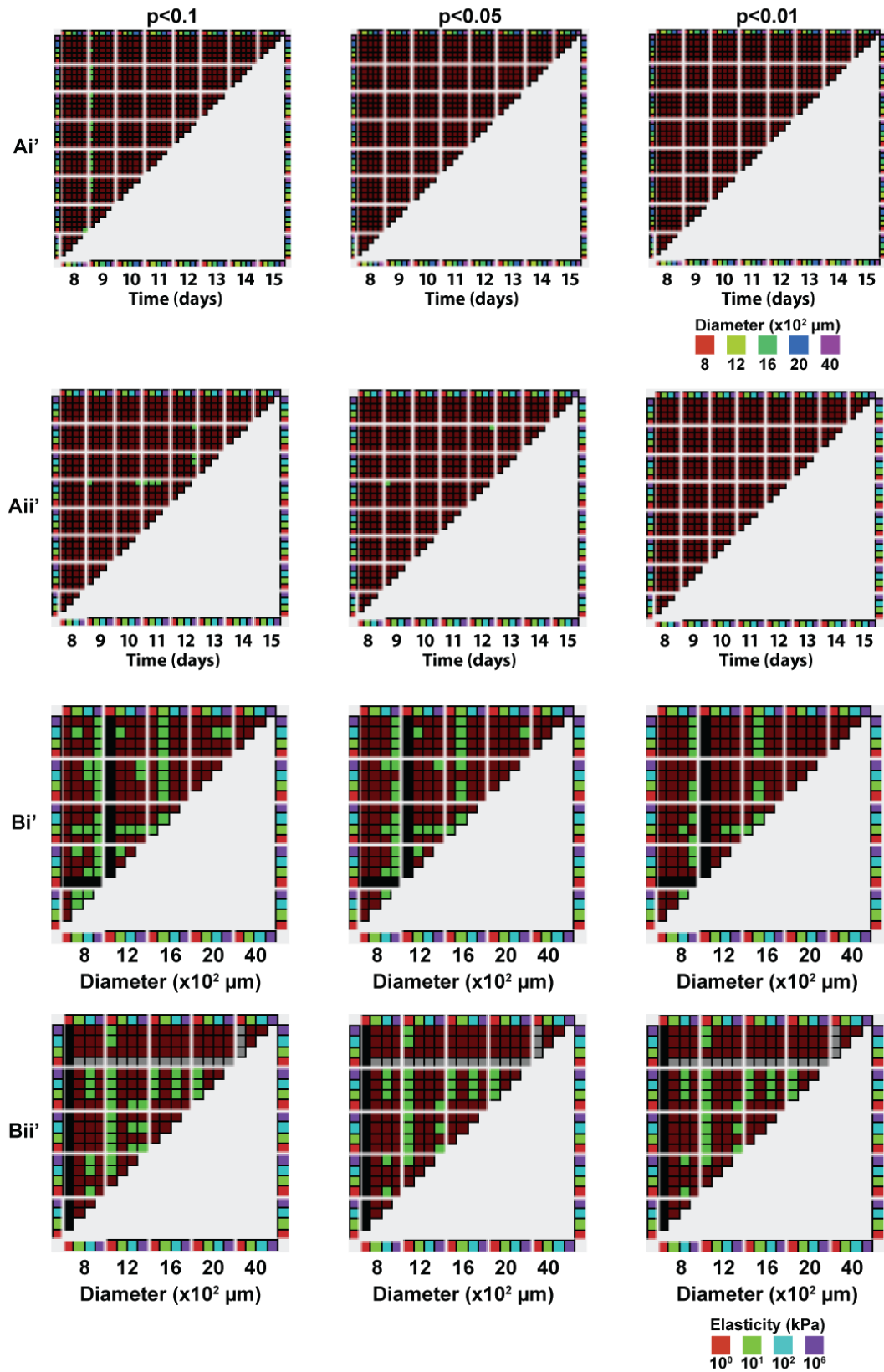
Supplementary Figure 5.3 Web diagram of gene expression for each condition of diameter and elasticity, day 15

Genes	Forward	Reverse
POU5F1(oct4)	ATCAAGCAGCGACTATGCAC	CCAGAGGAAAGGACACTGGT
SOX2	AGGAGTTGTCAAGGCAGAGAA	TCCTAGTCTTAAAGAGGCAGCA
NANOG	CTCAGCTACAAACAGGTGAAGA	GAGTAAAGGCTGGGGTAGGT
SOX1	GCTTTTGTACAGACGTTCCCA	CGCTTCCCTCCGTAGGTGATA
NES	TAGCTCCCAGAGAGGGGAAT	CCTCTCCAAGGAAACAGGGT
SOX17	GAGCAAGATGCTGGGCAAG	CTTCAGCCGCTTCACCTG
CER1	CAGCCAGACTATAACCCACG	GGAAAATGAACAGACCCGCA
GSC	GGAGAAAGTGGAGGTCTGGT	CAGCTGTCCGAGTCCAAATC
EOMES	TACCCAGACCCAACCTTTCC	GGAGGTCCATGGTAGTCCAG
MIXL1	AGTCCAGGATCCAGGTATGGT	GATAATCTCCGGCCTAGCCA
T	CCAGTGGCAGTCTCAGGTTA	CTACTGCAGGTGTGAGCAAG
KDR(FLK1)	GGCTGAAGCTAGGTAAGCCT	ATGCTCACTGTGTGTTGCTC
PDGFRA	AGCCTATGGATTAAGCCGGT	GTAATGGGGCCTGACTTGG
MESP1	GCGCTGTTCCGCCGAG	GGAAGGAGCGGGGACG
GATA4	GACACCCCAATCTCGATATGTT	GTTGCACAGATAGTGACCCG
ISL1	CCAGTCCAGAGAGACACGAC	AATTGACCAGTTGCTGAAAAGC
TBX5	GGTTTTGTCTCCTGCCTTCTCC	AAGATAGGATGCCAGGGAGC
MEF2C	ATACCAGTGGGTGGGAAAGG	GTTGCTGAGGCAAATTGCAG
TBX20	GCAGGAGGATGTTTCCAACC	GGACGATGTCCATCAGGACT
SIRPA	AGAGGGTGTGACCCAGTTAC	CCTGAGCCAGAAATCCCTTG
IRX4	TTCCGTTCTGAAGCGTGGTC	TGAAGCAGGCAATTATTGGTGT
ACTN2	TCTCTTGCTTCTACCACGCT	TCCATTCCAAAAGCTCACTCG
TNNT2	AATAGAGCCTGGCCTCCTTC	CCCCATTTCCAAACAGGAGC
TNNI1	TCCACAACACCAGGGAGATTA	GCAGATCCATGGACACCTTG
TNNI3	TGGACAAGGTGGATGAAGAGA	GATCTGCAATCTCCGTGATGT
MYL3	GAAGATCACCTACGGGCAGT	GTATTGAGCTCTTCTGTCTTGG
MYL4	AGGGATCAGCCTGTCCTAGA	AGTCTATCTTTACACTCTTGGGGT
MYL7	CAGACCTGAGGGAGACCTAC	GGTCTGTCCCATTGAGCTTCT
MYH6	TGACATTGGTGCCAAGCAAA	GTTGGCAAGAGTGAGGTTCC
MYH7	AAAGGTCAAGGCCTACAAGC	TGTGGCAAAGCTACTCCTCAT
PLN	CAGCTGCCAAGGCTACCTAA	CAGCAGGACAGGAAGTCTGA
ATP2A2 (SERCA2)	TCATCCGCTACCTCATCTCG	AGGAATCAAAGCCTCGGGAA
GJA1	CCTCTCGCCTATGTCTCCTC	CGGGGAAATCAAAGGCTGT
CDH5(VE-CADHERIN)	CTACCAGCCCAAAGTGTGTG	ATGTTGGCCGTGTTATCGTG
PECAM1(CD31)	TTGGACCAAGCAGAAGGCTA	TCCATGGGGCAAGAATGACT
ACTA2(SMA)	AAAATGAGATGGCCACTGCC	CGATGAAGGATGGCTGGAAC
CNN1(Calponin)	CAGCATGGCGAAGACGAAA	ATGATGTTCCGCCCTTCTCT
MYH11	GAGACAGCTTACGAGTATGAG	TTGCGTAGCTGCTTGATGG
NEUROD1	CGCGCTTAGCATCACTAACT	TGGTCATGTTTTCGATTTCTTTG
PAX6	CTGTTGGTACAATTGCCGGT	TCTCTGACAGTTCCCTCAGC
MAP2	GGCCAACTTCTCCAGTGAAC	TGCTGGAACCTCAGCAGGTAA
TUBB3	GAGGGCGAGATGTACGAAGA	CTCCGGGGGTTTAGACTG
RUNX2(Cbfa1)	TTAGACGGTCTCACTGCCTC	TGGTCCCTAATGGTGTGGAC
BGLAP(Osteocalcin)	TCACACTCCTCGCCCTATTG	CCATTGATACAGGTAGCGCC
SRP72	TGCTGCTGTGTTTACTCTG	GCAGCACCCATTCTTTCT
SLC4A1AP	CCTCTACGATCTGGGAAGCA	TCTGGTCCCTGCAGGATAAA

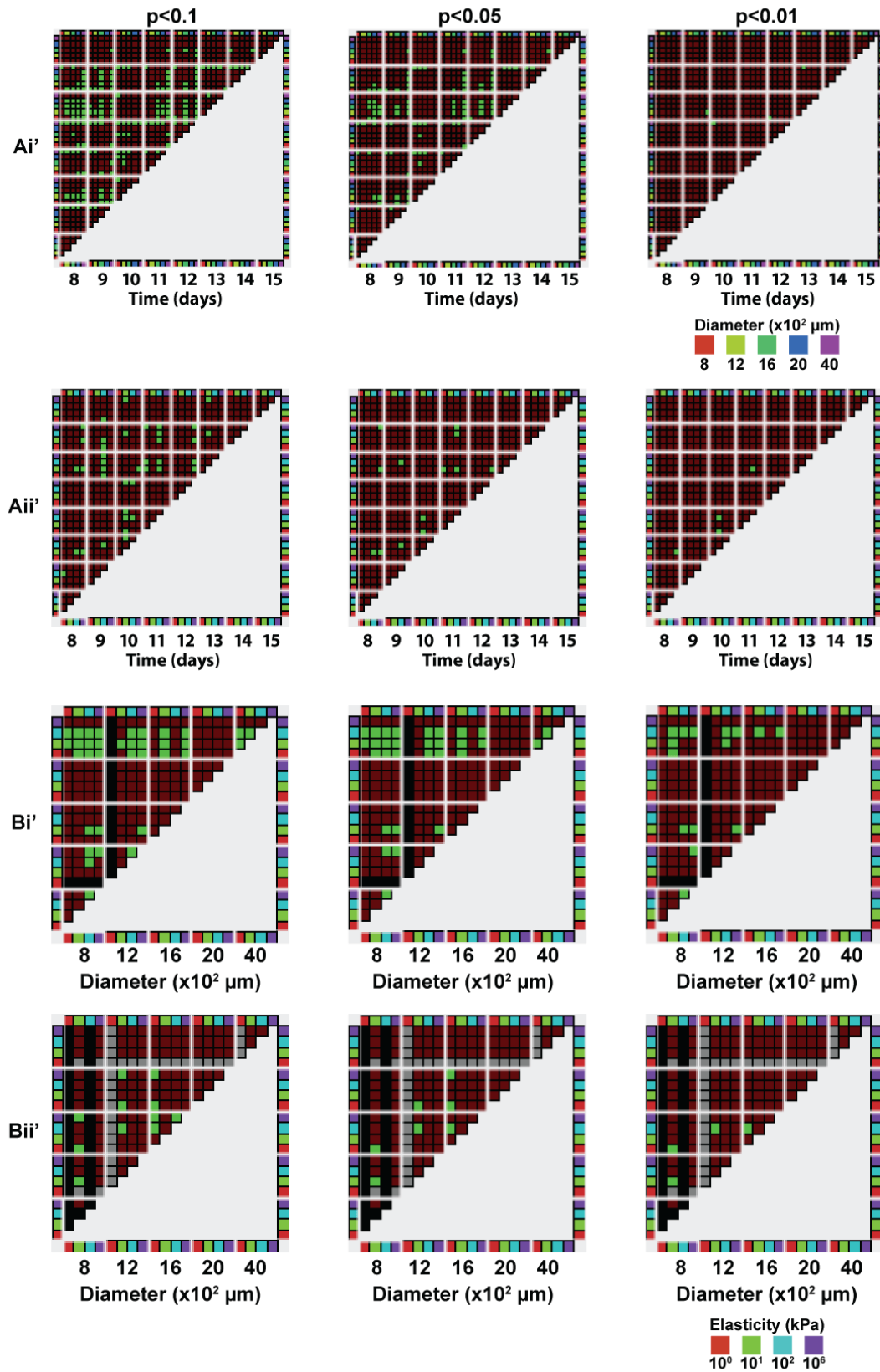
Supplementary Table 5.1 Primer sequences for qPCR experiments



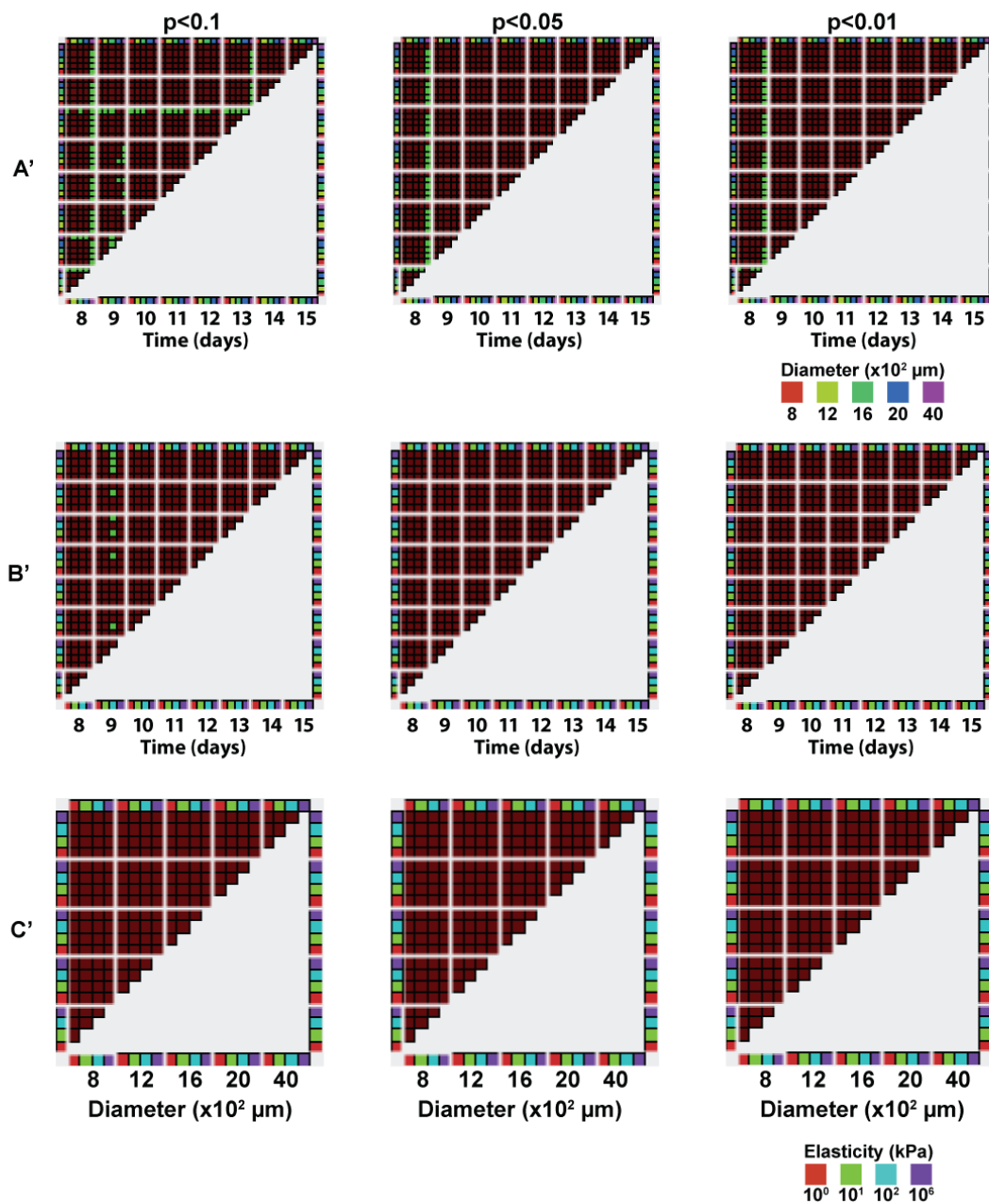
Supplementary Figure 5.4 p-value matrices corresponding to Figure 5.6 . Green represents significance.



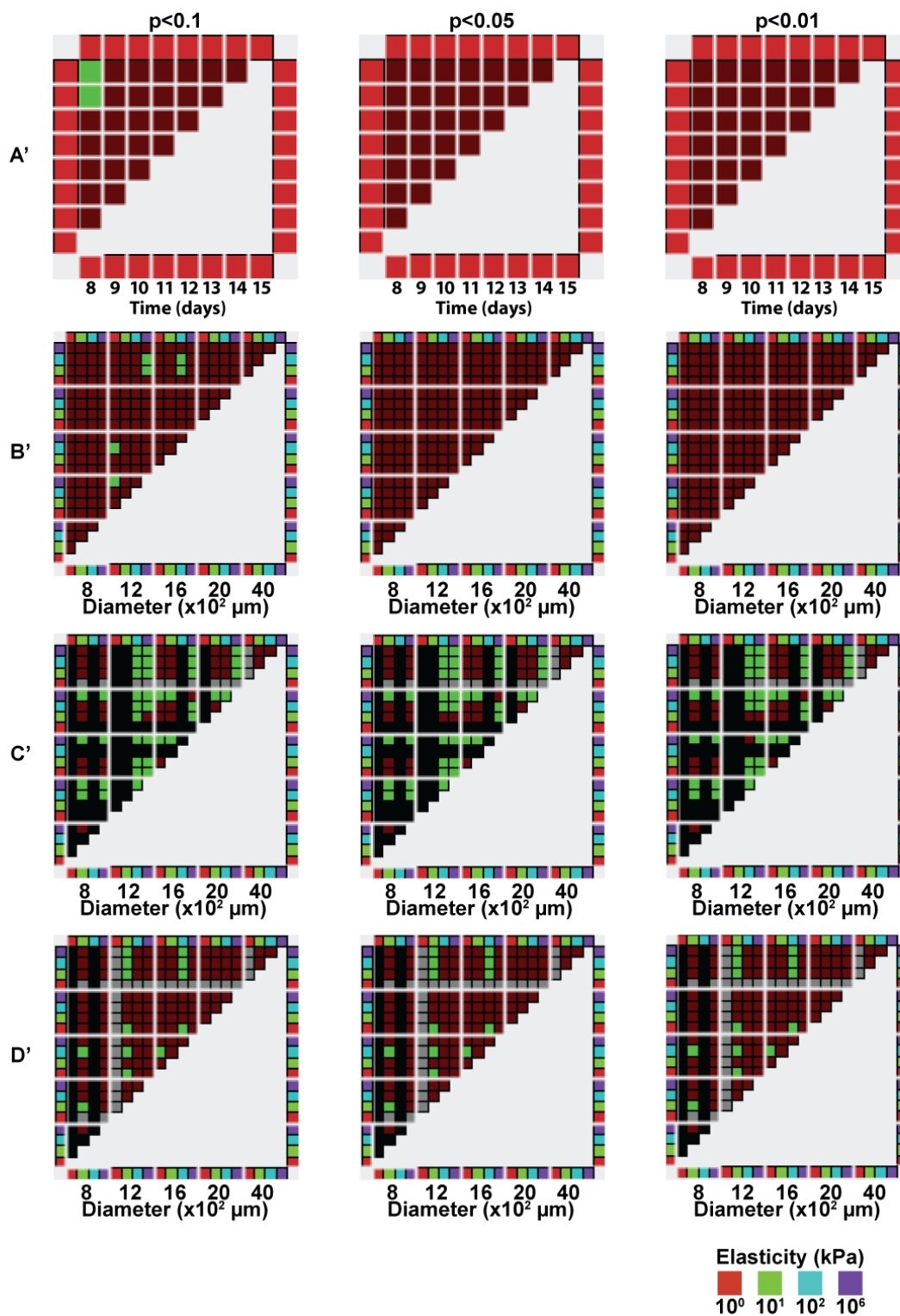
Supplementary Figure 5.5 p-value matrices corresponding to Figure 5.7. Green represents significance.



Supplementary Figure 5.6 p-value matrices corresponding to Figure 5.8. Green represents significance.



Supplementary Figure 5.7 p-value matrices corresponding to Figure 5.9. Green represents significance.



Supplementary Figure 5.8 p-value matrices corresponding to Figure 5.10. Green represents significance.

Chapter 6 – Back to the clinics: new design strategies for the fabrication of Engineering Cardiac Bands

Introduction

Congestive heart failure is characterized by a loss of cardiomyocytes usually due to an ischemic event. This loss is associated with interstitial fibrosis that weakens the contractile power of the myocardium [1]. To compensate for the loss of contractile tissue and the increased mechanical load, cardiomyocytes undergo hypertrophy. This adaptation induces ischemic cardiomyopathy responsible for congestive heart failure, which can lead to the death of the patient [2]. Spontaneous myocardial self-regeneration is limited by a poor mitotic capacity of cardiomyocytes that are terminally differentiated [3]. Stem cell transplantation appears to be a treatment of choice because of its regenerative potential. In a small animal model of myocardial infarction, Assmus et al. have established a limitation of the progression of heart failure, using stem cells [4]. Current protocols for cell delivery through direct injection are not optimal for cell survival and function. Therefore, based on a tissue engineering approach, the combination of cells with a biodegradable scaffold appears to be a suitable alternative [5]. This physical support for cells promotes cell differentiation through its elastic properties [6], avoids non specific homing and enhances *in situ* cell retention [7]. Among the numerous available scaffolds, fibrin has been extensively studied, in part because of its availability and approvability for clinical applications. However, fibrin scaffolds are not optimal. Like many hydrogels it does not exhibit high stretchability. Sun and colleagues have demonstrated that by mixing two polymers, here polyacrylamide (PAA) and alginate, some hydrogels could adopt hybrid mechanical properties [8]. Yet, if PAA usually shows good viability when perfectly crosslinked and when used as a 2D mattress, its use inside a hydrogel for 3D cell encapsulation can be toxic in case of the presence of highly reactive residual acrylamide monomers. We hence considered hyaluronic acid (HA) and alginate: two natural biomaterials known for their biocompatibility and tunable mechanical properties which can be mixed to fibrin to improve its characteristics.

Alginate is extracted from brown algae (Phaeophyceae) and is also synthesized by some bacteria. It is a whole family of linear copolymers, containing blocks of β -D-mannuronate (M) and α -L-guluronate (G) residues (**Figure 6.1**). Only the G-blocks are involved in the cross-linking process with divalent cations such as Ca^{2+} to form an hydrogel [9]. Even if there are still ambiguities about the immunogenicity of alginate [10], the foreign body reaction seems to be controlled by a multi-step extraction procedure [11]. Therefore, more and more applications are proposed with alginate scaffolds: ovarian follicle development [12], strengthening of MI walls [13] or dura mater repair [14].

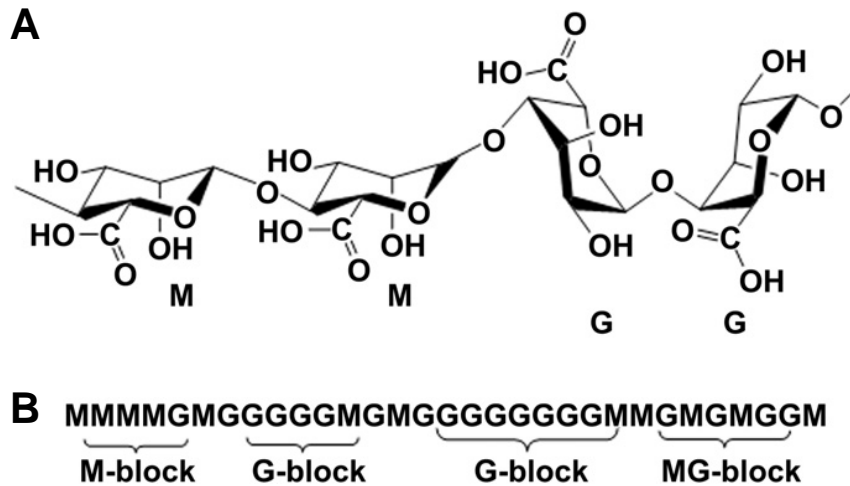


Figure 6.1 Representative alginate structure: (A) chain conformation and (B) block distribution. M: β -D-mannuronate; G: α -L-guluronate

Another way of adding physiological properties to the fibrin gel would be the addition of HA. Hyaluronic acid is a glycosaminoglycan (GAG) (Figure 6.2) present in the human extracellular matrix and responsible for activating many signaling cascades, with a low immunogenic profile and good biodegradable properties [15]. Weigel et al. have demonstrated that HA can also play an important role in the stabilization of fibrin blood clots, by enhancing its physical structure [16]. HA is also known for its impact on cell differentiation towards the cardiac lineage [17] [18, 19]. It has been shown that seeding embryonic stem cells on hyaluronic acid ease their differentiation in phenotypes of the cardiac lineage [20]. Luckily, some clinically approved formulations of hyaluronic acid exist, as it is routinely used as an intra-articular filler (to smoothen bone-bone friction) as well as in aesthetic surgery as a replacement for botulinum toxin.

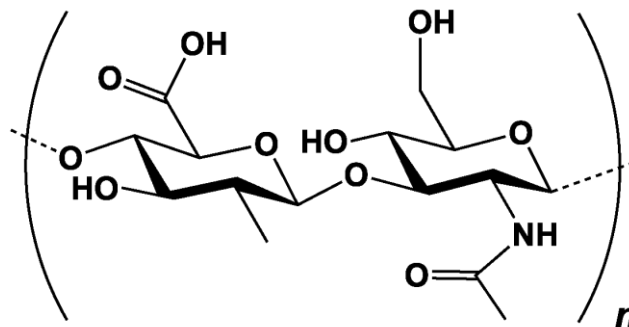


Figure 6.2 Representative structure of hyaluronic acid. Excerpt from <http://www.societechimiquedefrance.fr>

In the previous two chapters, we showed that fibrin scaffolds could be optimized for the operating theater in agreement with the regulatory authorities, in such a way that it supported pro-angiogenic effects and the improvement of cardiac function in rats, sheep and

more recently in the first human patient [21-23]. We also showed that microfabrication techniques could help the standardization of cell culture techniques for the differentiation of pluripotent stem cells into cardiomyocytes. However, although we used model materials such as polyacrylamide and a model cell type such as commercially available human iPSCs, we then sought to start the translation of these findings to the clinics, by applying our conclusions to the fabrication of smart patches that could integrate many physical, chemical and biological signals, using only clinically relevant (i.e. either already approved or easy to translate) raw materials and techniques.

In this chapter, we first extended our new microfabrication protocol for patterning hPSCs both to the culture and specification of clinical grade hESC and to the fabrication of various kinds of simple, patterned fibrin patches of similar composition as the ESCORT ones. Then, we aimed at improving our hydrogel's mechanical characteristics and enhance its biological properties by creating blends with other biomaterials. As cells are highly influenced by their mechanical environment, we fabricated fibrin-based scaffolds with various alginate concentrations to control their stiffness. We also varied the concentrations of hyaluronic acid, a GAG suspected to chemically affect cardiomyocyte mechanosensing [19]. Similar to what was described in chapter 4, we conducted histological analyses and mechanical measurements with conventional compressive tests and the SWE technique. As a model cell line, we have seeded hMSCs and conducted *in vitro* biological tests to assess cell behavior and see if selected scaffolds could promote muscular lineage differentiation, in similar ways as reported by Engler et al.[6].

Materials & Methods

Cell patterning on clinical fibrin hydrogels

Patterned polyacrylamide hydrogel fabrication

Polyacrylamide coverslips were fabricated as described in chapter 5. For hiPSCs culture and differentiation, the ECM was composed of Matrigel, fibronectin and fluorescent fibrinogen, as described before. For murine 3T3 or BJ + hESC experiments, the ECM solution used for patterning was composed of 50 µg/mL of human fibronectin supplemented or not with 5 µg/mL of Alexa-Fluor488® conjugated fibrinogen (Life Technologies).

Cell culture and differentiation

Human iPSCs were amplified and differentiated as previously described (Chapter 5). For murine 3T3 experiments, cells were cultured in capped flasks using DMEM supplemented with 10% Fetal Bovine Serum (FBS), 1% Non-essential amino-acids (NEAA) and 1% solution

of 100X penicillin-streptomycin. Medium was changed every three days and cells were split by trypsinization at 80% confluence.

For human ESCs experiments, the ESCORT's protocols have been used and later adapted to micropattern cell culture. Indeed, there are two widely spread ways for cultivating hESCs: either with a feeder layer, or in feeder free conditions, using Matrigel, a basal lamina extracted from mice with carcinoma. Matrigel is a very attracting solution because it removes one highly unreliable parameter in the culture system. However, even if cells can be differentiated on Matrigel, it is quite easy to expand hESCs on a feeder layer. The feeder layer provides adhesion sites through ECM-cell interactions as well as through cell-cell interactions. They also serve as secreting cells for helping maintaining the pluripotency of hESCs. Out of the many types of fibroblasts that can be used as feeders are the Mouse Embryonic Fibroblasts (MEFs) and the Human Foreskin Fibroblasts (HFFs). Before seeding, feeder cells need to either be treated with Mytomycin C or irradiated in order to stop their proliferation [24]. However, Mouse Embryonic Fibroblast are not suitable to the clinics, are highly heterogeneous and show low proliferation capabilities. While the ESCORT's protocol mentions the use of irradiated HFF of clinical grade (FPBT lineage), we started using these cells together with a new lineage of immortalized HFFs, called BJ, offering new opportunities for experimentations and validation of our microfabricated prototypes.

Transfer on fibrin hydrogels

Two techniques were used for transferring cells or ECM patterns on fibrin. Either the fibrin was cast from a solution of fibrinogen:thrombin F20T4 of Evicel® between two sandwiched patterned coverslips of PAA, or a homemade laser-cut Plexiglas ring was used on top of a patterned coverslip prior to the addition of the fibrinogen:thrombin mixture. Then, samples were incubated for at least 1 hour at 37 °C with a 5% CO₂ atmosphere.

Shear Wave Elastography and imaging

Constructs were imaged using either a Leica phase-contrast bright field microscope, a Zeiss epifluorescent microscope, a Zeiss confocal microscope or the ultrasound imaging system of the Aixplorer® apparatus, using a 15 MHz probe. Regarding the latter imaging technique, custom-made agarose multi-well plates had to be molded in order to transmit the ultrasound signal. Briefly, the cover of a polystyrene multi-well plate was placed upside down in a plastic recipient. Then, flat PDMS discs were punched and placed at the center of each well before pouring a solution of autoclaved agarose 2% in the recipient. Additionally, a lid made of unstructured agarose was molded in a 10-cm-diameter petri dish. After 40 min, agarose dishes were unmolded and immersed in RPMI supplemented with 2% B27 (with

insulin) until imaging was performed. The lid was used to create a solid interface to easily apply the standard echographic gel when imaging ZX and ZY planes of our samples (not shown here). For regular XY imaging, echographic gel was directly applied to the outer wall of the multi-well plate and the probe was kept in direct contact with the gel using a three-fingered grip.

Image and video processing

Contrast correction, merging and 3D reconstruction was performed using standard Image J toolboxes. Videos were recorded for 10 s at 20 fps and compressed into MP4 movies before being processed by the homemade Processing video analysis software described in Chapter 5 for contractility measurements. Briefly, after an ROI had been selected on the raw movie, frames were dilated or eroded and then filtered using a binary threshold, and the number of white pixels inside the ROI was recorded for each frame. Data were saved in both CSV files and in a SQL database for inter-experiment comparisons.

RT-qPCR and flow cytometry

RT-qPCR and flow cytometry have been performed in similar conditions, with similar primers and antibodies (respectively) as described in the ESCORT protocol [21, 22]. Flow cytometry data were then collected and further analyzed using a custom made software written in Processing.

Immunostaining

Samples were fixed and permeabilized using a warm solution of PBS with 3.7% paraformaldehyde (PFA) and 0.01% Triton X-100 for 15 min at RT. Then, coverslips were incubated for 1 to 2 hours on droplets of PBS containing DAPI, Alexa-567 conjugated phalloidin and an FITC-conjugated anti-human CD15 antibody. Coverslips were then mounted on rectangular coverslips with FluoroShield® as the preservative.

Preparation of composite 3D scaffolds

Fibrin-based hydrogels with hyaluronic acid or alginate

Agarose 2% was overlaid on the bottom of each well of a 24-well plate (2 cm²/well), so as to avoid an important adhesion of patches. For regular fibrin hydrogels, 150 µL of a 20 mg/mL fibrinogen solution (Evicel®) was poured into each well. Fibrinogen solution was then reacted with 4 UI/mL thrombin (Evicel®) at a ratio of 1:1 (v/v). Gels were incubated for 1 hour at 37 °C and 5% CO₂. For fibrin-HA hydrogels, HA was added to the thrombin preparation prior to polymerization. For fibrin-alginate hydrogels, agarose was supplemented with 5% CaCl₂ to allow alginate to crosslink. An additional slice of agarose was also placed on top of the

hydrogel to accelerate polymerization and improve homogeneity.

Cells seeding experiments

Human mesenchymal stem cells (hMSCs) were obtained from the Cell Therapy Laboratory of Saint Louis Hospital as a kind gift of J. Larghero and V. Vanneaux. MSCs were cultured in α MEM medium supplemented with 10% FBS and 1% penicillin-streptomycin. hMSCs used for *in vitro* and *in vivo* experiments were between passage 5 and 8.

Selected hydrogels were formed on agarose, with a thin glass coverslip on top. Agarose was supplemented with CaCl_2 5% for fibrin-alginate hydrogels. After 1 hour of polymerization at 37 °C and 5% CO_2 , glass-coverslips were flipped and transferred to 6-well plates. One hundred thousand MSCs were seeded in each well, culture medium was changed every 2 days and the experiment stopped at day 7. Cells were detached with Trypsin for 6 minutes and then centrifuged at 1,200 rpm for 6 min. The cell pellet was dried and stored at -80°C for further RNA extraction.

Histological analysis

After polymerization, patches were embedded in Tissue-Tek OCT compound Mounting Media, and cut into 10- μm -thick sagittal sections using a cryostat. A selected set of sections was mounted on microscope slides. After 24 hours, they were rinsed with ethanol 70% and washed with Phosphate Buffered Saline (PBS).

Hematoxylin Eosin staining

The sections were stained with hematoxylin for 30 seconds, and then rinsed with water. Next, they were stained with Eosin for 90 seconds, and then rinsed with water. Warm glycerol (60%) was added and slides were covered with glass coverslips. Afterwards, photomicrographs were taken using a Leica microscope equipped with a digital camera.

Dapi and phalloidin staining

3D cell cultures were fixed with 4% PFA and then rinsed 3 times with PBS. Cells were permeabilized with 0.25% Triton X-100, and further rinsed 3 times with PBS. Nuclei were stained with Dapi for 3 min and actin network was stained with fluorescently labelled phalloidin during 30 min.

Mechanical characterization

Compressive test

The Young's modulus in compression was derived from stress-strain curves obtained

using an Instron 5565 mechanical apparatus (Instron, Norwick, MA), equipped with a 10 N load cell. Briefly, fibrin and fibrin/hyaluronic acid hydrogels pieces were formed in flat-bottomed syringes to have a controlled geometry. Fibrin/alginate hydrogels were allowed to crosslink with agarose-CaCl₂ slices on top and at the bottom of the syringe. The height of cylinders was measured and placed in the apparatus and the strain was recorded at different loads. The Young's modulus in compression was calculated as the slope at the beginning of the deformation, where the stress-strain curve can be assumed to be linear.

Shear Wave Elastography (SWE) - Aixplorer Ultrasound Imaging

SWE provides in real-time a quantitative map of the soft tissues' shear modulus by tracking remotely induced shear waves at high spatial and temporal resolution. To our knowledge, this method has already shown success in breast cancer diagnosis but had never been exploited in the field of tissue engineering and biomaterial design. As hydrogels were transparent to ultrasounds we added agarose powder during preparation. Hydrogels required no specific geometry but cylinders appeared to be more practical. Hydrogels were prepared the same way, with cut syringe, as for compressive tests, and elasticity was directly displayed on the Aixplorer[®] ultrasound system after selecting a region of interest inside the hydrogel.

Results I: Soft micropatterning with the ESCORT protocol

The choice of the substrate: BJ vs. FPBT

It had previously been reported that murine feeders behaved differently than human feeders [25], but no major difference had been noted between two lineages of HFFs. Surprisingly, here, we observed dramatic differences between the two lineages. When kept in proliferation medium (Nutristem[®], to maintain stem cells' pluripotency and self-renewing capabilities), the I6 lineage of hESCs proliferated considerably faster on BJs than on FPBTs (**Figure 6.3-A**, blue histogram). Upon BMP-2 induction, stem cell colonies (already bigger on BJs than on FPBTs) started to spread and to show signs of spontaneous differentiation much earlier on BJs than on FPBTs. As a result, the surface area covered by the colonies was even higher for cells on BJs than on FPBTs, due to their wider spreading area (**Figure 6.3-A**, green histogram). At the end of the four days of BMP-2 induction, almost all the colonies had a « differentiated » morphology on BJs while a non negligible part of the colonies on FPBTs had kept their « pluripotent » morphology (**Figure 6.3-B**).

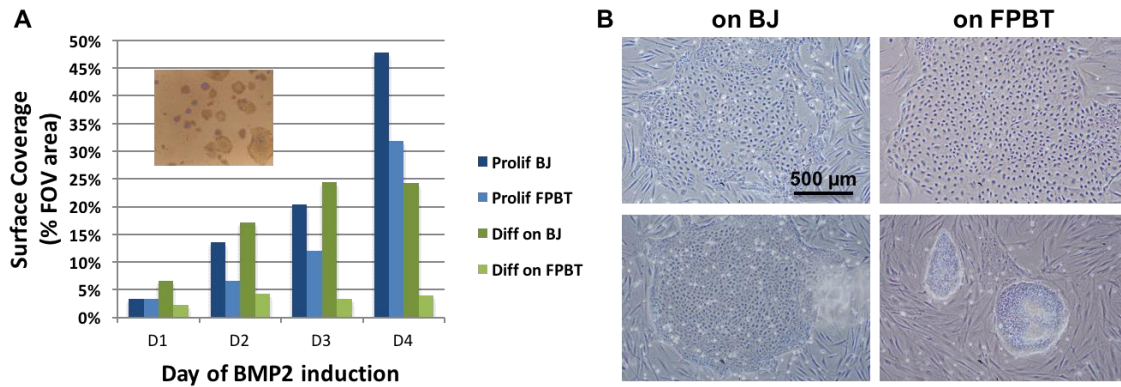


Figure 6.3 Comparative BMP-2 induction on BJ feeders or FPBT feeders. %FOV: % of field of view area. (A) Surface coverage of hESC colonies (B) Phase contrast pictures of the morphologies of the colonies.

After MACS sorting with anti-CD15 magnetic beads, it appeared that the yield of CD15⁺ cells was much higher on BJ feeders (1.8 million cells) than on FPBTs (0.86 million cells, [Table 6.1](#)). Surprisingly, the number of cells was not considerably higher on BJ feeders. Quantitative PCR analysis of early cardiac markers showed similar patterns of gene expression ([Figure 6.4-A](#)) between the two conditions, but results have to be taken very cautiously due to very important C_t variations in the GAPDH amplification. In addition, the expression pattern was quite different from previous data showing higher expressions of Tbx5, Nkx2.5 and Mef2c in the CD15⁻ population rather than in the CD15⁺ population, whereas only Isl1 was higher in the CD15⁺ population. As flow cytometry confirmed that the purity was above 90% in both conditions and that low amounts of CD15⁺ had been lost in the negative population ([Figure 6.4-B and C](#)), we started to question the expression pattern of the feeder cells and found out that HFFs already expressed high amounts of Tbx5 (data not shown). As they are the main component of the CD15⁻ population, it could explain these artifacts in the qPCR results.

	BJ		FPBT	
	Count	Proportion	Count	Proportion
Before sorting	5.3x10 ⁶		4.4x10 ⁶	
CD15⁻	1.5x10 ⁶	46%	2.1x10 ⁶	71%
CD15⁺	1.8x10 ⁶	54%	0.86x10 ⁶	29%

Table 6.1 Specification yields after culture on BJ or FPBTs feeders.

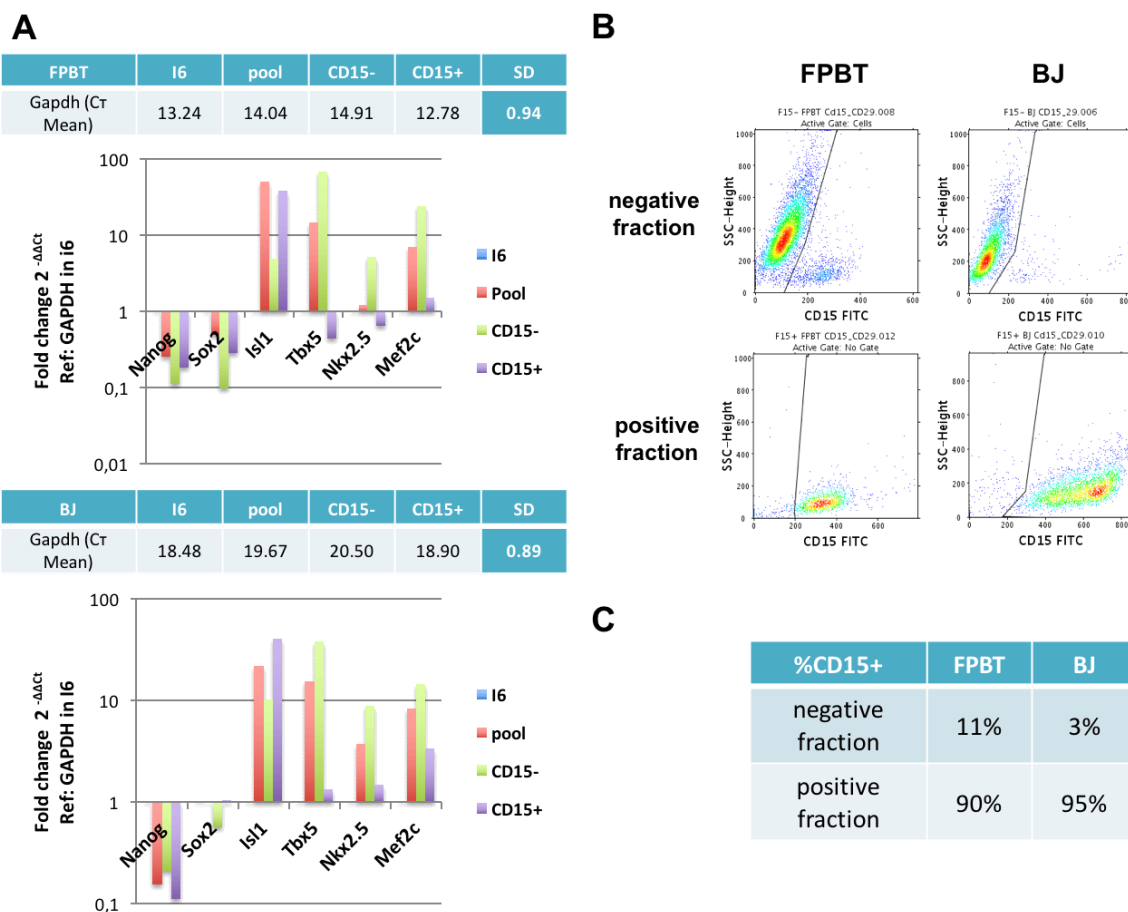


Figure 6.4 Gene expression and purity analysis after specification on FPBT or BJ (A) qPCR analysis of pluripotency (Nanog, Sox2) and early cardiac genes (Isl1, Tbx5, Nkx2.5, Mef2c) after BMP2 specification on FPBT (top) or BJ (bottom). (B-C) FACS analysis of post-sorting purity, x-axis: CD15-FITC, y-axis: SSC Height. Gates are based on Ig references (not shown).

As we repeated the experiment on either FPBTs or BJs feeders, we stopped observing differences in the specification yields, even though the total number of cells was higher on BJs than on FPBTs at the end of the specification (Table 6.2). The reason could be that the I6 cells that were used the second time had been amplified for a longer time on BJs, and thus behaved like on BJ. Indeed, other experiments in our laboratory suggested that transferring cells amplified on BJs from BJs to FPBTs and keeping them many passages on FPBTs led to the behavior observed for FPBTs and not for BJs.

	BJ		FPBT	
	Count	Proportion	Count	Proportion
Before sorting	12.5x10 ⁶		9.4x10 ⁶	
CD15-	2.0x10 ⁶	35%	1.1x10 ⁶	36%
CD15+	3.8x10 ⁶	65%	1.9x10 ⁶	64%

Table 6.2 Specification yields after culture on BJ or FPBT feeders.

Patterning and stem cell culture

Homogeneity of the seeding

Regardless of the choice of the substrate (Matrigel or a feeder layer), there are two requirements to be able to make sense out of cultures on micropatterns: (i) having the same cell behavior on all the patterns, to be able to make statistical analyses of the results, (ii) being able to precisely control cell density. However, preliminary experiments had showed that extensive agitation was need after cell seeding in order to avoid inhomogeneous cell sedimentation (see Chapter 5). This intensity of this phenomenon was found to depend on whether cells had been fully dissociated, or just separated in small clusters. As hESCs survive best in small clusters, we observed strong heterogeneities in the resulting seeding. Our initial solution was to decrease the number of conditions, gathering spot sizes by groups of two and performing the patterning on 30-mm diameter coverslips inside a 6-well plate, a dimension that prevents peripheral or central aggregation of falling cells. While central and peripheral aggregations were still present to a lower extent, they could be completely removed by shaking the plate every ten minutes for 1 to 2 hours.

Controlling spot cell density

The I6 lineage of hESCs has one major drawback: cells cannot be separated into single cells using tripsynization. Indeed, if they were not in small aggregates, they would not adhere and eventually died. Therefore, even with homogeneous seeding, it was not possible to precisely control cell density: in case aggregates were bigger than the spot size, proliferation and differentiation would lead to very peculiar morphologies on the spots (**Figure 6.5**).

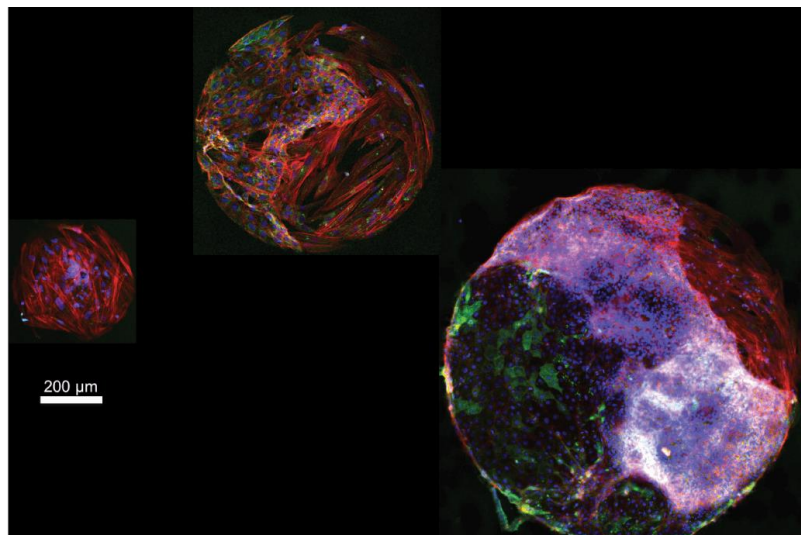


Figure 6.5 Immunostaining attempts on patterns with inappropriate pattern cell density. Red: actin, blue: chromatin, green: CD15

It has been suggested that hESC's survival in single cell suspensions can be promoted by the addition of a Rock inhibitor called Y-27632 [26-30]. Even though addition of Y-27632 did not permit to trypsinize the cells, it allowed for mechanical breaking of the aggregates into groups of cells that were smaller than the smallest patterns. On feeder cells that were patterned on gelatin or FN spots prior to I6 seeding, I6 would stay attached on the spots, but also on the supposedly cell-repellant regions of the coverslips (**Figure 6.6-A**).

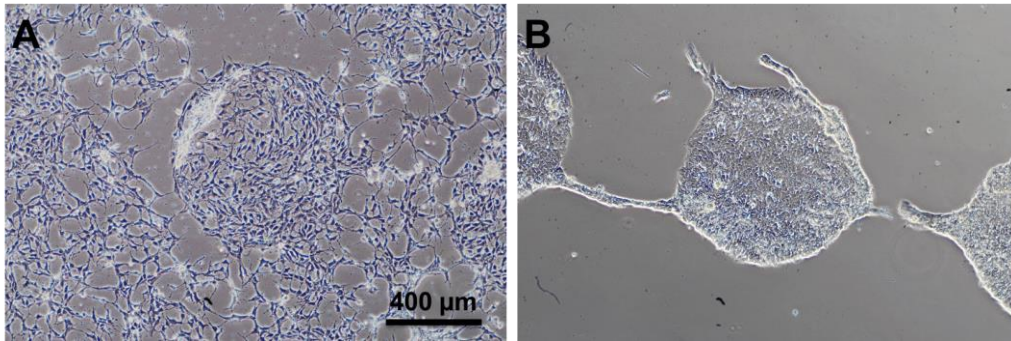


Figure 6.6 Effect of Y-27632 addition (A) and removal (B) from Nutristem® medium on hESCs seeded on spot patterns.

It was observed that when adding Y-27632 at 10 μM for the first two days of I6 culture, cells would adopt a single cell polygonal morphology and adhere everywhere in the dish. As soon as the Nutristem® + Y-27632 was removed and replaced by Nutristem® alone, cells on non adhesive regions of PLL-g-PEG2.5 would either detach or regroup on top of the spots (**Figure 6.6-B**). For an optimal I6 dilution close to ½ (instead of the 1/6 dilution ratio used in clinical settings) of a confluent culture of hESCs, the hES cells were able to force the feeder layer to progressively detach. As a result, cultures were left with only hESCs that were stably attached on the spots.

Initial Glass patterning success

The optimal technique was thus to pattern fibronectin spots and then to seed irradiated BJ fibroblasts to help ensure the adhesion of hESCs, as it had been observed that Matrigel® coatings led to more frequent contaminations and easy cell detachment.

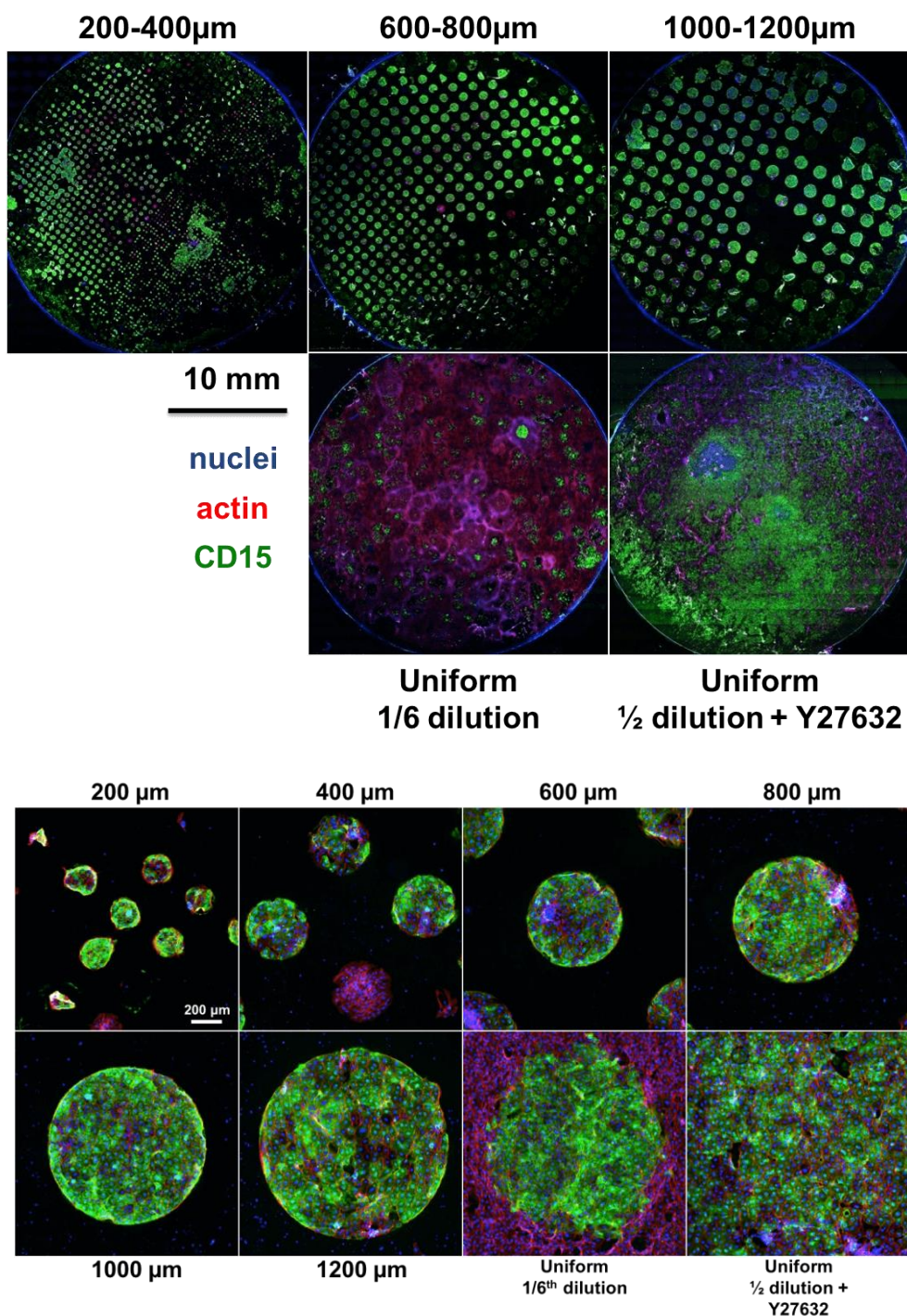


Figure 6.7 Immunostaining after BMP2 induction of hESCs on rigid spots. (top frames) global overview of the 30-mm coverslips (bottom frames) higher magnification, representative images of the hESCs after 4 days of BMP2 induction.

As shown on **Figure 6.7**, it seemed that the modification of the protocol to allow for good adhesion of the hESCs on the spots also led to improved specification into CD15⁺ cells on the new positive control (referred to as Uniform 1/2 dilution + Y-27632). This confirmed that the Rock Inhibitor had an important role to play, which is in agreement with the hypothesis that mechanical constraints participate in controlling stem cell's fate. It could also be that a three-

fold change in cell density (1/6 to 1/2), together with improved cell adhesion (thanks to the rock inhibitor), was enough to go from a sparse culture of CD15⁺ progenitors to an almost confluent culture of CD15⁺ cells.

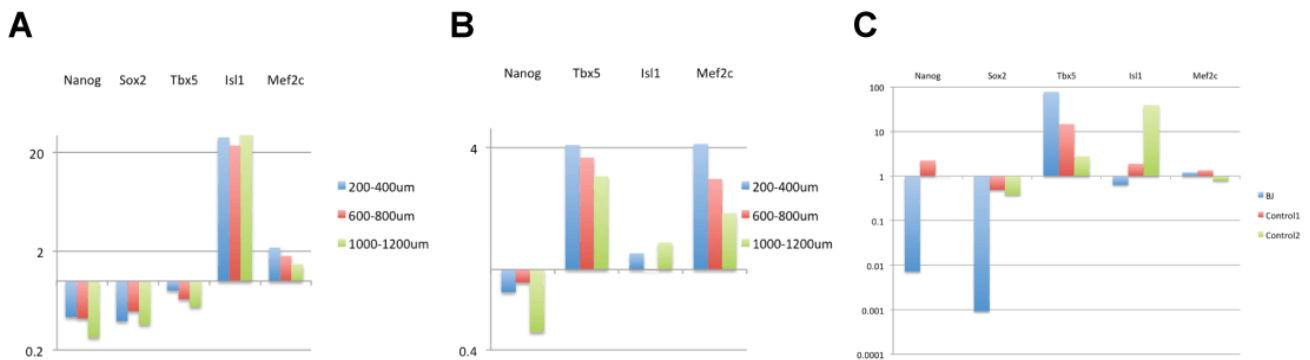


Figure 6.8 qPCR analysis

(A) Log₂ representation of fold change on patterns relative to Control 1 (1/6 dilution), (B) Log₂ representation of fold change on patterns relative to Control 2 (1/2 dilution with Y-27632), (C) Log₁₀ representation of fold change of pellets of BJ only, Control1 and Control2 relative to undifferentiated i6 hESCs

Quantitative PCR also confirmed this trend that differentiation was highly enhanced with the second protocol rather than with the initial one. However, differences of multiple orders of magnitude in the expression of Tbx5 have been noted, which was later identified as an artifact of the co-culture with BJ cells, that also overexpress Tbx5 in normal culture conditions, as compared to pluripotent I6 (**Figure 6.8-C**). Later on, hESCs could be successfully patterned on polyacrylamide substrates of controlled stiffness coated with spots of fibronectin, with the help of feeder cells as well as Rock Inhibitor, as shown in **Figure 6.9**. Now that similar efficiency in terms of hESC patterning have been achieved, more quantitative experiments can be performed to compare results from hiPSCs cultures to the I6 hESC lineage.

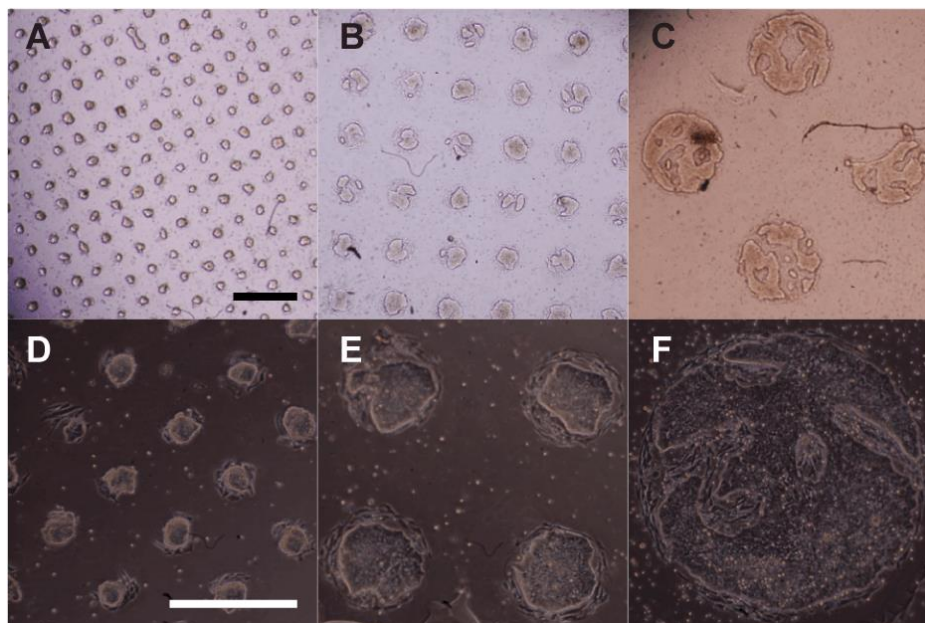


Figure 6.9 Example of patterning of BJs + hESCs on 10 kPa PAA substrates patterned with FN spots. (A, D) 200 μm (B, E) 600 μm (C, F) 1200 μm. Note the sublayer of fibroblasts at the periphery of the spots. Scale bars: 500 μm

Results II: Proof-of-concept patterning strategies using clinical fibrin hydrogels

First proof of concept for the transfer of patterned cells from PAA to clinical fibrin gels

We then wondered how we could clearly bridge the gap between in vitro studies and in vivo patch surgery. As a proof of concept, we showed that using a mixture of fibronectin and FITC-fibrinogen, it was possible to pattern lines on PAA of intermediate stiffness (10 kPa) and promote fibroblast adhesion and alignment. After one day in culture, a fibrinogen:thrombin mix was poured onto the cell culture and placed back in the incubator for the time of the polymerization. After one hour, the fibrin gel was peeled off and placed upside down into a new culture well. It is hypothesized that FITC-fibrinogen polymerized together with the rest of the fibrinogen, promoting the entrapment of the cells within the fibrin gel. Cells had been successfully transferred from the PAA (**Figure 6.10-B**) to the fibrin patch (**Figure 6.10-A**), and alignment had been preserved. More interestingly, after one additional day in culture, cells had continued proliferating and had kept their orientation throughout the entire patch (**Figure 6.10-C**).

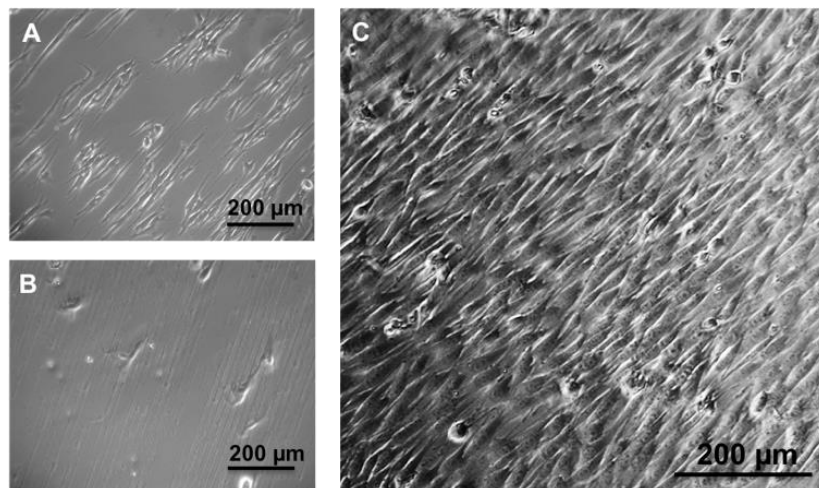


Figure 6.10 PAA to Fibrin patterned cell transfer.

(A) Cells on fibrin after unmolding. (B) cells left over on PAA after unmolding. This is actually the only field of view where we can see a few cells. (C) 3T3 on fibrin after 24 hours. Proliferation had continued and alignment is maintained.

Therefore, we decided to start showing the properties of transfer using the feeder cells, the BJ lineage. Unfortunately, afore mentioned observations have not been reproduced: cells started to pull on the fibrin gel, degrading it and compacting it. It could be because of the Plexiglas ring that had been used during transfer: while the fibrin gel had not detached from

the ring in the first experiment, it did detach and remained as a freely buoying sheet in the latter experiment. Therefore, alignment could only be observed immediately after transfer, as shown in **Figure 6.12**.

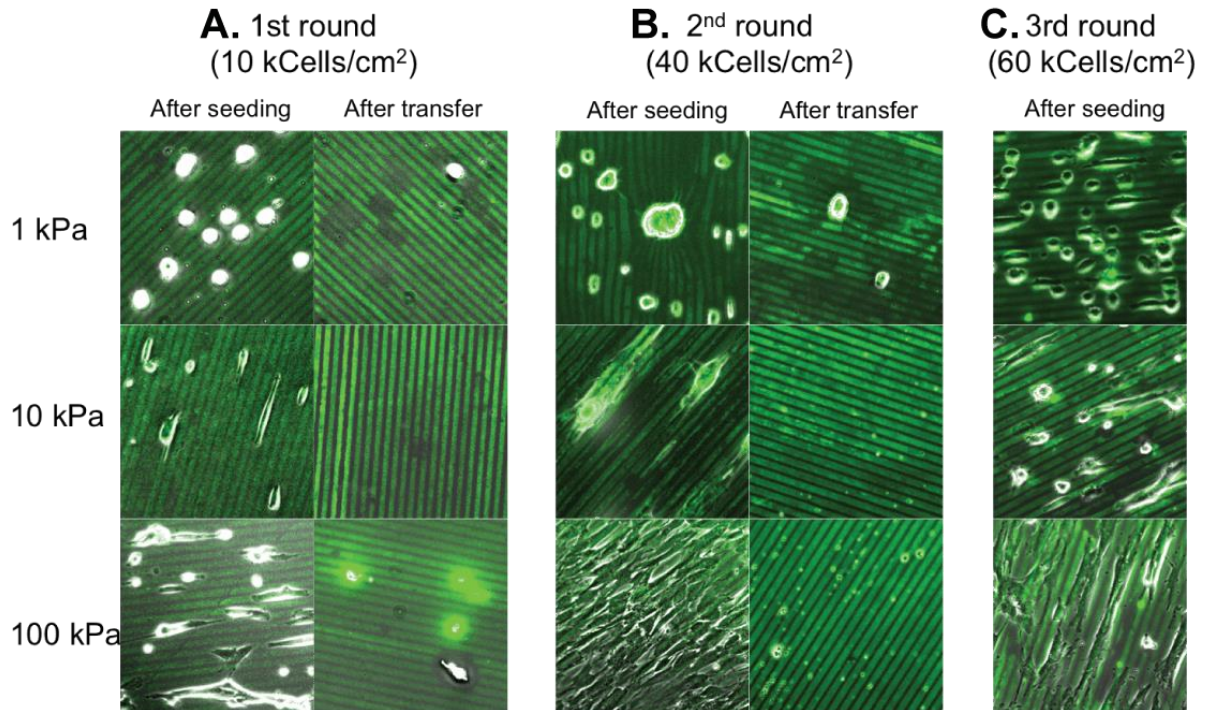


Figure 6.11 Surface of PAA before and after transfer on fibrin patch

In a nutshell, the transfer was still very efficient and very few cells were found on the PAA after transfer (**Figure 6.11**). Nevertheless, after transfer on fibrin (**Figure 6.12**), cells retained the shape they had acquired on PAA gels, which was either an elongated shape on gels above 10kPa, or round shapes on softer gels (**Figure 6.12**) but proliferation did not occur with the same alignment (not shown).

Of importance, no detectable fluorescent fibrinogen could be observed in the fibrin gel (**Figure 6.12**), except inside the cells that had *endocytosed* it. Also, fluorescent lines were still observed on the initial PAA gels. These two observations strongly affirmed the hypothesis that the fibrinogen pattern had been transferred together with the cells during fibrin polymerization, at least for this experiment.

When repeating the experiment, we tried seeding cells again on the exact same PAA coverslips. Not so surprisingly, cells adhered again and aligned in the same fashion (**Figure 6.11**, 2nd round). This was yet another confirmation that most of the ECM (fibronectin + fluorescent fibrinogen) had remained on the initial PAA hydrogels.

The transfer on fibrin gels led to the same observation as before: a good initial alignment on the patches but later degradation and compaction. We suspected that alignment might be preserved over time only when the cells had already reached a certain density. Consequently, we used the exact same PAA coverslips with increasing cell densities. This experiment is still in progress and the hypothesis cannot be verified yet. A surprising observation, though, was that after many rounds on the same hydrogels, the alignment of fibroblasts on 1 kPa hydrogels clearly improved (Figure 6.11, 3rd round). An explanation could be that cluster formation on 1 kPa resulted from initial spreading of the cells (accompanied by matrix secretion), followed by pulling and aggregation and detachment, as suggested by Figure 6.13. The secreted matrix would be aligned along the pattern and after a specific thickness would have been reached, then new cells would align more strongly on the hydrogel.

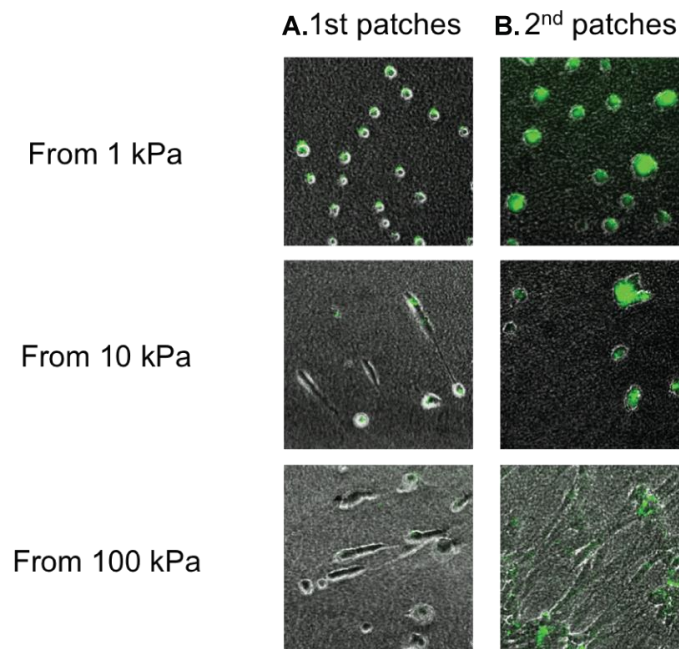


Figure 6.12 Surface of fibrin patches after transfer from PAA.

To confirm whether the fluorescent fibrinogen had been endocytosed by the fibroblasts, or if the cells just detached the fibrinogen from the substrate, 3D images were reconstructed from confocal observations. In the latter scenario, it would imply that integrin receptors might still be bonded to fibrinogen molecules, and thus, spreading and migration could become problematic when considering the grafting of the patch on an injured heart. While epifluorescence cannot discern between the two conditions, 3D Confocal images shown in Figure 6.13 revealed that fluorescent fibrinogen was distributed throughout the entire cytosol and not only at the cell's membrane, thus confirming that fibrinogen is being endocytosed in by the cells.

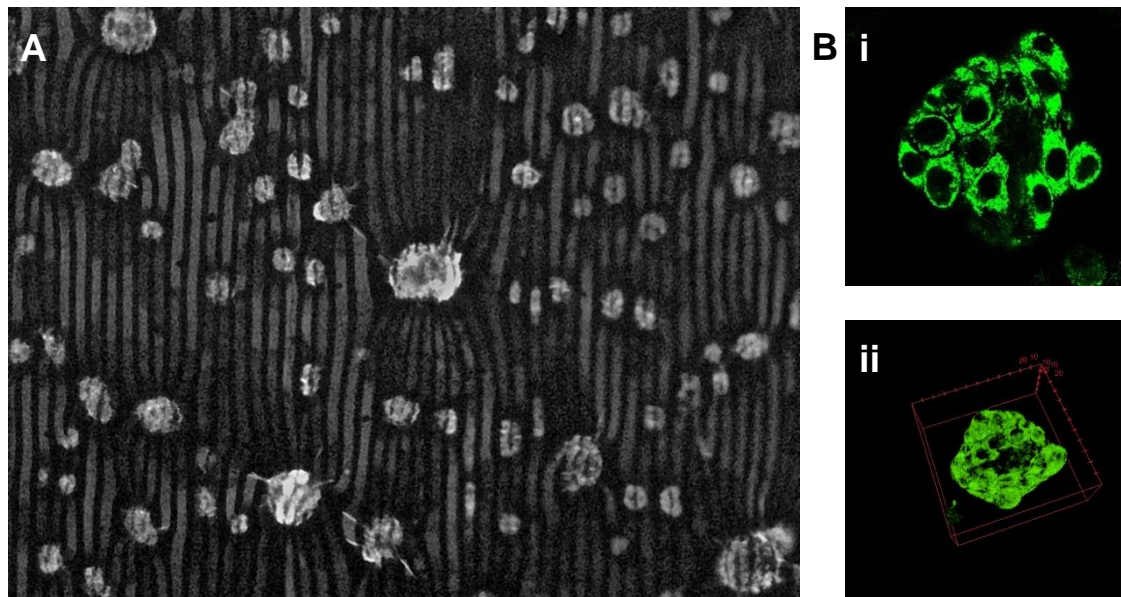


Figure 6.13 Fluorescent fibrinogen observation on 1 kPa PAA patterned with lines and seeded with BJ fibroblasts. (A) Epifluorescence. (B) LSCM of a cluster, (B-i) section, (B-ii) 3D reconstruction.

Importantly, it was noted that aggregates were strong enough to stay attached on 1 kPa gels while deforming it. Similar to Traction Force Microscopy (TFM) with embedded fluorescent nanobeads, this shows that measuring the deflection of the patterned lines from the orientation could help quantify the force exerted by the aggregates.

This observation will undoubtedly be very useful for further experiments with cardiomyocytes and systolic force quantification, as discussed at the end of Chapter 5. Designing different patterns could lead to an alternative to bead-based TFM. The advantages would be: (i) the insurance that nanobeads do not affect the hydrogel stiffness; as a consequence, there would be no need for testing the mechanical properties of both bead-free and bead-laden gels; (ii) a lower cost; (iii) the insurance of a “flat” topography; (iv) the controlled distribution of the fluorescence, which would facilitate automation of signal processing and analysis algorithms.

Of course, the main drawback is the stronger force needed to be able to observe the deformation. This minimal force is strongly related to the gel's stiffness but also to the resolution of the pattern. As a result, single cell TFM would only be possible with subcellular patterning.

Advanced proof of concept using an optimized geometry for single-material differentiation of hiPSCs into cardiomyocyte and subsequent transfer to clinical fibrin

In the previous chapter, we studied the influence of elasticity and topographical confinement on the differentiation of hPSCs into cardiomyocyte, using a small-molecule-based

protocol. We observed rings of differentiated beating cardiomyocytes. Although these rings seemed to have a constant thickness at first, deeper examination led to the understanding that the thickness of the ring depended on the diameter of the spots and, to a lower extent, on the elasticity of the substrate. However, while this is true for diameters ranging from 800 μm to 4,000 μm , it was not clear whether the ring size would still increase with even bigger spots. When looking at the dimension of tissue culture plate, we can find that bigger spots actually means getting closer and closer to the smallest multi-well plates commonly used in laboratories. As a matter of fact, 96-well-plate's wells have a diameter of 6.35 mm, i.e. 6,350 μm . Therefore, 4,000 μm can be considered as a “multi-well plate” control the same way a 96-well plate would be when performing high-throughput screening.



<https://goo.gl/gNDXF1>

As suggested by data presented in the previous chapter, while ring size increases for very large spots, it belongs to a quite narrow range for intermediate values of spot diameter, with an average of 380 μm .

Consequently, we hypothesized that any pattern with a constant thickness of approximately twice the average ring size would help fabricate cardiac microtissues with a very high cardiomyocyte yield. We thus designed simple patterns of periodic bands with a thickness of 700 μm and an interspace of 100 μm , on all 4 rigidities introduced before, and performed the differentiation protocol as described previously. We named the resulting beating structures **Engineered Cardiac Bands (ECBs)**.

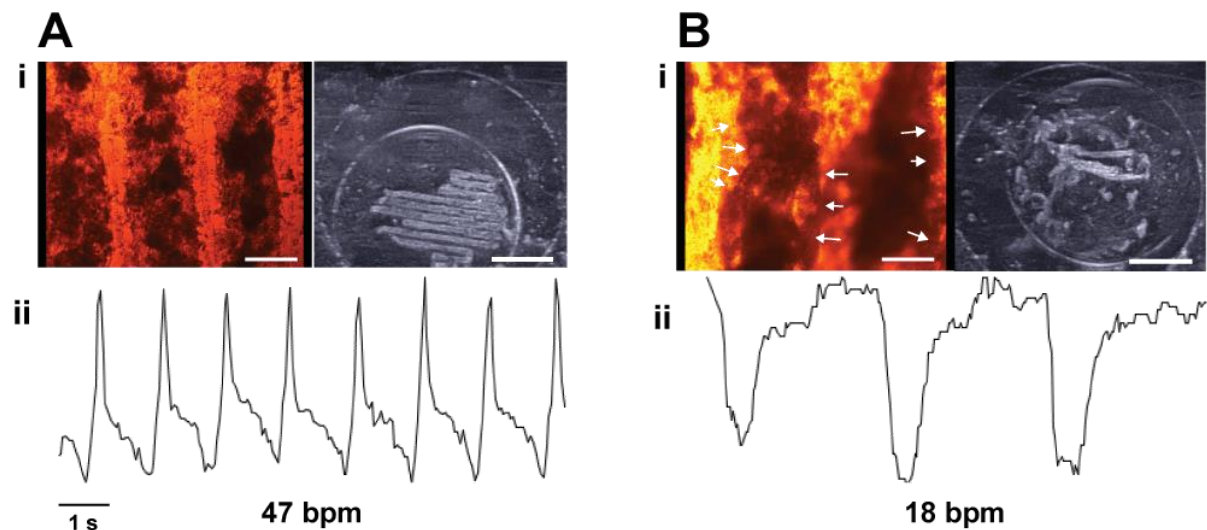


Figure 6.14 Beating patterns of engineered cardiac bands.

Proof-of-concept of regular (bright field, i.left) and ultrasound (i.right) imaging to characterize anisotropic cardiac microtissues before (A) and after (B) the fabrication of the fibrin patch. (ii) Beating pattern acquired by video analysis of the SWE. Scale bar: 500 μm .



<https://qoo.gl/APZ15p>

Results were striking. Not only was the entire culture beating, but contraction propagated solely in the direction of the lines (**Figure 6.14-A** and **Supplementary Movie 6.1**). Although this was repeatedly observed for low elasticity (1 kPa and 10 kPa), it was less reproducible on harder PAA (100 kPa) and on glass coverslips, where cells seemed to contract more heterogeneously. We think that while elasticity can have played a biomechanical role here, a simpler explanation would be that as cells adhere less strongly on soft substrates, contractions trigger the partial detachment of the cardiac band and promote synchronization along the band.

Performing cardiac differentiation on soft substrates would offer three main advantages. First, polyacrylamide is a very strong anti-adhesive for cell culture, and thus patterns can be generated very faithfully and be maintained for longer periods of time and in any medium. Second, partial detachment can promote better synchronization of independently beating clusters. Finally, transfer from the coverslips to the fibrin patch will work dramatically better.

Naturally, the second step was to demonstrate the feasibility of stacking multiple layers of aligned cardiac bands, by using fibrin as a cement between the different parts. Multiple PAA coverslips were then prepared, seeded with hiPSCs and differentiated into cardiomyocytes. At day 12, bands had already started to beat and fibrin hydrogels were cast.

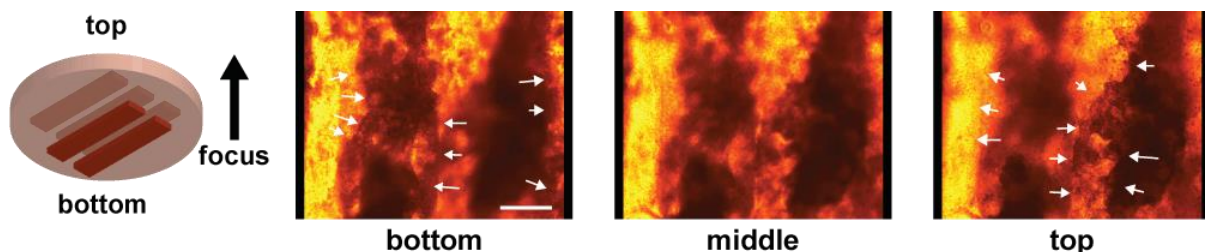


Figure 6.15 Proof-of-concept of a two-level fibrin patch made of parallel band of hiPSC-derived cardiomyocytes. The schematic (left) represents the way the movie was acquired, by slowly moving from the first layer of ECBs to the top layer of ECBs, at the surface of the fibrin patch. White arrows indicate the border of bands in focus. Scale bar: 500 μm .



<https://qoo.gl/wkABUO>

As suggested by the preliminary results using murine 3T3 and human BJ fibroblasts, after an incubation time of one hour, the fibrin patch could be easily unmolded and cardiac bands had transferred to the clinical fibrin. By taking care of aligning the coverslip in parallel, it was possible to create a two-layered clinical patch made out of hiPSC-derived cardiomyocytes (**Figure 6.15** and **Supplementary Movie 6.3**). Furthermore, we demonstrate that these patches can be monitored using SWE, by placing the samples in agarose multi-well plates (**Figure 6.14-B** and **Supplementary Movie 6.2**). Not only could they be visualized, thus allowing for contractility

frequency measurements (Figure 6.14-B), but cardiac bands have also been assessed for their elasticity (Figure 6.16 and Supplementary Movie 6.4).

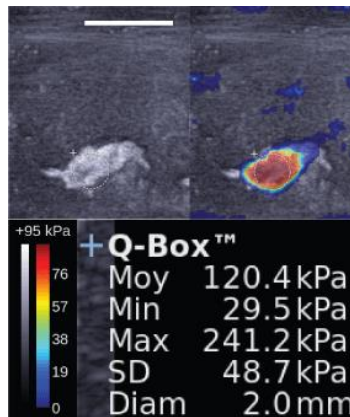


Figure 6.16 Evaluation of the stiffness of aggregated cardiac bands, free standing in agarose dishes.



<https://goo.gl/xUElha>

Obviously, there are still many limitations that need to be overcome, as the stability of these patches after unmolding. As illustrated in

Figure 6.16 and Supplementary Movie 6.4,

most fibrin patches were dissociated from the cardiac bands when transferred in the agarose dishes. It resulted in the anarchical aggregation of the bands. This could explain the high value of the Young's modulus observed for these bands (120.4 kPa). While it is in the range of pathological cardiac muscle (hypertrophied cardiomyocytes), this value should be interpreted with considerable caution because this aggregation of bands led to reaching the limits in spatial resolution for the

shear-wave model to be accurate. In fact, more recent measurements of the elasticity of cardiac balls detached from the spots described in the previous chapter suggest an elasticity of about 6 kPa, similar to the F20T4 fibrin patch and to fetal hearts. To prevent from this detachment and aggregation, a very simple solution could be to add an additional layer of fibrin in order to protect the cardiac bands from stresses generated by external manipulations.

Alternatives to cell transfer: direct ECM patterning on clinically-relevant hydrogels

Fibrin patterning

Being able to micropattern a cardiac patch, make it clinical and being able to graft it on the pericardium can be very challenging. Some solutions have been to use nanogrooved PEG hydrogels to culture either (rat) cardiomyocytes [31] or to help mature endogenous cardiac progenitor cells [32], then to transfer them on hearts using fibrin glue, in a similar way as presented here above. As an alternative, we show that instead of having to transfer the cells while polymerizing fibrin from fibrinogen, it is possible to prepare in advance fibrin patches exhibiting patterned lines of fibronectin on their surface.

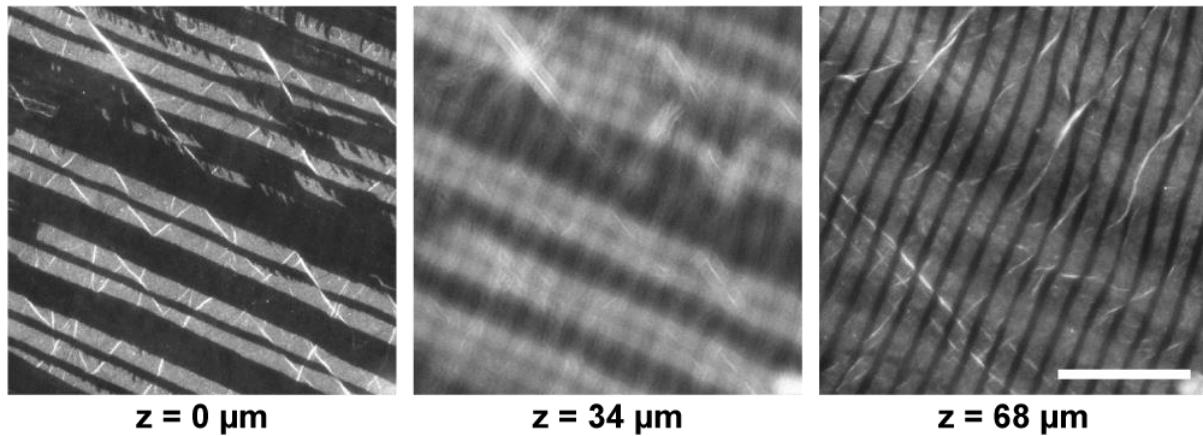


Figure 6.17 Confocal microscopy of the proof-of-concept fibrin micropatterning with lines of fibronectin + fibrinogen, after transfer from a 10-kPa polyacrylamide layer.

On **Figure 6.17**, we show that using the same technique as for transferring beating cardiac bands, it is in fact also possible to only transfer ECM proteins from the polyacrylamide to the fibrin hydrogel. If the two micropatterned PAA coverslips are placed orthogonally, then the resulting fibrin patch will have two sides coated with micropatterned ECM, forming orthogonal lanes (**Figure 6.17**). Consequently, patches could be prepared in advance and only used with already differentiated cardiomyocytes or cardiovascular progenitor cells. Using non adhesive culture dishes, it would also be possible to stack these fibrin constructs together with dissociated cells before surgery.

Results III: new blends of clinical materials

Preliminary observations regarding alginate micro-patterning

We had previously shown, using neonatal rat cardiomyocytes, that it was possible to engineer soft hydrogels so has to direct the elongation of cardiomyocytes and favor their anisotropic contraction when field stimulated (**Figure 6.18**) [33]. Originally, using alginate as a substitute for PDMS [34] was a way not only to soften the matrix – hence providing mechanical cues for healthier cardiomyocyte maturation and force generation – but also to translate this technology into a clinically relevant construct. Indeed, alginate would be able to resorb inside the body and is already being produced in GMP environments.

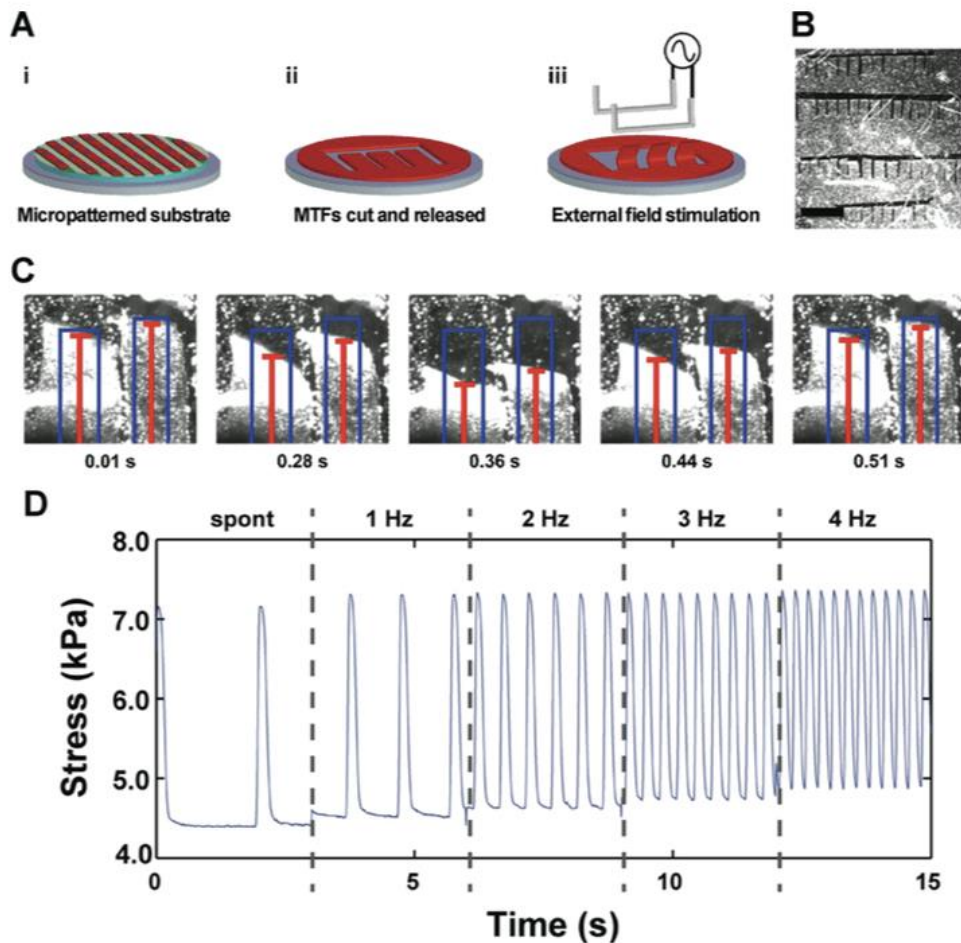


Figure 6.18 Cardiac muscular thin films constructed from micropatterned alginate substrates. (A) Schematic of the assay: cantilevers are cut and peeled out of the alginate film and exposed to external electrical field stimulation. (B) Optical photograph of the alginate coverslip after peeling the cut regions showing a high number of MTFs from a single experiment. Scale bar represents 5 mm. (C) Tracking of the horizontal projection of the 2 representative films during one contraction cycle at 2 Hz stimulation frequency. (D) Representative time trace of stress generated by one MTF at different pacing frequencies. Excerpt from [33].

However, because alginate is a non fouling material, it had to be chemically conjugated to either ECM proteins (as described by Agarwal and Farouz and colleagues[33] or synthetic polypeptides, like GRGDS (as experimented in our laboratory at ENS Paris), that can promote cellular adhesion. Additionally, when evaluated as a candidate for clinical applications, preliminary experiments showed that handling was complicated due to the brittleness of the gels. Even though the elastic modulus can be modulated in the appropriate range for cardiac therapies, alginate flaps do not resist to the stress generated during surgery. Finally, conservation happened to be problematic both because of the appeal of alginate to bacteria, and because of the dramatic swelling behavior observed for alginate hydrogels in medium that do not contain enough Ca^{2+} , such as RPMI, the medium used in our cardiomyocyte differentiation protocol. Consequently, we also investigated whether alginate could be used not as the main scaffolding material, but as a mechanical reinforcement material for the initial fibrin patch.

Handling test

For handling test of fibrin/alginate hydrogel, the chosen volume was 200 μ L.

Concentration F: mg/mL; T: UI/mL; A: mg/mL	Polymerization speed 37°C	Pinch grip	Retention: unfolding and respreading	Number of samples
F20T4	Ok 1h	No difficulty	No particular difficulty	3
F20T4A5	Ok 1h	No difficulty	No particular difficulty	3
F20T4A15	Ok 1h	No difficulty. Increase rigidity.	No particular difficulty	3
F20T4A30	Ok 1h	No difficulty. More rigid.	No particular difficulty	3

Table 6.3 Handling of patches as a function of fibrinogen, thrombin and alginate concentrations.

For fibrin/alginate-based hydrogels (**Table 6.3**), we decided to start with the concentration of fibrinogen and thrombin which is currently used in *in vivo* models and has already been investigated earlier (F20T4, see Chapter 4), and to add an increasing concentration of alginate to make the hydrogel stiffer. Handling properties seemed compatible with further *in vitro* and *in vivo* experiments for all the formulations of fibrin-alginate scaffolds.

Concentration F: mg/mL; T: UI/mL; HA: mg/mL	Polymerization speed 37°C	Pinch grip	Retention: unfolding and respreading	Number of samples
F35T7HA4	Ok 1h	Difficult	++	3
F35T7	Ok 1h	No difficulty	No particular difficulty	3
F30T6HA3.5	Ok 1h	Difficult	++	3
F30T6	Ok 1h	No difficulty	No particular difficulty	3
F25T5HA3	Ok 1h	No difficulty	No particular difficulty	3
F25T5	Ok 1h	No difficulty	No particular difficulty	3
F20T4HA2.5	Ok 1h	No difficulty	No particular difficulty	3
F20T4	Ok 1h	No difficulty	No particular difficulty	3
F15T3HA2	Ok 1h	No difficulty	No particular difficulty	3
F15T3	Ok 1h	No difficulty	No particular difficulty	3
F10T2HA1.5	Ok 1h	Difficult	++	3
F10T2	Ok 1h	Difficult	++	3

Table 6.4 Handling of patches as a function of fibrinogen, thrombin and hyaluronic acid concentrations.

However, for fibrin/hyaluronic acid-based hydrogels (**Table 6.4**), the complete screening showed that only intermediate concentrations of both fibrin and fibrin/HA seem compatible with further experiments, including surgeon work during the grafting procedure.

Histological profile

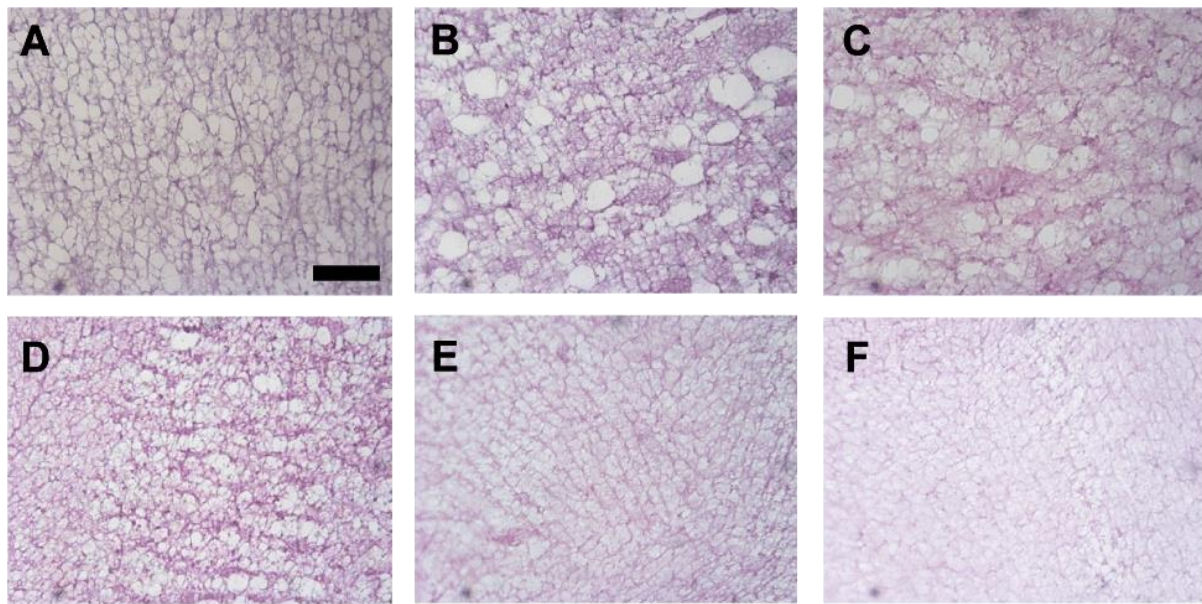


Figure 6.19 Histological sections of fibrin patches, stained with Hematoxylin/Eosin. (A) Patch with 10 mg/mL of fibrinogen and 2 U/ml of thrombin: F10T2. (B) F15T3, (C) F20T4, (D) F25T5, (E) F30T6, (F) F35T7. Scale bar: 200 μ m

In order to faithfully compare the results for the composite materials to those for the simple fibrin patches, we performed again a similar analysis as the one presented in Chapter 4. Conformingly to previous results, the fibrin network was different according to the initial concentration and pore diameter was dose-dependent. Indeed, the pore diameter was bigger in the case of the lowest concentration F10T2 (**Figure 6.19-A**) and the biggest pores corresponded to the lowest concentration in fibrinogen and thrombin, F35T7 (**Figure 6.19-F**). While we stated opposite results regarding microscopic pores in Chapter 4, histological sections obtained in this new series of experiments seemed to have been less *disturbed* and thus might correspond more to the confocal images shown in Chapter 4.



Figure 6.20 Histological sections of fibrin/alginate patches, stained with Hematoxylin/Eosin. (A) F20T4A5. (B) F20T4A15. (C) F20T4A30. Scale bar: 200 μ m.

The effect of progressive incorporation of alginate inside a F20T4 fibrin hydrogel resulted in very different structures. Pore sizes seemed to be equivalent in F20T4A5 (**Figure 6.20-A**) and in F20T4 (**Figure 6.19-C**) but we could observe a progressive disorganization of the mesoscopic fiber network for F20T4A15 (**Figure 6.20-B**) and F20T4A30 (**Figure 6.20-C**), with what

can be assumed as very large clusters in bright purple. In these two conditions, the nanoscale organization can be distinguished but the thick fibers observed in Chapter 4 looked more like individual elongated clusters, not necessarily connected in a network structure.

Regarding fibrin/HA hydrogels, we could observe the same histological profile as for fibrin/alginate hydrogels, as the amount of HA increased. The fibrin network showed progressive disorganization; microscopic pores were easily observable at low concentration (Figure 6.21, A-C) while there was a mixture of very thick pores and regions of nanoscopic networks at higher concentrations (Figure 6.21, D-F). Conversely to fibrin-alginate though, the meso-scopic pores present at high concentrations in fibrinogen for the fibrin-HA composite seemed connected by a network of thick fibrin fibers.

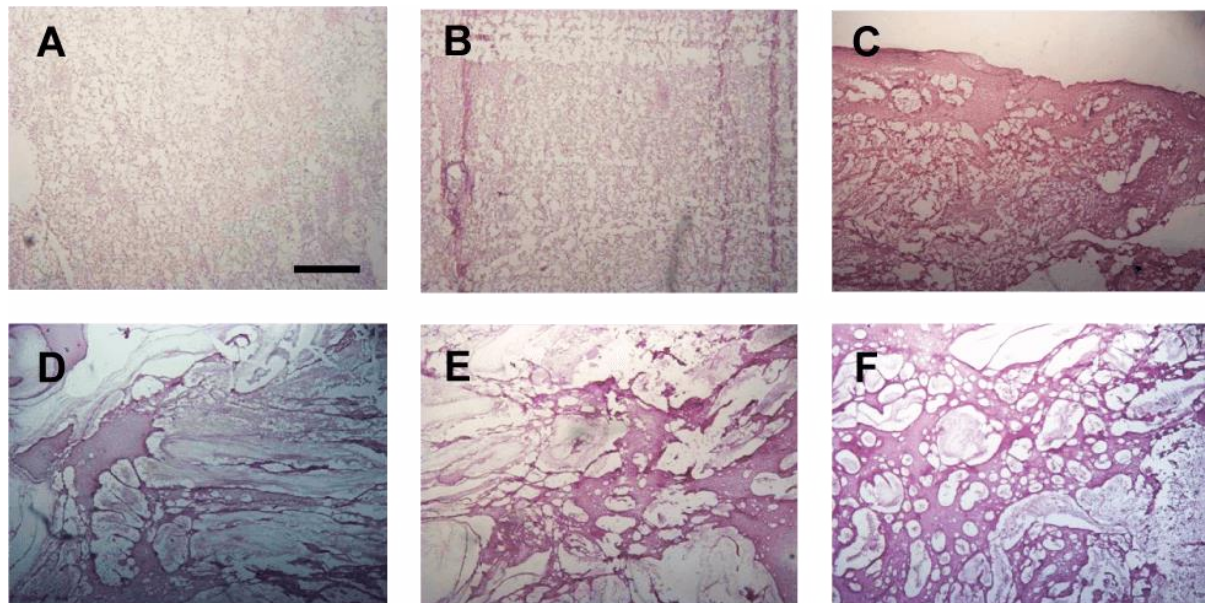


Figure 6.21 Histological sections of fibrin/hyaluronic acid patches, stained with Hematoxylin/Eosin. (A) F10T2HA1.5. (B) F15T3HA2. (C) F20T4HA2.5. (D) F25T5HA3. (E) F30T6HA3.5. (F) F35T7HA4. Scale bar: 200 μ m.

Mechanical properties

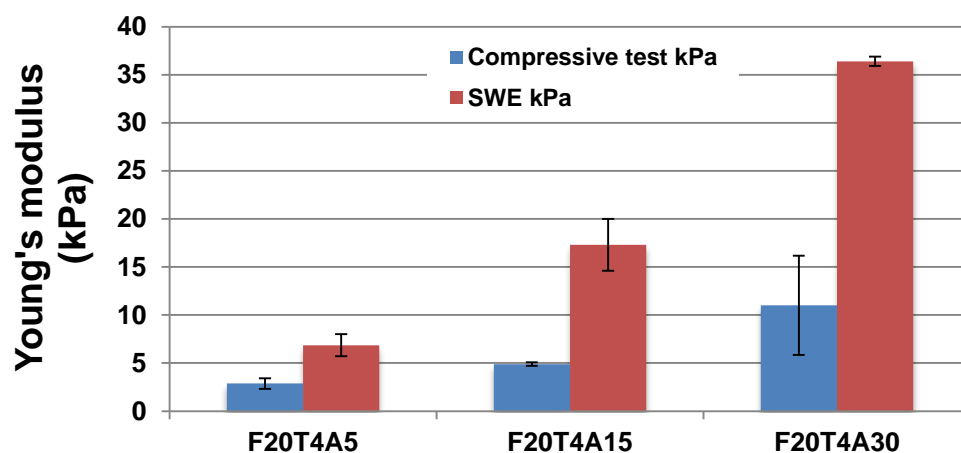


Figure 6.22 Compressive test and SWE results for fibrin/alginate hydrogels. F: fibrinogen in mg/mL, T: thrombin in U/mL, A: alginate in mg/mL. (elasticity is expressed in kPa: mean \pm SEM)

Fibrin/Alginate hydrogels, with a constant fibrin concentration, showed an increased modulus with increasing alginate concentration (Figure 6.22). As our previous experience with compressive testing had been disappointing (Chapter 4), we decided to take into account values measured through SWE. We could notice that compared to F20T4 hydrogels, F20T4A5 composite hydrogels showed equivalent elasticity (respectively 6.15 kPa and 6.85 kPa). Low concentrations of alginate did not seem to affect the stiffness but at higher concentrations, alginate clearly stiffened the structure (up to 36 kPa for F20T4A30).

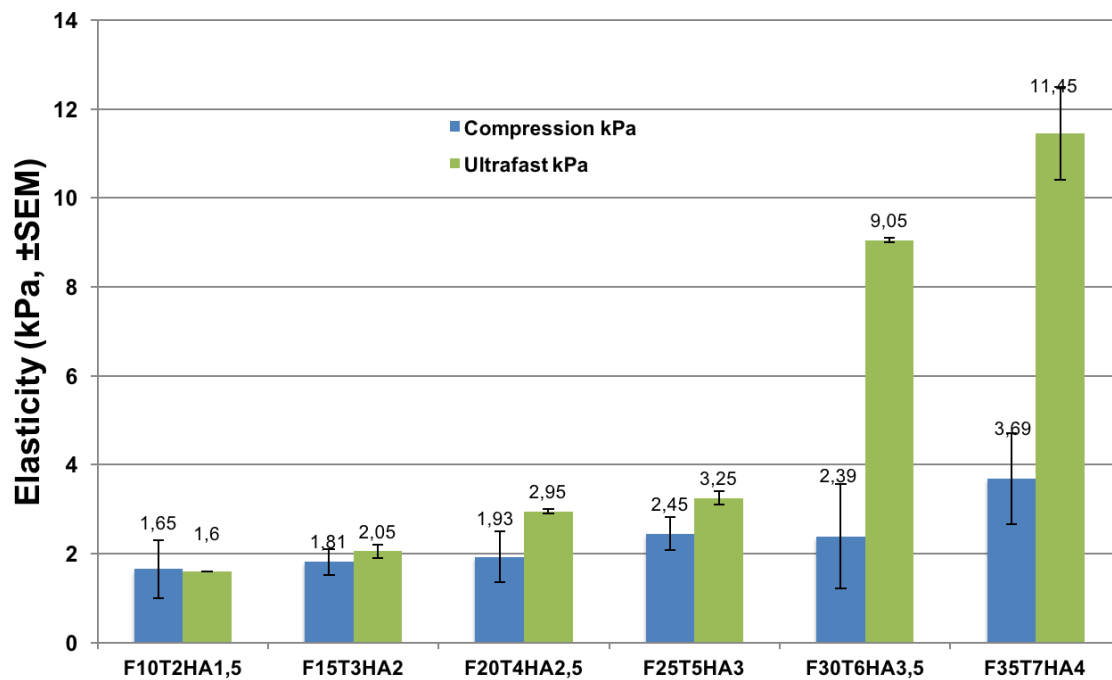


Figure 6.23 Compressive test and SWE results for fibrin/HA hydrogels.

On the other hand, even though fibrin/HA hydrogels presented increasing elasticity with increasing concentrations in hyaluronic acid (Figure 6.23), values were systematically lower than fibrin hydrogels. As HA polymeric chains did not form independent networks by themselves, they probably just hindered the fibrin network polymerization process by limiting the diffusion of thrombin due to increased viscosity. Again, although their respective trends were similar, compressive tests showed systematic lower values than SWE measurements.

In vitro experiment

One hundred thousand MSCs were seeded on 78.5 mm² circular hydrogels. Hydrogels were selected based on their mechanical properties, to see if the used stem cells will present specific shapes depending on matrix stiffness. These 2D cell cultures were stopped at day 7 and no chemical differentiation were used.

On the control fibrin patch, F20T4, which had an intermediate elasticity approaching that of reported muscular elasticity (about 6 kPa), hMSCs started to present actin alignment but

although some cells seemed to present thin elongated cytoplasmic extensions, others presented random polygonal shapes.

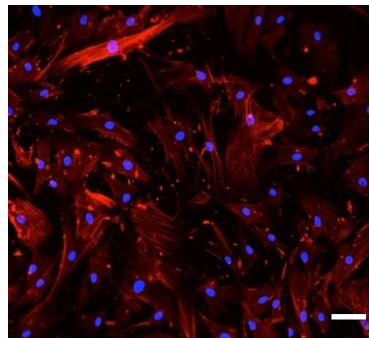


Figure 6.24 Microscopic image of F20T4 seeded with hMSCs at Day 7. Scale bar: 200 μ m

The F20T4A5 matrix showed a high concentration of cells presenting regions of parallel actin networks and anisotropic cells. Intermediate alginate concentrations (**Figure 6.25-B**) caused cell bodies to enlarge but cell alignment was not as good. Regarding the last condition (**Figure 6.25-C**), F20T4A30, cells seemed to lose the peculiar shape previously observed: they were polygonal with no particular anisotropy nor any remarkable morphology.

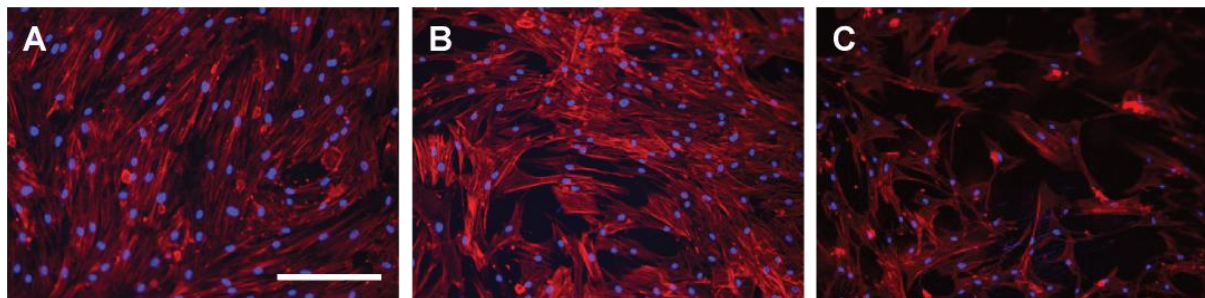


Figure 6.25 Microscopic images of fibrin/Alginate seeded with hMSCs at Day 7. (A) F20T4A5. (B): F20T4A15. (C): F20T4A30. Scale bar: 500 μ m

For the softest matrix, F10T2HA1.5 at 1.6 kPa (**Figure 6.26-A**), some of hMSCs showed thin long cytoplasmic extensions, characteristic of neuronal cells. As for the second matrix, F20T4HA2.5 at 2.95 kPa (**Figure 6.26-B**), cells started to exhibit a larger cell body as compared to the previous condition. Finally, on the stiffer matrix F35T7HA4 (**Figure 6.26-C**), some MSCs started to present parallel actin networks (at the single cell level) and larger cellular bodies, characteristic of muscular cells.

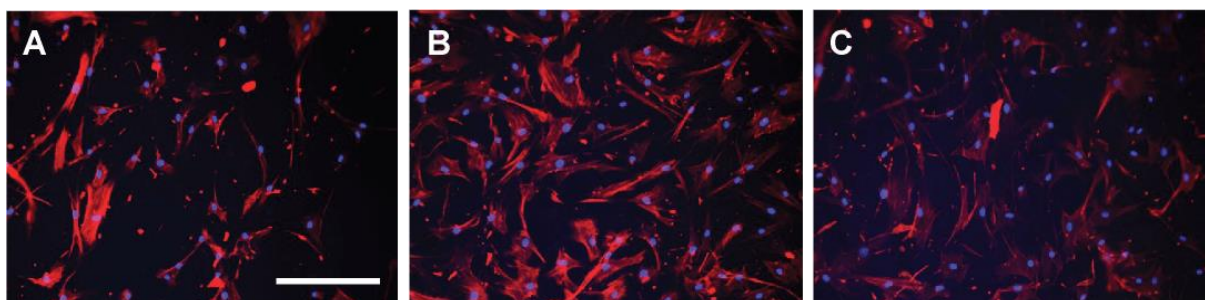


Figure 6.26 Microscopic images of fibrin/HA seeded with hMSCs at Day 7. (A) F10T2HA1.5 (B) F20T4HA2.5 (C) F35T7HA4. Scale bar: 500 μ m

Conclusion on the new blends

The aim of this preliminary study was to propose and mechanically characterize new scaffolds that could be used as a matrix for hESC-derived cardiovascular progenitors. First, handling tests showed that regardless of the scaffold composition, fibrin, fibrin/HA or fibrin/alginate, intermediate concentrations always seemed to be easier to use and to manipulate. Although in the case of pure Evicel® fibrin, histological stains showed a progressive narrowing of hydrogel's pores with increasing fibrinogen/thrombin concentrations, this behavior seemed disturbed by the progressive addition of both alginate and HA. Because we chose not to further crosslink the HA, it was surprising to observe that both using HA or [alginate:Ca²⁺], the fibrin polymerization process had been altered.

With regards to mechanical properties, the base material, fibrin, showed a progressive increase in stiffness with increasing concentrations of fibrinogen and thrombin. As the pore size is progressively reduced with increasing concentrations, the fiber density might produce a more rigid network. By adding HA, at equal fibrin concentrations, values dropped down. As for the histological aspect, HA may have disrupted the polymerization process, making the fibrin network softer. The opposite phenomenon was observed for fibrin/alginate hydrogels. The fact that these hydrogels were composed of an interpenetrating network could explain this significant increase of elasticity, as alginate alone can be very stiff when crosslinked with calcium ions.



Figure 6.27 Sheep surgery using a fibrin/HA patch loaded with CD15⁺ hESC-derived progenitors

In vitro experiments have shown that cell shape could be influenced by the scaffold's mechanical properties. For the matrix of lowest elasticity (F10T2HA1.5), cells presented long cytoplasmic extensions, while for stiffer matrices (F20T4, F35T7HA4, F20T4A5, F20T4A15), they presented a larger cell body, with a parallel actin network. On the stiffest matrix, F20T4A30, hMSCs tended to exhibit a slightly different shape, more polygonal in some cases.

This could correspond to the establishment of a phenotype corresponding to fibrous tissue, as these tissue have been reported to have an elastic modulus that belonged to this range of elasticity. Yet, all these observations have to be carefully interpreted, due to the limited amount of replicate and the well-known variability in hMSCs behavior. In fact, even though some morphologies could remind us of neuronal or muscular morphologies, one has to bear in mind that after a few cell cycles, some human MSCs start to show signs of senescence, whose morphological characteristics are similar to what has been presented here as fibrous tissue.

The next steps would be to determine at the gene level whether these observations can be confirmed. We will check, for each condition, several specific markers, such as β -tubulin III for neurons, MyoD for muscle cells, CBF α 1 for osteogenic cells. Yet, in the light of our attempts to perform surgery on sheep using composite fibrin/HA patches (Figure 6.27), where the patch had shrunk from a 10-cm² surface area down to nearly 1 cm², one will have to bear in mind that even in-laboratory handling tests may not suffice to assess clinical potential.

Conclusion and Perspectives

In this chapter, we described how we focused on making sure that the time spent on the development of new technologies in academic laboratories would not be wasted because of the lack of awareness of the clinical needs. Rather than following commonly reported timelines for drug or medical device research and development [35], where it can take up to 10 additional years between the first report of discovery and market availability, we always kept in mind the question of how the potential outcomes of the research described in the previous chapter could benefit patients as fast as possible. As Cedric Villani, a young Field Medal recipient, likes to point out (and I am poorly paraphrasing): adding constraints is a necessary condition for creativity to be transformed into innovative ideas.

Here, we started from a very complex protocol developed before the start of this PhD [33], alginate functionalization and micropatterning, and went many steps back to consider the numerous pitfalls that would appear when adapting this to human embryonic stem cell culture, and to rethink how simpler techniques could be used to answer real needs. While complex geometric shapes had been used to pattern neonatal rat cardiomyocytes, we found out that making large bands was enough to trigger uniform differentiation of pluripotent stem cells into synchronously beating assemblies named Engineered Cardiac Bands (ECBs). Instead of using biocompatible, resorbable and clinically relevant materials during differentiation, we replaced it with polyacrylamide, a quasi-perfectly elastic hydrogel that only requires raw materials that are commonly available in biological laboratories. Contrary to alginate, its conservation happened to be much simpler, and hydrogel's stability did not depend as much on the medium's salt composition. Rather than creating new synthetic polymers with an ever

growing processing complexity, like we can read in daily published research, we constrained ourselves to composites of well-known materials, and assessed whether we could combine them in new ways that would fit our requirements. Instead of wasting time trying to adapt new concepts to inappropriate and complex characterization techniques (like tensile testing or AFM), we preferred the simplicity of technologies still under development, but with tailored applications to our questions, like SWE.

Even though it can sound paradoxical, the fact that all the techniques presented here were developed in-house will be a determinant component in speeding up the translational process. In fact, when engineers and scientists develop a new technology that can be interesting for medical applications, a considerable amount of time is needed to take into account the hurdles and constraints of the biological world or of the clinics, whereas in our interdisciplinary environment, where every single scientist is facing these constraints on a daily basis, innovation naturally overcomes these problems. It has been argued that outsourcing enables faster development by taking advantages of the expertise of other groups, when in fact, outsourcing can slow down development by implying an additional time for the two sides to understand the real needs, while in-house engineers and biologists are already aware of these needs. Micropatterns can be outsourced, but what about the ECM protein coatings? Polyacrylamide hydrogels can be outsourced, but what about contamination issues? Cardiomyocyte production can be outsourced, but what about maturation stages? All these questions would have to be answered in discussion with these many industrial partners, when in fact, this can be solved faster, locally.

References

1. Braunwald E, Bristow MR: **Congestive heart failure: fifty years of progress.** *Circulation* 2000, **102**:IV14–23.
2. Jezierska-Woźniak K, Mystkowska D, Tutas A, Jurkowski MK: **Stem cells as therapy for cardiac disease - a review.** *Folia Histochem Cytobiol* 2011, **49**:13–25.
3. Beltrami AP, Urbanek K, Kajstura J: **Evidence that human cardiac myocytes divide after myocardial infarction.** ... *England Journal of ...* 2001, **344**:1750–1757.
4. Assmus B, Schachinger V, Teupe C, Britten M: **Transplantation of progenitor cells and regeneration enhancement in acute myocardial infarction (TOPCARE-AMI).** *Circulation* 2002.
5. Hamdi H, Furuta A, Bellamy V, Bel A, Puymirat E, Peyrard S, Agbulut O, Menasche P: **Cell Delivery: Intramyocardial Injections or Epicardial Deposition? A Head-to-Head Comparison.** *ATS* 2009, **87**:1196–1203.
6. Engler AJ, Sen S, Sweeney HL, Discher DE: **Matrix elasticity directs stem cell lineage specification.** *Cell* 2006, **126**:677–689.
7. Willerth SM, Arendas KJ, Gottlieb DI, Sakiyama-Elbert SE: **Optimization of fibrin scaffolds for differentiation of murine embryonic stem cells into neural lineage cells.** *Biomaterials* 2006, **27**:5990–6003.
8. Sun J-Y, Zhao X, Illeperuma WR, Chaudhuri O, Oh KH, Mooney DJ, Vlassak JJ, Suo Z: **Highly stretchable and tough hydrogels.** *Nature* 2012, **489**:133–136.
9. Lee KY, Mooney DJ: **Alginate: Properties and biomedical applications.** *Progress in Polymer Science* 2012, **37**:106–126.
10. Zimmermann U, Klöck G, Federlin K, Hannig K, Kowalski M, Bretzel RG, Horcher A, Entenmann H, Sieber U, Zekorn T: **Production of mitogen-contamination free alginates with variable ratios of mannuronic acid to guluronic acid by free flow electrophoresis.** *Electrophoresis* 1992, **13**:269–274.
11. Orive G, Ponce S, Hernández RM, Gascón AR, Igartua M, Pedraz JL: **Biocompatibility of microcapsules for cell immobilization elaborated with different type of alginates.** *Biomaterials* 2002, **23**:3825–3831.
12. Shikanov A, Xu M, Woodruff TK, Shea LD: **Interpenetrating fibrin-alginate matrices for in vitro ovarian follicle development.** *Biomaterials* 2009, **30**:5476–5485.
13. Rocca Della DG, Willenberg BJ, Ferreira LF, Wate PS, Petersen JW, Handberg EM, Zheng T, Steindler DA, Terada N, Batich CD, Byrne BJ, Pepine CJ: **A degradable, bioactive, gelatinized alginate hydrogel to improve stem cell/growth factor delivery and facilitate healing after myocardial infarction.** *Medical Hypotheses* 2012, **79**:673–677.
14. Nunamaker EA, Otto KJ, Kipke DR: **Investigation of the material properties of alginate for the development of hydrogel repair of dura mater.** *Journal of the Mechanical Behavior of Biomedical Materials* 2011, **4**:16–33.
15. Prestwich GD: **Hyaluronic acid-based clinical biomaterials derived for cell and molecule delivery in regenerative medicine.** *Journal of Controlled Release* 2011, **155**:193–199.
16. Weigel PH, Fuller GM, LeBoeuf RD: **A model for the role of hyaluronic acid and fibrin in the early events during the inflammatory response and wound healing.** *Journal of Theoretical Biology* 1986, **119**:219–234.

17. Maioli M, Santaniello S, Montella A, Bandiera P, Cantoni S, Cavallini C, Bianchi F, Lionetti V, Rizzolio F, Marchesi I, Bagella L, Ventura C: **Hyaluronan Esters Drive Smad Gene Expression and Signaling Enhancing Cardiogenesis in Mouse Embryonic and Human Mesenchymal Stem Cells.** *PLoS ONE* 2010, **5**:e15151–11.
18. Chan CK, Rolle MW, Potter-Perigo S, Braun KR, Van Biber BP, Laflamme MA, Murry CE, Wight TN: **Differentiation of cardiomyocytes from human embryonic stem cells is accompanied by changes in the extracellular matrix production of versican and hyaluronan.** *J Cell Biochem* 2010, **111**:585–596.
19. Maioli M, Santaniello S, Montella A, Bandiera P, Cantoni S, Cavallini C, Bianchi F, Lionetti V, Rizzolio F, Marchesi I: **Hyaluronan esters drive Smad gene expression and signaling enhancing cardiogenesis in mouse embryonic and human mesenchymal stem cells.** *PLoS ONE* 2010, **5**:e15151.
20. Chopra A, Murray ME, Byfield FJ, Mendez MG, Halleluyan R, Restle DJ, Raz-Ben Aroush D, Galie PA, Pogoda K, Bucki R, Marcinkiewicz C, Prestwich GD, Zarembinski TI, Chen CS, Puré E, Kresh JY, Janmey PA: **Augmentation of integrin-mediated mechanotransduction by hyaluronic acid.** *Biomaterials* 2014, **35**:71–82.
21. Bellamy V, Vanneaux V, Bel A, Nemetalla H, Boitard SE, Farouz Y, Joanne P, Périer M-C, Robidel E, Mandet C, Hagège A, Bruneval P, Larghero J, Agbulut O, Menasché P: **Long-term functional benefits of human embryonic stem cell-derived cardiac progenitors embedded into a fibrin scaffold.** *Journal of Heart and Lung Transplantation* 2014:1–10.
22. Menasché P, Vanneaux V, Fabreguettes J-R, Bel A, Tosca L, Garcia S, Bellamy V, Farouz Y, Pouly J, Damour O, Périer M-C, Desnos M, Hagège A, Agbulut O, Bruneval P, Tachdjian G, Trouvin J-H, Larghero J: **Towards a clinical use of human embryonic stem cell-derived cardiac progenitors: a translational experience.** *European Heart Journal* 2014.
23. Menasche P, Vanneaux V, Hagege A, Bel A, Cholley B, Cacciapuoti I, Parouchev A, Benhamouda N, Tachdjian G, Tosca L, Trouvin JH, Fabreguettes JR, Bellamy V, Guillemain R, Suberbielle Boissel C, Tartour E, Desnos M, Larghero J: **Human embryonic stem cell-derived cardiac progenitors for severe heart failure treatment: first clinical case report.** *European Heart Journal* 2015:1–7.
24. Llames S, García-Pérez E, Meana Á, Larcher F, del Río M: **Feeder Layer Cell Actions and Applications.** *Tissue Engineering Part B: Reviews* 2015, **21**:345–353.
25. Eiselleova L, Peterkova I, Neradil J, Slaninova I, Hampl A: **Comparative study of mouse and human feeder cells for human embryonic stem cells.** *Int J Dev Biol* 2008, **52**:353–363.
26. Claassen DA, Desler MM, Rizzino A: **ROCK inhibition enhances the recovery and growth of cryopreserved human embryonic stem cells and human induced pluripotent stem cells.** *Mol Reprod Dev* 2009, **76**:722–732.
27. Chen AK-L, Chen X, Lim YM, Reuveny S, Oh SKW: **Inhibition of ROCK–Myosin II Signaling Pathway Enables Culturing of Human Pluripotent Stem Cells on Microcarriers Without Extracellular Matrix Coating.** *Tissue Engineering Part C: Methods* 2013:130725070704006.
28. Watanabe K, Ueno M, Kamiya D, Nishiyama A, Matsumura M, Wataya T, Takahashi JB, Nishikawa S, Nishikawa S-I, Muguruma K, Sasai Y: **A ROCK inhibitor permits survival of dissociated human embryonic stem cells.** *Nature Biotechnology* 2007, **25**:681–686.
29. Martin-Ibanez R, Unger C, Stromberg A, Baker D, Canals JM, Hovatta O: **Novel cryopreservation method for dissociated human embryonic stem cells in the presence of a ROCK inhibitor.** *Human Reproduction* 2008, **23**:2744–2754.
30. Li X, Meng G, Krawetz R, Liu S, Rancourt DE: **The ROCK Inhibitor Y-27632 Enhances the Survival Rate of Human Embryonic Stem Cells Following Cryopreservation.** *Stem Cells Dev* 2008, **17**:1079–1086.

31. Kim D-H, Lipke EA, Kim P, Cheong R, Thompson S, Delannoy M, Suh K-Y, Tung L, Levchenko A: **Nanoscale cues regulate the structure and function of macroscopic cardiac tissue constructs.** *PNAS* 2010, **107**:565–570.
32. Kim D-H, Kshitiz, Smith RR, Kim P, Ahn EH, Kim HN, Marbán E, Suh K-Y, Levchenko A: **Nanopatterned cardiac cell patches promote stem cell niche formation and myocardial regeneration.** *Integr Biol* 2012, **4**:1019–1033.
33. Agarwal A, Farouz Y, Nesmith AP, Deravi LF, McCain ML, Parker KK: **Micropatterning Alginate Substrates for in vitro Cardiovascular Muscle on a Chip.** *Adv Funct Mater* 2013, **23**:3738–3746.
34. Grosberg A, Alford PW, McCain ML, Parker KK: **Ensembles of engineered cardiac tissues for physiological and pharmacological study: heart on a chip.** *Lab Chip* 2011, **11**:4165–4173.
35. Hench LL, Jones JR: **Biomaterials, artificial organs and tissue engineering.** *Book* 2005.

Supplementary Information

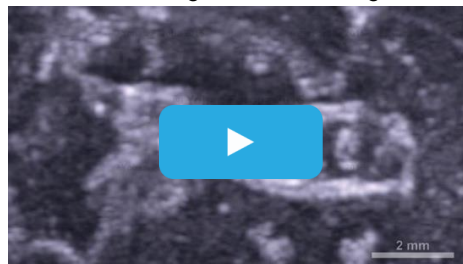
Supplementary Movie 6.1 Engineered Cardiac Bands, spontaneously beating on PAA substrates of variable stiffness

(click on any image, flash the QR code or go to the following address: <https://goo.gl/gNDXF1>)



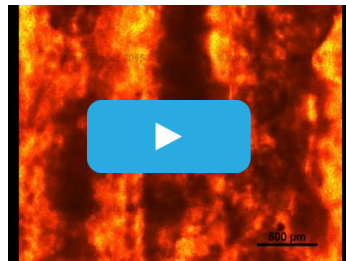
Supplementary Movie 6.2 Ultrasound imaging of a beating fibrin patch with 2 layers of cardiac bands

(click on any image, flash the QR code or go to the following address: <https://goo.gl/ApZ15p>)



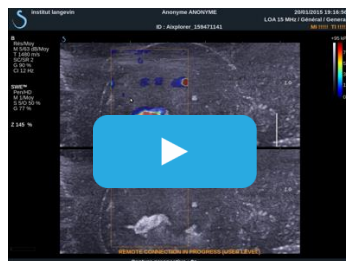
Supplementary Movie 6.3 Fibrin patch with 2 layers of cardiac bands, right after fibrin polymerization

(click on any image, flash the QR code or go to the following address: <https://goo.gl/wkABUO>)



Supplementary Movie 6.4 Shear Wave Elastography of free standing, clustered cardiac bands

(click on any image, flash the QR code or go to the following address: <https://goo.gl/xUElha>)



Chapter 7 – Conclusions and Perspectives

Summary

In this journey as a PhD trainee, I explored how biomaterials engineering could help design new solutions for the treatment of the most prevalent cardiovascular disease, congestive heart failure. By working hand to hand with engineers, chemists, biologists, pharmacologists, surgeons and members of the drug regulatory authorities, we have been able to identify what could be done in a reasonable amount of time in order to have the maximum impact on patient's quality of life. At the same time, we started to define the obstacles that remain to be overcome to bring still cutting edge technologies – like microfabrication on soft hydrogels, or microfluidics chips for high-throughput screening – to the clinics.

As illustrated by the outline of the present document, we perpetually went back and forth between the labs and the clinics, always trying to stay as close as possible to the medical reality, yet taking some distance when the constraints happened to be too limiting. At the beginning of my studies, the question we asked was how to make a patch that could deliver cardiovascular progenitors inside the myocardium. Previous studies had led our laboratories to abandon injections and adult stem cells. Therefore, the prerequisite to answer this question was a perfect control of the biology of hESCs and of their differentiation into cardiac progenitors. By being immersed in a clinical setting, I soon realized that unfortunately, developmental biomechanics are still in their infancy and, if data are now overabundant, the true meanings and implications of these data are yet to unravel. Therefore, we hypothesized that not only could biomaterials bring human embryonic stem cells to the clinics, but that they could also help answer scientific questions with undeniable practical applications.

First, I designed the protocol and formulation for the clinical fibrin patch. Before performing *in vivo* studies on the benefits of such a patch, we sought to make sure that the patch could be used in the operating theater. Using the surgical glue Evicel[®], the best formulation was found to be a patch made by mixing a solution of 20 mg/mL of fibrinogen with a solution of 4 UI/mL of thrombin. Two key parameters appeared to be involved in the simplicity, reproducibility and success of the clinical protocol: the control of the polymerization of fibrin as well as the conservation of the patch before surgery. To control the polymerization of fibrin, it was necessary to setup new collaborations to routinely and precisely determine the concentration of fibrinogen in the Evicel[®]'s solution and to make sure that thrombin's bioactivity was not impaired by the cell culture conditions. Indeed, initial attempts resulted in variable stiffness and cell retention within the patch either because the fibrinogen concentration was lower than expected, or because thrombin had been inactivated by proteins from the serum of the culture medium. To preserve the patch before surgery, no antifibrinolytic agent was

necessary, but the patch could not be detached from its petri dish without the help of an agarose coating. Therefore, we had to define a procedure for preparing and storing agarose petri dishes in a sterile environment. Eventually, this patch fabrication routine showed to be easily reproduced by the certified clinical personnel both in preclinical studies with sheep and later when the first patients had been treated.

Second, I went further on the control of the mechanical properties of the newly designed fibrin patches. Now that the more practical aspects had been solved, it was time to make a smarter patch, a patch that could enhance the therapeutic effects of the cardiac progenitors, rather than just posing as a delivery vector for cell survival. Before any attempt to incorporate bioactive drugs, we thus wondered how the mechanical properties alone could have a positive impact on the maturation of cardiovascular progenitors.

On one hand, we deepened our analysis of the mechanical properties of Evicel-based fibrin hydrogels to learn to control the structure of the patch over a wider range of elastic moduli. After comparing multiple techniques, shear wave elastography proved to be the simplest and most powerful technique for assessing the Young's modulus of hydrogels. We optimized the preparation steps for making echogenic biomaterials of various compositions at a higher scale and it allowed for the characterization of the entire spectrum of fibrin patches that can be prepared by just altering the fibrinogen concentration. As a matter of fact, this range of materials happened to be relatively narrow, since concentrations of fibrinogen higher than 35-40 mg/mL had a discriminatively short polymerization time whereas concentrations lower than 5 mg/mL did not lead to firm enough gels. Accordingly, the range of Young's moduli was only between about 2 kPa and 12 kPa (F20T4 gels having a stiffness around 6 kPa), but fortunately, it seems to be the range of elasticity corresponding to fetal hearts (below 10 kPa) and neonatal hearts (10-20 kPa), hence our confidence in future positive outcomes.

On the other hand, I had to define a technique for screening the interactions between model materials and hESCs or hESC-derived cardiac progenitors. As in any model, we soon came to the conclusion that strict clinical settings implied too many constraints and that by simplifying the study using hiPSCs, Polyacrylamide and Matrigel as our raw materials, we could unleash the scientific potential of this study. Nevertheless, the biggest constraint to overcome was of another kind. It was contamination. And here, working with clinical applications in mind helped face sooner this reality of stem cell therapies. While microfabrication techniques have been often used to address fundamental questions in mechanobiology and mechanotransduction, it was rare that it required more than a week of culture in complete absence of antibiotics. This sensitivity of hPSCs to external conditions pushed us to our limits to design a technology that in the end, would allow for prolonged culture of hPSCs on substrates of controlled elasticity and controlled ECM protein distribution. To my

knowledge, at the time this manuscript is being written, there is no reported protocol describing the culture and differentiation of human pluripotent stem cells on micropatterned matrices of controlled elasticity for long periods of time. Even though results will have to be replicated a few more times to confirm their reliability, we have been able to extract important information on the behavior of hiPSCs under confinement and in soft environments. While qualitative observations tended to suggest that beating appeared first in conditions of low elasticity, we showed that elasticity did not seem to have an important effect on the differentiation of hiPSCs into cardiomyocytes. However, the diameter of the ECM spots, that confined cells, seemed to confer, if not significant genetic expression variations, important structural and functional changes. Above 1600 μm in diameter, beating peripheral rings were observed in place of the beating clusters seen below 1600 μm , where the ring and the rest of the colony was hardly discernable. Additionally, small clusters showed the ability to synchronize and stabilize their beating frequency as well as strengthen their radial contractions relatively faster than wide rings, that exhibited irregular, fast-paced, circular (orthoradial) wave-like contractile behaviors. At the expression level, clustering analyses revealed groups of conditions with similar profiles of RNA expression, when genes had been grouped by categories of interest. If overall, it mostly resulted in a mixture of populations ranging from very early mesodermal cells to immature cardiomyocytes and vascular progenitors, the association of certain conditions in elasticity and diameters led to an enrichment of different stages of cardiac development. Indeed, the combination of soft hydrogels and large spots seemed to correlate with a more atrial and immature phenotype whereas hard substrates with small spots was linked to a more ventricular and mature phenotype, with a lower proportion of immature cells than on hard substrates with large spots. In summary, we have extracted the main characteristics of cardiac differentiation in a multitude of mechanically and topographically controlled environments. Not only does this microfabrication technique provide a way to standardize and scale up cardiomyocyte production for reliable experimentations and therapies, but it also helps define strategies for matching the right differentiation protocol and the right environment to the right biological, pharmacological or clinical application. As discussed earlier, since the best differentiation stage for the use of cardiomyocytes in the treatment of heart failure remains unknown, it is important to be able to isolate different populations at different stages of cardiac development.

Last but not least, the proximity with the clinical environment has been an opportunity for me to take some distance from *simplified* models and to look for *simple* solutions that would still take advantage of the conclusions drawn using complex microtechnologies and very specific setups. Rather than succumbing to the temptation of blindly generalizing to human stem cells the microfabrication of alginate substrate for neonatal rat cardiomyocyte contractility

assays, I focused on designing new ways of fabricating materials exhibiting similar properties, yet with simpler techniques, no chemical modifications and clinically-relevant raw materials.

This initially resulted in two new families of composite materials made of fibrin and calcium alginate or fibrin and hyaluronic acid. The competition between fibrin polymerization and alginate crosslinking on one side, and between fibrin polymerization and hyaluronic acid's inherent viscosity on the other side, strongly affected the structure of the fibrin network and its corresponding elasticity. If both alginate and hyaluronic acid hindered homogeneous fibrin polymerization, crosslinked alginate stiffened the final hydrogel (up to 37 kPa), whereas hyaluronic acid, non crosslinked, did not contribute to fibrin stability.

On another level, it also resulted in proof-of-concept techniques allowing for chemical-free and enzyme-free dissociation and transfer of anisotropic hiPSC-derived cardiac bands onto clinical fibrin patches. Subsequently, I showed that we could engineer new agarose petri dishes for the evaluation of their contractile and mechanical behavior using shear wave elastography. This work establishes the first stone of a stronger bridge between developmental biomechanics, *in vitro* toxicological assays and regenerative medicine. Undoubtedly, building on these proofs of principle could dramatically expand the ways we perform electrophysiological and contractility assays, by allowing researchers to compare and continue *in vitro* experiments into living beings, in a non-invasive fashion. *In vivo* mechanical characterization can lead to the design of *in vitro* biomimetic materials as well as the implementation of *in silico* predictive and personalized models that could translate back to efficient, scalable and disruptive therapies.

Perspectives

Stem cell differentiation, biomaterials and cell-free cell therapy

Important to the development of cellular therapy in regenerative medicine is a better understanding of the underlying mechanisms through which transplanted cells exert their biological effects. One puzzling observation has been that the therapeutic benefits of cellular therapy appear to outlast the physical presence of transplanted cells [1]. This is inconsistent with the idea that implanted cells colonise and directly replace the injured tissue. A hypothesis of paracrine signalling has therefore been suggested in which factors secreted by grafted cells promote endogenous healing [1]. This concept would also explain experiments in which cells remaining within a patch still show therapeutic benefit [2]. In support of this idea, pigs with myocardial infarctions and treated with human mesenchymal stem cell-conditioned media had higher myocardial capillary density, decreased myocardial infarct size, and better cardiac performance than pigs receiving non-conditioned media [3].

Additional investigations undertaken to determine which secreted factors could be important have identified a class of secreted microvesicles, exosomes, as a strong candidate [4, 5]. Exosomes are 40-100 nm diameter membrane-bound vesicles formed in the late endosome/multivesicular bodies [6]. Their cholesterol rich, sphingomyelin containing lipid bilayer membranes are punctuated with tetraspanin proteins such as CD63/CD9 and their lumen contains soluble proteins and biologically active mRNAs and miRNAs. Exosomes shuttle their contents from the shedding cell to recipient cells near or at great distance to exert biological effects; delivery of mRNAs and miRNA has been shown to affect gene expression in the recipient cell [7]. In a regenerative context, exosomes secreted by cardiosphere derived cells (CDCs) have been shown to recapitulate the therapeutic effects of CDC transplantation. As research in this area continues and bioactive vesicles or their contents are identified, this will open up new possibilities in regenerative medicine. Microvesicle-based therapies have the potential to be more clinically useful than their cellular counterparts, as they could be safer, more reproducible, scalable, and more amenable to quality control. Further, exosomes can be readily modified in the laboratory [8]. Their contents and surface components could therefore be optimised for improved target specificity, therapeutic potency, or stability. Small molecule pharmaceuticals can also be attached to the surface of microvesicles if targeted adjuvant therapy were of interest.

Yet, if cellular therapy evolves toward cell-free formulations, biomaterials would still represent an ally of importance. Secreted microvesicles could potentially be encapsulated in biomaterials, which would allow for optimised delivery modalities, such as suturable patches for surgical applications or microspheres for injectable suspensions. Encapsulation may improve tissue retention and could allow for time-release technologies. Additionally, the identification of targeting peptides by *in vivo* screening technologies such as phage display [9, 10] could lead to new materials with both gene delivery capabilities [11] and an improved affinity for the healthy or diseased heart [12].

In any case, if exosomes can be further modified, their production would have to be optimised and standardized. In the light of promising results claiming that myocardial infarction can be endogenously alleviated after injection of hESC-secreted exosomes [13], the question of the cellular source and their culture conditions will have to resurface. Hence, technologies such as our cardiac band differentiation on soft substrates will undoubtedly provide ways to control the generation of exosomes from anisotropic and synchronized cardiomyocytes.

References

1. Gnecci M, Zhang Z, Ni A, Dzau VJ: **Paracrine mechanisms in adult stem cell signaling and therapy.** *Circulation Research* 2008, **103**:1204–1219.
2. Menasché P, Vanneau V, Fabreguettes J-R, Bel A, Tosca L, Garcia S, Bellamy V, Farouz Y, Pouly J, Damour O, Périer M-C, Desnos M, Hagège A, Agbulut O, Bruneval P, Tachdjian G, Trouvin J-H, Larghero J: **Towards a clinical use of human embryonic stem cell-derived cardiac progenitors: a translational experience.** *European Heart Journal* 2014.
3. Timmers L, Lim SK, Hoefler IE, Arslan F, Lai RC, van Oorschot AAM, Goumans MJ, Strijder C, Sze SK, Choo A, Piek JJ, Doevendans PA, Pasterkamp G, de Kleijn DPV: **Human mesenchymal stem cell-conditioned medium improves cardiac function following myocardial infarction.** *Stem Cell Research* 2011, **6**:206–214.
4. Lai RC, Tan SS, Teh BJ, Sze SK, Arslan F, de Kleijn DP, Choo A, Lim SK: **Proteolytic Potential of the MSC Exosome Proteome: Implications for an Exosome-Mediated Delivery of Therapeutic Proteasome.** *International Journal of Proteomics* 2012, **2012**:1–14.
5. Vrijssen KR, Sluijter JPG, Schuchardt MWL, Van Balkom BWM, Noort WA, Chamuleau SAJ, Doevendans PAFM: **Cardiomyocyte progenitor cell-derived exosomes stimulate migration of endothelial cells.** *Journal of Cellular and Molecular Medicine* 2010, **14**:no–no.
6. Loyer X, Vion A-C, Tedgui A, Boulanger CM: **Microvesicles as cell-cell messengers in cardiovascular diseases.** *Circulation Research* 2014, **114**:345–353.
7. Valadi H, Ekström K, Bossios A, Sjöstrand M, Lee JJ, Lötvall JO: **Exosome-mediated transfer of mRNAs and microRNAs is a novel mechanism of genetic exchange between cells.** *Nat Cell Biol* 2007, **9**:654–659.
8. Johnsen KB, Gudbergsson JM, Skov MN, Pilgaard L, Moos T, Duroux M: **A comprehensive overview of exosomes as drug delivery vehicles — Endogenous nanocarriers for targeted cancer therapy.** *BBA - Reviews on Cancer* 2014, **1846**:75–87.
9. Zahid M, Phillips BE, Albers SM, Giannoukakis N, Watkins SC, Robbins PD: **Identification of a cardiac specific protein transduction domain by in vivo biopanning using a M13 phage peptide display library in mice.** *PLoS ONE* 2010, **5**:e12252.
10. McGuire MJ, Samli KN, Johnston SA, Brown KC: **In vitro selection of a peptide with high selectivity for cardiomyocytes in vivo.** *Journal of Molecular Biology* 2004, **342**:1–12.
11. Yoo SY, Jin H-E, Choi DS, Kobayashi M, Farouz Y, Wang S, Lee S-W: **M13 Bacteriophage and Adeno-Associated Virus Hybrid for Novel Tissue Engineering Material with Gene Delivery Functions.** *Advanced Healthcare Materials* 2015:n/a–n/a.
12. WILLEMS IE, ARENDS J-W, DAEMEN MJ: **Tenascin and fibronectin expression in healing human myocardial scars.** *The Journal of pathology* 1996, **179**:321–325.
13. Khan M, Nickoloff E, Abramova T, Johnson J, Verma SK, Krishnamurthy P, Mackie AR, Vaughan E, Garikipati VNS, Benedict C, Ramirez V, Lambers E, Ito A, Gao E, Misener S, Luongo T, Elrod J, Qin G, Houser SR, Koch WJ, Kishore R: **Embryonic Stem Cell-Derived Exosomes Promote Endogenous Repair Mechanisms and Enhance Cardiac Function Following Myocardial Infarction.** *Circulation Research* 2015, **117**:52–64.

Abstract

Cell therapy is a promising strategy to help regenerate the damaged heart. Recent studies have placed a lot of hopes in embryonic stem cells and our lab had previously found a way to differentiate them into cardiac progenitors, cells that can only differentiate into cardiomyocyte, endothelial cells or smooth muscle cells. This early commitment decreases their proliferative capabilities, yet maintains their plasticity for better integration inside the host tissue. However, clinical and pre-clinical injection studies did not really meet the expectations. Even though slight improvements in cardiac function were demonstrated, very low cell viability has been observed, as well as a very low retention of the cells inside the myocardium. To address this problem, my PhD projects not only focus on the design of new biomaterials to act as a vehicle for cell delivery and retention in the infarcted area, but also on the design of biomaterials that control the cellular environment during the differentiation of pluripotent stem cells into cardiomyocytes. Going back and forth between the labs and the clinics, we first developed new techniques for the fabrication and the characterization of a cell-laden fibrin patch that is now undergoing phase I clinical trial. From the approved clinical formulation, we then propose new blends of clinical materials that will eventually improve the maturation of the cardiac progenitors once grafted onto the failing heart. In this perspective, we developed an *in vitro* model to investigate the combined influence of matrix elasticity and topographical confinement on stem cell differentiation into cardiomyocytes. By using microfabrication techniques to pattern pluripotent stem cells on substrates of controlled stiffness, we demonstrate that even using a widely recognized chemical-based protocol to modulate signaling cascades during differentiation, much heterogeneity emerges depending on the cellular physical environment. We thus extracted the main features that led to controlled and reproducible cardiac differentiation and applied it to the fabrication of next generation of multi-layered anisotropic cardiac patches in compliances with clinical requirements. This work opens new routes to high-scale production of cardiomyocytes and the fabrication of cell-laden or cell-free clinical patches.

Keywords: Cell therapy, regenerative medicine, biomaterials and tissue engineering, cardiac development, mechanotransduction, microfabrication, human pluripotent stem cells.

Résumé

La thérapie cellulaire se positionne comme une stratégie prometteuse pour inciter le cœur infarcté à se régénérer. A cet effet, des études récentes placent des espoirs considérables dans l'utilisation des cellules souches embryonnaires et notre laboratoire a déjà démontré comment les différencier en progéniteurs cardiovasculaires, un type de précurseurs cellulaires qui ne peut aboutir qu'à la formation de cardiomyocytes, de cellules endothéliales ou de cellules de muscles lisses. Cet engagement précoce réduit leur capacité de prolifération anarchique et en même temps leur permet de rester suffisamment plastiques pour éventuellement s'intégrer plus facilement avec le tissu hôte. Cependant, les études précliniques et cliniques d'injection de ces cellules s'avèrent décevantes. Malgré de légères améliorations de la fonction cardiaque, on observa une trop faible survie cellulaire ainsi qu'un taux de rétention des cellules dans le myocarde remarquablement bas. Afin d'étudier ce problème, mes travaux de thèse ont porté non seulement sur la conception de nouveaux biomatériaux pouvant servir de moyen de transport et d'intégration des cellules dans la zone infarctée, mais aussi sur la conception de biomatériaux permettant de contrôler précisément l'environnement cellulaire au cours du processus de différenciation de cellules souches pluripotentes humaines en cardiomyocytes. Grâce aux importantes interactions entre nos laboratoires de recherche fondamentale et de recherche clinique, nous avons tout d'abord développé de nouvelles techniques de fabrication et de caractérisation de patches de fibrine cellularisés qui sont récemment entrés dans un essai clinique de phase I. A partir de cette formulation clinique approuvée par les autorités de régulation, nous avons élaboré toute une gamme de matériaux composites uniquement à base de matières premières pertinentes dans ce cadre clinique, dans le but d'améliorer la maturation des progéniteurs cardiovasculaires une fois greffés sur le cœur défaillant. Dans cette optique, nous avons également développé un modèle *in vitro* permettant d'étudier précisément l'influence combinée de la rigidité du substrat et du confinement spatial sur la différenciation des cellules souches en cardiomyocytes. Grâce à des techniques de microfabrication sur substrat mou, il a été possible de positionner précisément les cellules souches pluripotentes dans des espaces restreints d'élasticité variable. Ainsi, nous avons pu observer que même en utilisant des protocoles chimiques éprouvés basés sur la modulation de cascades de signalisation impliquées dans le développement cardiaque, une très forte hétérogénéité pouvait apparaître en fonction de l'environnement physique des cellules. Nous avons ainsi pu extraire les caractéristiques principales permettant une différenciation cardiaque efficace, reproductible et standardisée et les avons appliquées à la fabrication d'une nouvelle génération de patches composés de matériaux cliniques et de couches multiples de bandes synchrones de cardiomyocytes. De fait, ces travaux ouvrent de nouvelles voies dans l'utilisation de biomatériaux pour la production industrielle de cardiomyocytes et pour la fabrication de patches cliniques, cellularisés ou non, dans le traitement de l'insuffisance cardiaque.

Mots clés : Thérapie cellulaire, médecine régénératrice, biomatériaux et ingénierie tissulaire, développement cardiaque, mécanotransduction, microfabrication, cellules souches pluripotentes humaines.